A handwritten signature in black ink, consisting of several loops and strokes, located in the top right corner of the page.

CEREBROSPINAL FLUID PULSE PRESSURE
AND
CRANIOSPINAL DYNAMICS

A theoretical, clinical and experimental study

© 1984 ISBN 90 70062 07 0 A. Jongbloed en Zoon, Publishers, The Hague, the Netherlands.
All rights reserved. No part of this publication may be reproduced, stored in a retrieval system, or transmitted, in any form or by any means, electronic, mechanical, photocopying, recording or otherwise, without the prior permission of the publisher or the authors.

From the Department of Neurosurgery and the Department of Electro-Neurology,
Academic Hospital Rotterdam and Erasmus University,
Rotterdam, The Netherlands.

**CEREBROSPINAL FLUID PULSE PRESSURE
AND
CRANIOSPINAL DYNAMICS**

A theoretical, clinical and experimental study

PROEFSCHRIFT

TER VERKRIJGING VAN DE GRAAD VAN
DOCTOR IN DE GENEESKUNDE
AAN DE ERASMUS UNIVERSITEIT ROTTERDAM
OP GEZAG VAN DE RECTOR MAGNIFICUS
PROF. DR. M.W. VAN HOF
EN VOLGENS BESLUIT VAN HET COLLEGE VAN DEKANEN.
DE OPENBARE VERDEDIGING ZAL PLAATSVINDEN OP
WOENSDAG 1 FEBRUARI 1984 DES NAMIDDAGS
TE 2.00 UUR

DOOR

CORNELIS JACOBUS JOHANNES AVEZAAT
geboren te Amsterdam

1984

grafische verzorging:

ROECCDAVIDS
ALBLASSERDAM

PROMOTOREN : PROF. DR. S.A. DE LANGE
PROF. DR. M. DE VLIET

CO-REFERENTEN : PROF. DR. K.G. GO
PROF. DR. IR. H.G. STASSEN

**CEREBROSPINAL FLUID PULSE PRESSURE
AND
CRANIOSPINAL DYNAMICS**

A theoretical, clinical and experimental study

PROEFSCHRIFT

TER VERKRIJGING VAN DE GRAAD VAN
DOCTOR IN DE GENEESKUNDE
AAN DE ERASMUS UNIVERSITEIT ROTTERDAM
OP GEZAG VAN DE RECTOR MAGNIFICUS
PROF. DR. M.W. VAN HOF
EN VOLGENS BESLUIT VAN HET COLLEGE VAN DEKANEN.
DE OPENBARE VERDEDIGING ZAL PLAATSVINDEN OP
WOENSDAG 1 FEBRUARI 1984 DES NAMIDDAGS
TE 3.30 UUR

DOOR

JOHANNES HUBERTUS MARCELLIANUS VAN EIJNDHOVEN
geboren te Haarlem

1984

grafische verzorging:

ROEIJDAVIDS
ALBLASSERDAM

PROMOTOREN : PROF. DR. G. VAN DEN BRINK
PROF. DR. M. DE VLIENER

CO-REFERENTEN : PROF. DR. IR. H.G. STASSEN
PROF. DR. K.G. GO

In memory of my father
Cees J.J. Avezaat

CONTENTS

	PREFACE	15
CHAPTER 1	GENERAL INTRODUCTION	21
	<i>Aims</i>	25
CHAPTER 2	CRANIOSPINAL VOLUME-PRESSURE RELATIONSHIPS ...	27
	JOHN H.M. VAN EIJDHOVEN AND CEES J.J. AVEZAAT	
	2.1 The craniospinal system	29
	2.2 Historical survey	30
	2.3 Volume-pressure models	34
	<i>Linear models</i>	34
	<i>Non-linear models</i>	36
	<i>Distribution of compliance between cranial and spinal compartments</i>	39
	2.4 Analytical system description	41
	2.5 Clinical significance	45
	2.6 Discussion	47
	<i>Static and dynamic volume-pressure curves</i>	47
	<i>Mechanical basis of the volume-pressure curve</i>	50
	<i>Assessment of craniospinal volume-pressure relationships by means of the volume-pressure test</i>	53
	<i>Conclusions</i>	55
CHAPTER 3	CEREBROSPINAL FLUID PULSE PRESSURE	57
	CEES J.J. AVEZAAT AND JOHN H.M. VAN EIJDHOVEN	
	3.1 Historical survey	59
	3.2 CSF pulse pressure as a volume-pressure parameter	60
	<i>Introduction</i>	60
	<i>Analytical method</i>	61
	3.3 Pulsatile change in cerebral blood volume	62
	<i>Origin of the pulsatile change in cerebral blood volume</i>	62
	<i>Factors affecting the pulsatile change in cerebral blood volume</i>	64
	3.4 Discussion	66
	<i>Conclusions</i>	68

CHAPTER 4	CLINICAL OBSERVATIONS ON THE RELATIONSHIP BETWEEN CEREBROSPINAL FLUID PULSE PRESSURE AND INTRACRANIAL PRESSURE	71
	CEES J.J. AVEZAAT AND JOHN H.M. VAN EIJNDHOVEN	
4.1	Introduction	73
4.2	Material and methods	73
	<i>Material</i>	73
	<i>Relationship between CSF pulse pressure and ICP</i>	74
	<i>Volume-pressure relationship</i>	78
4.3	Results	79
	<i>Volume-pressure relationship</i>	79
	<i>Relationship between CSF pulse pressure and ventricular fluid pressure</i>	81
	<i>Observations during plateau waves</i>	87
4.4	Discussion	91
	<i>Volume-pressure relationship</i>	91
	<i>CSF pulse pressure</i>	93
	<i>The conflict between CSF pulse pressure and volume-pressure response during plateau waves</i>	95
	<i>Clinical implications</i>	96
	<i>Conclusions</i>	98

CHAPTER 5	CEREBROSPINAL FLUID PULSE PRESSURE AND CRANIOSPINAL VOLUME-PRESSURE RELATIONSHIPS DURING EXPERIMENTAL BRAIN COMPRESSION	101
	CEES J.J. AVEZAAT AND JOHN H.M. VAN EIJNDHOVEN	
5.1	Introduction	103
5.2	Experimental methods	104
	<i>Preparation and Measurements</i>	104
	<i>Experimental protocol and Data collection</i>	105
5.3	Results	107
	<i>Relationship between volume-pressure response and ventricular fluid pressure</i>	107
	<i>Relationship between CSF pulse pressure and ventricular fluid pressure</i>	113
5.4	Discussion	117
	<i>Volume-pressure relationship</i>	117
	<i>CSF pulse pressure</i>	122
	<i>The constant term P_0</i>	127
	<i>Clinical implications</i>	128
	<i>Conclusions</i>	129

CHAPTER 6	EFFECTS OF HYPERCAPNIA AND ARTERIAL HYPOTENSION AND HYPERTENSION ON CEREBROSPINAL FLUID PULSE PRESSURE AND INTRACRANIAL VOLUME-PRESSURE RELATIONSHIPS DURING CEREBRAL COMPRESSION IN DOGS	131
	CEES J.J. AVEZAAT AND JOHN H.M. VAN EIJNDHOVEN	

6.1	Introduction	133
6.2	Experimental methods	134
	<i>Protocol hypercapnia</i>	135
	<i>Protocol arterial hypotension and hypertension</i>	136
6.3	Results	136
	<i>Effects of hypercapnia</i>	136
	<i>Effects of changes in systemic arterial pressure</i>	143
6.4	Discussion	151
	<i>Volume-pressure relationship and CSF pulse pressure</i>	151
	<i>Effects of hypercapnia</i>	153
	<i>Effects of changes in systemic arterial pressure</i>	156
	<i>Conclusions</i>	159

CHAPTER 7	THE PULSATILE CHANGE IN CEREBRAL BLOOD VOLUME IN DOGS ASSESSED BY ELECTROMAGNETIC FLOWMETRY UNDER VARIOUS EXPERIMENTAL CONDITIONS	161
	JOHN H.M. VAN EIJNDHOVEN AND CEES J.J. AVEZAAT	

7.1	Introduction	163
7.2	Experimental methods	164
	<i>Preparation and Measurements</i>	164
	<i>Experimental protocol</i>	166
	<i>Computation of the pulsatile change in cerebral blood volume</i>	167
7.3	Results	169
	<i>Effects of changes in arterial carbon dioxide tension</i>	169
	<i>Effects of changes in systemic arterial pressure</i>	175
	<i>Effects of raised ICP</i>	179
7.4	Discussion	185
	<i>Normal vertebral artery blood flow</i>	186
	<i>The pulsatile change in cerebral blood volume under basal conditions</i>	187
	<i>Effects of changes in systemic arterial pressure</i>	188
	<i>Effects of changes in arterial carbon dioxide tension</i>	189
	<i>Effects of raised ICP</i>	194
	<i>Conclusions</i>	197

CHAPTER 8	GENERAL DISCUSSION OF THE CRANIOSPINAL VOLUME-PRESSURE RELATIONSHIPS AND THE ROLE OF THE CEREBROSPINAL FLUID PULSE PRESSURE IN THEIR ASSESSMENT	199
8.1	Introduction	201
8.2	Craniospinal volume-pressure relationships	201
	<i>Volume compensation versus volume buffering</i>	201
	<i>Clinical significance</i>	204
	<i>The exact shape of the volume-pressure curve</i>	207
8.3	CSF pulse pressure	210
	<i>CSF pulse pressure as a volume-pressure parameter</i>	210
	<i>CSF pulse pressure and cerebral vasomotor tone</i>	213
CHAPTER 9	DYNAMICS OF THE CEREBROSPINAL FLUID CIRCULATORY SYSTEM	217
	A mathematical description JOHN H.M. VAN EIJNDHOVEN AND CEES J.J. AVEZAAT	
9.1	Introduction	219
9.2	CSF formation and absorption	220
9.3	Mathematical CSF circulation model	223
9.3.1	<i>Steady state conditions</i>	224
	<i>Pressure-independent CSF formation</i>	225
	<i>Pressure-dependent CSF formation</i>	228
	<i>Conclusions</i>	229
9.3.2	<i>Dynamic behaviour of the CSF circulation</i>	229
	<i>Infusion test</i>	232
	<i>Volume-pressure test</i>	233
9.4	Discussion	234
	<i>Conclusions</i>	238
CHAPTER 10	EVALUATION OF THE CEREBROSPINAL FLUID CIRCULATION MODEL	239
	An experimental study in dogs JOHN H.M. VAN EIJNDHOVEN AND CEES J.J. AVEZAAT	
10.1	Introduction	241
10.2	Experimental methods	242
	<i>Preparation and Measurements</i>	242
	<i>Experimental protocol and Data collection</i>	243
10.3	Results	245
	<i>Infusion test</i>	245
	<i>Volume-pressure test</i>	249
	<i>Comparison between infusion test and volume-pressure test</i>	254
10.4	Discussion	257
	<i>CSF formation</i>	258
	<i>CSF absorption</i>	259
	<i>Storage capacities of the craniospinal system</i>	261

<i>Comparison with the Marmarou model</i>	262
<i>Clinical significance</i>	264
<i>Conclusions</i>	266

CONCLUDING REMARKS AND RECOMMENDATIONS FOR FURTHER RESEARCH	269
--	-----

APPENDIX 1	FREQUENCY ANALYSIS OF THE ICP MEASURING SYSTEM	275
APPENDIX 2	RELATIONSHIP BETWEEN CSF PULSE PRESSURE AND ICP: COMPARISON BETWEEN PLOTTING PULSE PRESSURE AGAINST MEAN ICP AND AGAINST DIASTOLIC ICP	278
APPENDIX 3	RELATIONSHIP BETWEEN VOLUME AND PRESSURE WITHIN A CLOSED SPHERE	280
APPENDIX 4	EFFECT OF SYSTEMIC ARTERIAL PRESSURE ON THE CRANIOSPINAL VOLUME-PRESSURE RELATIONSHIP	282
APPENDIX 5	STRAIN IN THE CEREBRAL ARTERIAL WALL DURING CHANGES IN SYSTEMIC ARTERIAL PRESSURE AND IN ARTERIAL CARBON DIOXIDE TENSION	285
APPENDIX 6	SOLUTION OF THE NON-LINEAR DIFFERENTIAL EQUATION DESCRIBING THE DYNAMIC BEHAVIOUR OF THE CEREBROSPINAL FLUID SYSTEM	287
APPENDIX 7	COMPUTATION OF THE MODEL PARAMETERS P_0 AND E_1 FROM THE CONSTANT RATE INFUSION TEST	290
APPENDIX 8	COMPUTATION OF THE MODEL PARAMETERS P_0, E_1 AND C_1 FROM THE VOLUME-PRESSURE TEST	292
	SUMMARY	295
	SAMENVATTING	303
	REFERENCES	311
	SYMBOLS AND ABBREVIATIONS	334
	ACKNOWLEDGEMENTS	336
	CURRICULA VITAE	338



PREFACE

"If the difficulty of a physiological problem is mathematical in essence, ten physiologists ignorant of mathematics will get precisely as far as one physiologist ignorant of mathematics and no further. If a physiologist who knows no mathematics works together with a mathematician who knows no physiology, the one will be unable to state his problem in terms that the other can manipulate, and the second will be unable to put the answers in any form that the first can understand."

N. Wiener (1948).

The theoretical, clinical and experimental studies brought together in this work are the fruits of the close collaboration between the authors over many years. This cooperation started in 1975 with the preparation for our contribution to the Third International Symposium on Intracranial Pressure in Groningen (1976). In this paper, a method for assessment of craniospinal elastance using the cerebrospinal fluid pulse pressure was described for the first time. We spent four months at the Institute of Neurological Sciences in Glasgow in 1977 where we carried out part of the animal experimental work. In the following years the volume-pressure studies in clinical patients were continued and the method for computer analysis of the intracranial pressure recordings was further developed. Additional animal experiments were performed in our own laboratory for experimental neurosurgery. Throughout this period we regularly discussed together the results of our studies and the theoretical concepts involved.

One of the authors is a clinically engaged neurosurgeon, whereas the other is an engineer and thus represents the natural sciences. The reasons for a cooperation of this kind are obvious. The time when an individual investigator could explore wide fields of scientific interest on his own has gone for good. The attainments of contemporary research are the result of scientists from various disciplines thinking together and working together.

This is particularly true of the subject of the present investigation, which deals with such a complicated structure as the craniospinal system. The dynamics of this system, such as the relationship between volume and pressure, the circulation of cerebrospinal fluid and the cerebral blood flow, can only be understood through a knowledge of the physical and system theoretical principles by which they are controlled. Many pathological states which are of interest to the neurosurgeon are directly associated with the geometry of the system concerned and with the physical properties of both its confining structures and its contents.

Furthermore, both animal experimental and clinical research often requires a sophisticated methodology for which the contribution of natural scientists is indispensable.

Biological systems, however, can never be satisfactorily described by the laws of inanimate matter. The contributions of natural scientists therefore have to be appreciated in the light of anatomical and physiological knowledge. The clinician finally tries to understand pathological processes and to interpret theoretical and empirical findings in practical terms of patient management.

Most of our studies have appeared in a number of publications, a list of which is given at the end of this preface. However, since we were about to enter upon the final phase of the investigations on the present subject, we decided to give an overview of the entire work in the form of a thesis. As we consider our work to be the result of joint efforts, we were very much in favour of the idea of a joint thesis. In the preparatory discussions with parties involved, however, this idea met with some opposition. It appeared that a thesis is still regarded by some people as a highly individual piece of work. The main concern seems to be that, in a metaphorical sense, one author might hide behind the other.

The ultimate consequence of this view would have been the presentation of our studies in two separate contributions. However, our views and ideas on the problems presented here have intermingled throughout the years to such an extent that it is no longer possible to separate out our individual contributions retrospectively. Even if this were at all feasible, such a presentation would show a considerable overlap.

There was also a more positive reason for our decision to present a joint thesis and this was connected with the approach which we chose. A mainly clinically oriented presentation would appeal to a reading public with a clinical background only, whereas a more basic approach would likewise limit the sphere of influence of our work. We should like, on the contrary, to encourage readers from various disciplines to explore beyond their own territory and to try to understand each other's languages. Because of this approach we had to exercise restraint in the elaboration of some ideas, but this was always done in the conviction that it would benefit the study as a whole.

We therefore accept joint responsibility for the complete contents of this thesis. Nevertheless, because this has been especially requested, we have shown in the Table of Contents which of us has been mainly responsible for each chapter; this is indicated by the order of our names.

While this research project was in progress, the following publications appeared:

AVEZAAT CJJ; EIJNDHOVEN JHM VAN; JONG DA DE; MOOLENAAR WCJ: A new method of monitoring intracranial volume-pressure relationships. In: Intracranial Pressure III eds. JWF Beks, DA Bosch, M Brock, Springer-Verlag, Berlin-Heidelberg-New-York, 308-313, 1976.

AVEZAAT CJJ; EIJNDHOVEN JHM VAN; WYPER DJ: Cerebrospinal fluid pulse pressure and intracranial volume-pressure relationships. J. Neurol. Neurosurg. Psychiat., 42, 687-700, 1979.

EIJNDHOVEN JHM VAN; AVEZAAT CJJ; WYPER DJ: The CSF pulse pressure in relation to intracranial elastance and failure of autoregulation. In: Intracranial Pressure IV eds. K Shulman, A Marmarou, JD Miller, DP Becker, GM Hochwald, M Brock, Springer-Verlag, Berlin-Heidelberg-New York, 153-158, 1980.

AVEZAAT CJJ; EIJNDHOVEN JHM VAN; WYPER CJ: Effects of hypercapnia and systemic arterial hypo- and hypertension on the interrelation between CSF pulse pressure and volume-pressure response. In: Intracranial Pressure IV eds. K Shulman, A Marmarou, JD Miller, DP Becker, GM Hochwald, M Brock, Springer-Verlag, Berlin-Heidelberg-New York, 159-162, 1980.

EIJNDHOVEN JHM VAN; AVEZAAT CJJ: The analogy between CSF pulse pressure and volume-pressure response. In: Intracranial Pressure IV eds. K Shulman, A Marmarou, JD Miller, DP Becker, GM Hochwald, M Brock, Springer-Verlag, Berlin-Heidelberg-New York, 173-176, 1980.

AVEZAAT CJJ; EIJNDHOVEN JHM VAN; WYPER DJ: Effects of hypercapnia and arterial hypotension and hypertension on cerebrospinal fluid pulse pressure and intracranial volume-pressure relationships. J. Neurol. Neurosurg. Psychiat., 43, 222-234, 1980.

EIJNDHOVEN JHM VAN; AVEZAAT CJJ: Cerebrospinal fluid pulse pressure as parameter of intracranial elastance. In: Neurobiology of cerebrospinal fluid 2 ed. JH Wood, Plenum, New York, 643-660, 1983.

EIJNDHOVEN JHM VAN; AVEZAAT CJJ: The CSF pulse pressure as parameter of intracranial elastance: The role of the pulsatile change in cerebral blood volume. In: Intracranial Pressure V, in press 1983.

AVEZAAT CJJ; EIJNDHOVEN JHM VAN: The conflict between CSF pulse pressure and volume-pressure response during plateau waves. In: Intracranial Pressure V, in press 1983.

EIJNDHOVEN JHM VAN; AVEZAAT CJJ: New aspects of cerebrospinal fluid circulation models with emphasis on the stability of the model parameters. In: Intracranial Pressure V, in press 1983.

CHAPTER 1

GENERAL INTRODUCTION

"No, we haven't done any ICP measurements in the last six months, not since Dr. Keenboy left to go to St. Elsewhere's Clinic."

B. Jennett (1975)

Since the introduction of continuous recording of intracranial pressure (ICP) in neurosurgical practice (Guillaume and Janny, 1951; Lundberg, 1960) this method has greatly contributed to clinical research in the field of intracranial hypertension. Numerous publications have enriched the literature on ICP and five International Symposia (1972, 1974, 1976, 1979 and 1982) on the subject have been held. The knowledge gained from these investigations has considerably benefited the management of patients suffering from raised ICP. However, in spite of the enthusiasm among those who practise ICP monitoring, the method has not yet gained universal acceptance as a routine procedure with regard to the various aspects of care of the individual patient: diagnosis, surveillance, treatment and prognosis.

The question of the clinical value of ICP monitoring is, of course, closely related to the question as to what extent ICP truly reflects central nervous system function. In our view the answer to this question must be sought somewhere between the two extremes expressed in the statements of Stern (1963) "that ICP should be given a subsidiary role in the assessment of the fluid-mass dynamics in neurological disease" and of Langfitt (1969) "that uncontrolled, increased ICP is one of the most common causes of neurological death". This dilemma is clinically illustrated by the common experience that high levels of ICP may be sustained by normal subjects without evidence of neurological impairment (Evans et al., 1951), whereas patients with large space-occupying lesions may have clinical signs of brainstem distortion without significant elevation of ICP.

Much of this controversy results from the two-fold meaning of increased ICP. On the one hand it may be regarded as a symptom indicating the presence of a space-occupying process, of whatever nature, which can no longer be compensated for. On the other hand intracranial hypertension may be a pathogenetic factor causing brain dysfunction *per se*. The latter aspect in particular is still controversial; for instance, it is not yet

known for certain which level of ICP is so critical that it requires treatment. The interaction between ICP and brain function is apparently so complex that no simple deductions can be made from the level of ICP alone. It is therefore necessary to consider many other aspects of ICP that 'matter' (Jennett, 1976) such as: the cause and rate of development of intracranial hypertension, the presence of pressure waves, brain shift, and of pressure gradients, the cerebral perfusion pressure, and the craniospinal volume-pressure relationships.

In the neurosurgical department of the Academic Hospital of Rotterdam continuous ICP recording has been practised since the late sixties (de Lange et al., 1967 and 1968). However, in the light of the experience thus gained we have not yet been able to take a firm stand with regard to the controversy outlined above. We have, therefore, oriented our research towards those aspects of raised ICP that would help us to interpret pressure recordings in terms of their clinical relevance. In this respect we were particularly interested in the rapid fluctuations in ICP synchronous with the heart beat, which we shall henceforth refer to by the term 'cerebrospinal fluid (CSF) pulse'. When looking at the pulse wave on the oscilloscope its shape appeared to vary considerably. Sometimes it was rounded, at other times sharper and it showed a varying number of superimposed smaller peaks. Also the amplitude of the pulse wave, hereafter termed the 'pulse pressure', varied in magnitude from one patient to the other. Furthermore, it increased concomitantly with the ICP and, when so-called plateau waves (Lundberg, 1960) appeared, the pulse pressure would rise disproportionately. We were challenged by these observations to study these phenomena more closely.

At the same time our attention was drawn to the work of Marmarou (1973), Miller (1973), and Löfgren (1973) who established the modern concept of craniospinal volume-pressure relationships as well as the methods for assessing these relationships in clinical patients. These developments opened up important clinical perspectives by setting the actual level of ICP in a wider context. The value of volume-pressure considerations was demonstrated in various clinical situations (Shulman and Marmarou, 1971; Miller et al., 1973, 1975, 1977 and 1977; Miller and Pickard, 1974; Hase et al., 1978).

Techniques designed for the assessment of the volume-pressure

relationships involve rapid volume loading of the craniospinal system. Volume-pressure parameters are computed from the resulting pressure response. The analogy with the CSF pulse pressure, i.e., the pressure response to the pulsatile volume load of blood to the craniospinal system, became immediately obvious to us. This analogy gave birth to the idea of using the CSF pulse pressure as a volume-pressure parameter. It would thus become possible, by using the ICP signal itself, to assess the craniospinal volume-pressure relationship continuously and non-invasively; this would contribute to the clinical value of ICP monitoring. The pursuit of this idea constitutes the main theme of this thesis.

In the course of these investigations we became more and more aware of the relative importance of the volume-pressure relationship in determining the actual level of ICP as compared with the craniospinal spatial compensatory capacities. Since the main ability for spatial compensation is offered by the volume of CSF, we felt the need to study more closely the parameters governing the dynamics of CSF formation, circulation and absorption. These investigations have therefore been included in this thesis.

Aims

The aims pursued in the investigations contained in this thesis can be summarized as follows:

1. a mathematical description of the relation of volume to pressure within the craniospinal system based on data from the literature (Chapter 2),
2. the verification of the mathematical volume-pressure model in animal experiments (Chapter 5),
3. a mathematical description of the CSF pulse pressure as a volume-pressure parameter (Chapter 3),
4. a preliminary assessment of the CSF pulse pressure as a volume-pressure parameter in a group of clinical patients (Chapter 4),
5. the establishment of the role of the CSF pulse pressure as a volume-pressure parameter under various experimental conditions (Chapters 5, 6, and 7),
6. a mathematical description of CSF dynamics (Chapter 9),

7. the evaluation of various methods for assessing the parameters of the CSF circulation model in animal experiments (Chapter 10).

The first part of the thesis deals with the CSF pulse pressure as a measure of craniospinal volume-pressure relationships (Chapters 2-7). It concludes with a general discussion (Chapter 8) which also introduces the second part of the thesis on CSF circulation (Chapters 9 and 10).

CHAPTER 2

CRANIOSPINAL VOLUME-PRESSURE RELATIONSHIPS

"The cranial contents cannot any longer be regarded as a fixed quantity without the power of expanding or contracting in volume."

W.E. Dixon and W.D. Halliburton (1914)

2.1 The craniospinal system

The craniospinal system within the rigid skull and vertebral column comprises a multi-compartmental space which consists of brain and spinal cord (which are largely water), CSF and blood. Neural tissue accounts for about 70% of the total volume; the remaining 30% is made up of CSF, blood and extracellular fluid in about equal portions of 10% each.

The craniospinal constituents are contained within the dura mater which is a firm membrane consisting of fibrous tissue. In the cranial vault the dura is immediately adjacent to the inner table of the skull, but in the spinal canal the dura is separated from the vertebral lining of the canal by fatty tissue and a venous vascular plexus. The craniospinal contents can thus expand at the expense of epidural venous blood which is easily expelled from the spinal canal. We shall therefore use the term 'craniospinal system' to mean all that is contained within the dural envelope. Under normal circumstances there is free communication of CSF between the cranial and spinal compartments at the foramen magnum, which is why both are regarded as belonging to one system. It should be noted that the skull is not completely closed as it is perforated at its base by numerous smaller openings.

The CSF and blood contents are parts of circulatory systems. The CSF is mainly formed within the cerebral ventricles. Its flow is caudally directed towards the openings in the fourth ventricle where it reaches the subarachnoid space. It bathes brain and spinal cord and is finally absorbed in the venous system at the sagittal sinus. Normally, the processes of CSF production and absorption are in equilibrium. The craniospinal blood volume is part of the cerebral and spinal cord blood flow regulation. The system is, within limits, able to maintain a constant flow, in spite of changes in perfusion pressure, by controlling the diameter of part of its vascular bed. This phenomenon is called autoregulation.

ICP is a function of all the above mentioned factors. Except for the vascular bed which has its own pressures, the ICP is the same in every compartment as long as the CSF is able to circulate freely.

2.2 Historical survey

Any discussion of the craniospinal volume-pressure relationships must necessarily start from the doctrine named after Monro (1783) and Kellie (1824), which has dominated thought for such a long time on the mechanisms involved in the genesis of intracranial hypertension. The historical development of the Monro-Kellie doctrine has been described by various authors (Weed, 1929; Masserman, 1934; Evans, 1956; Stern, 1963; Langfitt, 1969). The original hypothesis propounded a rigid and inextensible cranial cavity, filled to capacity with incompressible brain tissue and blood, from which it was concluded that the volume of the latter must at all times be constant. The doctrine took into account neither the CSF, although Alexander Monro's father had described the interventricular foramen, nor the spinal portion of the craniospinal compartment.

Burrows (1846) modified the hypothesis in this respect by postulating that the volume of blood could vary reciprocally with the volume of CSF. The experiments of Weed and McKibben (1919) showed that by intravenous injections of hypo- and hypertonic solutions the volume of brain bulk could also be markedly altered. The negative ICP which developed after the administration of strongly hypertonic solutions was held as proof of the Monro-Kellie postulate of the rigid container with a constant total volume. Negative pressures were not obtained when the cranial contents were exposed to the atmospheric pressure by removing part of the cranial vault (Weed and Hughson, 1921). The modified hypothesis, allowing for reciprocal changes in the volumes of all the craniospinal constituents, was introduced into neurosurgery by Cushing (1925).

However, this rather mechanistic hypothesis, if 'rigidly' applied, fails to explain many significant aspects of intracranial dynamics. When, in the experimental animal, an intracranial balloon is slowly expanded (Fig. 1), the ICP will not significantly rise at first. This is because in accordance with the Monro-Kellie doctrine the additional volume of the balloon is accommodated by a reduction in volume of one of the intracranial

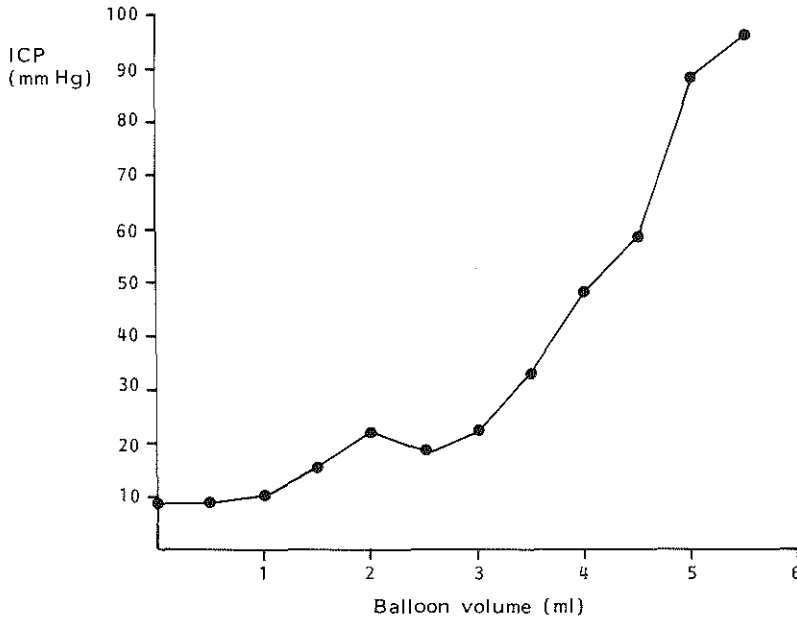


Fig. 1. Intracranial pressure (ICP) plotted against volume of intracranial extradural balloon, expanded at constant rate of 1 ml/40 min, in an experimental animal (dog).

contents, probably the CSF. Finally, when this process of spatial compensation, as it is called, is exhausted, ICP increases rapidly. Strictly speaking, the extra balloon volume which is in excess of the compensated volume can only be accommodated if the cranial contents are compressible or if the craniospinal coverings are distensible.

When a normal subject, with a needle in the lumbar subarachnoid space, is tilted from the recumbent into the sitting position, the lumbar CSF pressure rises. If the system fulfilled the Monro-Kellie requirements, the pressure would not rise at all, as the fluid in the needle but not the fluid in the head is exposed to atmospheric pressure (Langfitt, 1969). On the other hand, if the system were completely open, the pressure rise would be equal to the height of the hydrostatic column in the vertical position. The actual increase in pressure, however, is less, as had already been noted by Barré and Schrapf (1921) and Zylberlast-Zand (1921) and thus the system represents a state of affairs intermediate between the completely closed and the completely open system.

Dixon and Halliburton (1914) were the first to question the constancy of the total craniospinal volume, although this did not seem fully justified by their experimental evidence. Ayala (1923 and 1925) studied

the fall in pressure when a given quantity of spinal fluid was removed from clinical patients. Among the factors which he mentioned as determining the degree of decline in pressure was not only the volume of CSF removed, but also the elasticity of the meninges. The quotient 'fall in pressure divided by volume of fluid removed' went down in history as Ayala's index and is related to the modern term 'elastance'. The index was found to be low in benign intracranial hypertension and high in cerebral tumours.

The first systematic investigations into the relationship between changes in total intradural volume and changes in ICP was conducted by Weed and his associates (Weed, 1929; Flexner et al., 1932; Weed and Flexner, 1932; Weed et al., 1932; Flexner and Weed, 1933; Weed and Flexner, 1933). When dogs were tilted from the horizontal position to the vertical head-down and tail-down positions, pressure changes were observed in the cisterna magna, but their magnitude was less than would have been expected from the change in the height of the hydrostatic column. The spinal tube was, consequently, regarded as an only partially rigid container and the resistance exerted against the hydrostatic column was ascribed to an elastic force. The dislocation of fluid into the manometer in the head-down position was explained by an inward collapse of the spinal dura, and vice versa for the tail-down position. Consequently, the volume of the craniospinal compartment was restricted to that of the intradural space and was no longer considered constant. The system was compared with an elastic container in which changes in pressure were, within the limits of its elasticity, directly proportional to changes in volume. By using so-called bubble-manometers instead of open-end manometers the escape of fluid from the system is prevented and pressure readings are thus more accurate. By relating the difference in pressure as measured by both methods to the volume of fluid passing into or out of the open-end manometer, Weed et al. computed a coefficient of elasticity, which was found to be constant under various experimental conditions. Weed and his collaborators conceived the elastic properties of the craniospinal system as a complex function determined by many factors, among which were not only the collapsibility and distensibility of the dural sac but also intradural and extradural vascular factors.

Forty years later the variable capacity of the spinal dural sac and its role in CSF dynamics were demonstrated by Martins et al. (1972) in

myelographic studies in patients. The work of Ayala and Weed was critically reviewed by Masserman who studied the pressure changes after withdrawal of CSF in patients (1934 and 1935).

Ryder et al. (1953) gave the impulse to modern concepts on the relationship between craniospinal volume and pressure by describing this property as a non-linear function. These concepts were further developed in the early seventies by three groups of investigators: those of Marmarou, Miller and Löfgren.

After having shown the importance of volume-pressure considerations in infantile hydrocephalus (Shulman and Marmarou, 1971), a detailed mathematical description of the volume-pressure function was given by Marmarou (1973, 1975 and 1978). In his conception, its physiological basis is provided by the collapsibility of the cerebral venous vasculature rather than by the elasticity of the dural sac.

Miller (Miller and Garibi, 1972; Miller et al., 1973; Miller and Pickard, 1974; Leech and Miller, 1974; Miller and Leech, 1975) has emphasized the clinical application of volume-pressure parameters. The volume-pressure relationships were tested under various experimental and clinical conditions and the influence of physiological variables and therapeutic agents on the relationships were studied.

Löfgren (Löfgren et al., 1973; Löfgren and Zwetnow, 1973; Löfgren, 1973; Löfgren and Zwetnow, 1973; Löfgren, 1973; Löfgren, 1975) systematically examined the exact shape of the volume-pressure curve over the whole range of ICP, including the negative range, in experimental animals. The curve was shown to be the sum of two separate curves representing the cranial and spinal portions of the system. The mechanical basis of the curve was attributed equally to the spinal dural sac and to the cerebral venous vascular bed.

Since that time the non-linear nature of the relation of volume to pressure within the craniospinal axis has been confirmed by numerous workers (Guinane, 1972, 1974 and 1975; Lim et al., 1973; Cohadon et al., 1975; Nakatani and Ommaya, 1975; Furese et al., 1976; Sklar and Elashvili, 1977; Sullivan et al., 1977) and its role in the dynamics of ICP has been generally recognized.

2.3 Volume-pressure models

After the introduction into the rigid Monro-Kellie doctrine of the concept of elasticity, implying a variable total craniospinal volume, the modified hypothesis postulates:

$$V_{\text{tissue}} + V_{\text{blood}} + V_{\text{csf}} = V_{\text{total}} = V_{\text{eq}} + V_{\text{e}},$$

where: V_{eq} = equilibrium volume of the craniospinal system, where the ICP is within the normal range, and

V_{e} = 'elastic' volume, the change in volume with respect to the equilibrium volume.

Within V_{eq} the craniospinal contents, including space-occupying lesions, can alter their volumes by reciprocal changes without affecting V_{e} . In that case the total volume remains constant as does the ICP. However, each volume increment which cannot be accommodated by reciprocal volume changes has to encroach on V_{e} , thereby causing a change in the total craniospinal volume and a corresponding change in pressure.

Linear models

Several investigators have tried to establish the elastic properties of the system. Ayala (1923 and 1925) found that the quotient of pressure changes (ΔP) occurring with volume changes (ΔV), which he considered to be a measure of meningeal elasticity, varied only within very narrow limits in the same individual:

$$\frac{\Delta P}{\Delta V} = \text{constant.}$$

Weed, Flexner and Clark (Flexner et al., 1932; Weed et al., 1932; Weed and Flexner, 1932) tried to quantify the elastic properties of the craniospinal system by comparing it with an elastic container. By analogy with Young's modulus of elasticity (E_o):

$$E_o = \frac{\text{stress}}{\text{strain}}, \quad (\text{Hooke's law})$$

they introduced a coefficient of volume elasticity (E_v) substituting

ΔP for stress and $\Delta V/V$ for strain, where V represents the total volume of the dural contents:

$$E_v = \frac{\Delta P}{\Delta V} V.$$

The fraction $\Delta P/\Delta V$ was derived from experiments dealing with the abrupt tilting of animals from the horizontal to the vertical head-down and tail-down positions. The ICP was determined in the cisterna magna by successive use of the bubble-manometer (permitting measurement without dislocation of fluid) and of open-end manometers of various bores. ΔP was given by the difference of the pressure change on tilting between that recorded by the bubble-manometer and those of any of the open-end manometers, while ΔV was given by the amount of fluid displaced into or from any of the open-end manometers. It was found that as the bore of the manometer was increased the pressure changes on tilting became less, though the volume of fluid displaced became greater. Hence, the values of both ΔP and ΔV increased, but the ratio $\Delta P/\Delta V$ remained fairly constant in any one animal of the same size and age. The total intradural volume was determined after the animals had been killed. Substitution in the above equation yielded the coefficient of volume elasticity.

Weed et al. were wrong in simply applying Hooke's law to the craniospinal system, as this system corresponds to an elastic tube or sphere filled with an incompressible fluid rather than to a uniform elastic body (Davson, 1967). The reciprocal of the last equation, i.e., $\frac{\Delta V}{\Delta P} \cdot \frac{1}{V}$, gives what is known as the volume distensibility, which is not constant, but increases as the elastic material is stretched (King and Lawton, 1950; Burton, 1954). The experiments of Weed et al., however, were conducted around the physiological steady state volume and pressure and, presumably, the system may not have been sufficiently disturbed to reveal significant changes in the ratio $\Delta P/\Delta V$.

A constant fraction $\Delta P/\Delta V$ at different levels of ICP implies a linear relationship between elastic volume and pressure (P) in the craniospinal compartment:

$$P = EV_e + P_{eq},$$

where E is the gradient of the relationship ($= dP/dV_e$), generally termed the elastance, and P_{eq} is the normal ICP under equilibrium conditions corresponding with the equilibrium volume. The elastance may thus be considered as a measure of the stiffness or rigidity of the system. The term 'compliance' is also often used to express the inverse of elastance

(dV_e/dP) ; it is the compliance, consequently, which determines the give or the distensibility of the system.

Non-linear models

Ryder and co-workers (1953 and 1953) were the first to demonstrate that volume and pressure in the craniospinal compartment are not linearly related, describing this relationship by a hyperbolic function, which implies an increase in elastance as pressure increases. This became the starting-point for further research into the exact nature of the craniospinal volume-pressure relationships. Marmarou and his associates employed the technique of bolus injection into the CSF space. Pre-requisites for this method are that no spatial compensation should take place during the procedure, and that the injection should provoke no secondary responses which could alter the volumes of the other craniospinal contents. Two guidelines were therefore formulated by Marmarou et al. (1975):

1. The rate of volume addition must be considerably higher than the rate of CSF absorption.
2. The magnitude of volume addition and the rate of injection must be below that level which causes vasodilatation and alteration of the original resting pressure.

For this reason volume insertion by constant infusion was rejected. Moreover the method of stepwise addition, without waiting after each injection for the pressure to return to the resting level, as originally employed in the assessment of the volume-pressure relationships in hydrocephalic children (Shulman and Marmarou, 1971), was later abandoned. The pressure-volume curve was established by rapid serial injections of increasing amounts of volume into the CSF space of the cat (Marmarou, 1973; Marmarou et al., 1975). The plot of volume increments against pressure showed an exponential shape: the slope $\Delta V/\Delta P$, or compliance, decreased as pressure increased (Fig. 2). When the curve was plotted on a logarithmic pressure axis a straight line was obtained. The slope of this line was defined as the pressure-volume index (PVI), the numerical value of which, expressed in units of volume (ml), was defined as that amount of volume necessary to raise the resting pressure by a factor of 10. The PVI, unlike the elastance or compliance, characterizes the volume-pressure relationship for the whole range of ICP, as it is a

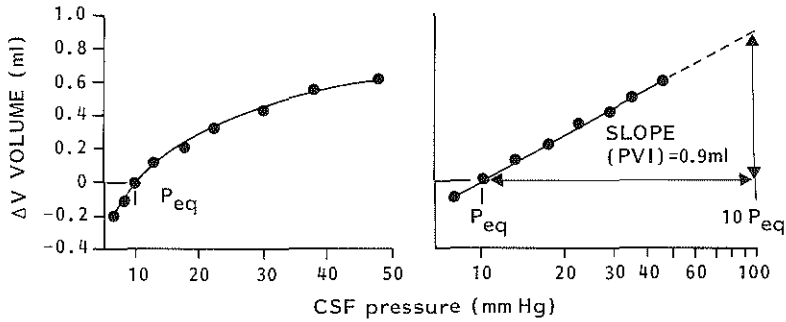


Fig. 2. CSF pressure-volume curve obtained in the cat by injecting volume increments of 0.1 to 0.6 ml into the cisterna magna and recording the pressure response. (Reproduced from Marmarou A; Shulman K; LaMorgese J: Compartmental analysis of compliance and outflow resistance of the cerebrospinal fluid system. *J. Neurosurg.*, 43, 523-534, 1975). The curve plotted on a linear axis (left) was found to be exponential. The same data plotted on a semilogarithmic axis can be approximated by a straight line (right). The slope of this line is equal to the pressure-volume index (PVI), and can be defined as the amount of volume necessary to raise equilibrium pressure (P_{eq}) by a factor of 10.

pressure independent term. The PVI can also be determined from a single volume injection since, as the volume versus log pressure plot is a straight line and the initial base-line pressure is given, only one additional point is required to establish the slope. When a volume ΔV_i is injected raising the base-line pressure (P_b) to a peak pressure (P_p), the PVI can be computed according to:

$$PVI = \frac{\Delta V_i}{P} = \frac{\Delta V_i}{0.4343 \ln \frac{P}{P_b}}$$

Miller et al. (Miller and Garibi, 1972; Miller et al., 1973) also used bolus injection to assess the volume-pressure relationship, but they did not develop a particular mathematical concept. Their work was especially oriented towards the clinical application of information obtained from measurement of craniospinal elastance. For this purpose the volume-pressure test was introduced, involving the rapid injection, within one second, of a uniform amount of fluid into the lateral ventricle through the ventricular catheter used for the recording of ICP. In patients the amount of volume injected was 1 ml. The instantaneous rise in ICP resulting from this injection was termed the volume-pressure response (VPR). The VPR, expressed in mm Hg/ml, is thus a direct measure of the elastance. In a group of patients a positive linear relationship between VPR and ICP was observed. This was accepted as proof of the exponential

nature of the volume-pressure relationships, although, strictly speaking, this cannot be inferred from group data. As a volume-pressure parameter the VPR is less complete than the PVI. Since it is pressure dependent, it must always be evaluated in the context of the level of ICP at which it was established.

By means of continuous infusion of saline into the cisterna magna, Löfgren et al. (1973) systematically studied the craniospinal volume-pressure curve in dogs for an extended range of ICP from a pressure of -10 mm Hg to a level exceeding the blood pressure. A very restricted range of rates of volume forcing proved to be suitable, since too rapid infusion resulted in pressure gradients within the CSF space, whereas too slow infusion produced considerable volume distortion caused by CSF absorption. The highest infusion rate which did not cause pressure gradients was finally chosen: 0.25 ml/sec. The curve thus obtained and corrected for CSF absorption shows a complex shape with two plateaus of relatively low elastance (Fig. 3). These segments of the curve were

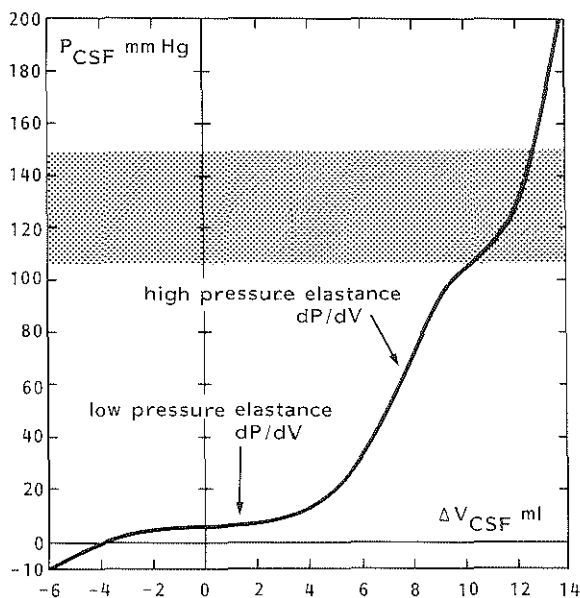


Fig. 3. CSF pressure-volume curve obtained in the dog with rapid infusion of fluid (0.25 ml/sec) into the cisterna magna. (Reproduced from Löfgren J; Essen C von; Zvetnow NN: The pressure-volume curve of the cerebrospinal fluid space in dogs. *Acta Neurol. Scand.*, 49, 557-574, 1973). Systolic and diastolic blood pressures are indicated by shaded area. In clinical ICP range the curve can be characterized by two straight-line segments: low pressure and high pressure elastance respectively.

thought to be related to interactions between the CSF system and the venous and arterial systems respectively, as they occur at corresponding pressure levels. The decrease in elastance close to the diastolic blood pressure was attributed to displacement of blood from the cerebral vascular bed, when cerebral blood flow (CBF) ceases. In the pressure range usually encountered in the clinical situation, the volume-pressure curve can be characterized by two approximately linear segments with a constant elastance: the low pressure elastance at normal ICP and the high pressure elastance, which is about 20 times larger, at elevated ICP. The exponential transition zone around an ICP of 15 mm Hg has a relatively small volume range. The results of Löfgren's work, therefore, seem to indicate that the generally held concept of an exponential volume-pressure curve is only valid for a restricted range of ICP.

Distribution of compliance between cranial and spinal compartments

Several investigators have examined the relative contributions of the cranial and spinal compartments to the compliance of the total system. Gilland (1965) was the first to determine the isolated spinal volume-pressure curve in patients with a spinal block and found it to be of exponential shape. Löfgren and Zwetnow (1973) recorded the isolated intracranial volume-pressure curve in dogs after the exclusion of the spinal compartment by a cervical block at C 1. The spinal curve was obtained by subtracting the intracranial curve from the curve of the whole system. It was demonstrated that at low and normal pressures most of the volume changes take place in the spinal section, whereas at higher pressures, above 20 mm Hg, there is an approximately equal partitioning of the added volume between both compartments (Fig. 4). Lim et al. (1973) compared the compliance of dogs with and without a stereotaxically produced aqueductal block. The compliance, calculated from bolus injections into the lateral ventricle, was reduced by 48% in the dogs with the aqueductal block. However, because of the large variation between the animals, these group results cannot be directly applied to the distribution of compliance in individual animals.

In contradiction with the above results, Marmarou et al. (1975) found a two to one distribution of compliance between cranial and spinal compartments in cats with a cervical block at C 6. The compliances of

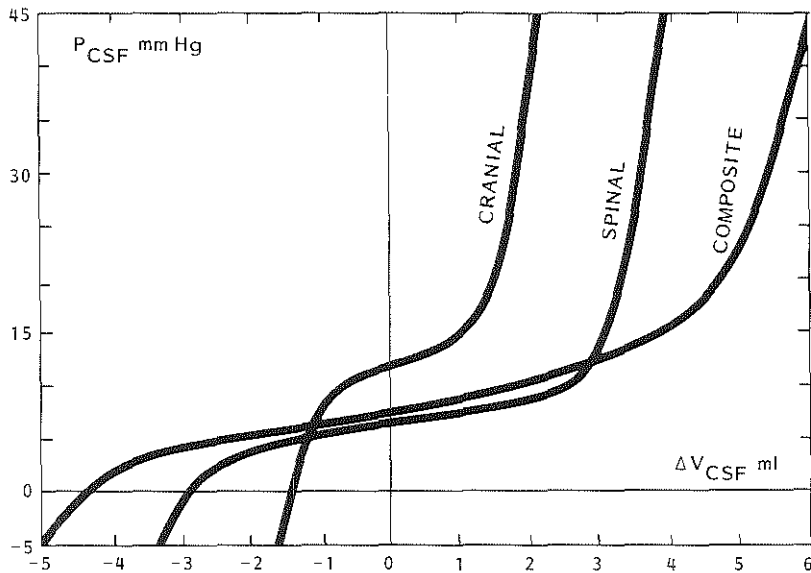


Fig. 4. Interrelations between cranial and spinal components and composite pressure-volume curve in the dog showing greater contribution of spinal compartment to cranio-spinal compliance in low pressure range. (Reproduced from Löfgren J; Zwetnow NN: Cranial and spinal components of the cerebrospinal fluid pressure-volume curve. *Acta Neurol. Scand.*, 49, 575-585, 1973).

both compartments were separately, experimentally determined and their sum was not significantly different from the total compliance measured prior to block.

These contradictory results may be explained by several factors:

1. Rate of volume addition. With the continuous infusion technique used by Löfgren and Zwetnow volume was more rapidly added than with the manual injection method of Marmarou et al.: 0.25 ml/sec versus 0.1 ml/sec. If spatial compensation were to take place during volume loading, for example by means of compression of the venous vascular bed in the cranial compartment, this would particularly affect the slower rate of volume loading. This may explain the larger compliance of the cranial compartment found by Marmarou et al.

2. Type and level of CSF block. The blocks isolating both compartments were all at different levels (aqueduct, C 1, and C 6), so that the relative volumes of the compartments were also different. Furthermore, the spinal blocks produced a complete separation between cranial and spinal compartment, whereas the aqueductal block caused only a partial

obstruction of CSF flow between both compartments. When, in the latter case, the ventricle is loaded with a volume, expansion of the cerebral mantle may still cause CSF in the cranial subarachnoid space to run into the spinal compartment.

3. Difference in animal species. Since craniospinal compliance is proportional to total neural axis volume, the distribution between cranial and spinal compliance will depend on the relative volumes of the respective compartments, which may vary according to the animal species.

2.4 Analytical system description

In accordance with the generally accepted concept of a non-linear volume-pressure relationship, as discussed in the previous section, we have described the craniospinal volume-pressure curve by an exponential function, which we have extended with a constant term (Fig. 5):

$$P = P_1 e^{E_1 V_e} + P_0, \quad (2.1)$$

where: P = ICP,

P_1, P_0 = constant pressure terms,

E_1 = elastance coefficient,

V_e = elastic volume, change in total craniospinal volume (V_{total}) with respect to equilibrium volume (V_{eq}).

When V_e equals zero ($V_{total} = V_{eq}$), the ICP is at its equilibrium pressure (P_{eq}): $P_{eq} = P_1 + P_0$.

The elastance (inverse compliance) E , defined as the slope (dP/dV_e) at any one point of the volume-pressure curve, can be directly derived from Equation 2.1:

$$E = dP/dV_e = E_1 (P - P_0). \quad (2.2)$$

Since E_1 determines the elastance at a given pressure, it was termed the elastance coefficient. The elastance increases as ICP increases, whereas the elastance coefficient, just like the PVI of Marmarou, is a pressure independent term, which remains constant so long as the volume-pressure curve does not alter its shape.

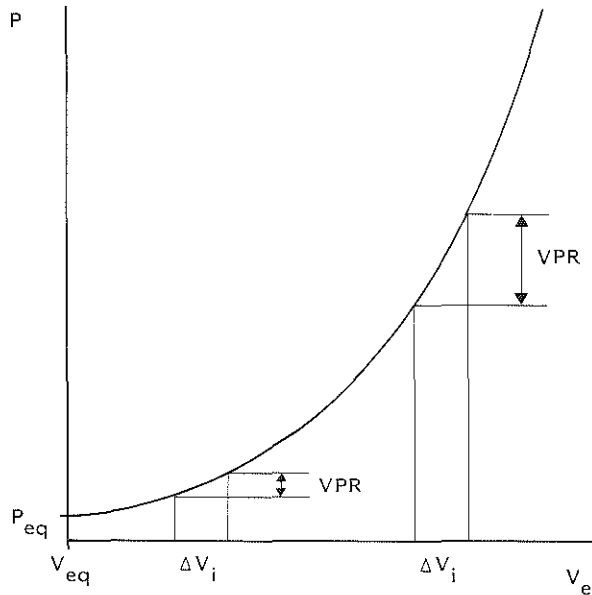


Fig. 5. Exponential craniospinal volume-pressure curve. Volume axis has its origin at normal equilibrium volume (V_{eq}) of craniospinal system, so that $V_{total} - V_{eq}$ represents increase in total craniospinal volume, in system description referred to as elastic volume (V_e). The curve intercepts pressure axis at normal equilibrium ICP (P_{eq}). Slope ($\Delta P/\Delta V_e$) at any point of curve is termed elastance (inverse compliance), of which volume-pressure response (VPR) per unit of volume increment (ΔV_i) is a measure.

The term P_o was primarily introduced for mathematical reasons without a physiological concept. Changes in P_o will cause the volume-pressure curve as a whole to shift along the pressure axis without its shape being affected. For example, the ICP is always measured with respect to a chosen reference level, at which level the external pressure transducer is placed. Changes in the height of the reference level will thus accordingly affect the magnitude of the ICP measured. It is, however, very unlikely that changing the height of the reference level will alter the elastic properties of the craniospinal system. Nevertheless, assessment of the volume-pressure relationship with a model which does not take into account P_o or, more correctly, which assumes that $P_o = 0$ will produce different results according to the reference level of the ICP. This error is prevented by the introduction of P_o .

The same applies to changes in ICP due to postural changes. In this case also the volume-pressure relationships are not likely to be influenced. With a model including P_o the same volume-pressure relationship will be found irrespective of body position.

From Equation 2.2 it can be derived that P_o is the pressure at which the elastance equals zero. It can be inferred from the volume-pressure curves shown in Figures 2, 3 and 5 that this point, corresponding with a completely flat course of the curve and with an infinitely small craniospinal volume, is never reached. As changes in P_o affect the equilibrium ICP, it is suggested that P_o is related to those physiological mechanisms that determine the equilibrium pressure of the craniospinal system.

Another clue with regard to the physiological meaning of the constant term can be found in a study by Löfgren et al. (1973). The volume-pressure curve was recorded in dogs during variations in central venous pressure, which were produced by applying a positive or negative pressure to the outlet tube of the respirator. The curve was found to be displaced upwards in a parallel manner along the pressure axis with positive central venous pressures, and in the reverse direction with negative pressures; this suggests that P_o may be related to the pressure in the extradural venous system, constituting the basic hydrostatic pressure level of the system.

When the volume of the system, at any one stage, increases by an extra amount ΔV_e , the ICP rises by a pressure response ΔP :

$$P + \Delta P = P_1 e^{E_1(V_e + \Delta V_e)} + P_o, \quad (2.3)$$

or:

$$P + \Delta P = P_1 e^{E_1 V_e} e^{E_1 \Delta V_e} + P_o,$$

or:

$$\Delta P = (P - P_o) (e^{E_1 \Delta V_e} - 1). \quad (2.4)$$

The last equation describes the relationship between the pressure response resulting from an increase in volume of the craniospinal system and the ICP. In the case of external volume forcing, as in the volume-pressure test, Equation 2.4 describes the relation between the volume-pressure response and ICP, if VPR is substituted for ΔP and the amount of volume injected (ΔV_i) for ΔV_e :

$$VPR = (P - P_o) (e^{E_1 \Delta V_i} - 1). \quad (2.5)$$

In this case it is assumed that $\Delta V_i = \Delta V_e$, which is only true if all the

injected volume contributes to the elastic volume, and consequently to the increase in total craniospinal volume, and if nothing is accommodated by spatial compensation (reciprocal volume changes). Volume loading should, therefore, be carried out according to the guidelines mentioned in section 2.3, implying the injection of a small volume at a rapid rate.

With regard to the shape of the above relationship it can be seen that it is linear if both E_1 and ΔV_i are constant, or, more correctly, if their product is constant. ΔV_i is constant by definition and E_1 is constant so long as the volume-pressure curve does not alter its shape. Conversely, it can be inferred that a linear correlation between VPR and ICP should be accepted as proof of the exponential nature of the volume-pressure relationship. Such a correlation has indeed been confirmed, both in clinical and in experimental studies, as discussed in the previous sections.

E_1 can be computed from the slope (S_1) of the VPR-ICP relationship (Equation 2.5):

$$S_1 = e^{E_1 \Delta V_i} - 1,$$

or:

$$E_1 = \frac{1}{\Delta V_i} \ln [S_1 + 1]. \quad (2.6)$$

Consequently, the computation of E_1 requires the assessment of the VPR-ICP relationship which, in turn, requires multiple volume-pressure tests carried out at different levels of ICP. In the experimental situation the ICP can be raised by various means, but in the clinical situation this seems less practical. Moreover, the risk of intracranial infection, associated with bolus injection into the CSF space, will increase with the number of injections. Computation of E_1 from a single volume-pressure test is, however, impossible as the equation, derived from Equation 2.5, contains the constant term P_o :

$$E_1 = \frac{1}{\Delta V_i} \ln \frac{P_p - P_o}{P_b - P_o}, \quad (2.7)$$

where: P_b = base-line ICP prior to injection, and

P_p = peak pressure following injection: $P_p - P_b = \text{VPR}$.

As can be seen from Equation 2.5, P_o is given by the intercept of the linear VPR-ICP relationship with the pressure axis. It would thus require

at least two volume-pressure tests at different pressure levels to determine this intercept.

E_1 can be calculated from a single bolus injection, if it is assumed that P_o equals zero, or, in other words, that the linear VPR-ICP relationship passes through the origin of the axes. In that case our volume-pressure model conforms to that of Marmarou, in which case E_1 is inversely related to the PVI according to the relationship:

$$E_1(P_o=0) = \frac{1}{0.4343 \text{ PVI}} \cdot \quad (2.8)$$

2.5 Clinical significance

Patients with intracranial disorders of a space-occupying nature, whether there is a tumour, haematoma, hydrocephalus, or brain swelling due to edema or vascular engorgement, will develop intracranial hypertension as soon as the spatial compensatory capacities, in which CSF absorption plays a major role, become exhausted. The rate of expansion of the mass lesion is of decisive importance in this respect. ICP measurements can provide information only as to whether or not ICP is raised and to what extent it is raised. Since ICP is known to fluctuate, prolonged ICP recording is sometimes required in order to answer these questions. If the intracranial mass continues to increase in size the ICP will start to rise, at first slowly but then more and more rapidly in accordance with the exponential configuration of the craniospinal volume-pressure curve.

We can now understand why volume increments in the craniospinal compartment have a more profound effect on ICP when the pressure is raised, than when it is in the normal range. This applies, for example, to the pulsatile increments in blood volume originating from the cardiac action and causing the CSF pulse, the amplitude of which increases when the ICP rises. The same holds for the effect on ICP of increments in cerebral blood volume (CBV) resulting from cerebral vasodilatation as caused by hypercapnia (Miller, 1975) and hypoxia (Small et al., 1960; McDowall, 1966), both constituting insults to the brain to which critically ill patients are often exposed. Vasodilatation as a result of instability of the cerebral vascular muscle tone may provoke large

pressure waves if intracranial compliance is reduced (Langfitt et al., 1965; Langfitt, 1975). Elevation of the systemic blood pressure may also cause a significant increase in ICP on the steep portion of the volume-pressure curve, even if CBF autoregulation is still unimpaired, as shown by Langfitt et al. (1965 and 1975).

Exact knowledge of the relation of volume to pressure would enable the clinician to predict the course of ICP if a patient were exposed to further intracranial volume additions, and, thereby, to select those patients who were particularly at risk. However, this knowledge would be of no use at all if the volume-pressure curve had a single, uniform shape, since in that case measurement of the ICP alone would suffice. Miller and his collaborators in particular have shown that this relationship is variable, not only between patients but also in the individual patient under a variety of circumstances. In patients with head injury the VPR was found to correlate more closely with the degree of brain shift than with the level of ICP, which led Miller to decide on the basis of the VPR whether surgical decompression was required. In different publications values from 3 to 5 mm Hg/ml have been mentioned as critical levels (Miller and Pickard, 1974; Miller et al., 1975; Miller, 1975). A decrease in VPR was found after surgical decompression in patients with cerebral tumours and head injury, even when the ICP was not significantly reduced (Miller et al., 1973; Hase et al., 1978). This means that the volume-pressure curve had taken a flatter course in these patients, whose ability to tolerate further volume additions had thus been improved.

It is a well known fact that several volatile anaesthetic agents may increase ICP by producing cerebral vasodilatation. These pressure increments have been found to be more pronounced in the presence of space-occupying lesions, even when the resting ICP was not increased (Fitch et al., 1969; Jennett et al., 1969; Shapiro et al., 1972).

These findings indicate that intracranial mass lesions cause an increase in slope of the volume-pressure curve. It seems plausible that by producing brain distortion and brain shift these lesions alter the geometry of the system, especially by disturbing the free communication of CSF between the various compartments. The volume of the craniospinal system is thus reduced to that of the compartment harbouring the mass and so is the compliance. This is in accordance with the results of Löfgren and Zwetnow (1973) who found a 30% decrease in cranial compliance when

transtentorial herniation occurred during the expansion of intracranial balloons in dogs.

The evidence with regard to the influence of systemic arterial pressure and arterial carbon dioxide tension on the volume-pressure relationship is conflicting. A positive correlation between the blood pressure level and elastance was found by Löfgren (1973) and Leech and Miller (1974), but this could not be confirmed by Cohadon et al. (1975), Marmarou et al. (1975), and Takagi et al. (1980). A decrease in elastance during hypercapnia was found by Takagi et al. (1980), which is at variance with the results of Löfgren (1973), Leech and Miller (1974), and Rowed et al. (1975).

Therapeutic agents such as mannitol and steroids are known to reduce ICP (Wise and Chater, 1962; Kullberg and West, 1965; Brock et al., 1975 and 1976; Kullberg and Sundbärg, 1976), but they have been demonstrated to reduce the elastance proportionally more, both in experimental animals and in patients (Leech and Miller, 1974; Miller and Leech, 1975; Brock et al., 1975 and 1976; Miller et al., 1977).

It will be evident from this brief clinical review that the volume-pressure relationship is a variable property of the craniospinal system, influenced by disease entities, physiological variables and drugs. In practical terms the sensitivity to further elevation of ICP varies between different patients, as well as in the individual patient under different circumstances. This kind of information, which cannot be obtained from measurement of the level of ICP alone, may prove useful in diagnosis and as a therapeutic and prognostic guide to clinical management. It seems worthwhile, therefore, for the clinician to have at his disposal a simple and reliable method for the assessment of craniospinal volume-pressure relationships.

2.6 Discussion

Static and dynamic volume-pressure curves

In considering craniospinal volume-pressure curves particular attention

should be paid as to whether the ICP is plotted against the volume of an expanding intracranial mass or against additions to the *total* volume of the neural axis.

We prefer to call the first type of curve, which is found in Langfitt (Langfitt et al., 1966; Langfitt, 1975) and in the early work of Miller (Leech and Miller, 1974), the 'static' volume-pressure curve. It is usually obtained by expansion of an intracranial balloon at a slow rate. An example of this type of curve, taken from our own experiments, is given in Figure 6. Part of the balloon volume is compensated for by a reciprocal reduction in the volume of one of the normal craniospinal constituents, probably the CSF. The remaining part, which cannot be compensated for, has to be stored or buffered by the system, thus causing an increase in its total volume and, consequently, a rise in pressure. The distribution of these volume portions and the resulting

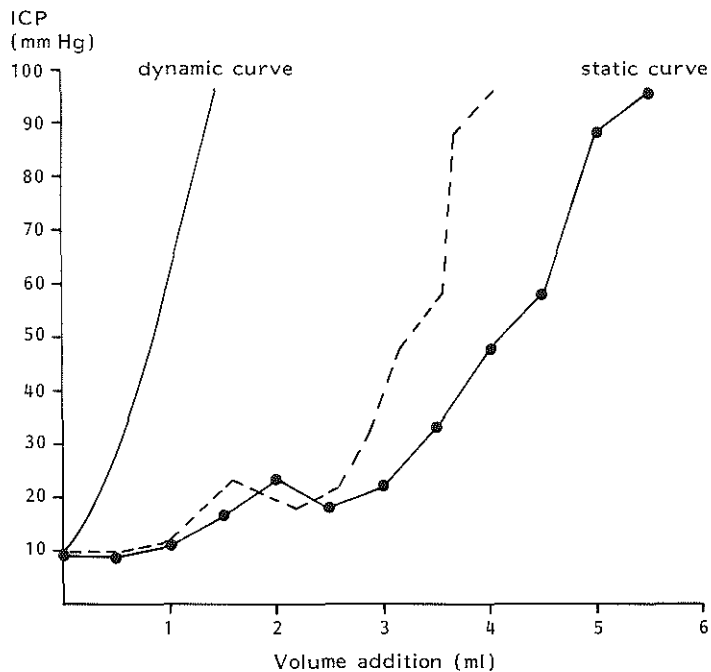


Fig. 6. Composite plot of dynamic and static volume-pressure curves in a single experimental animal (dog) during continuous inflation of intracranial extradural balloon (1 ml/40 min.). Static curve was obtained by plotting steady state ICP against balloon volume. Dynamic curve was constructed by means of mathematical volume-pressure model described in paragraph 2.4 and using bolus injection technique. Volume axis of latter curve represents true increase in craniospinal volume. Dashed curve was obtained by subtracting dynamic from static curve and indicates amount of compensated balloon volume at each pressure. Note that elastic volume is relatively small compared to compensated volume. Furthermore, during elevation of ICP volume compensation is still effective though gradually less so.

rise in ICP depend on the spatial compensatory capacities and the elastic properties or storage capacities of the system. The capacities of the craniospinal contents to compensate for volume increments are determined by several factors, among which are the cause and localization of the expanding lesion and, most important, its rate of development. The static curve is thus the resultant of the spatial and elastic contributions to the adaptation of any space-occupying lesion.

The 'dynamic' volume-pressure curve, as opposed to the 'static' curve, truly reflects the elastic properties of the system. This is due to the fact that spatial compensation has been excluded in its construction, so that each volume increment as a whole represents an increase in the total volume. Figure 6 shows the dynamic curve, obtained by volume-pressure testing, of the same experimental animal in which the static curve was recorded. The amount of compensated volume at any pressure level is found by subtracting the dynamic from the static curve. In this way the importance of spatial compensation of the craniospinal compartment in coping with volume additions, even in processes which are relatively rapid compared with most clinical situations, is clearly demonstrated. Even when ICP is considerably raised, spatial compensation still appears to be effective. Langfitt (1966 and 1975) has suggested that spatial compensation is a finite process, and that ICP only starts to rise once this process is exhausted. It appears, however, that failure of spatial compensation is a relative concept, the limits of which are set by time factors rather than by the absolute amount of volume available for compensation. The static curve is also a function of the dynamic curve, since the latter determines the extent to which the uncompensated volume portion will increase ICP. Hypothetically, an increase in compliance by a factor 2 may be expected to cause the static curve to take a flatter course given the same compensatory capacities. This has been worked out in Figure 7.

In the clinical context, where we are dealing with considerably 'slower' processes than in the experimental situation, the significance of the static relationship is presumably predominant. However, when spatial compensation becomes more and more compromised, it is the dynamic relationship which sets the actual pressure level.

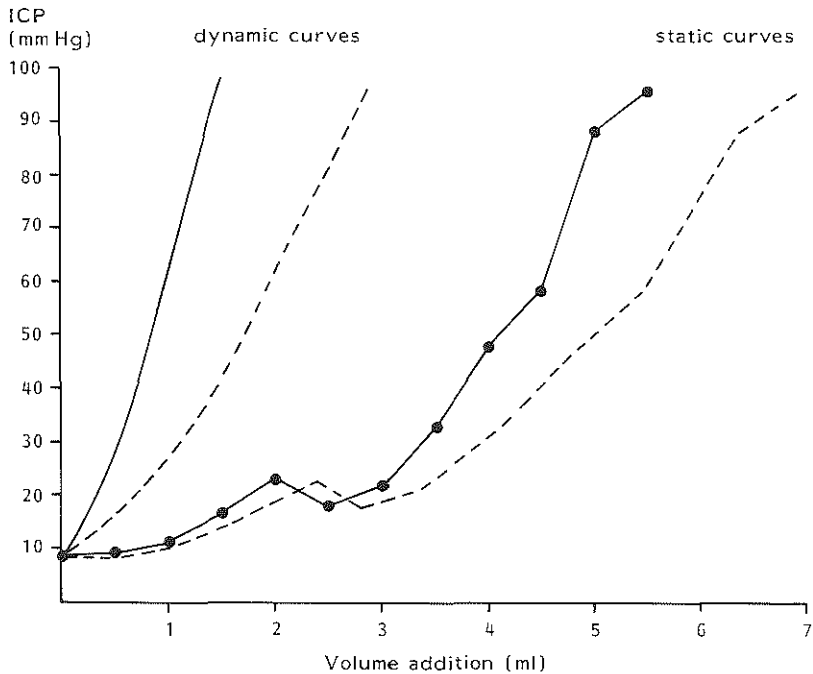


Fig. 7. Dynamic and static volume-pressure curves in same animal as in Figure 6. Compliance has been hypothesized as being increased by a factor 2 (dashed line). Hypothetical effect on static volume-pressure curve, given the same volume compensatory ability, is shown by dashed curve. It is suggested that with ICP rising and spatial compensation failing steady state ICP in response to an expanding mass lesion is increasingly determined by elastic properties of craniospinal system.

Mechanical basis of the volume-pressure curve

Another problem is the question of the mechanical and physiological basis of the dynamic volume-pressure curve. In this respect the role of the spinal dural sac and that of the intracranial haemodynamics have been alternately emphasized. Figure 8, taken from Löfgren (1975), illustrates these two factors.

The role of the dural sac as an important CSF reservoir for the cranial compartment has been well established (Pollock and Boshes, 1936; Foldes et al., 1958; Kety, 1965; de Boulay and El Gammal, 1966; Ponsen and van den Bos, 1971; Martins et al., 1972; Löfgren, 1973). Martins et al. (1972) have pointed out that the dura expands in the spinal canal like an unfolding leather bag rather than an elastic rubber tube. Since it is contained within the rigid vertebral canal, its distensibili-

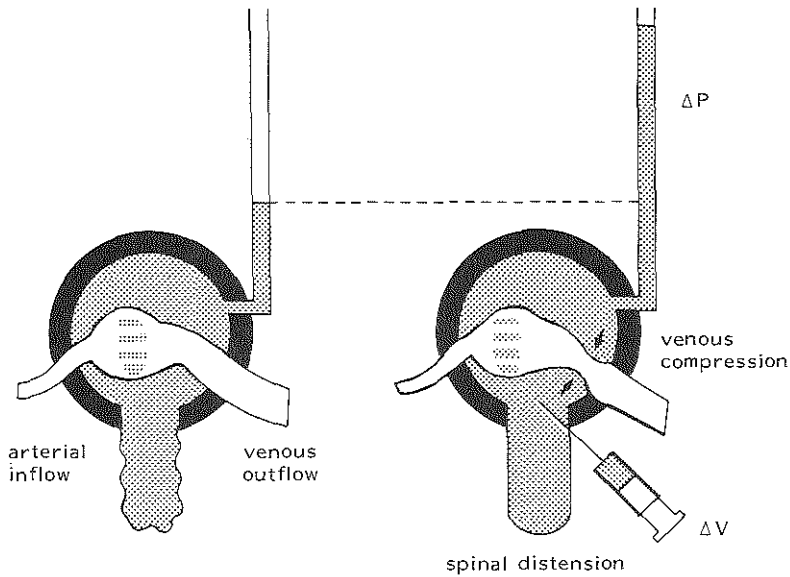


Fig. 8. Simplified model of craniospinal system demonstrating effect of volume addition (ΔV). Height of pressure response (ΔP) is determined by spinal distensibility and venous compressibility. (Reproduced from Löfgren J: Mechanical basis of the CSF volume-pressure curve. In: Intracranial Pressure II eds. N Lundberg, U Pontén, M Brock, Springer-Verlag, Berlin-Heidelberg-New York, 79-81, 1975).

ty will depend on the vascular pressure inside the epidural venous plexus. Moreover the epidural fatty tissue may alter its intraspinally located volume by sliding the intervertebral foramina in and out. The spinal dural sac is a highly compliant subdivision of the whole system and defines to a large extent the shape of the volume-pressure curve in its low pressure range (Fig. 4). However, when the sac is filled to capacity, it becomes a stiff, elastic structure. This explains why Löfgren and Zwetnow (1973) found an almost equal distribution of added volume between the cranial and spinal compartment when ICP exceeded 20 mm Hg.

The fundamental question with regard to the compliance of the cranial cavity is whether volume additions cause an increase in total volume or whether they are compensated for by reciprocal volume changes. The first possibility seems very unlikely at first sight in view of the bony encasement of the brain which is immediately adjacent to the dura. In the case of the second possibility the cerebral vascular bed needs to be considered, since this is the compartment which is pre-eminently

capable of rapid volume adjustments. The vascular factor has received particular attention from Löfgren (1973) and Marmarou (Marmarou et al., 1975). The pressure response following volume forcing was believed to be determined by the compressibility of the low-pressure, venous segment of the vascular bed. Provided that the supply of blood is constant, venous compression by a volume increment in the CSF space will, through the increased outflow resistance and consequent stagnation of flow, result in an increase of intravascular pressure which is transmitted to the surrounding CSF. The problem with regard to this explanation, in our opinion, lies in the introduction of reciprocal volume changes into the volume-pressure concept; this is, strictly speaking, not allowed, since they do not contribute to changes in total volume. If part of the injected volume is compensated for, it is no longer justifiable to plot this volume against pressure and to regard the curve thus obtained as a volume-pressure curve truly reflecting craniospinal elasticity. This criticism applies, for example, to the low elastance plateau at the blood pressure level of Löfgren's curve (Fig. 3), where the decrease in elastance was explained by rapid egress of blood from the cranial cavity.

The concept of the vascular bed as a compliant reservoir for the cranial compartment is contradicted by the experimental evidence that the cerebral vascular bed is extremely resistant to a reduction in volume. Compression of cerebral veins occurs only at a very specific and limited site: at their junction with the dural sinuses, a phenomenon which is known as the 'cuff constriction' (Wright, 1938; Bedford, 1942; Hedges et al., 1964; Nakagawa et al., 1974). The rest of the vascular bed does not collapse and even dilates when ICP is raised (Cushing, 1902; Wolff and Forbes, 1928; Fog, 1933; Wright, 1938; Greenfield and Tindall, 1965). The CBV has accordingly been shown to remain constant or to become slightly increased during elevation of ICP (Nagai et al., 1972; Grubb et al., 1975; Löfgren and Zwetnow, 1976). However, during rapid volume loading short-lasting reductions in CBV can occur, as was demonstrated by Benabid et al. (1976 and 1980) who measured CBV by an impedance method during bolus injection and rapid infusion. We agree, therefore, that some spatial compensation in the volume of cerebral blood does take place during rapid processes.

It thus appears that, under certain conditions, the injected volume $\Delta V_i = \Delta V_e + \Delta V_c$, where ΔV_c is the volume part which is compensated for.

The compressibility of the cerebral veins determines the distribution between the two volume portions: when ΔV_c is small, ΔV_e and, consequently, the pressure response will be large, and vice versa. The situation is even more complex, since by increasing the venous outflow resistance with consequent stagnation of the venous outflow, the volume load will, at the same time, cause an increase in CBV. ΔV_e is thus augmented by an extra volume originating from the vascular compartment.

In our opinion it is highly questionable that this complex mechanism, triggered off by volume forcing, could produce a pressure response without affecting the total cranial volume. We would thus suggest that even in the rigid skull volume changes can occur which are not necessarily reciprocal, although they will be very small indeed. The increase in total cranio-spinal volume of the animal depicted in Figure 6, for example, is approximately 1.2 ml in the pressure range from 20 to 100 mm Hg. On the basis of an equal partitioning of this volume between the cranial and spinal compartments the increase in cranial volume, i.e. 0.6 ml, can be estimated to amount to less than 0.7% of the total cranial volume. The mechanical basis for such volume changes could be provided by the numerous orifices in the skull base and also by a partial collapse of the dural venous sinuses occurring at high ICP (Langfitt et al., 1966; Shapiro et al., 1966). The latter structures we do not consider to belong to the total volume comprised within the dural envelope. Furthermore, when the foramen magnum is occluded by tonsillar herniation or by high cervical ligation, as in the experiments designed to study the compliance of the isolated cranial compartment, it may still function as an elastic membrane to the closed container.

Assessment of craniospinal volume-pressure relationships by means of the volume-pressure test

We have chosen the volume-pressure test as the technique for testing our volume-pressure model for two reasons: 1. its clinical applicability and 2. the analogy between VPR and CSF pulse pressure as will be discussed in the next chapter. In order to be clinically applicable a method should be simple, safe, reliable and repeatable. These requirements make infusion techniques impractical for routine clinical use. However, the volume-pressure test has also a number of disadvantages. ICP measurements in the lateral ventricle carry a potential risk of infection, the inciden-

ce of which has been reported to be in the order of 0.5% to 5% (Lundberg, 1960; Sundbärg et al., 1972; Wyler and Kelly, 1972; Smith and Alksne, 1976; Troupp and McDowall, 1976). The causative microorganism is usually staphylococcus epidermidis which responds well to antibiotic treatment. However, infections may unfavourably affect the outcome of these patients who are often already seriously ill and may also delay CSF shunting procedures if indicated. In our own material of over 300 continuous ICP recordings, five were complicated by a ventriculitis. Most of these measurements were made for diagnostic purposes and did not last longer than 12 to 24 hours. With ICP monitoring over periods exceeding two to three days, as in head injury patients for example, the chance of infection will certainly increase. The risk will be even greater if fluids are repeatedly injected through the ventricular catheter as in volume-pressure testing, in which case it will be difficult to maintain meticulous sterility standards.

The risk of infection as well as other problems related to ventricular puncture have led to the development of techniques in which ICP is measured at the convexity of the brain, either in the subarachnoid or in the epidural space. In these techniques, especially in the latter where the transducer is directly applied to the dura, fluid injections are not feasible and the impossibility of assessing the volume-pressure relationships would thus limit the use of these techniques.

Another problem with regard to the addition of extra volume to the CSF compartment is that, in our experience, this may cause dangerous pressure rises especially when the ICP is already high and the compliance is reduced. Large pressure waves may be induced as a result of secondary, vasodilatory responses. The alternative of fluid injection, i.e., withdrawal of CSF, is less practical, as this may lead to blockage of the ventricular catheter. It is also methodologically unsound, as withdrawal of fluid cannot be carried out sufficiently rapidly.

Finally, in our experience the VPR shows, in the individual patient, a rather wide variability in consecutive measurements at the same level of ICP. Some of the causes may be related to the injection manoeuvre. The exact amount of fluid injected may vary slightly as may the rate of injection. In restless and 'uncooperative' patients it may be difficult to get a stable base-line pressure on which to perform the volume-pressure test. Moreover the pressure response itself may be affected by spontaneous bodily activity of the patient. Studying the variability of the VPR in

consecutive measurements, Miller and Leech (1975) regarded a change of 2 mm Hg/ml or more as significant. The VPR over the entire study, however, ranged only from 0 to 6 mm Hg/ml. In our own clinical study of 65 ICP registrations the VPR ranged from 0 to 12 mm Hg/ml and the vast majority of the responses was lower than 6 mm Hg/ml. Bearing this in mind it seems unlikely that different volume-pressure relationships could be reliably discriminated on the basis of a single test. In order to improve the accuracy of the assessment more than one test would thus be required, so that significance could be attained at a smaller change. However, the increase in the number of tests would, in turn, increase the risk of infection.

In view of the above disadvantages associated with the clinical use of the volume-pressure test we have examined an alternative method, based on the CSF pulse pressure, for the continuous assessment of the craniospinal volume-pressure relationships during ICP monitoring in patients.

Conclusions

1. The total volume of the craniospinal system is variable.
2. In true craniospinal volume-pressure relationships the ICP should be compared with increments in the total volume of the system.
3. The mechanical basis of the dynamic volume-pressure curve is formed by the physical properties of the craniospinal coverings rather than by vascular factors, as the latter involve reciprocal volume-changes which interfere with the definition of true volume-pressure relationships.
4. The compliance of the craniospinal system is largely determined by the spinal compartment.
5. Most reports from the literature have treated the elastic properties of the craniospinal system as an exponential function and this has been the starting-point of our mathematical volume-pressure model.
6. This model is further characterized by the introduction of a constant pressure term: P_0 .
7. It follows from the exponential shape of the volume-pressure curve that the relationship between the ICP and any pressure response resulting from a rapid and uniform volume load is linear.

8. In clinical patients the volume-pressure function has been shown to be a variable property.
9. The disadvantages associated with the clinical use of the volume-pressure test motivate the search for an alternative method of assessment of craniospinal volume-pressure relationships.

CHAPTER 3

CEREBROSPINAL FLUID PULSE PRESSURE

"It is oversimple and illogical to state that CSF pulsations are purely arterial or purely venous in nature."

G. Dardenne et al. (1969)

3.1 Historical survey

The first observations of cardiac pulsations of the brain must be as old as mankind itself, since they can be made at the fontanelles of neonates and at the site of traumatic cranial defects. According to Mosso (1881), Galen already knew of the respiratory and cardiac movements of the brain.

A more systematic study of the CSF pulse was initiated with the first attempts to direct measurement of the ICP by Leyden (1866), Key and Retzius (1875) and Knoll (1886). Through the introduction of lumbar puncture by Quincke in 1891 the CSF pulse became familiar to the clinician. Early reports on the amplitude of the pulse mention values of 1 mm saline in the cat (Weed and McKibben, 1919) and of 2-3 mm saline in man (Howe, 1928). Antoni (1931 and 1946) examined the CSF pulse in various conditions, particularly spinal block. O'Connell (1943), reducing the effects of damping on the recording of the pulse by using a wide-bore needle, found an average pulse pressure of 15 mm saline in man. Gerlach (1952) studied the form of the pulse wave extensively and showed how it changed with the ICP. With the introduction of modern isovolumetric electronic manometers larger amplitudes were reported ranging from 20 to 40 mm saline (Goldensohn et al., 1951; Bering, 1955). It still holds true today that absolute values for the pulse amplitude from different studies cannot be compared without taking into account the physical characteristics of the recording system.

The classic studies of Bering (Bering and Ingraham, 1953; Bering, 1955) inaugurated a new era of interest in the CSF pulse, especially with regard to its origin and site of transfer. Although the choroid plexus is no longer regarded as the main source of the pulse, the question as to whether it is arterial (Becher, 1922; Tinel, 1927; Antoni, 1931 and 1946; O'Connell, 1943; Goldensohn et al., 1951; Gerlach, 1952; Dunbar et al., 1966; du Boulay, 1966) or venous (Turchetti, 1946; Hamit et al.,

1965) in origin, or both arterial and venous (Adolph et al., 1967; Dardenne et al., 1969; Dereymaeker et al., 1971) has not been definitively solved to the present day.

The CSF pulse has also attracted attention as a pathogenetic factor in the development of various clinical conditions, such as syringomyelia (Gardner, 1965), intracranial cystic cavities (du Boulay, 1966), hydrocephalus (Bering, 1962; Bering and Sato, 1963; Wilson and Bertan, 1967; Maira et al., 1975; Sato et al., 1975; Pettorossi et al., 1978; Di Rocco et al., 1979), and the empty sella syndrome (Kaufman, 1968).

Those who practise ICP monitoring have tried to use the CSF pulse as a diagnostic aid. Maira et al. (1975) and Sato et al. (1975) observed differences in the configuration of the pulse wave in various forms of hydrocephalus. Castel and Cohadon (1976), using Fourier analysis, examined the morphology of the pulse during elevation of ICP as well as in hydrocephalus and expansive tumoral processes. They related both wave form and amplitude to the elastic condition of the craniospinal system. A method using the amplitude of the CSF pulse as a measure of craniospinal elastance was introduced by ourselves and constitutes the main topic of this thesis.

3.2 CSF pulse pressure as a volume-pressure parameter

Introduction

With regard to the present studies our main interest concerns the CSF pulse in so far as it can be used as a diagnostic tool in the assessment of craniospinal elastance. In view of this aim, the importance of the amplitude overshadows that of the other aspects of the pulse: origin, morphology and pathogenesis, which will, therefore, not be discussed.

The pulse pressure has been found to increase concomitantly with the ICP, irrespective of the cause of intracranial hypertension (Leyden, 1866; Mosso, 1881; Wright, 1938; Goldensohn et al., 1951; Ryder et al., 1952; Bering, 1955; Janny, 1974). An explanation of this phenomenon was given by Davson (1967). The pulsatile blood flow to the craniospinal system produces a pulsatile expansion of the walls of the cerebral arteries. In

this way the arterial pulse is transmitted to the surrounding brain and CSF. The arteries will only be able to expand at the expense of the veins. The collapsibility of the veins thus provides a damping in the transfer of the arterial pulse to the CSF compartment. The magnitude of the damping depends on the ease with which blood can be expelled from the veins, which in turn, is determined by the venous pressure. This pressure is equal to or slightly larger than the ICP (Hill, 1896; Noell and Schneider, 1948; Shulman, 1965). When the ICP rises, the venous pressure increases concomitantly and, consequently, the damping effect of the veins is reduced, resulting in an increase in pulse pressure.

Analytical method

Apart from the above physiological explanation of the increase in CSF pulse pressure with rising ICP, the problem can be tackled from another angle. Any pressure change within the craniospinal cavity must be the result of a change in the total volume of the system, the magnitude of the pressure change depending on the nature of the craniospinal volume-pressure relationships. The increase in pulse pressure with rising ICP, therefore, directly follows from the exponential shape of the volume-pressure curve, as already pointed out by Marmarou et al. (1975; Fig. 9). The magnitude of the pulse pressure thus appears to be a function of:

1. the shape of the volume-pressure curve, and
2. the magnitude of the volume change underlying the pulse.

Comparison of the Figures 9 and 5 shows that the CSF pulse pressure, just like the VPR, can be regarded as a measure of craniospinal elastance. In accordance with the analogy between pulse pressure and VPR, Equation 2.4 can also be applied to the relationship between CSF pulse pressure (CSFPP) and ICP, if the pulsatile change in craniospinal volume is assumed to originate from a change in CBV (ΔV_b):

$$\text{CSFPP} = (P - P_0) (e^{\frac{E_1 \Delta V_b}{P - P_0}} - 1). \quad (3.1)$$

With regard to the nature of this relationship, it can be predicted that, given a mono-exponential volume-pressure relationship (constant E_1), it will be linear if ΔV_b is constant. In that case the pulsatile change in CBV can be calculated from the slope (S_2) of the linear relationship and from E_1 , which can be determined by volume-pressure testing using

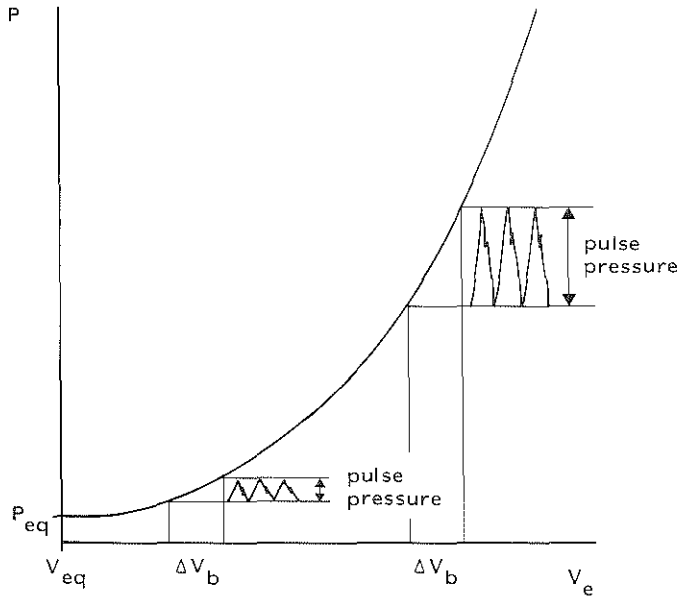


Fig. 9. Amplitude of CSF pulse (pulse pressure) increases with rising ICP in accordance with exponential shape of craniospinal volume-pressure curve. Magnitude of pulse pressure is determined by shape of curve and by amount of pulsatile change in cerebral blood volume (ΔV_b).

Equation 2.6, or Equation 2.7 in the case of a single test:

$$S_2 = e^{E_1 \Delta V_b} - 1,$$

or:

$$\Delta V_b = \frac{1}{E_1} \ln(S_2 + 1). \quad (3.2)$$

It is obvious that the CSF pulse pressure can never replace the VPR in the computation of the elastance coefficient, since the magnitude of the pulsatile change in CBV is unknown. However, assuming that ΔV_b is constant, changes in the slope of the CSFPP-ICP relationship truly reflect changes in volume-pressure relationship (E_1).

3.3 Pulsatile change in cerebral blood volume

Origin of the pulsatile change in cerebral blood volume

The change in craniospinal volume giving rise to the CSF pulse is generated within the cerebral vascular compartment. Concerning the magnitude of the

volume change, it should be clearly understood that it is not equivalent to the pulsatile amount of blood supplied to the craniospinal system by the afferent vascular system: the carotid, vertebral and spinal arteries. This is because part of this volume of blood is immediately compensated for by a simultaneous outflow of blood through the efferent venous system. This compensated blood volume does not contribute to an increase in total craniospinal volume and thus not to the formation of any pressure response. As a matter of fact, if the arterial inflow and venous outflow rates were identical at any point of time of the cardiac cycle, no volume change and, consequently, no pulse pressure would occur at all! The very fact that the in-and outflow curves are pulsatile and different in shape is responsible for the transient, time dependent change in CBV during a cardiac cycle, to which the following equation can be applied:

$$\Delta V(t) = \int_0^t [F_a(t) - F_v(t)] dt, \quad (3.3)$$

where: $\Delta V(t)$ = change in CBV as a function of time,

$F_a(t)$ = cerebral arterial blood flow as a function of time, and

$F_v(t)$ = cerebral venous blood flow as a function of time.

Inflow and outflow integrated over the cardiac cycle are, as a matter of course, equal. The maximum change in $\Delta V(t)$ within a cardiac cycle is equivalent to ΔV_b , the volume change underlying the CSF pulse pressure. The extreme values for $\Delta V(t)$ within a cardiac cycle are found when:

$$\frac{d \Delta V(t)}{dt} = 0, \quad \text{implying: } F_a(t) = F_v(t). \quad (3.4)$$

The interaction, or the timing, between the pulsatile inflow and outflow curves with the resultant change in CBV during a cardiac cycle is schematically demonstrated in Figure 10. The arterial inflow equals the venous outflow at times t_1 , t_2 , t_3 and t_4 . The blood volume increases when inflow exceeds outflow, i.e., during the intervals t_1-t_2 and t_3-t_4 , and decreases in the reverse situation. The change in CBV ($\Delta V(t)$) reaches its maximum at t_2 and its minimum at t_1 . The volume change underlying the CSF pulse pressure is determined by the difference between the maximum and the minimum volume of cerebral blood during a cardiac cycle.

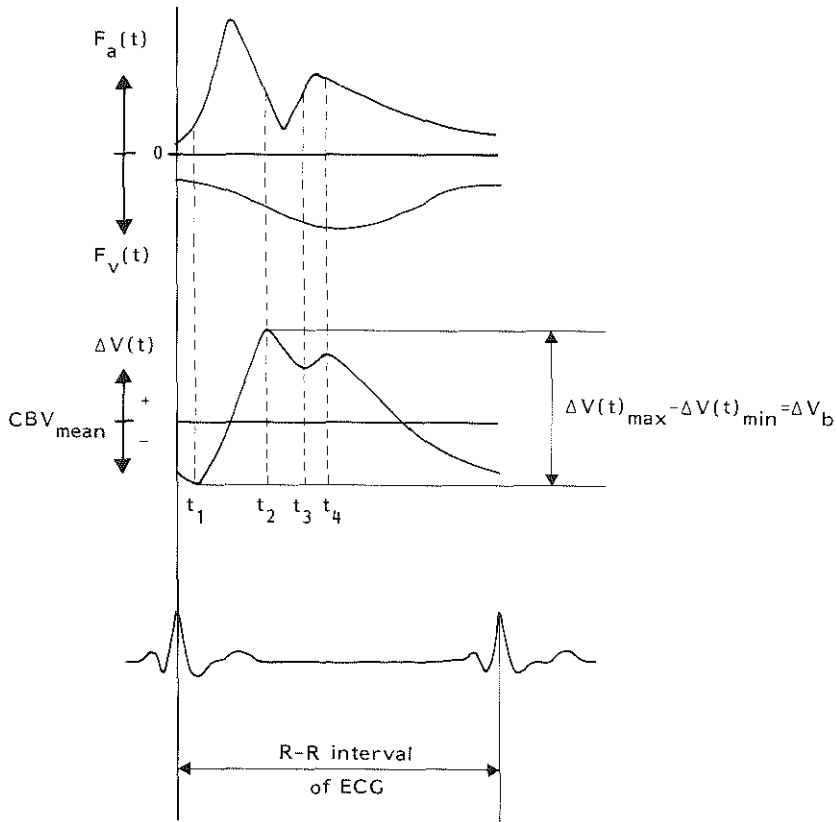


Fig. 10. Schematic drawing of cerebral arterial inflow ($F_a(t)$) and venous outflow ($F_v(t)$) curves, interaction between which determines change in cerebral blood volume ($\Delta V(t)$) during cardiac cycle. Maximum volume change ($\Delta V(t)_{max}$), occurring at time t_2 , minus minimum volume change ($\Delta V(t)_{min}$), occurring at time t_1 , is defined as pulsatile change in CBV (ΔV_b).

Factors affecting the pulsatile change in cerebral blood volume

As outlined above, ΔV_b depends on the time lag between the inflow and outflow curves and on their respective shapes. These, in turn, will depend on the impedances of the arterial and venous sections of the cerebral vasculature. The inflow impedance is to a large extent controlled by the vasomotor tone of the so-called cerebral resistance vessels, playing a major role in the CBF autoregulatory mechanism, whereas the outflow impedance is passively influenced by compression of part of the venous outflow tract. For example, a decrease in cerebral perfusion pressure will, by evoking an autoregulatory vasodilator response, cause a decrease in inflow resistance and, consequently, facilitate the inflow

of blood. The time lag between inflow and outflow will thus be increased, resulting in an augmentation of ΔV_b . The opposite effect may be expected to result from an increase in perfusion pressure.

The time lag may also be increased by factors acting upon the other side of the cerebral vascular bed. An increase in the CBF outflow resistance, as caused by venous compression during elevation of the ICP, will cause a delay in the pulsatile outflow, thus further enlarging the pulsatile volume change. The effect of the time lag or phase shift between the in- and outflow curves is schematically shown in Figure 11.

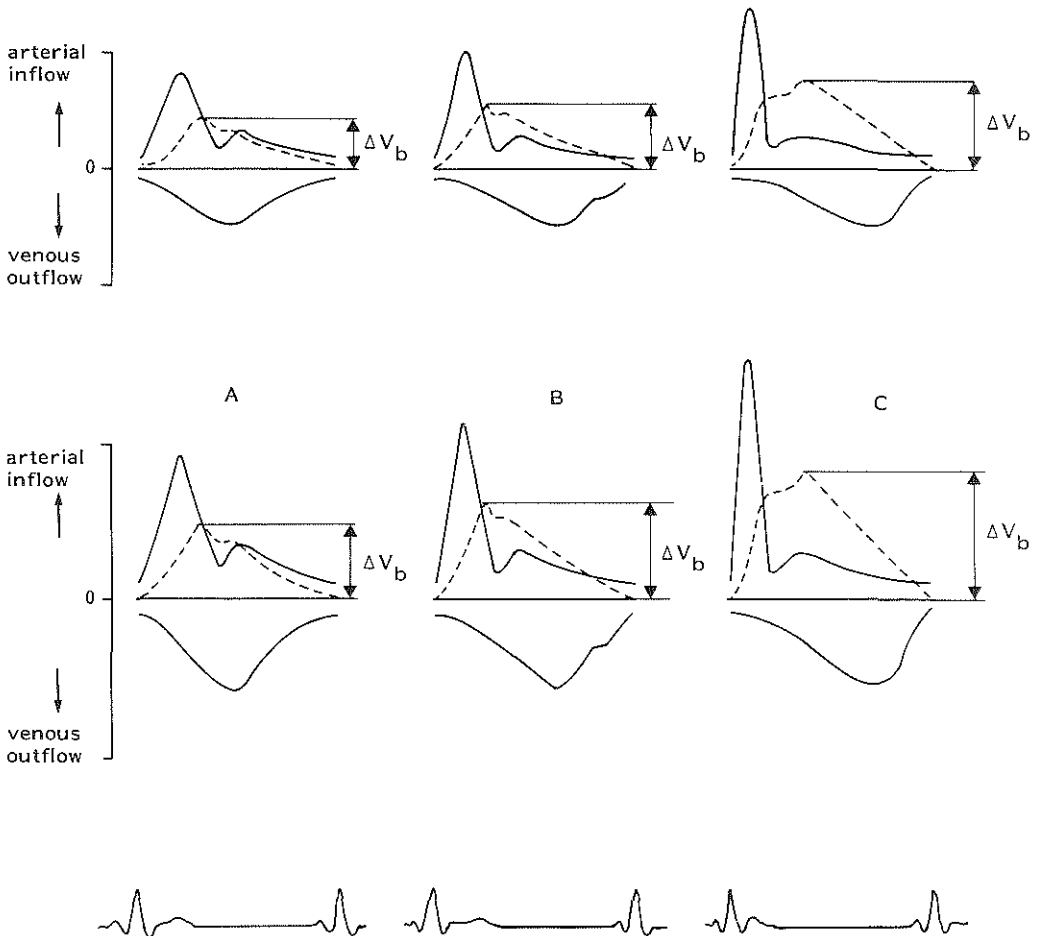


Fig. 11. Schematic drawing of pulsatile cerebral arterial inflow and venous outflow curves under various circumstances. Pulsatile change in cerebral blood volume has been plotted by dashed curves. ΔV_b is maximum change in CBV per cardiac cycle. Two mechanisms affecting magnitude of ΔV_b are shown. 1) From A through B to C effect of increase in phase shift between inflow and outflow curves on ΔV_b is shown. 2) From upper to lower part of figure effect of increase in CBF on ΔV_b is shown.

The magnitude of ΔV_b also depends on the pulsatile volume load of blood to the craniospinal system, which is determined by the CBF, leaving aside spinal cord flow, and by the heart rate. Figure 11 shows that, given a constant heart rate and assuming unaltered relative flow profiles (no change in phase shift), an increase in CBF may be expected to cause an increase in ΔV_b . The effect of the heart rate on the pulsatile volume load, which is actually the CBF per cardiac cycle, and thus on ΔV_b will be most pronounced at low heart rates as is shown in Figure 12.

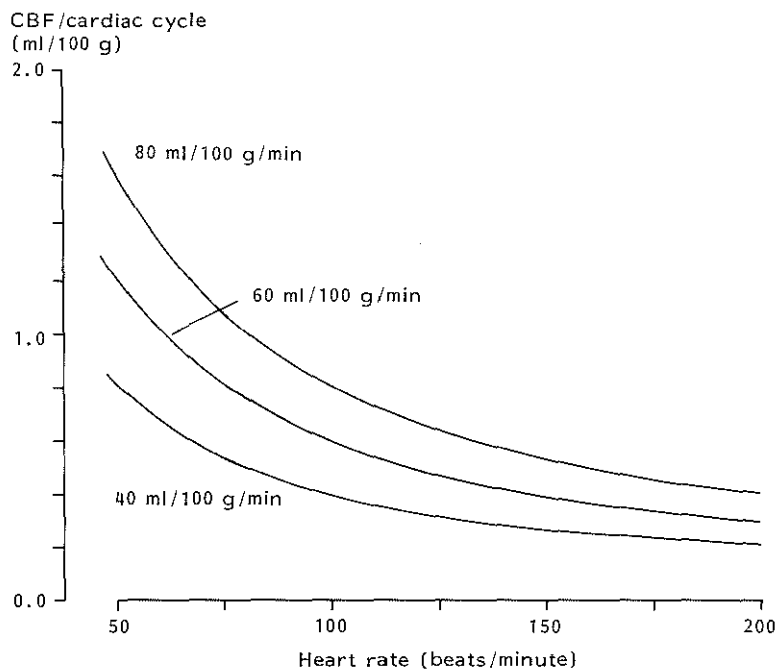


Fig. 12. Diagram showing dependence of pulsatile cerebral blood supply (CBF/cardiac cycle) on CBF (ml/100 g/min) and heart rate.

3.4 Discussion

The validity of the analogy between CSF pulse pressure and VPR depends on the similarity between the respective underlying volume changes. Here, several problems arise. The volume increment causing the VPR is artificially induced within the CSF compartment; its magnitude is known and constant at all times. The pulsatile volume change, on the other hand, is a

physiological phenomenon occurring in another craniospinal compartment; its magnitude is unknown and may vary under the influence of the ICP as well as of intracranial and extracranial haemodynamic factors.

Sullivan et al. (1978) have claimed that equivalent volume loading of different intracranial compartments may produce different pressure responses, so that the concept of a single volume-pressure curve for the craniospinal compartment is not valid. In experimental animals, paired bolus injections, first into the lateral ventricle and next into an epidural balloon, showed a divergence in the ICP response beyond a critical volume of the balloon; the pressure change after balloon injection became progressively larger than that after ventricular injection. When the group results were considered, the difference between the responses attained statistical significance above an ICP of 60 mm Hg.

In our view, this phenomenon can be explained by taking into account that the expanding balloon causes brain herniation resulting in impairment of CSF flow from the cranial to the spinal compartment. Bolus injection into the CSF space tends to open up the CSF pathways, whereas injection of the relatively large volume as used by Sullivan et al. (0.3 ml in the cat) into the balloon will increase the impairment of CSF flow by furthering herniation. The pressure response following balloon injection will thus be determined by the cranial compliance to a greater extent than the pressure response following ventricular injection; as discussed in Chapter 2.3, the cranial compliance is smaller than that of the total craniospinal system. This problem is not encountered when volume increments in the CSF and vascular compartments are compared, as in the case of the VPR and the CSF pulse pressure.

In defining the volume change underlying the CSF pulse pressure as the pulsatile change in CBV we have supposed the volumes of brain and CSF to remain constant during the cardiac cycle. The constancy of the latter volume may be questioned. However, if pulsatile changes in the CSF volume occur, they will be small compared to the pulsatile changes in blood volume. Assuming a CSF absorption rate of about 0.35 ml/min in man, the largest possible CSF volume change per cardiac cycle would be in the order of 0.005 ml. This value is negligible compared to the values for ΔV_b , which have been found to vary in man between 0.36 to 4.38 ml, as will be reported in the next chapter.

There are no methods available for direct, quantitative assessment of ΔV_b , although methods such as: rheoencephalography, pulsatile echo-encephalography, Doppler ultrasound and electromagnetic flow measurement might provide semi-quantitative information on changes in ΔV_b . Therefore, as the magnitude of ΔV_b remains unknown, the CSF pulse pressure can never provide a direct measure of craniospinal elastance. However, according to Equation 3.2, ΔV_b can be computed from the CSFPP-ICP relationship and E_1 . Further study of this relationship in combination with the volume-pressure relationship may thus yield information on how ΔV_b is affected by the variables discussed in the previous section: cerebral perfusion pressure, CBF, and heart rate, and on the extent to which it varies between patients. With the help of this knowledge it may become possible to interpret changes in CSF pulse pressure in terms of changes in E_1 . For example, if the CSFPP-ICP relationship turned out to be linear in nature, implying a constant ΔV_b , the slope of this relationship would become a relative measure of E_1 as long as the variables affecting ΔV_b remained unchanged. An increase in slope would mean an increase in E_1 and vice versa. In that case the CSFPP-ICP relationship could be used to monitor the volume-pressure relationship during continuous ICP recording.

With these aims in mind we examined the relation of CSF pulse pressure to ICP in experimental animals and in clinical patients. For historical reasons the clinical study will be reported first. This study was conducted in a group of patients who had been subjected to continuous ICP recording and volume-pressure testing as part of their diagnostic investigations. The ICP measurements had been recorded on magnetic tape. The pressure recordings were retrospectively analysed with respect to the CSFPP-ICP relationship. These investigations should, therefore, be regarded as a pilot study for the more detailed and more systematically conducted animal experiments.

Conclusions

1. The CSF pulse pressure is determined by the magnitude of the pulsatile change in CBV and by the craniospinal elastance.
2. The magnitude of the pulsatile change in CBV is determined by the interaction between the pulsatile inflow and outflow curves and by the pulsatile volume load of blood to the craniospinal system.

3. Given a constant elastance coefficient, the CSF pulse pressure will be linearly related to the ICP so long as the pulsatile change in CBV remains constant.
4. So long as the pulsatile change in CBV is constant, changes in CSF pulse pressure will reflect changes in elastance.

CHAPTER 4

**CLINICAL OBSERVATIONS ON THE RELATIONSHIP BETWEEN
CEREBROSPINAL FLUID PULSE PRESSURE
AND INTRACRANIAL PRESSURE**

"In view of the fact that a major part of the neurosurgeon's time, skill and effort is devoted to combating intracranial hypertension and its consequences, it is a priori astonishing that more objective and exact methods for investigating this pressure have not found wider use."

N. Lundberg (1960)

4.1 Introduction

The aims of the clinical study were:

1. to examine the relationship between CSF pulse pressure and ICP during continuous ICP recording in patients, and
2. to compare this relationship with the volume-pressure relationship as determined by volume-pressure testing.

It was not intended at this stage of the investigation to evaluate the clinical relevance of the volume-pressure function itself, e.g., with respect to the underlying disease entity or the clinical state of the patient. For that purpose volume-pressure studies should be performed on groups of patients with similar disease states so that valid comparisons can be made. A variable volume-pressure relationship in a series of patients in different clinical states and suffering from a variety of intracranial disorders was accepted as the basis of the present study.

4.2 Material and methods

Material

A total number of 65 ICP recordings carried out in 58 patients was retrospectively analysed. All these patients had undergone continuous pressure recording as part of their investigation or management. The neurological disorders are listed in Table 1. The ages varied between two months and 77 years with a mean age of 37.1 years. The sex distribution was 28 females and 30 males. The length of the recording periods varied between 12 and 24 hours.

Table 1. Diagnostic categories of patients studied.

Diagnostic category	Number
Infantile hydrocephalus	7
Non-tumorous adult hydrocephalus	9
Normal pressure hydrocephalus	7
Infratentorial tumour and hydrocephalus	11
Supratentorial tumour and hydrocephalus	4
Supratentorial tumour	3
Head injury	5
Benign intracranial hypertension	3
Miscellaneous	7
No pathology	2
Total	58

Relationship between CSF pulse pressure and ICP

The ICP was measured by means of a ventricular catheter with a Rickham reservoir (Rickham and Penn, 1965) placed through a right frontal burr hole in the lateral ventricle, so that in fact the ventricular fluid pressure (VFP) was recorded. A butterfly needle (Abbott 21G) was percutaneously inserted into the reservoir, fixed to the skin, and connected to an external pressure transducer (Statham P37) via a stiff manometer line (length: 100 cm; internal diameter: 1.5 mm). The frequency response of the measuring system was examined in a separate study (Appendix 1) and was found to be flat up to 20 Hz. For this reason we were satisfied that the pulse wave amplitude was undamped. The frequency response appeared to be considerably influenced by the presence of air-bubbles in the system and great care was therefore taken to obtain an air-free system.

The reference level for the transducer was chosen at a plane midway between the upper surface of the calotte and the external auditory meatus, a level roughly corresponding with the external projection of the foramen of Monro, with the patient lying in the supine position, the head slightly elevated on a small pillow. The pressure signal was amplified (HP 78205B), displayed on an oscilloscope (HP 78304A) and recorded on a chart recorder (W&W, Model 312). At the end of each recording CSF was withdrawn for cell count and culture. One patient developed a mild ventriculitis following

the pressure recording caused by staphylococcus epidermidis, which was successfully treated with cloxacillin.

Continuous recording of the CSF pulse pressure to ICP ratio requires automatic data processing. The VFP signal together with the electrocardiogram (ECG) was, therefore, recorded on magnetic tape (Philips Analog 7) and analysed off-line by computer (PDP 11/34). The pressure signal was sampled at a rate of 80 Hz. The mean VFP was computed by averaging the samples within the R-R interval of the ECG. A problem arises with regard to the computation of the amplitude of the pulse wave, since the heights of ascending and descending portions of the wave are not equal; this is because the pulse is superimposed on the respiratory VFP wave as shown in Figure 13. To overcome this problem a trend correction procedure was carried out as shown in Figure 14.

Plots of the mean VFP per cardiac cycle and the corresponding pulse pressures against time were constructed for consecutive intervals of 4000 heart beats each, equivalent to periods of approximately 45 to 60 minutes depending on the heart rate. The average values of VFP and pulse pressure over 20 consecutive cardiac cycles were taken and plotted against

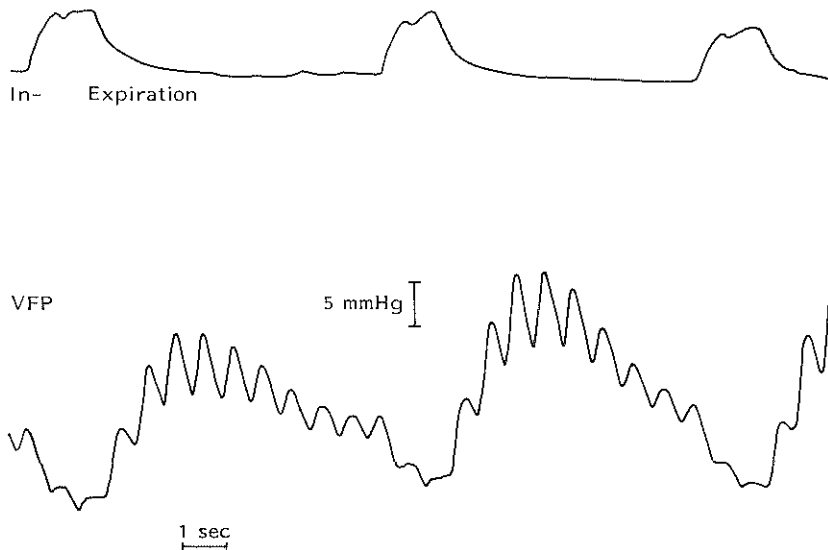


Fig. 13. Tracings of ventricular fluid pressure (VFP) and respiration (impedance plethysmography) showing cardiac pulsations superimposed on respiratory VFP wave. Note inequality of ascending and descending slopes of CSF pulse pressure during change in VFP.

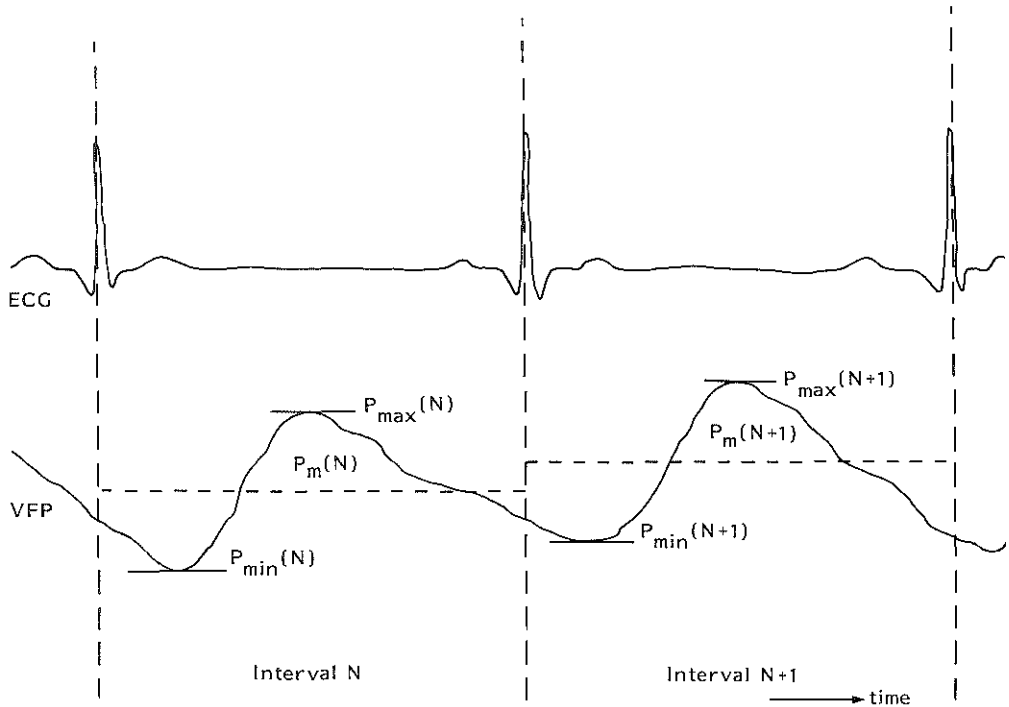


Fig. 14. Computer analysis of ventricular fluid pressure (VFP) signal in combination with electrocardiogram (ECG). Sampling frequency of signal is 80 Hz. Mean VFP in N-th R-R interval of ECG ($P_m(N)$) is arithmetical average of samples. Due to fluctuation of mean VFP, pulse pressure ($P_{max} - P_{min}$) is different for ascending and descending slope of pulse. To overcome this problem pulse pressure for interval N ($\Delta P(N)$) is calculated according to:

$$\Delta P(N) = \frac{1}{2} [2P_{max}(N) - P_{min}(N) - P_{min}(N+1)].$$

each other in a graph which thus consisted of 200 data pairs. Linear regression analysis was applied to these data. Finally, a pressure histogram was constructed for each recording interval. An example of such a computer plot is shown in Figure 15.

Volume-pressure testing was carried out at the beginning of each pressure recording. Since the aim of this study was to compare the CSFPP-VFP relationship with the volume-pressure relationship, only the first interval of 4000 heart beats of each pressure recording was considered, as the volume-pressure relationships might have changed during the subsequent time intervals.

If the relationship between CSF pulse pressure and VFP is linear, as in Figure 15, and Equation 3.1 is applied to this relationship, it follows that P_0 is given by the intercept of the regression line with

the pressure axis and that the slope of the line is determined by the product of the elastance coefficient (E_1) and the pulsatile change in CBV (ΔV_b). If E_1 is determined by volume-pressure testing, ΔV_b can be computed from Equation 3.2.

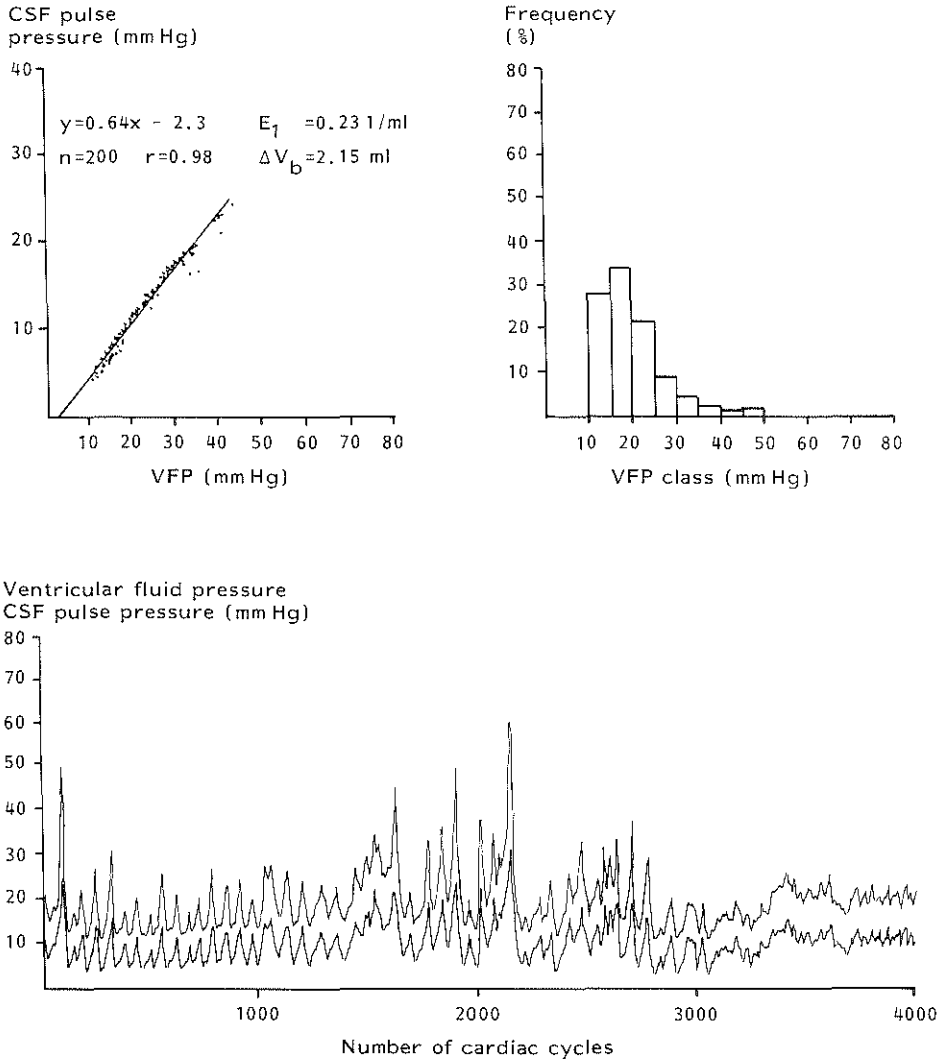


Fig. 15. Computer plot of ventricular fluid pressure (VFP) recording, comprising period of 4000 cardiac cycles, in patient with supratentorial tumour. Bottom: tracings of mean VFP (upper) and CSF pulse pressure (lower). Top left: relationship between CSF pulse pressure and mean VFP. Regression equation and calculated values for elastance coefficient (E_1) and pulsatile change in cerebral blood volume (ΔV_b) are shown. Top right: frequency distribution of VFP represented as histogram with pressure classes of 5 mm Hg.

Volume-pressure relationship

At the beginning of each pressure recording, volume-pressure testing was carried out by rapid injections, within one second, of 1 ml aliquots of normal saline into the lateral ventricle from a syringe interposed via a three-way stopcock in the tubing connecting the pressure transducer to the patient. During this manoeuvre the speed of the chart recorder was increased to ensure a more accurate reading of the pressure response. The peak pressure following injection was taken from the first clearly discernable cardiac pulse wave and calculated from the diastolic pressure plus one third of the pulse pressure. The VPR was calculated by relating this pressure to the base-line pressure immediately prior to ventricular loading but at the same point of the respiratory VFP cycle. The number of tests varied for each patient, with a total of 290 tests in 65 recordings. After the completion of each test the pressure was allowed to return to a stable base-line pressure.

The computation of the elastance coefficient from the data collected in the above manner poses a problem. As discussed in Chapter 2.4, E_1 cannot be computed from a single volume-pressure test, using Equation 2.7, as there is no P_0 available. This term is given by the intercept of the relationship between VPR and VFP with the pressure axis. In order to obtain a reliable relationship, a series of volume-pressure tests would have to be performed at various levels of VFP. In the present study, the VFP levels at which the tests were performed were usually within a close range; consequently no linear relationship between VPR and VFP could be obtained for each individual patient so as to yield a reliable value for P_0 . This was partly due to the retrospective nature of the study, but also because of the risks involved in unduly perturbing the volume and pressure of the craniospinal system in patients with already elevated VFP. There are two solutions to this problem. It would still be possible to calculate E_1 from Equation 2.7 by using P_0 of the CSFPP-VFP relationship which, theoretically, may be expected to be identical to P_0 of the VPR-VFP relationship. The alternative solution would be to compute E_1 assuming that P_0 equals 0. For the purpose of comparison both methods have been used.

In order to reduce the error caused by the variability of the VPR, the elastance coefficient of each patient was taken to be the average

value of the coefficients calculated from the various tests performed on that patient.

Another problem arises when, on the basis of the mathematical model, the CSFPP-VFP relationship is compared with the volume-pressure relationship. For, in the computation of the former relationship, the pulse pressure was related to the *mean* VFP of a cardiac cycle, whereas with regard to the latter relationship the VPR was related to the base-line VFP before injection. Thus, strictly speaking, either the pulse pressure should be related to the diastolic pressure, or the VPR should be related to the mean of the base-line and peak pressure. This problem will be dealt with in Appendix 2.

4.3 Results

Volume-pressure relationship

In order to indicate the ICP range from which the results of this study were obtained, a combined pressure histogram of the group of patients is given in Figure 16. The variation of the VPR with the VFP is shown in Figure 17. Linear regression analysis yielded the following relationship:

$$\text{VPR} = 0.14 \text{ base-line VFP} + 1.0 \quad (n=290, r=0.52, p < 0.001).$$

According to Equation 2.5 this linear relationship is in accordance with the concept of a mono-exponential volume-pressure relationship. Strictly speaking, it cannot be accepted as definite proof, since in that case the relationship should be demonstrated for each patient individually. As pointed out in the methodology section, the number of volume-pressure tests per patient was too small and the pressure range in which they were performed too narrow to allow for a reliable computation of the VPR-VFP relationship in each individual patient.

The elastance coefficients were calculated according to the two methods with respect to P_0 as previously explained and the mean results are given in Table 2. The P_0 used was that of the CSFPP-VFP relationship which usually had a positive value. E_1 calculated by using P_0 yielded, therefore, the larger value. The E_1 of each single patient was the mean value of the coefficients calculated from the various volume-pressure

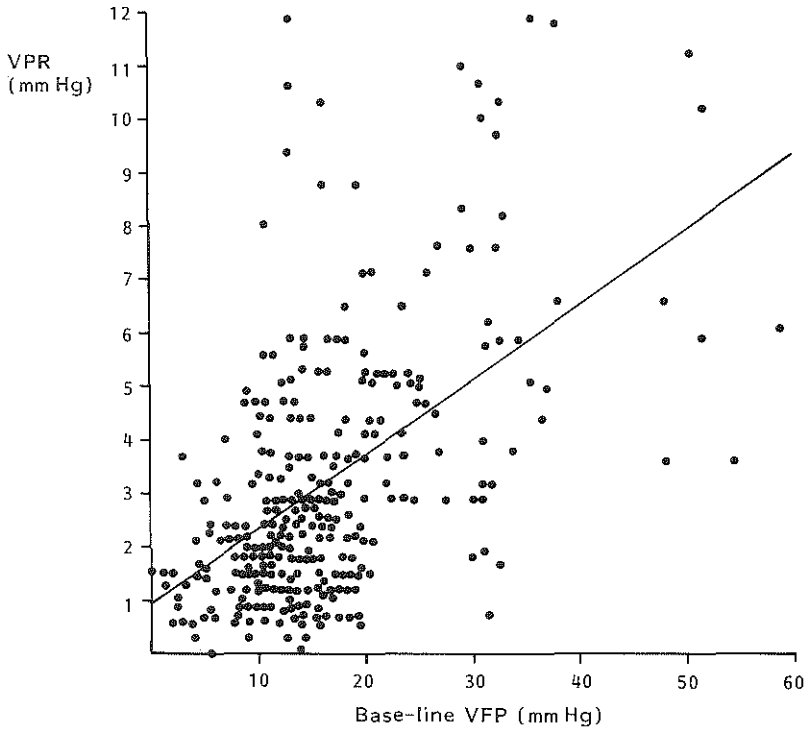


Fig. 16. Relationship between volume-pressure response (VPR) following bolus injection of 1 ml aliquots into ventricular catheter and base-line or pre-injection ventricular fluid pressure (VFP). 290 Bolus injections were performed during 65 continuous VFP recordings. Regression line is shown: $y=0.14x + 0.99$; $r=0.52$; $p<0.001$.

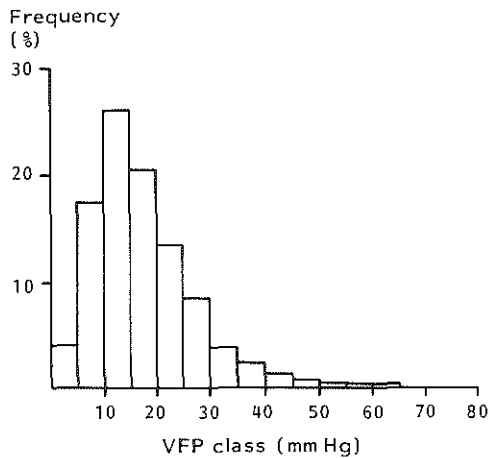


Fig. 17. Ventricular fluid pressure (VFP) class frequency distribution of 65 continuous VFP recordings in 58 patients. Skewness towards the higher pressure classes indicates moderately raised VFP for the group as a whole.

Table 2. Mean group values of elastance coefficient (E_1), computed using P_0 and assuming $P_0=0$ respectively.

	E_1 with P_0 (1/ml)	E_1 with $P_0=0$ (1/ml)
Mean	0.26	0.21
Standard deviation	± 0.17	± 0.15
Range	0.05 - 0.99	0.04 - 1.10

tests performed on that patient. Ideally, given a stable volume-pressure relationship, the various coefficients calculated for each single patient should be identical. The standard deviation of the mean E_1 per patient may, therefore, be considered to reflect the variability of the VPR due to methodological errors. The mean group standard deviation was 0.07 1/ml for E_1 with $P_0=0$ and 0.10 1/ml when P_0 was used in the computation of E_1 . These values are relatively large compared with the magnitude of the mean E_1 , suggesting that in clinical practice the volume-pressure relationship cannot be accurately assessed on the basis of a single volume-pressure test. Apparently, the use of P_0 did not reduce the standard deviation. In order to comply with the requirements of the mathematical model it was decided to take E_1 computed by using P_0 of the CSFPP-VFP relationship for further consideration.

Relationship between CSF pulse pressure and ventricular fluid pressure

The plots of CSF pulse pressure versus VFP always showed a linear relationship with high correlation coefficients (Figs. 15, 19, 20, 21, and 22). The mean results of the regression equations are given in Table 3.

Table 3. Mean group results of linear relationship between CSF pulse pressure (CSFPP) and ventricular fluid pressure (VFP) ($CSFPP = aVFP + b$), P_0 (pressure axis intercept), and pulsatile change in cerebral blood volume (ΔV_b).

	a (slope)	b (mm Hg)	Correlation coefficient	P_0 (mm Hg)	ΔV_b (ml)
Mean	0.40	- 1.6	0.85	3.2	1.67
Standard deviation	± 0.16	± 2.9	± 0.08	± 5.1	± 0.96
	0.09	-17.3	0.65	- 7.4	0.36
Range	-	-	-	-	-
	1.06	2.4	0.99	16.3	4.38

The finding of a linear relationship implies, in accordance with Equation 3.1, that the product of E_1 and ΔV_b was constant for the recording interval concerned. If it is assumed that no change in volume-pressure relationship occurred during the duration of a recording interval (approximately one hour), it follows that ΔV_b also remained constant. The mean group results for ΔV_b are given in Table 3.

In order to examine whether the CSFPP-VFP relationship could serve as a reliable parameter of the volume-pressure relationship, the gradients of the regression lines were compared with the elastance coefficients. Figure 18 shows that there is indeed a statistically significant positive correlation. However, the correlation is too weak to allow for a confident prediction of E_1 on the basis of the CSFPP-VFP relationship in individual patients. The explanation for this is that the second determinant of the pulse pressure, the pulsatile change in CBV, evidently varies considerably between patients (Table 3). This is demonstrated with the help of a few

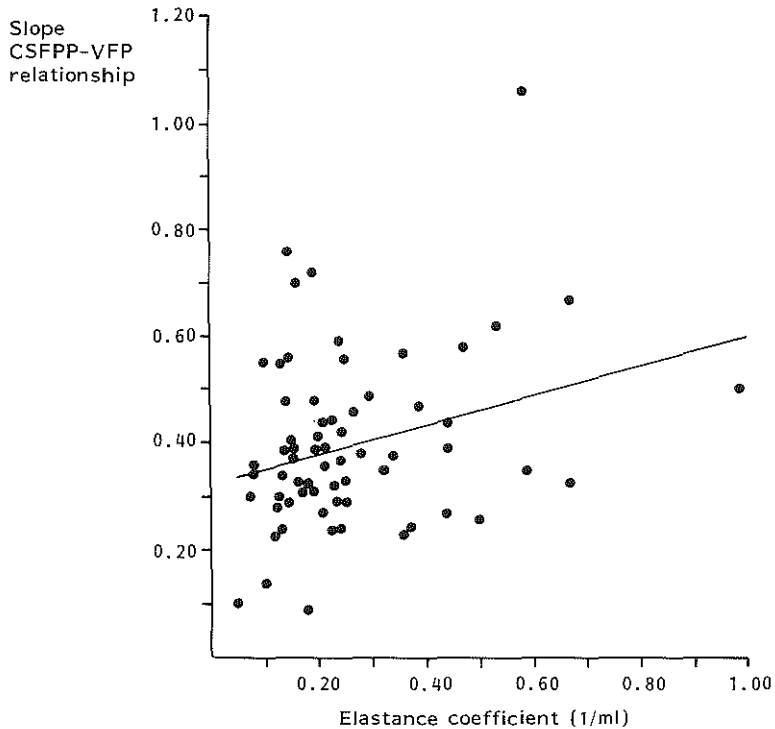


Fig. 18. Slope of relationship between CSF pulse pressure (CSFPP) and ventricular fluid pressure (VFP) plotted against elastance coefficient in 65 continuous VFP recordings. Regression line is shown: $y=0.27x + 0.3$; $r=0.28$; $p<0.05$.

examples. Comparison between Figures 19 and 20 shows that the difference in slope of the regression line is fully explained by the difference in E_1 , since the calculated values for ΔV_b are equivalent. However, Figure 21 shows a steep slope in spite of a small E_1 and, conversely, Figure 22 shows the coincidence of a weak slope and a large E_1 . According to the mathematical model these discrepancies are directly attributable to ΔV_b .

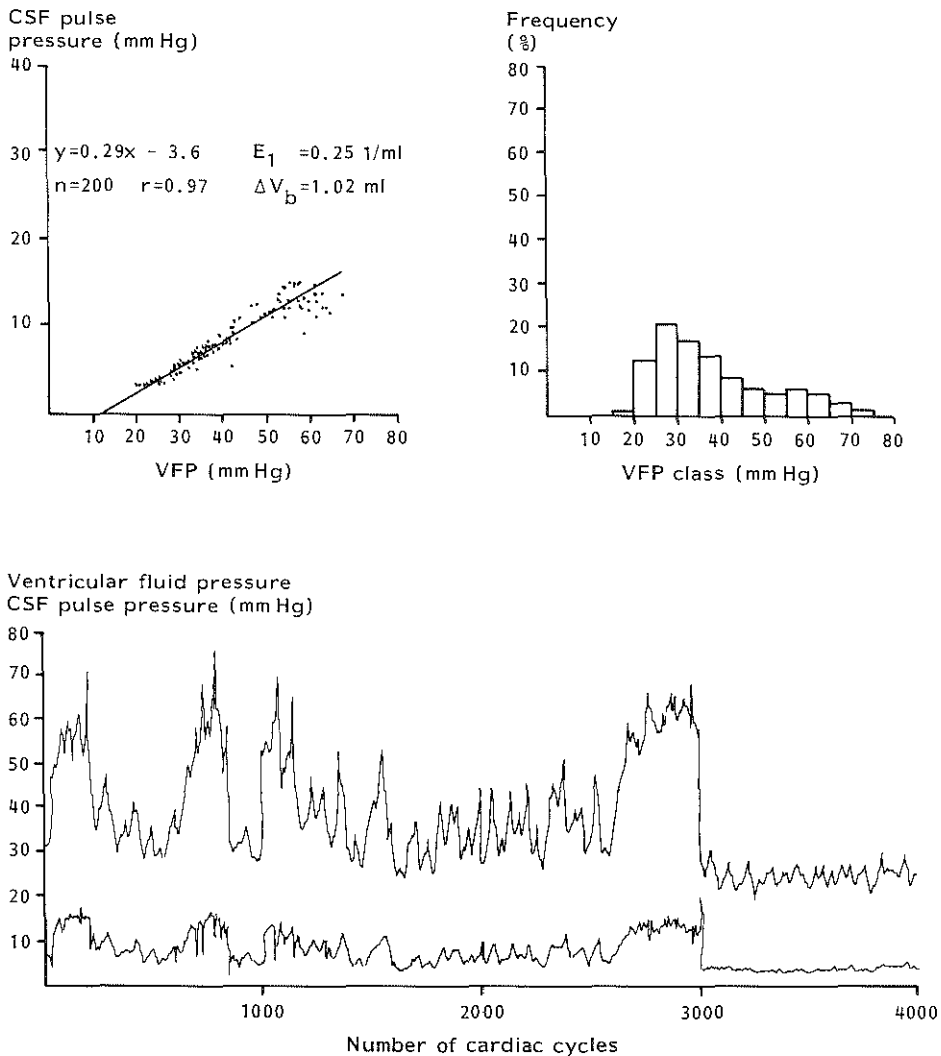


Fig. 19. Computer plot of ventricular fluid pressure recording in 4 year old child with communicating hydrocephalus and malfunctioning CSF shunt. Compare with Figure 20.

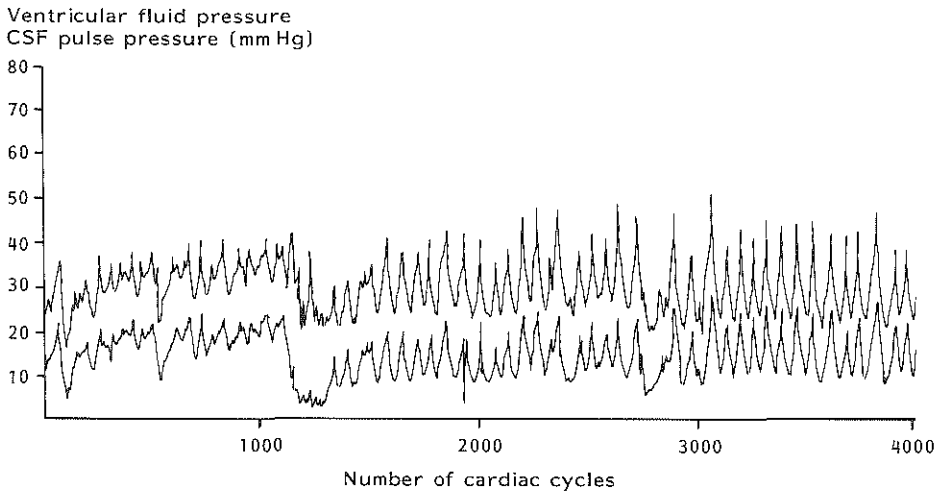
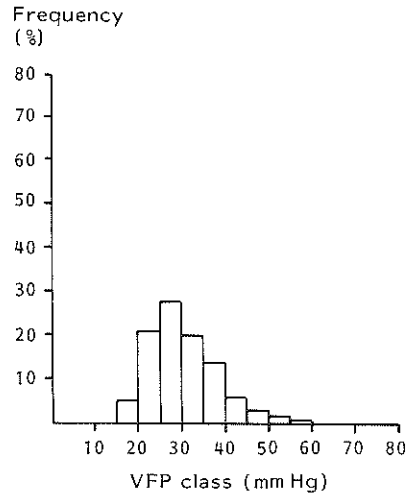
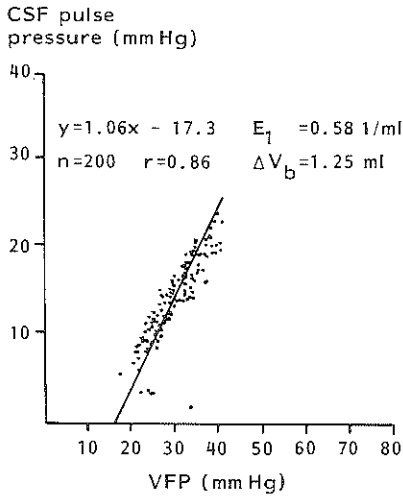


Fig. 20. Computer plot of ventricular fluid pressure recording in 2 year old child with communicating hydrocephalus and malfunction of CSF shunt. Compare with Figure 19. Note that difference in E_1 is accurately reflected by difference in slope of relationship between CSF pulse pressure and VFP. This is because magnitude of ΔV_b is approximately the same in both patients.

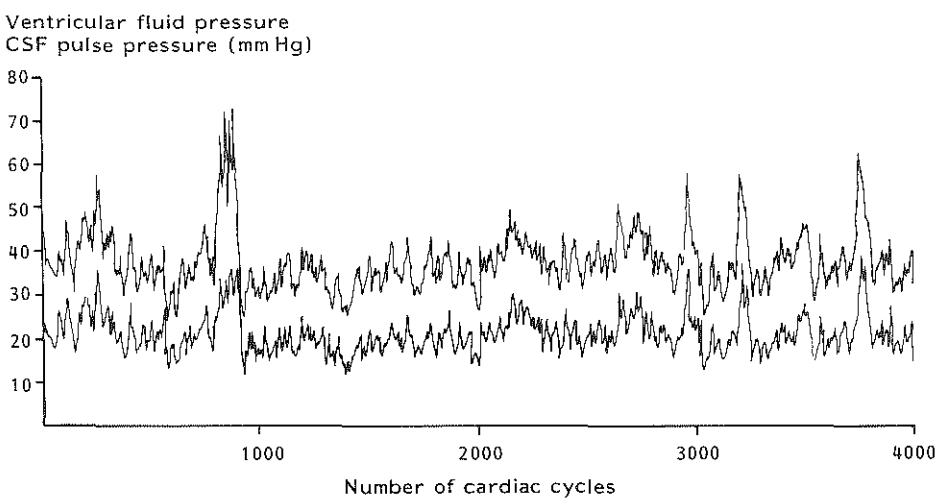
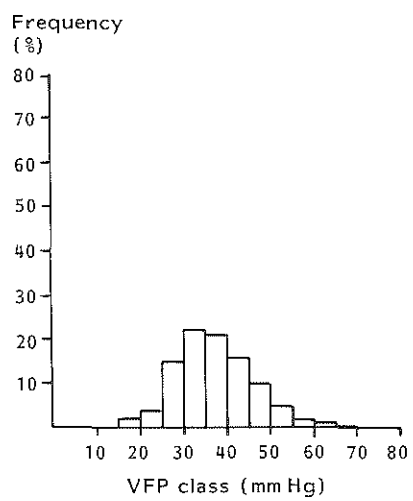
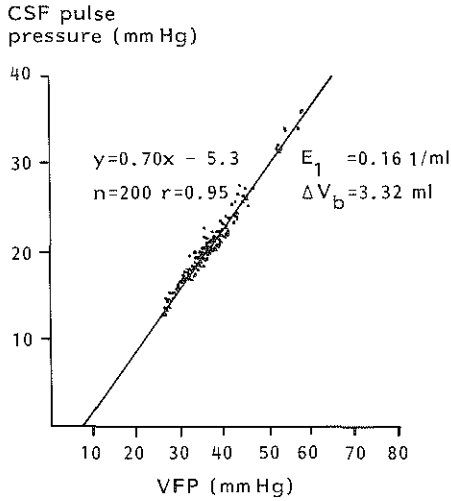


Fig. 21. Computer plot of ventricular fluid pressure recording in adult patient suffering from benign intracranial hypertension. Note steep slope of CSF pulse pressure versus VFP relationship in spite of relatively low E_1 . As a result calculated value for ΔV_b is high.

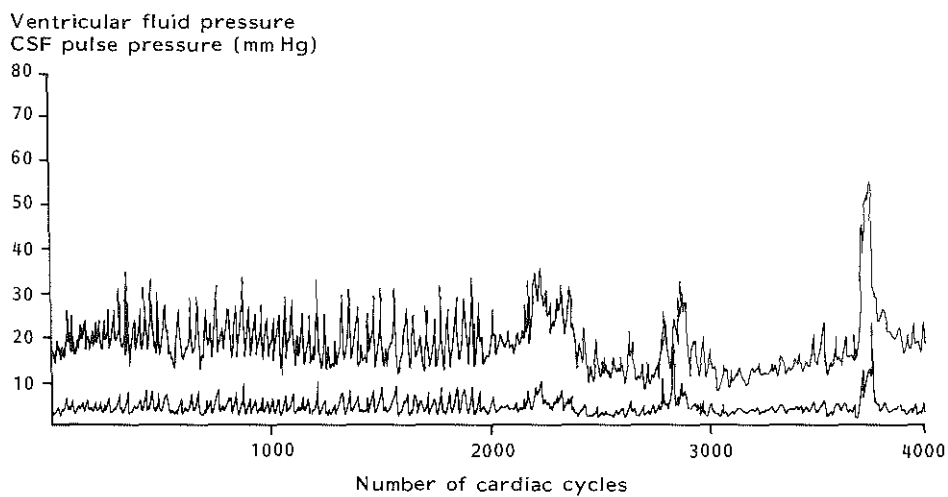
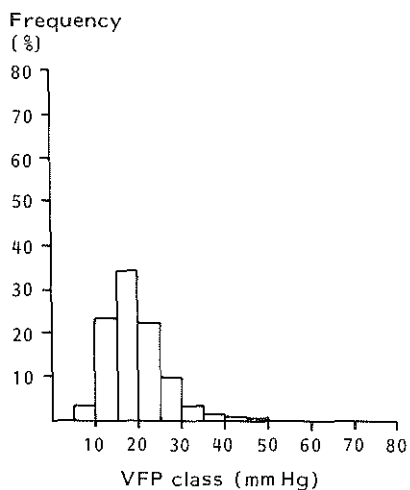
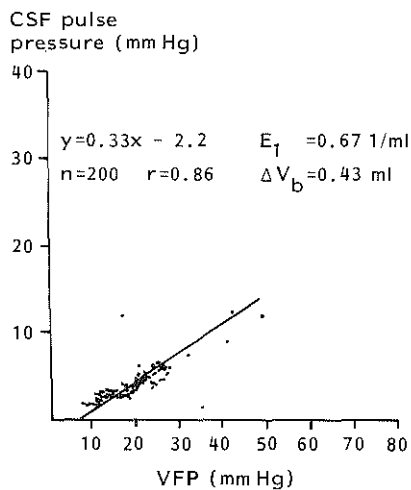


Fig. 22. Computer plot of ventricular fluid pressure recording in 8 year old child with non-communicating hydrocephalus and malfunction of CSF shunt. Note weak slope of relationship between CSF pulse pressure and VFP in spite of large E_1 , resulting in low value for ΔV_b .

Observations during plateau waves

An interesting observation was made when so-called plateau waves occurred during the pressure recording. These pressure waves, first described by Janny (1950) and later by Lundberg (1960), are characterized by large, plateau-like formations with steeply ascending and descending slopes and with a duration of 5 to 20 minutes. Figure 23 shows an example of this

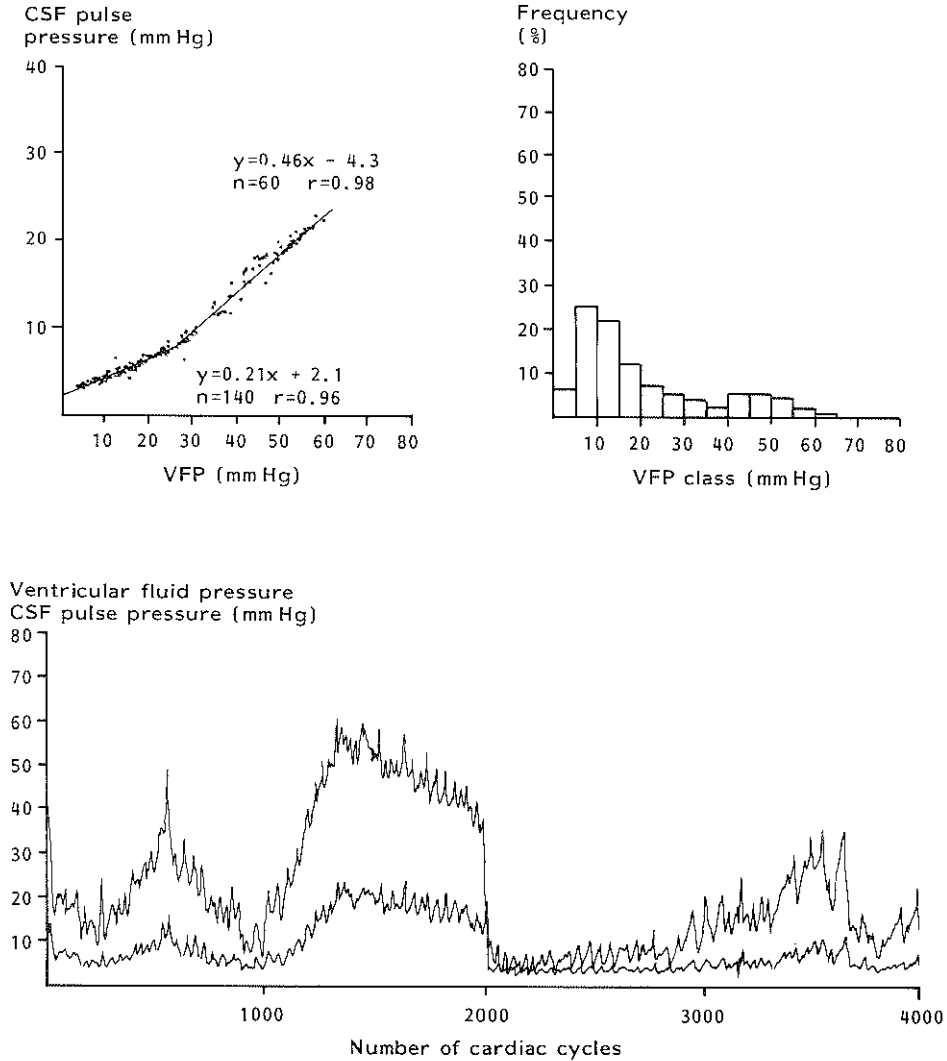


Fig. 23. Computer plot of ventricular fluid pressure recording in adult patient with hydrocephalus due to glioma of pons. Tracing shows typical plateau wave and some abortive waves. Data of baseline VFP (3-24 mm Hg) and of waves (25-60 mm Hg) were treated separately. Note breakpoint in relationships between CSF pulse pressure and VFP of both pressure ranges. During plateau wave CSF pulse pressure increases more rapidly.

type of wave. In the recording intervals during which they occurred a breakpoint in the CSFPP-VFP relationship was observed, caused by a steepening of the regression line during the pressure wave. As the slope of the relationship is determined by both E_1 and ΔV_b , we wondered which of these had caused the increase in slope. An increase in E_1 , implying a steeper volume-pressure curve, seemed the most plausible explanation at first sight, as it is generally believed that plateau waves occur when the elastance is high (Langfitt et al., 1965; Lundberg et al., 1968; Miller, 1975). Therefore, it was decided to devote a separate study to this problem by determining E_1 and ΔV_b both at base-line VFP and during the plateau wave. As the plateau waves happened to occur during later intervals of the pressure recordings, these data are not included in the material upon which the results of the main study are based.

Four patients exhibiting plateau waves were studied. At base-line ICP VPRs were obtained in the usual manner. At the crest of nine plateau waves (two in each of three patients and three in one patient) volume-pressure testing was performed either by rapid withdrawal of CSF or by bolus injection immediately followed by aspiration of fluid. The combined results of the volume-pressure tests are given in Figure 24. The VPRs obtained at the base-line VFP showed a significant linear relationship with the VFP with the following regression equation:

$$\text{VPR} = 0.12 \text{ base-line VFP} + 1.5 \quad (n = 30, r = 0.51, P < 0.001).$$

In contrast to these results, those obtained during the plateau waves showed a scatter of data without any significant correlation. Moreover, the latter responses were generally lower than was expected on the basis of linear extrapolation of the base-line data. The mean E_1 at the base-line VFP, computed from the regression line using Equation 2.6, was 0.11 l/ml. The lack of correlation between VPR and VFP at the plateaus indicates that the volume-pressure relationship has lost its exponential nature and, consequently, the mathematical model can no longer be applied. These data were therefore analysed by calculating the elastance at the mean plateau VFP which was 58.5 mm Hg. The mean elastance at this pressure level was 5.2 mm Hg/ml. This was lower than expected, since extrapolation of the regression line would have yielded, at the same VFP, a mean plateau elastance of 8.5 mm Hg/ml.

Since the shape of the above plateau waves was disturbed by the

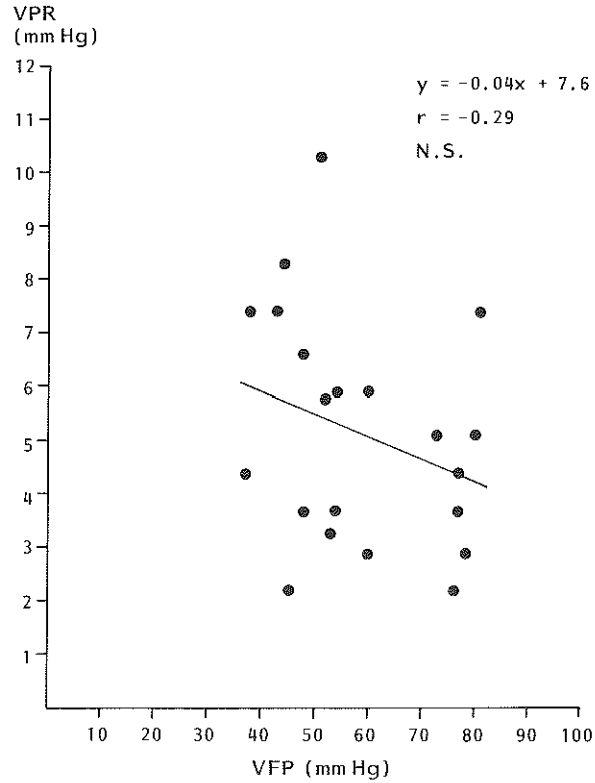
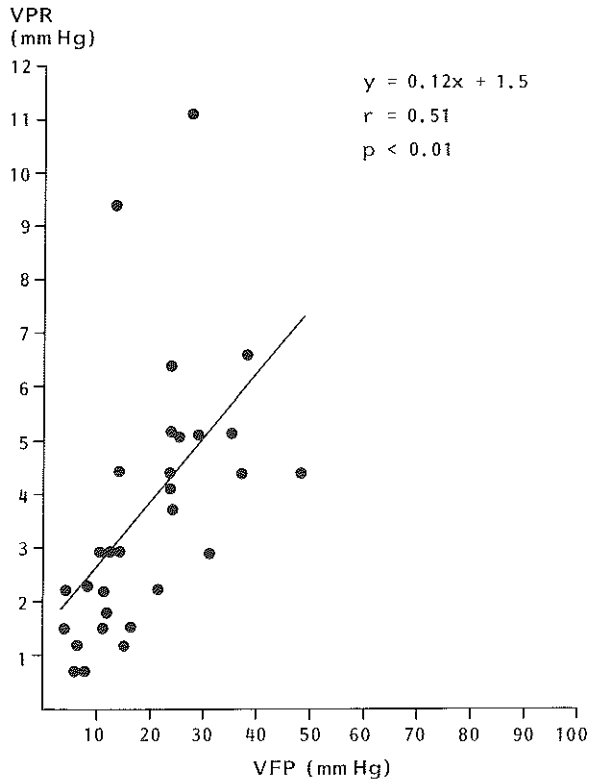


Fig. 24. Plots of volume-pressure response (VPR) against ventricular fluid pressure (VFP) at base-line VFP (left) and during plateau waves (right) in four patients. At base-line significant linear relationship is observed (regression equation given) which is lost during plateau waves. VPR obtained during plateau waves was generally lower than expected on the basis of extrapolation of regression line at base-line, indicating increase in compliance during plateau waves.

volume-pressure tests, they were not considered suitable for pulse pressure analysis. For this purpose one typical, neighbouring plateau wave was selected in each patient. The recording intervals in which they occurred were analysed as previously described, but the CSFPP-VFP relationship was calculated separately for the VFP range of the base-line and of the plateau wave as shown in Figure 23. Linear relationships with high correlation coefficients were always obtained, both during and outside the pressure waves. The regression equations are given in Table 4. The gradient of the regression line always increased during the plateau wave, the mean result showing a two-fold increase. The mean group ΔV_b for the VFP range exclusive of the pressure waves, calculated from E_1 and the mean slope of the regression lines, was 1.5 ml. ΔV_b at the mean plateau VFP can be calculated from the mean CSF pulse pressure at this VFP and from the mean plateau elastance according to:

$$E = \frac{\Delta P}{\Delta V_e} = \frac{\text{CSFPP}}{\Delta V_b} .$$

The CSF pulse pressure was computed from the mean regression equation yielding a value of 18.3 mm Hg at a VFP of 58.5 mm Hg. With a mean plateau elastance of 5.2 mm Hg/ml, the mean value for ΔV_b at the plateaus was found to be 3.5 ml, representing a more than two-fold increase compared with ΔV_b at the base-line.

In conclusion, these results show that the disproportionate increase in CSF pulse pressure during plateau waves is due to an increase in ΔV_b and not to a disproportionate increase in elastance.

Table 4. Regression equations of relationship between CSF pulse pressure (y) and ventricular fluid pressure (VFP; x) at base-line VFP and during plateau wave in four patients. VFP ranges, correlation coefficients (r), and mean results are given.

No	Base-line			Plateau wave		
	VFP range (mm Hg)	Regression equation	r	VFP range (mm Hg)	Regression equation	r
1	10-30	y=0.18x+0.1	0.86	31-70	y=0.30x-1.9	0.92
2	10-30	y=0.18x+0.9	0.88	31-90	y=0.48x-7.6	0.96
3	10-34	y=0.15x+2.0	0.79	35-70	y=0.27x-1.6	0.79
4	3-24	y=0.21x+2.1	0.96	25-70	y=0.46x-4.3	0.98
Mean		y=0.18x+1.3			y=0.38x-3.9	

4.4 Discussion

Volume-pressure relationship

As mentioned before, a linear relationship between VPR and ICP, demonstrated by pooling the results of a group of patients, cannot be held as definite proof of the exponential nature of the craniospinal volume-pressure relationship in the individual patient, as was done in the original work of Miller et al. (1972 and 1973). However, as discussed in Chapter 2.3, there is sufficient evidence from both animal experimental and clinical research to make an exponential relationship acceptable as a workable model. The experimental work described in the subsequent chapters will provide further evidence in this respect.

The slope of the VPR-VFP relationship found in this study is less steep than that reported by Miller et al.: 0.14 versus 0.20 respectively. In a later study Miller and Leech (1975) found a slope of 0.16. These differences are probably due to the difference in composition of the clinical material of the various series with respect to intracranial pathology and also to age, as will be discussed later. With regard to intracranial pathology the variation in ventricular size may be an important factor, although the opinions on how ventricular volume affects the craniospinal volume-pressure relationship differ. Cohadon et al. (1975) reported a negative correlation between the size of the ventricles and the slope of the volume-pressure curve. Miller and Leech (1975) also found low values of VPR in patients with ventricular enlargement. According to these results the small VPR-VFP slope in our study might be explained by the large proportion of patients with hydrocephalus (Table 1). Sklar et al. (1980), on the other hand, found the elastance to be directly proportional to ventricular size. We believe that it is incorrect in any case to compare the volume-pressure functions of series of patients by pooling the VPR data per series. The data should be used to calculate volume-pressure parameters for each patient individually, after which the mean group value may be used to characterize the volume-pressure relationship of a particular group of patients. For example, the mean group E_1 calculated from the slope of the combined VPR versus VFP plot is 0.13 l/ml, which is half the mean value of the coefficients calculated for each individual patient.

Since the VPR varies with the ICP, the volume-pressure relationship of an individual is best characterized by a pressure independent term such as the elastance coefficient. As mentioned before, the computation of E_1 from the model equations poses a problem, since it requires knowledge of the term P_0 which cannot be supplied by a single volume-pressure test. The assessment of P_0 requires at least two volume-pressure tests at different levels of ICP, but preferably a number of tests on account of the variability of the VPR. This is less practical in the clinical situation as it increases the hazards related to volume-pressure testing, i.e., infection and secondary pressure rises. In the present study the problem of the missing P_0 was handled by taking the P_0 from the CSFPP-VFP relationship. The mean value of P_0 was relatively small (3.2 mm Hg), but nonetheless as Table 2 shows, by ignoring P_0 E_1 was on average underestimated by approximately 20%. From the Equations 2.6 and 2.9 it is clear that the error in the computation of E_1 introduced by ignoring P_0 will be greatest in the low ICP range.

A few studies have provided data on the volume-pressure relationship in normal patients, which can be used as a reference for the values of E_1 found in this series of mixed pathology and consisting of both adults and children.

Fridén and Ekstedt (1980), in 18 patients selected as normal from a total of 105 patients, found a value of 0.21 ± 0.09 for the slope of the linear fit of elastance versus ICP. According to Equation 2.2 this slope parameter is equal to E_1 . Shapiro et al. (1980) found a mean PVI of 25.9 ml (range 21.5-30.5 ml) in seven adults without intracranial mass pathology. As discussed in Chapter 2, the PVI as a parameter of compliance is inversely related to E_1 and can be converted into E_1 by using Equation 2.8. This yields for Shapiro's data an E_1 of 0.09 l/ml (range 0.08-0.11 l/ml). Since the PVI is established from the Marmarou volume-pressure model, which does not take account of P_0 , this value should be compared with that of the E_1 in our study calculated on the assumption that P_0 equals 0. The same authors found lower PVI values, ranging from 8.2 ml to 30.1 ml (converted E_1 values: 0.08-0.28 l/ml), in a group of 23 normal children. The reduced compliance in children was shown to correlate with their smaller neural axis volume as determined by external measurements. The relatively high values for E_1 in this study (Table 2) are thus in agreement with its pathological setting. One should, however, be cautious

in comparing volume-pressure parameters from different studies because of the differences in the technique used for their assessment.

CSF pulse pressure

As stated before, the study of the craniospinal volume-pressure relationship and its clinical significance was not the primary aim of these investigations, which was rather to establish the relationship between CSF pulse pressure and ICP, as well as to compare this relationship with the volume-pressure relationship. The patients in this study underwent ICP recording for a limited period of time and mainly for diagnostic purposes. During this time they were in a stable condition with regard to both their neurological state and their vital functions. We have assumed, therefore, that their volume-pressure relationship did not change during the recording. This assumption will be even more valid with regard to the first interval of 4000 heart beats of the recording period which was considered in this study and during which the volume-pressure relationship was assessed.

The results show that under these circumstances the relationship between CSF pulse pressure and ICP can be accurately described by a linear function. Janny (1974) was one of the first to report a linear CSFPP-ICP relationship. He found an average gradient of 0.36 in five patients in the ICP range up to 40 mm Hg. Slopes of 0.33 ± 0.08 , 0.34 ± 0.15 and 0.47 ± 0.06 were found in normal patients without intracranial pathology by Szewczykowski et al. (1977), Godin et al. (1980) and Fridén and Ekstedt (1980) respectively. The relatively steep mean slope of 0.40 ± 0.16 found in this study may be attributed to the intracranial mass pathology of the majority of our patients and may, as such, be taken as consistent with the high elastance coefficient of this series.

If the mathematical model is applied to the result of a linear CSFPP-ICP relationship, the important conclusion is that, under stable clinical conditions, the second variable determining the height of the CSF pulse, the pulsatile change in CBV, is constant and independent of the ICP. In other words, during elevation of the ICP the increase in CSF pulse pressure is solely determined by the increase in elastance. This is contradictory to what would have been expected on the basis of the outcome of the discussions in Chapter 3.3 on the factors affecting ΔV_b . Among these

factors was the ICP, which may influence ΔV_b by means of two mechanisms: alterations in the cerebral perfusion pressure and compression of the venous outflow tract. During elevation of the ICP both mechanisms are operative in increasing the time lag, or phase shift, between the pulsatile inflow and outflow of cerebral blood, resulting in a gradual increase in ΔV_b as demonstrated in Figure 11. It can be easily seen that a steadily increasing ΔV_b with rising ICP implies a non-linear relationship between CSF pulse pressure and ICP.

Some authors have indeed described the CSFPP-ICP relationship by a non-linear, exponential function. Guinane (1975) found an exponential relationship in cats in the ICP range from normal up to 60 mm Hg. Hartmann (1980) found an exponential relationship in the same ICP range by pooling the data obtained in a group of 25 patients with acute subarachnoid haemorrhage. The discrepancy between these results and ours may be explained by the relatively small pressure ranges examined in the individual patients of this study. With the exception of intervals showing plateau waves, the spontaneous fluctuations of the ICP did not usually exceed 20 to 30 mm Hg. This could mean that the increase in ΔV_b during elevation of the ICP is apparently so small that the data can also be analysed by linear fits, suggesting a constant ΔV_b .

In this respect the increase in slope of the CSFPP-ICP relationship observed during plateau waves is of interest. Here, the increase in ΔV_b at the beginning of the pressure waves is large enough to cause a marked increase in slope. The origin of plateau waves is generally attributed to an increase in CBV due to a sudden loss of vasoconstrictor tone in the cerebral resistance vessels (Guillaume and Janny, 1951; Lundberg, 1960; Lundberg et al., 1968; Risberg et al., 1969), a phenomenon which has been termed cerebral vasomotor paralysis by Langfitt et al. (1965). At the same time this explanation may serve to explain the increase in ΔV_b , as the reduction in CBF inflow resistance during vasoparalysis affects the pulsatile flow profile as previously argued. The increase in ΔV_b is magnified by the effect of the markedly increased ICP on the venous outflow.

With regard to the values for ΔV_b found in this study (mean value: 1.67 ml) it should be noted that they have to be considered with caution, since they were derived from pulse pressure data and from E_1 on the basis of a mathematical concept, and were not empirically determined. The order

of their magnitude, however, seems plausible in the light of the following argument. Assuming a CBF of 50 ml/100 g/min, a brain weight of 1300 g and a heart rate of 72/min, the CBF per cardiac cycle can be calculated to amount to approximately 9 ml in normal man. If the CBF were nonpulsatile in nature, no change in CBV would occur at all. The same would apply to identical pulsatile inflow and outflow profiles. If inflow and outflow were completely separated in time, the resulting transient increase in CBV per cardiac cycle would be 9 ml. Consequently, we have to assume that the time lag between pulsatile inflow and outflow of CBF is such that during the maximum change in CBV approximately 80% of the inflow of blood is compensated for by venous outflow and 20% (i.e. 1.67 ml) has to encroach on the volume buffering capacities of the craniospinal system. If the spinal cord flow, which in our view also contributes to the formation of ΔV_b , is taken into account, the actual percentage would become even lower. When the total volume of the craniospinal system is considered, the magnitude of the pulsatile change in CBV is thus far less than 1% of this volume. From the relationship between CSF pulse pressure and ICP found in this study (Table 3) the pulse pressure at the modal ICP of 15 mm Hg (Fig. 17) can be calculated as amounting to 4.4 mm Hg, which is about 30% of the modal ICP. It may thus be concluded that the volume changes occurring with pressure changes in the craniospinal system are very small indeed, so that the requirements of the Monro-Kellie doctrine seem almost fulfilled.

The conflict between CSF pulse pressure and volume-pressure response during plateau waves

From the results of the separate study with regard to the phenomenon of the divergence of CSF pulse pressure and VPR during plateau waves, several conclusions can be drawn. The value of 0.11 l/ml for the elastance coefficient at the base-line ICP is surprisingly low compared with that of 0.26 l/ml found in the main study consisting of patients with normal as well as with elevated ICP. The E_1 found here is within the normal range of 0.09 to 0.11 l/ml as reported by Shapiro et al. (1980). This seems to indicate that, in contrast with what is generally believed, a 'tight-brain' situation is not an absolute precondition for the emergence of plateau waves. Furthermore, the VPR data obtained during the plateau waves suggest that the exponential nature of the craniospinal volume-pressure relation-

ship is lost and that the system has become relatively more compliant. This would imply a bend in the volume-pressure curve towards a more horizontal course, much like the low elastance plateau close to the level of the blood pressure of Löfgren's curve (Fig. 3).

It should be noted that part of the VPRs during the plateau waves were obtained by withdrawal instead of injection of fluid. Miller et al. (1973) have found the VPR to be lower following withdrawal than following injection, suggesting some form of hysteresis of the craniospinal system. This may thus account for the low value of some of our responses, although the VPRs following injection were also generally lower than expected. Moreover, Shapiro et al. (1980) did not find a difference between withdrawal and injection.

The increase in ΔV_b at the plateau waves lends support to our concept of the origin of ΔV_b , if the causative mechanism of plateau waves, cerebral vasoparalysis causing an increase in CBV, is taken into consideration. As argued before, cerebral vasoparalysis lowers the arterial inflow impedance resulting in a shift of pulsatile flow from diastole to systole. The effect of this event on the time lag between the pulsatile inflow and outflow is reinforced by the delay in venous outflow as a result of the increase in outflow resistance under the influence of the high plateau ICP.

Clinical implications

The elastance provides information on the actual volume-pressure relationship in a patient at a given point in time, irrespective of the ICP: a high elastance implies that a small change in craniospinal volume causes a large change in ICP, and vice versa. An increase in elastance with rising ICP has been shown to be a general and fundamental property of the craniospinal system. In that light, calculations of elastance do not add new information to that already obtained from measurement of the level of ICP alone. Elastance calculations do become of importance when the elastance is related to the ICP, as this relationship reflects the elastic properties of the craniospinal system which are unique for each individual patient and within a patient for each specific clinical situation. For the same reason, before it can be used as a volume-pressure parameter, the CSF pulse pressure has to be related to the ICP. In clinical practice this will make it necessary for some form of automatic data processing to be used,

requiring more complicated technical equipment and thereby affecting the simplicity of ICP recording. On the other hand, statistical analysis of the ICP has already been advocated by many authors as a means of condensing and ordering the huge amount of data collected by ICP monitoring over extended periods of time (Janny et al., 1972; Kullberg, 1972; Hulme and Cooper, 1975; Barnes and McGraw, 1975; Brock et al., 1975; Brock et al., 1976; Turner et al., 1976; Corbin et al., 1980; Graham et al., 1980; Mason et al., 1980; Stalhammer et al., 1980; Takizawa et al., 1980). It has been claimed that in this way characteristics may be revealed that are clinically useful but are not seen by scanning the raw data. According to the results of this study, the relationship between CSF pulse pressure and ICP can be treated by simple linear regression analysis, the slope of which would provide the clinician with a continuously available volume-pressure parameter. Furthermore, in view of the high correlation coefficients of the linear fits and the variability of the VPR, the reliability of volume-pressure relationship assessment would be enhanced. The major advantage of this method lies in the extraction of information from the ICP signal itself, doing away with the necessity of access to the CSF space with the associated risks of infection.

However, before this method can be put into practice, the second determinant of the CSF pulse pressure, the pulsatile change in CBV, still constitutes a serious problem. It has been shown that the slope of the CSFPP-ICP relationship can never be taken as an absolute parameter of the volume-pressure relationship without taking into account the magnitude of ΔV_b . The magnitude of ΔV_b , however, is unknown and can only be calculated after the volume-pressure relationship has been assessed. During ICP monitoring in the individual patient the slope could still function as a relative measure of the volume-pressure relationship, as changes in slope reflect changes in E_1 so long as ΔV_b remains constant. On theoretical grounds we have established that ΔV_b is determined both by extracranial and intracranial haemodynamic factors (Chapter 3.3). Clinical variables such as the blood pressure, the carbon dioxide content of the blood and the heart rate, among other factors, may thus affect the magnitude of ΔV_b and thereby the CSF pulse pressure and its relationship with the ICP. Some of these factors may simultaneously affect the volume-pressure relationship. The interaction of variables that act upon the pulse pressure in clinical practice may therefore be so complex that changes in slope

become difficult to interpret. It remains to be seen, however, to what extent the slope is altered by changes in ΔV_b . At any rate, as can be seen from Table 3 and Figure 18, variations in ΔV_b between patients are sufficiently large as to prevent confident discrimination between their volume-pressure functions on the basis of the CSFPP-ICP relationship.

The phenomenon of a relatively low VPR in contrast with a high CSF pulse pressure observed during plateau waves suggests that under these circumstances the CSF pulse pressure is a better clinical parameter than the VPR. Of course, a plateau wave in itself is an ominous clinical sign. It would therefore be of interest to know whether under other circumstances of defective cerebral vascular muscle tone, such as impairment of CBF autoregulation, the same phenomenon was to be found. In that case the clinical state of a patient would be determined by the defective autoregulation rather than by the increased craniospinal compliance, and, again, the pulse pressure would be the better parameter.

In view of the results of this study it seems worthwhile to explore the relationship between pulse pressure and ICP further, in more detail and under controlled conditions in the laboratory, and to see how it relates to the volume-pressure relationship. In patients, these relationships could only be examined in a restricted range of ICP. How would the CSF pulse pressure behave in the full range of ICP up to the level of the blood pressure? How does the pulsatile change in CBV affect the pulse pressure when changes in intracranial haemodynamics are induced and what are the net effects on the pulse pressure when the volume-pressure relationship is simultaneously altered? Will it be possible to assess the mechanisms involved in the origin of ΔV_b in a more direct way? These questions will be dealt with in the following chapters.

Conclusions

1. In clinical patients in whom the relationship between CSF pulse pressure and ICP was examined in restricted pressure ranges, a linear relationship was found.
2. A weak correlation was found between the slope of this relationship and the elastance coefficient.

3. Calculated values of the pulsatile change in CBV showed considerable variation between patients.
4. During plateau waves craniospinal compliance was found to be increased.
5. The disproportionate increase in CSF pulse pressure during plateau waves was attributed to an increase in the pulsatile change in CBV.

CHAPTER 5

**CEREBROSPINAL FLUID PULSE PRESSURE AND CRANIOSPINAL VOLUME-
PRESSURE RELATIONSHIPS DURING EXPERIMENTAL
BRAIN COMPRESSION**

"There are other points of interest concerning which my curtailed time forbids making more than passing mention. The pulsation of the brain, for instance, which increases pari passu with the increase of intracranial tension, may give the surgeon at times valuable data."

*H. Cushing,
The Mütter Lecture, Philadelphia, December 3, 1901*

5.1 Introduction

Two factors have been identified which influence the CSF pulse pressure: firstly, the pulsatile change in CBV (ΔV_b) and secondly, the slope of the craniospinal volume-pressure curve as determined by the elastance coefficient (E_1). In the clinical study a linear relationship was established between the pulse amplitude and the ICP and it was mathematically derived that the slope of the regression line is determined by the product of ΔV_b and E_1 . This implies that, given a constant E_1 , ΔV_b can also be regarded as constant for the relatively narrow pressure ranges encountered clinically. It may be further inferred that, so long as ΔV_b remains constant, changes in slope occurring during continuous ICP recording truly reflect changes in E_1 .

A disturbing factor in this respect, however, is that there are many variables that may be expected to affect the magnitude of ΔV_b . It was these variables which were apparently responsible for the lack of strong correlation between the slope of the CSFPP-ICP relationship and E_1 in the patients. ΔV_b may also vary in the individual patient who passes through the whole range of ICP. Cerebral vasodilatation occurring during plateau waves, for example, was demonstrated to produce an increase in the pulsatile volume change. The same may be expected to occur when CBF autoregulation is lost as a result of cerebral vasoparesis.

In order to study the relationship between CSF pulse pressure and ICP for the whole range of ICP more precisely and under controlled conditions, a series of experiments was designed in dogs. The craniospinal volume-pressure relationship was simultaneously assessed and compared with the CSFPP-ICP relationship from which inferences were made with regard to the behaviour of ΔV_b with rising ICP.

5.2 Experimental methods

Preparation and Measurements

The experiments were performed on six adult mongrel dogs of either sex weighing from 10 to 19 kg. Anaesthesia was induced with intravenously administered thiopentone (30 mg/kg) and maintained with a mixture of nitrous oxide and oxygen (2:1) supplemented by choralose (50 mg/kg) intravenously. The animals were ventilated using a modified Starling pump, the stroke volume of which was adjusted to maintain normocapnia (PaCO_2 : 37-43 mm Hg). Body temperature was maintained between 36° C and 38° C by heating lamps. Throughout the experiment normal saline was slowly infused intravenously.

The animals were placed in a stereotaxic frame in the sphinx position. The scalp and temporal muscles were reflected. A balloon made from glove rubber was used for elevating the ICP by cerebral compression; it was placed epidurally through a burr hole in the right frontotemporal area and connected to a variable speed infusion pump (Sage Instruments, model 351). The VFP was measured bilaterally using needles (inside diameter 1.5 mm) introduced by the continuous infusion method (Fig. 25) into the lateral ventricles through small burr holes in the parietal area. The coordinates of the burr holes were: 8 mm lateral to the median sagittal plane and 10 mm anterior to the centre of the external auditory meatus. All bone defects were sealed with acrylic dental cement. The cisterna magna pressure (CMP) was measured by means of a needle inserted percutaneously into the cisterna magna. Systemic arterial pressure (SAP) was monitored from an aortic catheter introduced via the femoral artery. Central venous pressure was measured in the inferior vena cava by catheterization of the femoral vein. The electrocardiogram (ECG) was recorded via needle electrodes placed in the limbs of the animal. All pressures were measured continuously by pressure transducers (Bell and Howell) placed at the level of the right atrium. Details with regard to the frequency response of the ventricular needle to manometer system are given in Appendix 1. The various signals were displayed on two chart recorders (Devices M4 and M2) and stored on tape (Philips Analog 7). Arterial blood gases were measured at 30 minute intervals throughout the experiment using a direct reading electrode system (Radiometer BMS 3),

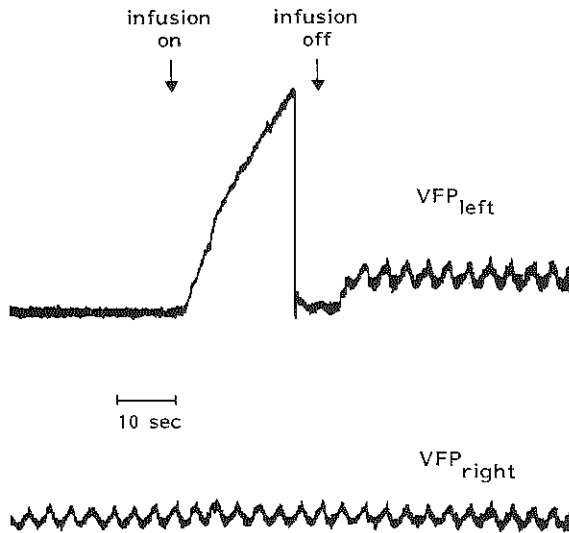


Fig. 25. Introduction of needles for measurement of ventricular fluid pressure (VFP) by means of continuous infusion method. Needle in right ventricle has already been inserted (lower tracing). During passage of needle through cerebral mantle pressure rise is built up (upper tracing). Sudden drop in pressure indicates perforation of ventricular wall. Average insertion depth was 19 mm measured from outer table of skull.

and values were corrected for temperature differences between the animal and recording system (Severinghaus, 1966).

Experimental protocol and Data collection

After all pressures had stabilized the extradural balloon was distended by continuous inflation with normal saline at a rate of 1.0 ml per 15 minutes, and after each experiment the balloon was checked for leaks. The volume-pressure test was used as a method of acquiring volume-pressure data. A cluster of four tests was carried out at five minute intervals by rapid serial injection of 0.05 ml of normal saline into the left ventricle using a three-way stopcock interposed in the tubing connecting the ventricular needle to the pressure transducer (Fig. 26). The VPR was read from the injected ventricle and calculated from the immediate change in mean VFP in corresponding parts of the VFP respiratory cycle. All mean pressures including SAP were calculated from the diastolic pressure plus one-third of the pulse pressure. In order to reduce the variability from errors inherent in the manoeuvre, the mean VPR of each cluster of four tests was taken and related to the mean pre-injection VFP. After completion of the four tests the VFP always returned to the

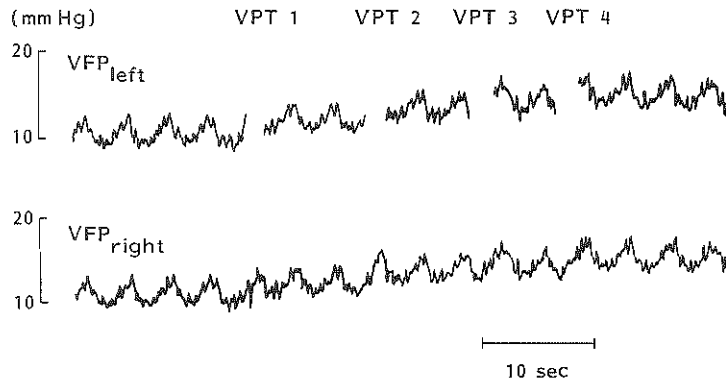


Fig. 26. Series of four volume-pressure tests (VPT 1-4) by rapid injection of 0.05 ml aliquots into left ventricle (upper tracing). Volume-pressure response was read from injected ventricle and defined as immediate change in ventricular fluid pressure (VFP) in corresponding parts of respiratory VFP wave. Note similarity of responses in both ventricles.

steady state level before the next time interval was reached.

During the tests the speed of the chart recorder was increased, so that the amplitude of the CSF pulse could be distinguished clearly. Eight pulse pressures were calculated per interval of five minutes by taking the average values of the pulse pressures over the last respiratory cycle before and the first cycle after each bolus injection. The means of the four pulse pressures before and after each test were related to the mean pre-injection and peak VFP respectively. As a result of this procedure each time interval yielded one VPR and two pulse pressures.

When changes in SAP occurred, as they sometimes did in the advanced stages of cerebral compression, no special measures were taken to keep the SAP at a constant level. But, since changes in SAP are known to affect the craniospinal volume-pressure relationships (Löfgren, 1973; Leech and Miller, 1974) and, probably, the CSF pulse pressure as well, all values of both VPR and pulse pressure obtained at levels of SAP deviating more than 15% from the mean SAP of the experiment were discarded.

The experiment was terminated when the VFP had reached the level of the SAP, except in the case of three animals in which it was continued far beyond this level. The brains were transected at the foramen magnum, weighed (brain weights between 72 and 92 grams), fixed in formalin, and sectioned coronally at 5 mm intervals for pathology. Proper placement of the ventricular needles was verified and major brain lesions from surgical preparation were excluded.

5.3 Results

Relationship between volume-pressure response and ventricular fluid pressure

In the plots of VPR versus VFP three zones could be defined to an extent (Fig. 27). At first, the VPR increased linearly with the VFP. Next, the VPR levelled off or even decreased, and finally, at the advanced stage of cerebral compression, the response started to rise again but more rapidly than before. The regression equations of the first zone are given in Table 5. These linear relationships are in accordance with the mono-exponential volume-pressure model, implying a constant elastance coefficient. E_1 was calculated from the slopes of the regression lines using Equation 2.6. The constant term P_0 followed from the intercepts of

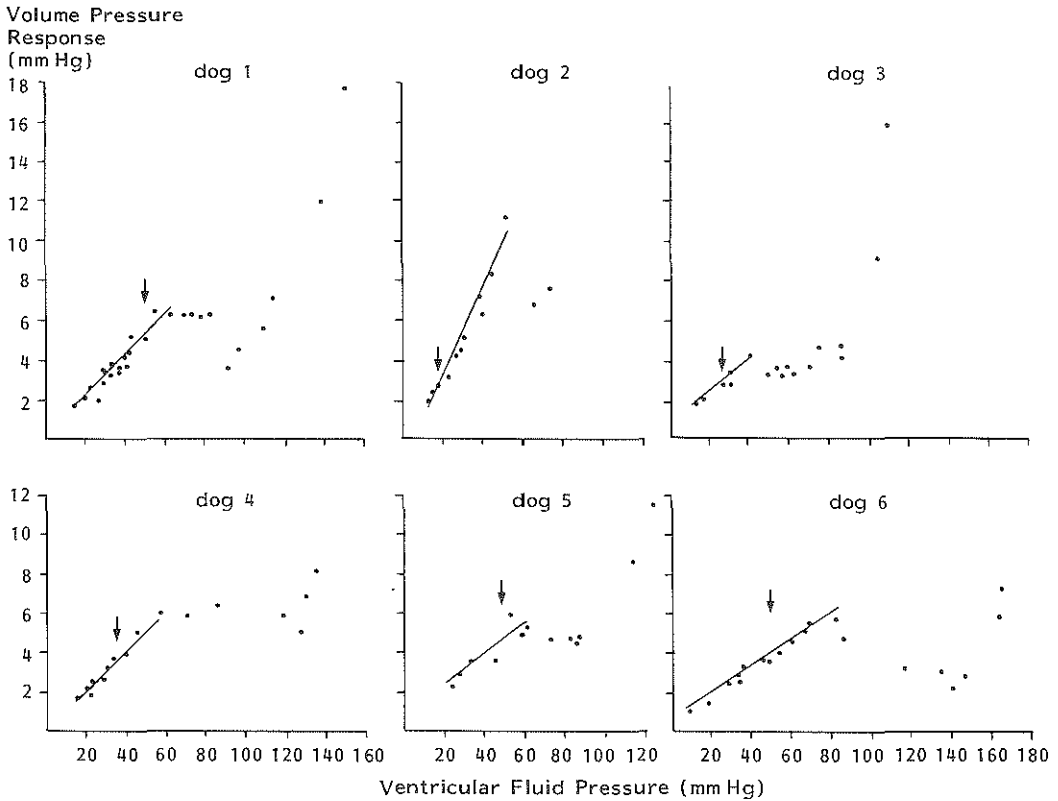


Fig. 27. Plots of volume-pressure response (VPR) against ventricular fluid pressure (VFP) during continuous inflation of extradural balloon in six dogs. Three different zones can be recognised. In first zone VPR increases linearly with VFP. Regression lines are shown and regression equations are given in Table 5. In second zone VPR remains constant and/or decreases, and finally in third zone VPR increases again but more rapidly than in first zone. Arrows indicate onset of tentorial herniation.

Table 5. Relationship between volume-pressure response (VPR) and ventricular fluid pressure (VFP); regression equation, number of datapoints (n), correlation coefficient (r), P_0 , and elastance coefficient (E_1) below first breakpoint, and mean VPR (\pm SD) and elastance above breakpoint. VFP ranges are given.

Animal no	Below breakpoint						Above breakpoint			
	Regression equation	n	r	P_0 (mm Hg)	E_1 (1/ml)	VFP range (mm Hg)	Mean VPR (mm Hg)	n	Elastance (mm Hg/ml)	VFP range (mm Hg)
1	$y=0.10x-0.1$	18	0.95	1.4	1.9	17.1 - 66.3	5.5 ± 1.0	8	110	66.3 - 111.8
2	$y=0.22x-1.5$	11	0.98	6.8	4.0	13.4 - 52.0	7.1 ± 0.6	2	142	65.4 - 72.5
3	$y=0.08x+0.7$	6	0.97	- 8.9	1.5	14.3 - 41.6	3.7 ± 0.6	9	74	49.4 - 87.2
4	$y=0.10x+0.0$	10	0.99	- 0.3	2.0	14.8 - 57.7	5.7 ± 0.6	5	114	57.7 - 126.5
5	$y=0.08x+0.8$	7	0.89	-10.5	1.5	24.0 - 60.1	4.7 ± 0.2	5	94	60.1 - 85.0
6	$y=0.07x+0.6$	13	0.99	- 9.3	1.3	8.8 - 81.0	3.2 ± 0.9	5	64	85.3 - 145.5
Mean	$y=0.11x+0.1$			- 3.5	2.0	15.4 - 59.8	5.0 ± 1.4		100	64.0 - 104.8

Table 6. Ventricular fluid pressure (VFP), systemic arterial pressure (SAP), cerebral perfusion pressure (CPP), and balloon volume at first and second breakpoint.

Animal no	First breakpoint				Second breakpoint			
	VFP (mm Hg)	SAP (mm Hg)	CPP (mm Hg)	Balloon volume (ml)	VFP (mm Hg)	SAP (mm Hg)	CPP (mm Hg)	Balloon volume (ml)
1	66.3	162.3	96.0	5.7	111.8	136.7	24.9	8.3
2	52.0	128.3	76.3	3.3	-	-	-	-
3	41.6	126.6	85.0	1.7	104.6	116.0	11.4	6.0
4	57.7	156.0	98.3	3.0	130.3	153.7	23.4	5.0
5	60.1	134.3	74.2	2.0	112.5	131.3	18.8	5.3
6	81.0	164.0	83.0	4.0	163.9	165.7	1.8	6.7
Mean	59.8	145.3	85.5	3.3	124.6	140.7	16.1	6.3

the lines with the pressure axis. The results are given in Table 5.

The data with regard to the breakpoint between the first and second zone are presented in Table 6. It occurred at a mean VFP of 60 mm Hg but with considerable variation between the animals. A significant positive correlation was found between the VFP and SAP at the breakpoints (Fig. 28) and, consequently, less variation was found when the cerebral perfusion pressures (SAP-VFP) at the breakpoints were considered (Table 6). The

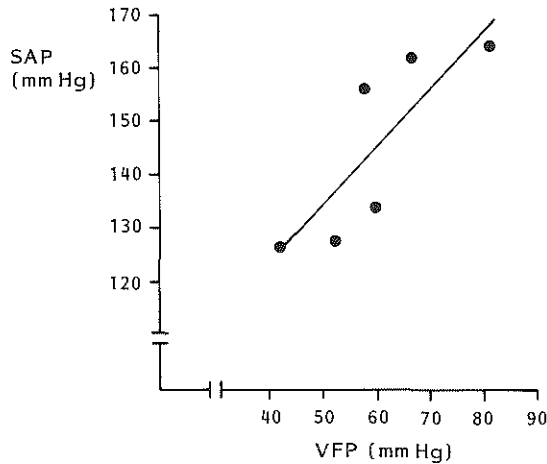


Fig. 28. Plot of systemic arterial pressure (SAP) against ventricular fluid pressure (VFP) at first breakpoint in relationship between volume-pressure response and VFP (Table 6), showing significant positive correlation. Regression equation: $y=1.06x + 80.4$; $r=0.83$; $p<0.05$

question as to whether the breakpoint was related to transtentorial herniation was also considered. With regard to the occurrence of tentorial herniation two stages could be recognized (Fig. 29). Early herniation was defined as the first appearance of a pressure gradient between the lateral ventricle and the cisterna magna. When the CMP did not rise any further and it was no longer possible to detect a VPR in the CMP tracing, tentorial obstruction was considered complete. The corresponding VFPs and balloon volumes are given in Table 7. Comparison of these results with those of Table 6 show that the breakpoint never coincided with either of the two stages of herniation, usually falling in between.

The second zone in the plots of VPR versus VFP poses a problem with regard to the analysis of the data. Fewer data points were available, as the animals passed through this phase of the experiment more rapidly and the blood pressure sometimes fell below acceptable levels. In addition,

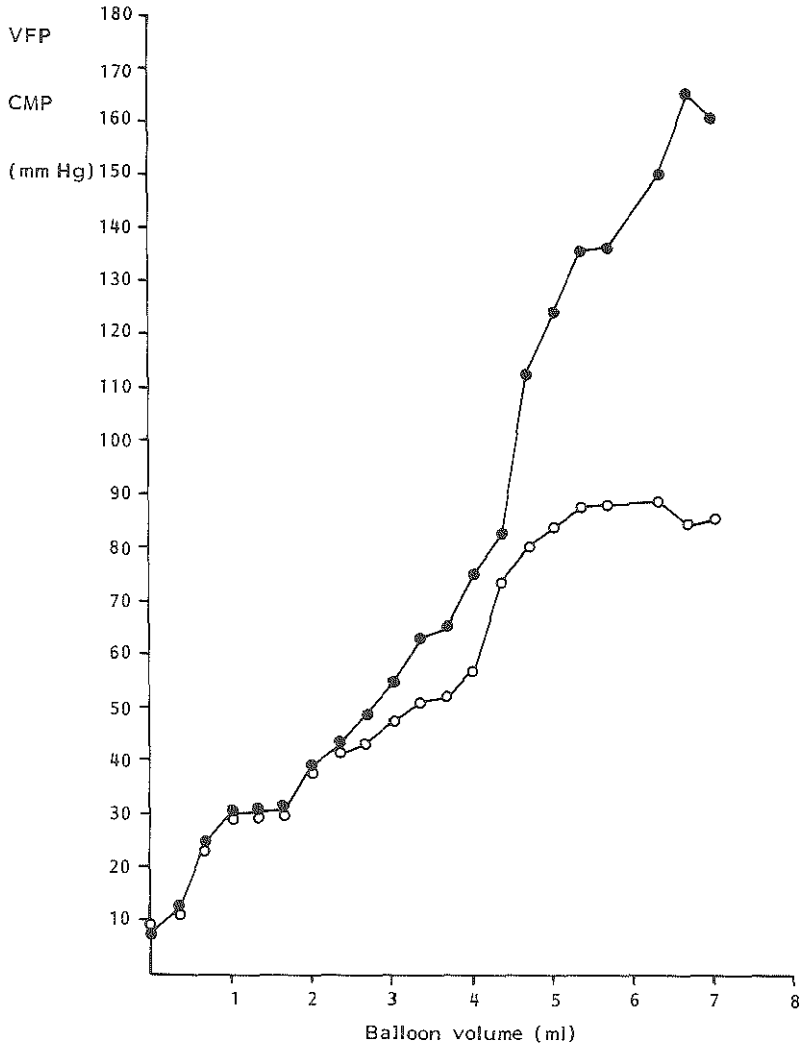


Fig. 29. Ventricular fluid pressure (VFP, filled circles) and cisterna magna pressure (CMP, open circles) against volume of extradural balloon, inflated at rate of 1 ml/15 min, in single animal (no 6), showing development of pressure gradient indicative of progressive cerebral herniation.

the VPR in the injected ventricle was often small in contrast with the much higher response in the contralateral ventricle consisting of a high peak followed by a very rapid return to the pre-injection level (Fig. 30). There was never any reason to doubt the patency of the ventricular needle in these cases. Apparently, the high initial peak response was missing in the injected ventricle because of the time involved in turning the three-way stopcock back into the recording position. The rapid return of the pressure towards the base-line suggests a very rapid compensation of

Table 7. Ventricular fluid pressure (VFP) and balloon volume at early and complete herniation.

Animal no	Early herniation		Complete herniation	
	VFP (mm Hg)	Balloon volume (ml)	VFP (mm Hg)	Balloon volume (ml)
1	52.3	5.3	72.7	6.7
2	16.3	0.7	24.7	1.7
3	24.5	1.0	54.3	2.7
4	35.0	2.3	114.0	4.0
5	48.5	1.3	79.0	2.7
6	48.3	2.7	113.0	4.7
Mean	37.5	2.2	76.3	3.8

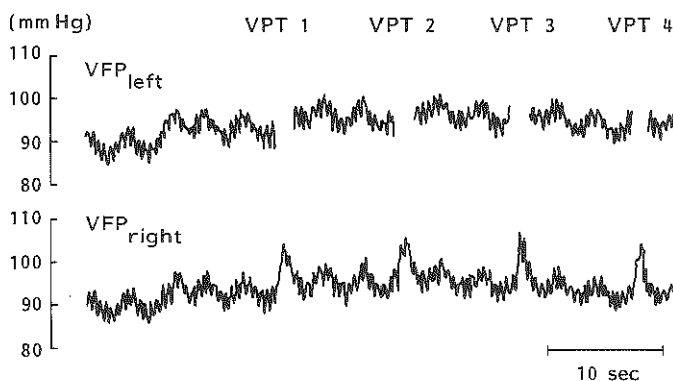


Fig. 30. Comparison between volume-pressure response in injected ventricle (upper tracing) and in non-injected ventricle (lower tracing) following four volume-pressure tests (VPT 1-4) performed at extremely high levels of ventricular fluid pressure (VFP). Compare also with Figure 26. Note that high peak pressure observed in non-injected ventricle is missed in injected ventricle because of time involved in turning three-way stopcock into recording position.

the volume added. In view of these findings we consider the fall in VPR observed in the second zone to be at least partly an artefact produced by failure of the bolus injection technique to detect rapid spatial compensatory mechanisms. Figure 31 shows the VPR from both ventricles plotted against the VFP in one of the animals, demonstrating that the phenomenon described is responsible for the decrease in VPR, but does not explain the levelling off: the VPR remained lower than would have been expected on the basis of extrapolation of the responses of the first zone.

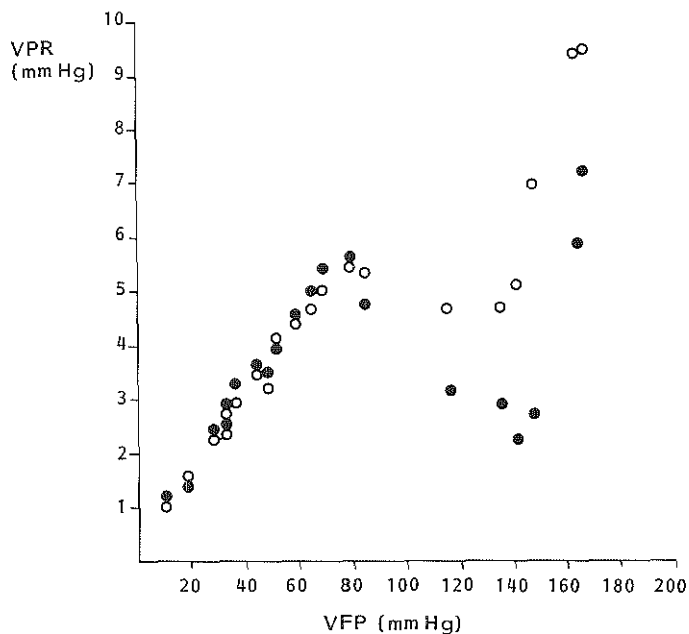


Fig. 31. Plot of volume-pressure responses (VPR) in injected (filled circles) and non-injected (open circles) ventricle against ventricular fluid pressure (VFP) in single animal (no 6). Note that fall in VPR above VFP of 80 mm Hg, observed in injected ventricle, is almost absent in non-injected ventricle. See also Figure 30.

Unfortunately, these observations could not be made in all animals with falling VPRs, as the recording needle in the contralateral ventricle was sometimes blocked at this stage because it was closest to the epidural balloon. It should be emphasized that the high initial peak and the discrepancy between the VPRs of both ventricles was never observed in the first zone of the VPR versus VFP relationship.

The above findings led us to conceive the VFP range where the VPR levelled off as a zone with a constant VPR and thus with a constant elastance. The important implication is that the craniospinal volume-pressure relationship is no longer exponential but linear in nature and that the mathematical model hitherto applied should be adjusted accordingly. The constant elastance zone can be described by:

$$P = E(V_e - V_{br}) + P_{br} ,$$

where: P = ICP,
 E = elastance,
 $V_e - V_{br}$ = increase in elastic volume with respect to volume at breakpoint, and
 P_{br} = ICP at breakpoint.

The elastance was computed from the mean VPR of this zone according to:

$$E = \frac{\Delta P}{\Delta V_e} = \frac{VPR}{0.05} \quad (\text{mm Hg/ml})$$

and the results are given in Table 5.

The data with regard to the second breakpoint in the VPR-VFP relationship, at which the VPR began to increase again, are given in Table 6. It occurred at a mean VFP of 125 mm Hg and it was related in each animal to the diastolic level of the SAP. In three animals sufficient data were available to calculate the regression lines for the pressure range above this breakpoint. The slope was always steeper than in the first pressure zone, and, as a result, a larger E_1 was found (Table 8).

Table 8. Relationship between volume-pressure response and ventricular fluid pressure (VFP) above level of diastolic blood pressure: regression equation, number of datapoints (n), correlation coefficient (r), elastance coefficient (E_1), and VFP range.

Animal no	Regression equation	n	r	E_1 (1/ml)	VFP range (mm Hg)
1	$y=0.26x-23.6$	4	0.98	4.6	111.8 - 155.3
3	$y=0.27x-15.4$	5	0.93	4.8	104.6 - 159.2
6	$y=0.31x-44.7$	4	1.00	5.4	163.9 - 207.8

Relationship between CSF pulse pressure and ventricular fluid pressure

The relationships between CSF pulse pressure and VFP are shown in Figure 32. The pulse pressure was found to increase linearly with rising ICP. The increase was more rapid in the high pressure range although this was not equally distinct in each animal. When the VFP approached the level of the SAP the amplitude of the pulse levelled off, and finally decreased above this level.

Since the VPR versus VFP plots had shown three zones with different volume-pressure relationships, it was decided to analyse the CSF pulse pressure data for each zone separately. The linear regression equations, including values for P_0 , are given in Table 9. In all but one animal a significant difference in slope was found on either side of the first breakpoint, the slope always becoming steeper (F distribution: $P < 0.01$ in four animals and $P < 0.05$ in one animal). Variables with possible effect

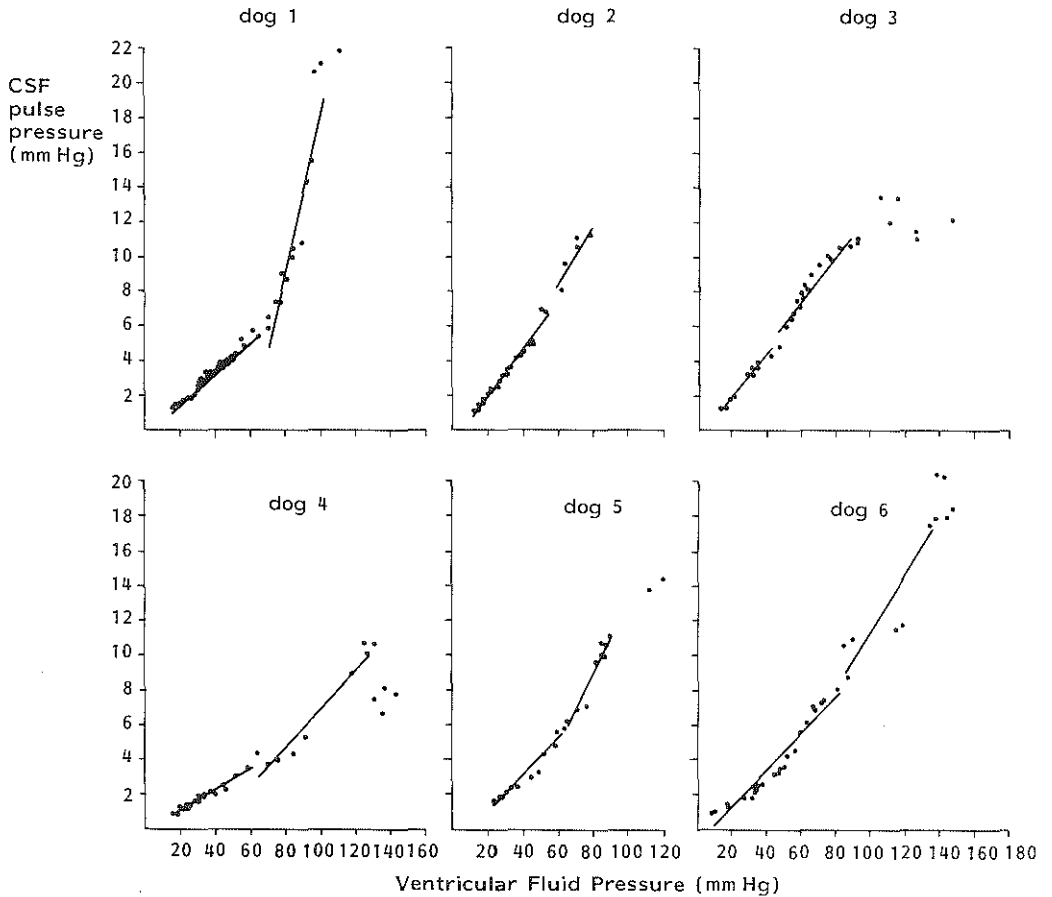


Fig. 32. Plots of CSF pulse pressure against ventricular fluid pressure (VFP) during cerebral compression by extradural balloon in six dogs. Data were analysed for first and second zone in plots of volume-pressure response versus VFP as shown in Figure 27. CSF pulse pressure rises linearly with VFP. Regression lines are shown and regression equations are given in Table 9. Slope of regression line above breakpoint was always steeper except in animal no 3.

on the CSF pulse pressure, such as the SAP, arterial pulse pressure and heart rate, remained stable throughout the experiment (Table 10).

The linearity of the relationship has a different meaning on either side of the breakpoint if the volume-pressure relationship is taken into consideration. Figure 33 shows the combined plot of both relationships in a single animal. Below the breakpoint, where the concept of a mono-exponential volume-pressure model holds true, it means, according to Equation 3.1, that the pulsatile change in CBV is constant. Using Equation 3.2, ΔV_b was calculated for the various animals and the results

Table 9. Relationship between CSF pulse pressure and ventricular fluid pressure (VFP) below and above first breakpoint: regression equations, number of datapoints (n), correlation coefficients (r), P_0 , pulsatile change in cerebral blood volume (ΔV_b), and increase in ΔV_b per mm Hg rise in VFP.

Animal no	Below breakpoint					Above breakpoint			
	Regression equation	n	r	P_0 (mm Hg)	ΔV_b (ml)	Regression equation	n	r	Increase in ΔV_b (ml/mm Hg)
1	$y=0.09x-0.5$	35	0.99	5.5	0.047	$y=0.45x-27.5$	14	0.96	0.0041
2	$y=0.14x-0.9$	21	0.99	6.2	0.033	$y=0.19x-3.5$	5	0.93	0.0013
3	$y=0.13x-0.6$	11	0.98	4.7	0.082	$y=0.13x-0.3$	18	0.97	0.0018
4	$y=0.06x-0.1$	19	0.98	1.5	0.029	$y=0.11x-4.2$	8	0.96	0.0010
5	$y=0.11x-1.2$	13	0.97	10.9	0.072	$y=0.22x-8.5$	8	0.94	0.0023
6	$y=0.11x-1.0$	25	0.97	9.1	0.081	$y=0.17x-5.3$	10	0.92	0.0027
Mean	$y=0.11x-0.7$			6.3	0.057	$y=0.21x-8.2$			0.0022

Table 10. Means (\pm SD) of systemic arterial pressure (SAP), arterial pulse pressure (Δ SAP), and heart rate (HR) below and above first breakpoint.

Animal no	Below breakpoint			Above breakpoint		
	SAP (mm Hg)	Δ SAP (mm Hg)	HR (beats/min)	SAP (mm Hg)	Δ SAP (mm Hg)	HR (beats/min)
1	159.5 \pm 8.1	56.3 \pm 8.3	114.2 \pm 11.4	144.9 \pm 11.9	54.1 \pm 6.4	114.0 \pm 12.4
2	126.4 \pm 2.6	39.8 \pm 1.3	151.5 \pm 10.7	122.0 \pm 2.8	39.5 \pm 4.9	134.5 \pm 3.5
3	118.8 \pm 5.8	34.0 \pm 1.7	132.0 \pm 3.3	119.6 \pm 4.7	35.1 \pm 1.5	134.7 \pm 2.8
4	151.6 \pm 3.6	46.1 \pm 2.2	144.5 \pm 5.3	156.4 \pm 6.2	43.7 \pm 2.6	175.0 \pm 14.2
5	135.6 \pm 2.9	53.9 \pm 6.6	165.3 \pm 1.6	130.8 \pm 9.3	50.3 \pm 2.1	168.3 \pm 2.3
6	167.8 \pm 1.8	50.8 \pm 4.3	168.0 \pm 6.6	158.4 \pm 4.7	46.0 \pm 4.2	156.0 \pm 9.5
Mean	143.3 \pm 19.4	46.8 \pm 8.6	145.9 \pm 20.5	138.7 \pm 17.0	44.8 \pm 7.0	147.1 \pm 23.3

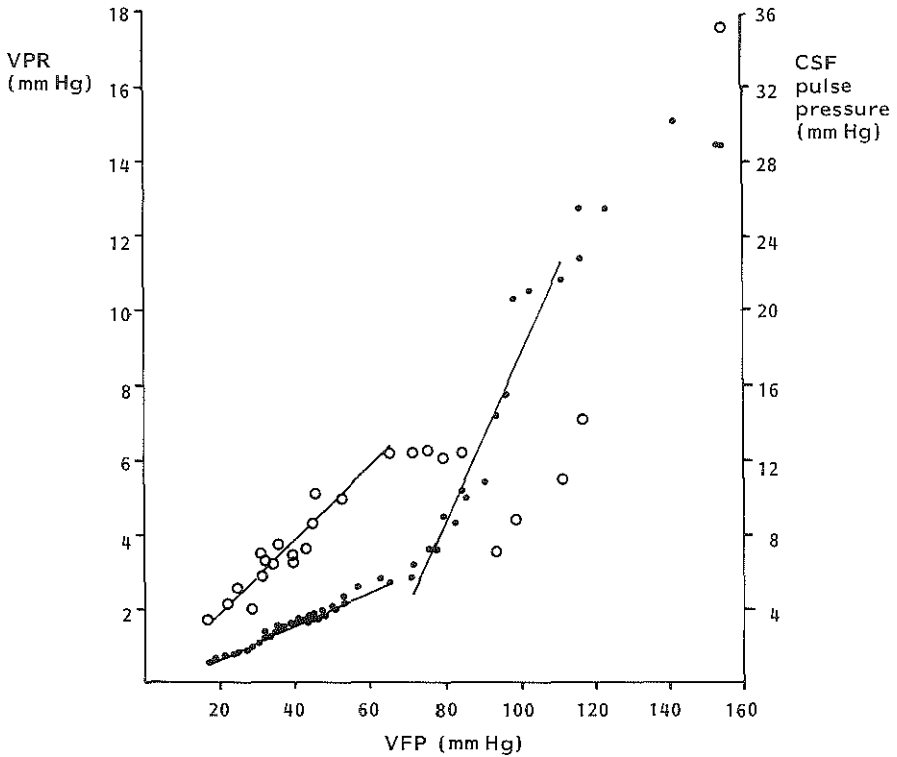


Fig. 33. Combined plot of volume-pressure response (VPR, open circles) and CSF pulse pressure (filled circles) in single animal (no 1). Note breakpoint in both relationships above which VPR levels off and CSF pulse pressure increases more rapidly.

are given in Table 9. The magnitude of ΔV_b varied considerably between the animals, which explains the lack of correspondence between the slopes of the CSFPP-VFP relationships and E_1 . The variation in ΔV_b could not be explained from differences in SAP, arterial pulse pressure, or heart rate.

Above the breakpoint the volume-pressure relationship is linear in nature, implying a constant elastance so that:

$$E = \frac{\Delta P}{\Delta V_e} = \frac{\text{CSFPP}}{\Delta V_b} = \text{constant.}$$

Consequently, the increase in CSF pulse pressure in this pressure zone must be explained by an increase in ΔV_b . The increase in ΔV_b per mm Hg rise in VFP was computed and the results are given in Table 9.

In the animals with data above the second breakpoint, coinciding with the diastolic blood pressure, no specific analysis was possible. A decrease in CSF pulse pressure was generally observed.

5.4 Discussion

This series of experiments was designed to study the relation of the CSF pulse pressure to both ICP and VPR with the clinically motivated objective of investigating whether the ratio of pulse pressure to ICP could serve as a reliable guide in the continuous assessment of craniospinal volume-pressure relationships. The results, however, also give rise to a critical review of the volume-pressure relationship itself, which will be discussed first.

Volume-pressure relationship

The validity of the mono-exponential volume-pressure model follows directly from the linear correlation between VPR and VFP. This is consistent with the findings of other authors (Marmarou, 1973; Miller et al., 1972 and 1973; Sklar and Elashvili, 1977). Sullivan and associates (1977), using the Marmarou pressure-volume model, reported a progressive elevation in PVI with rising ICP during cerebral compression in cats (Fig. 34). Since the PVI, as a parameter of compliance, is inversely related to E_1 , this finding would indicate a decrease in E_1 , thereby invalidating the mono-exponential model implying a constant E_1 or PVI. In Figure 34 we have plotted the elastance data of their study against the ICP instead of against balloon volume, and this yielded a linear relationship. This is consistent with our findings and, consequently, confirms the mono-exponential nature of the volume-pressure relationship during progressive cerebral compression at a constant rate.

This paradox originates from the application by Sullivan et al. of the Marmarou model to the single elastance data. This model, as discussed in Chapter 2.4, assumes that the constant term P_0 of our model equals zero, implying that the linear fit of the elastance versus ICP data always passes through the origin of the axes. So long as the values for P_0 are close to the origin, the computation of E_1 or the PVI will not be seriously disturbed. However, as is apparent from both Sullivan's (Fig. 34) and our results (Table 5), P_0 is a real quantity. In that case, the assumption of $P_0=0$ introduces an error into the computation of the PVI from single elastance data, which will be greatest in the low ICP range. Furthermore, a variable PVI will be found: a decrease in PVI with rising ICP when $P_0 > 0$ and an elevation in PVI when $P_0 < 0$. These arguments provide

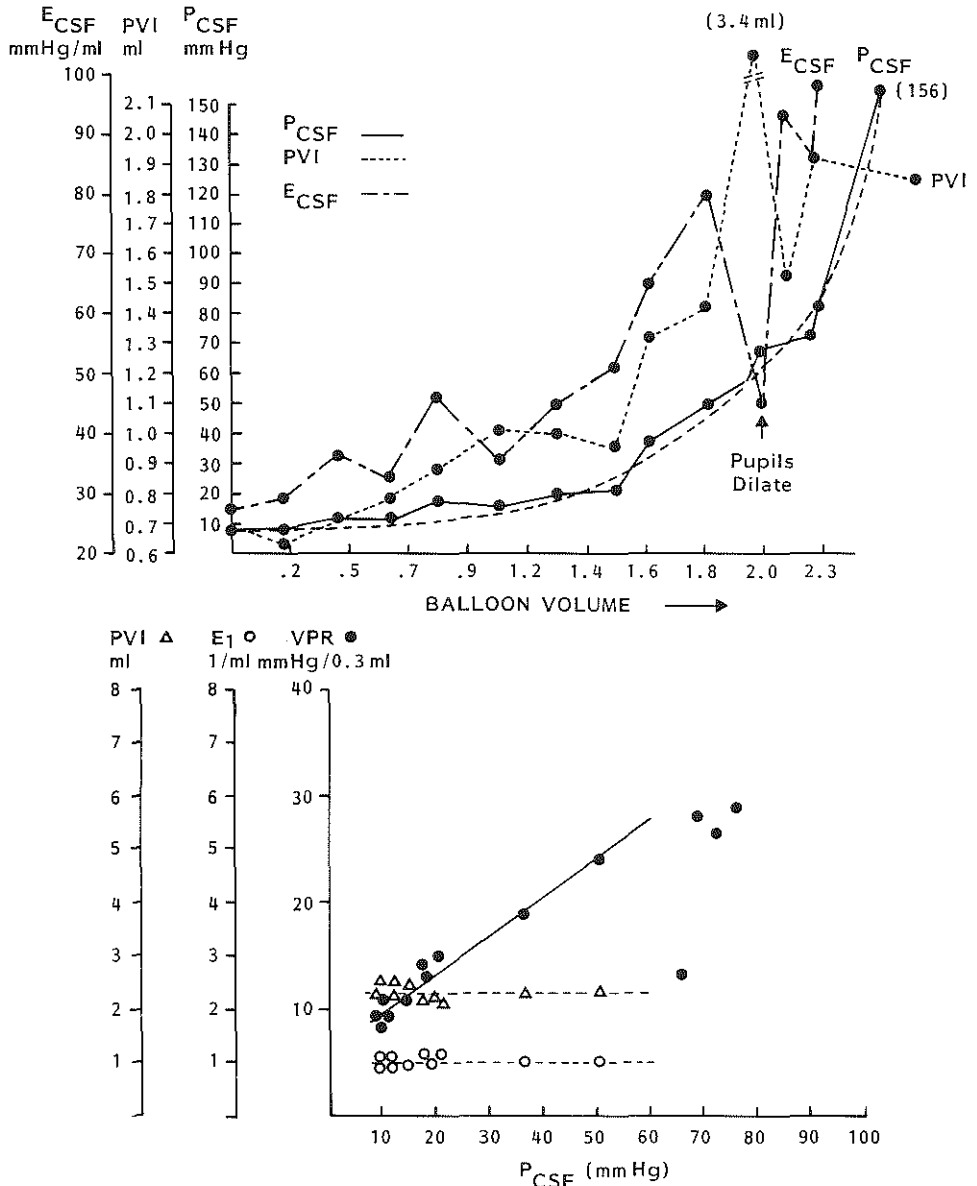


Fig. 34. Analysis of experimental data from Sullivan et al. (1977; upper figure) using our mathematical volume-pressure model (lower figure). Top figure was reproduced from Sullivan HG; Miller JD; Becker DP; Flora RE; Allen GA: The physiological basis of intracranial pressure change with progressive epidural brain compression. An experimental evaluation in cats. *J. Neurosurg.*, 47, 532-550, 1977. Intracranial pressure (P_{CSF}), pressure-volume index (PVI), and elastance (E_{CSF}) are plotted as a function of balloon volume in single experimental animal. Note progressive rise in both E_{CSF} and PVI with increasing balloon volume. These volume-pressure parameters were determined from bolus injections of 0.3 ml. Volume-pressure response (VPR) derived from Sullivan's data shows linear relationship with P_{CSF} ($y=0.36x+6.4$; $r=0.98$) up to P_{CSF} of 50 mmHg. Note fall in VPR in high pressure range. P_0 (intercept of regression line with pressure axis) is -17.8 mmHg. Calculation of elastance coefficient (E_1) for each bolus injection, using P_0 (Equation 2.7), yields constant E_1 . Consequently, PVI calculated by using P_0 is also constant. In conclusion, elevation of PVI as found by Sullivan et al. is caused by not taking into account constant term P_0 .

additional justification in our view for the introduction of the constant term into our model.

Confusion has been caused when discussing craniospinal volume-pressure relationships in the past, because reference was made to curves constructed by plotting the steady state ICP against the volume of an expanding mass (Langfitt et al., 1965; Leech and Miller, 1974). However relevant these curves may be from a clinical point of view, they do not reflect the elastic properties of the system, since the process of spatial compensation is involved as discussed in Chapter 2.6. This view is supported by the results of the present study, which fail to show a correspondence between the magnitude of E_1 and the balloon volume accommodated over the ICP range for which E_1 is valid. This is demonstrated by animal no. 2 for example. If, for convenience, the spatial compensatory capacity is defined as the rise in ICP per unit increase in balloon volume, this animal has the second largest compensatory capacity (Table 6). At the same time, however, in view of its large E_1 , it has the steepest volume-pressure curve (Table 5). This is probably due to the early occurrence of tentorial herniation in this animal (Table 7), which causes the volume of the total craniospinal compartment to be reduced to that of the supratentorial space. This confirms the findings of Lim et al. (1973), Löfgren and Zwetnow (1973 and 1973), and Marmarou et al. (1975), who reported an increase in elastance when the communication between the cranial and spinal compartments was impaired (Chapter 2.3).

How does the mean group E_1 of 2.0 l/ml found here compare with values of other volume-pressure parameters reported in the literature? As discussed in Chapter 2.3 and shown in Figure 3, Löfgren et al. (1973) characterized the volume-pressure curve of the dog in the pressure range usually encountered clinically by two linear segments, i.e., a low pressure elastance of 1.3 mm Hg/ml around an ICP of 3 mm Hg and a high pressure elastance of 25.2 mm Hg/ml usually determined at an ICP of 60 mm Hg. Application of Equation 2.2 to these results gives an E_1 of 0.42 l/ml. Sklar and Elashvili (1977), also in the dog, determined the slope relating elastance to pressure, termed the elasticity slope, by serial injection of 0.2 to 0.5 ml aliquots into the CSF space. A mean slope of 1.01 was found in a group of six animals. According to Equation 2.6 this result is consistent with an E_1 of 0.70 l/ml.

The considerably higher value in the present study is explained in our view by the balloon inflation technique used to raise the ICP, which causes transtentorial herniation with consequent reduction of the total neural axis volume to that of the supratentorial space, as argued above. This view is supported by the result of another study, that of Leech and Miller (1974), which used the cerebral compression model for elevation of the ICP, albeit in the baboon. From the data of that study a VPR versus VFP slope of 0.16 can be derived, yielding for E_1 the high value of 3.0 l/ml. Marmarou et al. (1975), using bolus injection with increasing volumes, found a PVI of 0.9 ml in the cat, which is consistent with an E_1 ($P_0=0$) of 2.6 l/ml. In this case the large E_1 can be explained by the smaller craniospinal volume of the cat as compared with the dog. The influence of neural axis volume on the volume-pressure relationships was demonstrated by Shapiro et al. (1980) who found, in a group of 23 children, a correlation between the PVI actually measured and the predicted PVI based on estimates of intracranial and spinal volumes obtained from external measurements. The concept of craniospinal volume as the major determinant of craniospinal elastance also explains the difference in E_1 between this experimental study and the clinical study.

An important finding of the present study was the validity of the exponential volume-pressure model for a restricted range of ICP only. At a mean ICP of 60 mm Hg a breakpoint occurred, above which the volume-pressure relationship became a linear function with a slope equal to the elastance at that point. The change in nature of the relationship lends particular significance to the breakpoint, the explanation of which should obviously be sought in those physiological mechanisms which are at the root of the concept of craniospinal compliance and which were discussed in Chapter 2.6. In Appendix 3 we have derived a linear volume-pressure function for the craniospinal system by conceiving the system and its confining structures as a fluid filled elastic container to which the laws of Laplace and Hooke can be applied. Consequently, the question should be raised as to why the relationship of the biological system is exponential below the breakpoint.

The magnitude of the rise in ICP in response to a rapid volume addition depends on two factors. The first is determined by the purely physical properties of the craniospinal system as a whole. The second factor is related to the interaction between the system and the cerebral

vascular bed. The added volume compresses the venous outflow section and, through the increased outflow resistance, produces a temporary rise in the upstream intravascular volume and pressure; this pressure is transmitted through the thin venous wall to the surrounding CSF. Part of the ultimate pressure response is thus determined by the compressibility of the venous vascular bed. According to Poisseuille's law, the resulting venous pressure is inversely proportional to the square of vascular volume. It thus appears that the craniospinal volume-pressure relationship derives its non-linear nature from the non-linear volume-pressure relationship of the venous vascular bed.

The above inference from Poisseuille's law postulates a constant flow. When flow is reduced, it also follows from this law that the same volume increment will result in a lower pressure response. Consequently, during progressive reduction in CBF the pressure responses will become less pronounced and the volume-pressure curve will lose its exponential shape. The integrity of CBF seems thus to be a precondition for the exponential shape of the volume-pressure curve. This strongly suggests that the breakpoint in the VPR-ICP relationship found in this study marks the failure of CBF autoregulation. Since CBF was not measured in this series, we have no solid evidence for this assumption. However, subsequent experimental work reported in Chapters 6 and 7 will provide additional evidence in this respect. The fact that, at the breakpoint, the range of the cerebral perfusion pressure is much narrower than that of the ICP (Table 6) may already be significant; this is because failure of CBF autoregulation is related to the cerebral perfusion pressure, which reflects the transmural pressure, rather than to the absolute level of ICP.

Additional support for the above arguments can be derived from Löfgren's volume-pressure curve (1973), showing a linear course in the pressure range coinciding with that of the present study (Fig. 3). The recording of this part of the curve by the rapid infusion technique (0.25 ml/sec) usually took less than ten seconds. It has been well documented (Fog, 1934; Hirsch and Körner, 1964; Rapela and Green, 1964; Yoshida et al., 1966; Ekström-Jodal et al., 1970; Kogure et al., 1970) and also shown by ourselves (Chapter 6) that this time interval is too short for an autoregulatory vasodilator response to become fully established. We therefore believe that during the recording of Löfgren's

curve CBF was reduced as a result of the decrease in cerebral perfusion pressure, giving that part of the curve its linear shape.

The elastance in the linear part of the volume-pressure relationship is four times higher than the high pressure elastance reported by Löfgren et al. (1973): 100.0 and 25.2 mm Hg/ml respectively. The difference can be explained by the same mechanism responsible for the high elastance coefficients of our study, i.e., transtentorial herniation isolating the supratentorial from the infratentorial and spinal compartments. Beyond the first breakpoint in the VPR-ICP relationship, herniation always became fully established as was also evident from the widely dilated pupils.

From the difference between the VPRs in the injected and in the contralateral ventricle, the inference was made that the decrease in elastance occurring when the ICP had come within reach of the blood pressure level, an observation also made by Löfgren et al. (Löfgren et al., 1973; Löfgren and Zwetnow, 1973) and by Leech and Miller (1974), is an artefact caused by some rapid spatial compensatory mechanism. It was suggested by Löfgren et al. that this mechanism was the displacement of venous blood from the cranial cavity. Since, on account of the cuff constriction phenomenon at the subarachnoid vein sinus junction (Chapter 2.6), the egress of blood will become more and more impaired rather than facilitated as ICP increases, we would suggest that the dural sinuses, acting as a low pressure reservoir, may offer spatial compensation at this high level of ICP. A partial collapse of the sinuses during intracranial hypertension was postulated by Shulman et al. (1964) and by Rowan et al. (1972) and actually demonstrated in morphological studies by Shapiro et al. (1966).

In the ICP range above the blood pressure level, when CBF has completely ceased, the craniospinal compartment almost fulfils the requirements of the Monro-Kellie doctrine, and its volume-pressure relationships approach that of a filled, rigid container, resulting in a volume-pressure curve with a very steep slope.

CSF pulse pressure

This study has shown that the linear relationship between the ICP and

its pulse related variations, already found in clinical patients for small pressure ranges, is valid for the entire range of elevated ICP usually encountered clinically, i.e., up to 60 mm Hg on average. Above this pressure the relationship is still linear but usually with a steeper slope, indicating that the CSF pulse pressure increases more rapidly with the ICP than before. Whenever there was a breakpoint between the two relationships, it coincided with the breakpoint in the VPR-ICP relationship. In Figure 35 we have summarized these results by averaging the various regression equations.

By application of the mathematical model to the relationships of the ICP with both pulse pressure and VPR, it was demonstrated that the pulsatile change in CBV has a constant value below the breakpoint in

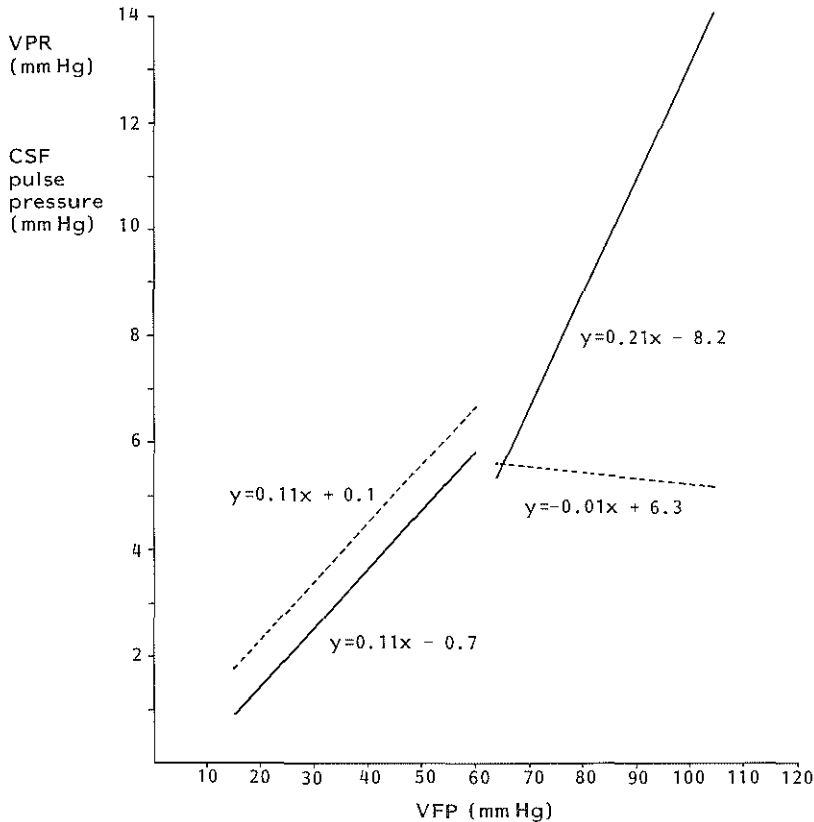


Fig. 35. Composite graph of relationships of both volume-pressure response (VPR, dashed line) and CSF pulse pressure (continuous line) with ventricular fluid pressure (VFP) during cerebral compression in six dogs. Mean regression lines and regression equations are shown (Tables 5 and 9. Regression analysis of VPR data above breakpoint was applied to pooled data). Note breakpoint in both relationships at VFP of 60 mm Hg.

contrast with a progressively larger value above the breakpoint. Given the coincidence of the breakpoints in both relationships in the individual animals, it seems plausible that the increase in ΔV_b can be explained by the same mechanism responsible for the breakpoint in the VPR-ICP relationship, i.e., a change in cerebral haemodynamics. Supportive evidence for this view can be found in the experiments of Symon and associates (1970, 1973, 1974, 1975 and 1976). They recorded pressure and pulsation in a pial artery and in Labbé's vein in baboon preparations and used the ratio of venous to arterial pulse height, termed the *pulse index*, as a parameter of cerebrovascular resistance. The pulse index increased in response both to increased arterial carbon dioxide tension and to cerebral vascular occlusion, indicating vasodilatation in response to biochemical and autoregulatory stimuli. When ICP was raised by cisterna magna infusion, pulse transmission steadily increased linearly but with a sharp inflexion point at an ICP of about 70 mm Hg, similar to the breakpoint observed in the present study (Fig. 36). During balloon

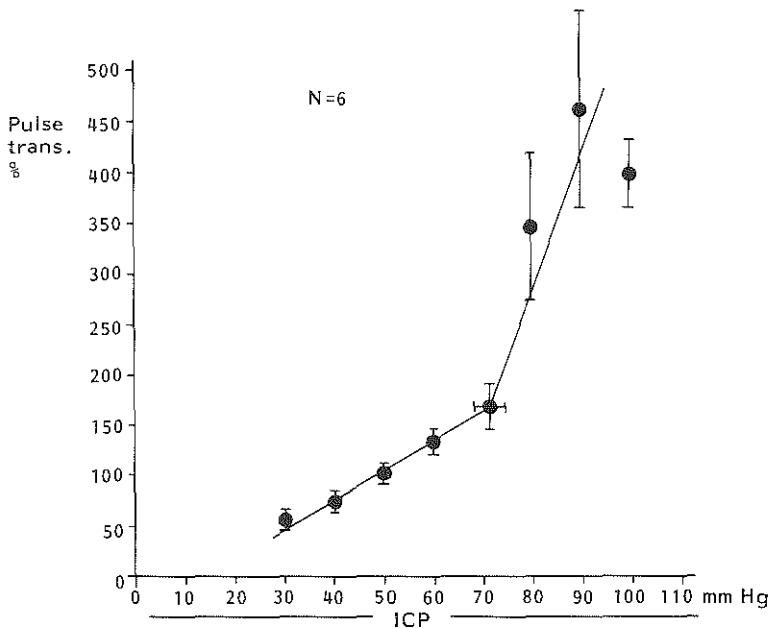


Fig. 36. Relationship between pulse transmission from cerebral artery to vein and intracranial pressure (ICP) during cisternal infusion in six baboons (Reproduced from Symon L; Crockard H; Juhasz J: Some aspects of cerebrovascular resistance in raised intracranial pressure: an experimental study. In: Intracranial Pressure II eds. N Lundberg, U Pontén, M Brock, Springer-Verlag, Berlin-Heidelberg-New York, 257-262, 1975). Pulse transmission % = venous pulse height in mm H₂O divided by arterial pulse height in mm Hg times 100%. Note breakpoint in relationship around 70 mm Hg.

expansion it was shown that CBF, measured by the hydrogen clearance method, was maintained up to an ICP of 70 mm Hg. From these results it was inferred that the inflexion point in the pulse transmission versus ICP relationship indicates that CBF autoregulation is beginning to fail and that maximal vasodilatation or even vasoparalysis has developed.

The findings of Symon et al. on the pulse transmission from cerebral artery to vein are quite consistent with our observations on the CSF pulse pressure, suggesting that the inflexion point in the pulse transmission and the breakpoint in the CSFPP-ICP relationship are caused by the same physiological mechanisms. This links up well with our concept of the origin of ΔV_b as outlined in Chapter 3.3. If, at the breakpoint, the active autoregulatory vasodilator response is exhausted, the cerebrovascular resistance cannot be reduced any further in order to accommodate a further decrease in cerebral perfusion pressure, so that from this point onwards CBF starts to decrease. On the one hand, provided that no change in heart rate occurs, a decreased flow implies a smaller volume load of blood to the brain per cardiac cycle. If there is also no change in the phase shift between the pulsatile inflow and outflow curves, this will result in a smaller ΔV_b , as shown schematically in Figure 11. On the other hand as shown by Langfitt and associates (1965 and 1965), cerebral ischaemia produced by reduced CBF leads to a stage of progressive cerebrovascular decompensation, during which period the normal resting tone of the cerebral vessels is gradually abolished (cerebral vasomotor paralysis). This causes further, passive, vasodilatation and reduction of the inflow resistance, thereby facilitating the pulsatile inflow of blood. In other terms, the loss of vasomotor tone renders the arterial vascular bed highly compliant, so that the arterial wall is more easily distended by the arterial pressure head. We suggest that this causes a change in the cerebral arterial inflow profile consisting of an increase in pulsatile flow due to a shift of flow from diastole to systole. At the same time, as previously argued, the outflow resistance at the venous side of the vascular bed is increased because of the cuff constriction mechanism at the vein sinus junction, and finally because of compression of the dural sinuses themselves under the influence of the elevated ICP; both these factors cause a delay in the pulsatile venous outflow towards the end of the cardiac cycle. The idea of a shift of the cerebrovascular resistance from the arterial to the venous side during elevation of the ICP is consistent with the findings of Lowell and Bloor (1971) and of Shulman and

Verdier (1967) who actually demonstrated such a shift in experimental animals. Both effects are operative in enlarging the phase shift between the pulsatile inflow and outflow of cerebral blood which thus disintegrate, as far as timing is concerned, into two separate processes. This will result in a progressive increase in ΔV_b , as shown in Figure 11. Since the results of the present study show an increase in ΔV_b above the breakpoint, the conflict between the opposite effects of the reduced CBF and the increased phase shift between inflow and outflow on ΔV_b is apparently settled in favour of the latter.

Evidence in support of the above explanation with regard to the paradox of an increase in the pulsatile change in CBV in spite of a reduced CBF can be derived from a study by Nornes and associates (1977). In this study the internal carotid artery blood flow was measured in patients by means of electromagnetic flowmeters. The progressive fall in mean carotid artery flow during the rise in ICP, caused by rupture of a cerebral aneurysm, was found to result from a decrease in the continuous portion of flow. The amplitude of the flow pulse, on the other hand, was found to increase. The plot of the flow pulse amplitude against the cerebral perfusion pressure showed a breakpoint around a pressure of 20 mm Hg with a disproportionate increase in flow pulse amplitude below this point. The same type of relationship was observed in the plot of CSF pulse pressure against perfusion pressure.

In Chapter 3.3 changes in the continuous portion of flow were not explicitly considered. In Figure 11 the effect of an increase in CBF on ΔV_b was shown for the situation in which the increase in mean flow was accompanied by an increase in the pulsatile amplitude. It can be easily seen that changes in the amount of continuous flow will not contribute to a change in the magnitude of ΔV_b provided that the changes affect the arterial inflow and venous outflow to the same extent. Since the venous outflow is relatively nonpulsatile compared with the arterial inflow, ΔV_b will be mainly determined by the arterial flow pulse, and *not* by the *total* volume load of blood per cardiac cycle as previously stated. The pulsatile volume load of blood to the brain, as a major determinant of the CSF pulse pressure, can now be defined more precisely as the volume of the systolic flow pulse, not including the continuous portion of flow. A decrease in CBF will thus cause a reduction in ΔV_b only if the flow pulse is reduced as well, and vice versa.

Consequently, the first part of the paradox of a decrease in CBF and an increase in ΔV_b , occurring above the breakpoint, can be explained by the finding of Nornes et al. that only the continuous portion of flow is reduced, and this does not have a decremental effect on ΔV_b . The second part of the paradox, the increase in ΔV_b , is explained by the increased phase shift between inflow and outflow, which is confirmed by Nornes' finding of an increase in the systolic flow pulse amplitude resulting from a shift of flow from diastole to systole. The largest flow pulse amplitudes were observed by Nornes et al. at extremely low perfusion pressures and correspondingly low mean flow values. They were caused by the phenomenon of negative or reverse flow in the carotid artery during diastole. This explains why high CSF pulse pressures can still be recorded when the ICP has been raised above the blood pressure level, as in the three animals of the present study, and complete cerebral circulatory arrest may be assumed to exist. In that case inflow and outflow, both taking place at the arterial side of the cerebral vascular bed, are two completely separate processes, implying a maximal phase shift.

The constant term P_o

The mathematical and physiological meaning of the constant term P_o in the volume-pressure model has been discussed in Chapter 2.4. When the relationships of the VPR and the CSF pulse pressure with the ICP in the present study are compared it can be observed that, in conflict with the mathematical model, the values of P_o are different in each animal (Tables 5 and 9). The question then arose as to whether these differences were statistically significant. Regression analysis of the relationships yielded the 95% confidence limits of P_o . The intervals showed a degree of overlap in four animals (nos. 1, 2, 4 and 5), so that the values for P_o of both relationships were statistically different in two animals only.

The problem of the difference in P_o is probably associated with the difficulty of defining the breakpoints exactly. The way in which CBF autoregulation is lost will affect the transition from the first to the second zone in the relationships (Figs. 27 and 32). When CBF is lost more gradually, the breakpoint will become less sharp. Since the VPR levels off, the slope of its relationship with the ICP will tend to decrease. This is probably why in this relationship most values of P_o are in the negative range. The CSF pulse pressure, on the other hand, begins to rise

disproportionately around the breakpoint. The slope of the CSFPP-ICP relationships tends therefore to be overestimated. This is why in this case P_o has positive values. Consequently, the problem encountered in defining the breakpoint will shift the P_o s of the relationships in opposite directions.

Finally, the reality of P_o as a valid model parameter with some physiological meaning is supported by the finding that in eight cases the origin of the axes did not fall within the 95% confidence limits of P_o .

Clinical implications

The finding of a constant pulsatile change in CBV below the breakpoint under the controlled conditions of these experiments is of importance as far as the clinical application of the CSF pulse pressure as a measure of craniospinal elastance is concerned. It means that changes in the slope of the CSFPP-ICP relationship observed during ICP monitoring, irrespective of the level of ICP, truly reflect changes in the volume-pressure relationship, so that the slope index becomes a relative measure of the elastance coefficient.

However, the results confirm those of the clinical study in that the slope cannot be used as an absolute measure of E_1 , since the magnitude of ΔV_b varied between the different animals to the extent that any correlation between the slope and E_1 was obscured. This variation could not be attributed to those measured variables which, from a theoretical point of view, may be assumed to exert influence on ΔV_b , such as the blood pressure, the arterial pulse pressure, and the heart rate. However, the effect of these factors on ΔV_b might be the result of a very complex interaction. Moreover, another important variable, the CBF, was not measured. Finally, the physiological state of the cerebral vasculature may also be regarded as an important factor with regard to the biological variation in ΔV_b .

In clinical practice the above factors may be expected to vary not only between patients but also within the same patient depending on his clinical state. In that case the slope of the CSFPP-ICP relationship will be affected by alterations in ΔV_b . It seems thus that the variability of ΔV_b as well as the fact that there is no method available for reliable, quantitative assessment of ΔV_b limit the use of the CSF pulse pressure as a measure of elastance.

The inference made from the results of this study, that loss of CBF autoregulation causes a breakpoint in the relationships of both CSF pulse pressure and VPR with the ICP, opens up a new perspective with respect to the use of the pulse pressure as a diagnostic aid. When autoregulation is impaired, the increase in CSF pulse pressure with rising ICP is no longer caused by an increase in elastance but by an increase in ΔV_b . This means, in view of the explanation for the latter, that under these circumstances the CSF pulse pressure is a measure of the dilatory state of the cerebral vascular bed rather than of the elastance. The finding of high pulse pressures, especially in combination with a low VPR, during ICP monitoring would thus indicate defective autoregulation and vasoparesis. In that case, assessment of the state of the patient on the basis of the VPR only would be falsely optimistic. This situation is analogous to that found in the clinical study of Chapter 4 during plateau waves. In the present study the level of the breakpoint ICP (60 mm Hg) was related to the particular cerebral compression model used. In the clinical situation CBF autoregulation may become impaired by various pathological conditions at much lower levels of ICP, so that the breakpoint ICP with associated discrepancy between CSF pulse pressure and VPR may be reduced accordingly.

Conclusions

1. During cerebral compression in dogs both CSF pulse pressure and VPR were found to rise linearly with the ICP up to a breakpoint, above which the pulse pressure continued to rise linearly but with a steeper slope, whereas the VPR remained constant.
2. With regard to the pulsatile change in CBV, the breakpoint marks the transition from a constant ΔV_b to a progressively increasing ΔV_b .
3. With regard to the craniospinal volume-pressure relationship, the breakpoint marks the transition from an exponential to a linear relationship.
4. The cause of the breakpoint, occurring at a mean ICP of 60 mm Hg, was attributed to failure of CBF autoregulation.
5. No correlation was found between the slopes of the CSFPP-ICP relationship and the elastance coefficients of the various animals due to the variation in ΔV_b .
6. No correlation was found between the elastance coefficient, as a parameter of the volume buffering capacities, and the volume

compensatory capacities of the craniospinal system.

7. The elastance coefficient seems to be largely determined by the volume of the craniospinal system. Compartmentation, as occurring in cerebral herniation, causes an increase in E_1 .
8. The decrease in VPR close to the level of the blood pressure is an artefact caused by a rapid spatial compensatory mechanism.

CHAPTER 6

EFFECTS OF HYPERCAPNIA AND ARTERIAL HYPOTENSION AND HYPERTENSION ON CEREBROSPINAL FLUID PULSE PRESSURE AND INTRACRANIAL VOLUME-PRESSURE RELATIONSHIPS DURING CEREBRAL COMPRESSION IN DOGS

"Changes in the arterial pulse pressure and the state of the vessels will change the CSF pulse. Goldensohn and associates have reported that the cisternal CSF pulse pressure of dogs was markedly increased by the inhalation of CO₂. Several things contribute to this change. There is a change in the state of the vessels caused by the CO₂; the general intracranial blood flow increases, and the mean CSF pressure rises. Which of these factors is the most important is not known at present."

E.A. Bering (1955)



6.1 Introduction

In the previous studies, both clinical (Chapter 4) and experimental (Chapter 5), the interrelationship between CSF pulse pressure and VPR during elevation of the ICP was established. At the same time it was shown that the fact that the magnitude of the pulsatile change in CBV is both unknown and variable constitutes a serious problem with regard to the replacement of the VPR by the CSF pulse pressure in the assessment of craniospinal volume-pressure relationships. In order to appreciate the slope of the CSFPP-ICP relationship in terms of a volume-pressure relationship, one would first have to assess ΔV_b so as to 'calibrate' the slope. However, the computation of ΔV_b in turn requires the VPR to be measured, so that bolus injection remains indispensable. A dominant role in the formation of ΔV_b was ascribed to the interaction between extracranial and intracranial haemodynamic factors (Chapter 3.3). It is therefore important to learn how and to what extent these factors affect ΔV_b . It might then become possible in clinical practice to predict changes in ΔV_b from changes in these factors without actually measuring ΔV_b . The study of some of the factors involved was the aim of the next series of experiments.

Changes in the arterial carbon dioxide tension (PaCO_2) and SAP may constitute major insults to the brain in a variety of clinical conditions. These variables form part of the standard monitoring procedure in the intensive care unit. Hypercapnia (increased PaCO_2), systemic arterial hypotension and hypertension were therefore selected from the haemodynamic factors affecting the CSF pulse pressure for the purpose of the present study.

The pulse pressure is known to be increased during hypercapnia (Goldensohn et al., 1951; Symon, 1970; Hamer et al., 1977). It may well

be, however, that this is the concomitant effect of the rise in ICP which is also produced by hypercapnia. Since hypercapnia is known to increase ICP through the mechanism of cerebral vasodilatation, which causes an increase in CBV as well as in CBF, we would anticipate a disproportionate increase in pulse height on the basis of our concept of ΔV_b .

Contradictory results have been reported with regard to the effects of changes in SAP on the CSF pulse pressure. Hamer et al. (1977) found an increase by lowering the SAP. This is difficult to reconcile with the finding by Symon (1970) of an increased pulse transmission from cerebral artery to vein during arterial hypotension. Moreover, it is often the case that no clear distinction is made in the various reports between the effect of the level of SAP and that of the height of the arterial pulse (Δ SAP). As discussed in Chapter 3.3, we would expect a decline in CSF pulse pressure from induced systemic hypertension for the reason that the consequent increase in cerebral perfusion pressure elicits an autoregulatory response of the cerebral resistance vessels, consisting of vasoconstriction. The converse argument goes for the effect of lowering the SAP.

A concomitant effect of PaCO_2 and SAP alterations is that they may also affect the craniospinal volume-pressure relationship, as reported by several authors (Löfgren, 1973; Leech and Miller, 1974; Cohadon et al., 1975; Tagaki et al., 1980). They may thus influence the CSF pulse pressure by acting upon both factors by which it is determined, i.e., ΔV_b and E_1 .

In the present study, changes in PaCO_2 and SAP were artificially induced in order to examine their effects on the volume-pressure relationship as well as on the CSFPP-ICP relationship. By comparing these relationships on the basis of the mathematical model, the effect of these changes on the pulsatile change in CBV was derived.

6.2 Experimental methods

Twelve anaesthetised, ventilated adult mongrel dogs of both sexes (body weights 14 to 28 kg) were studied. The anaesthesia, surgical preparation and methods of continuous recording of cisterna magna pressure, SAP, and central venous pressure have been described in the previous chapter. After all pressures had stabilized, an extradural balloon in the right frontal

region was gradually distended by continuous infusion of normal saline at a rate of 1 ml/40 minutes.

The VPR was used as a measure of the elastance. It was determined by bolus injections of 0.05 ml aliquots into the lateral ventricle. The VPR and CSF pulse pressure data were collected in the same way as in the previous series of experiments. The SAP was calculated as the diastolic pressure plus one third of the pulse pressure. Arterial blood gases were sampled periodically throughout the experiments and measured using a direct reading electrode system (Radiometer BMS 3). The readings were corrected for temperature differences between the animal and the recording system (Severinghaus, 1966).

On conclusion of the experiments the animals were killed and the brains removed. After weighing (brain weights between 71 and 102 g) the brains were fixed in formalin and then sectioned coronally at 5 mm intervals. The correct position of the VFP recording needles was verified and major brain lesions other than those produced by the expanding balloon were excluded.

The 12 animals were divided into two groups of six each. In the first group the effects of hypercapnia were investigated and in the second the effects of systemic arterial hypotension and hypertension on the CSF pulse pressure and the VPR were studied. The experimental design was such that each animal served as its own control.

Protocol hypercapnia

Brain compression was started at normocapnia. Hypercapnia was then produced by administering 5% carbon dioxide to the inspired gases for five minutes; at the end of this period a steady state was reached, as indicated by an infrared analyser monitoring the end-tidal CO_2 . During the following 15 minutes the animal was allowed to stabilize at a normocapnic level. At time zero and five minutes volume-pressure tests were performed and blood gases taken. The same manoeuvre was repeated at intervals of 20 minutes until the VFP approached the level of the blood pressure, at which point the experiment was terminated. Thus VPRs and CSF pulse pressures were obtained at normocapnia ($\text{PaCO}_2 = \text{M} \pm \text{SD} = 40.9 \pm 2.7$ mm Hg) and hypercapnic (57.8 ± 3.3 mm Hg) levels throughout the period of brain compression.

Protocol arterial hypotension and hypertension

Brain compression was started at the normal, resting SAP of the animals. SAP was reduced over five minutes by intravenous titration of a 0.1% solution of trimethaphan (Arfonad). For the next five minutes SAP was increased by continuous intravenous infusion of angiotensin (Hypertensin-CIBA, 3 μ g/ml). The animal was then allowed to stabilize at a normotensive level for ten minutes. The VPR was measured and data were collected at zero, five, and ten minutes. The same procedure was repeated every 20 minutes. In this way VPRs and CSF pulse pressures were obtained throughout the period of brain compression at normal SAP ($M \pm SD = 135.5 \pm 5.9$ mm Hg), hypotension (89.0 ± 5.2 mm Hg), and hypertension (175.3 ± 9.2 mm Hg). The experiment was terminated when the VFP had reached the normotensive SAP level. $PaCO_2$ was maintained within normal limits (37-43 mm Hg).

6.3 Results

Effects of hypercapnia

Figure 37 illustrates the effect of hypercapnia on the VFP in a single animal. The rise in VFP became progressively larger throughout the period of brain compression, but at a particular pressure level the CO_2 response of the VFP began to decline and, finally, CO_2 was no longer capable of increasing the VFP. Whenever there was a difference in VFP between normocapnia and hypercapnia in the extremely high pressure range, it was due to the slightly elevated SAP during hypercapnia. The course of events with regard to the CO_2 response of the VFP is clearly demonstrated when the response of each time interval is plotted against the VFP at normocapnia (Fig. 38).

During both normocapnia and hypercapnia, the VPR increased linearly with the VFP until a breakpoint was reached above which the VPR levelled off and sometimes decreased slightly, as had been observed in the previous series (Fig. 39). When the VFP approached the SAP level, the VPR started to increase again, but this pressure range was not studied further. The 'normocapnic' breakpoint occurred on average at a VFP of 53.4 mm Hg

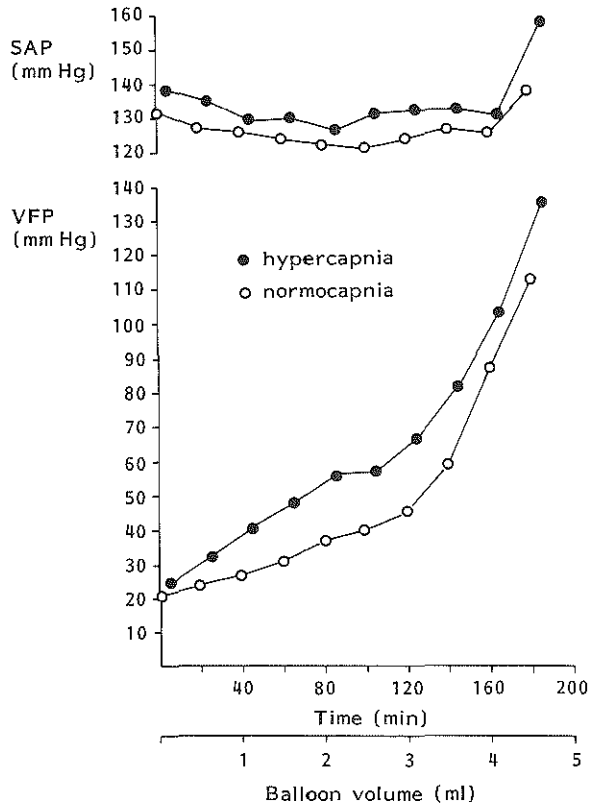


Fig. 37. Plots of ventricular fluid pressure (VFP) and systemic arterial pressure (SAP) at normocapnia and hypercapnia during steady rate inflation (1 ml/40 min) of extradural balloon in single animal of series (no 1). Initially, hypercapnia produced progressively larger rises in VFP. Above VFP of 45 mm Hg, however, CO₂ reactivity decreased. See also Figure 38 where this animal is represented by open circles. SAP was slightly elevated during hypercapnia. This may have accounted for some residual increase in VFP in extremely high VFP range when autoregulation was completely lost.

(range 42.8–64.6 mm Hg) and the 'hypercapnic' breakpoint at a VFP of 60.8 mm Hg (range 47.8–72.0 mm Hg). The difference between both breakpoint VFPs was statistically significant (Wilcoxon matched-pairs test: $p < 0.05$). Below the breakpoint significant relationships between VPR and VFP were always obtained ($p < 0.05$). The regression equations are given in Table 11. By applying the equations of the mathematical model to these relationships, the elastance coefficients were calculated and the results are given in Table 11. Hypercapnia produced a decrease in E_1 , indicating a flatter course of the volume-pressure curve, in five animals and an increase in E_1 in one animal. However, none of the differences between normocapnia and hypercapnia attained statistical significance (F-test applied to the slopes of the regression lines from which E_1 was calculated).

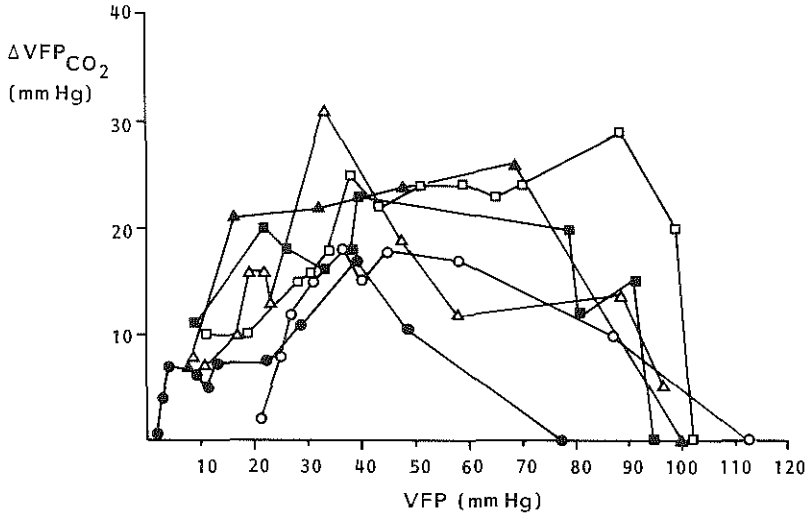


Fig. 38. Increase in ventricular fluid pressure produced by hypercapnia (ΔVFP_{CO_2}) in each time interval plotted against ventricular fluid pressure (VFP) during cerebral compression in 6 dogs. Animals are represented by different symbols. For data acquisition see also Figure 37. Data were corrected for increase in balloon volume during elevation of $PaCO_2$. Average increase in VFP reached its maximum around VFP of 50 mm Hg, corresponding with breakpoint pressure in relationship between volume-pressure response and VFP (53.5 mm Hg; see text).

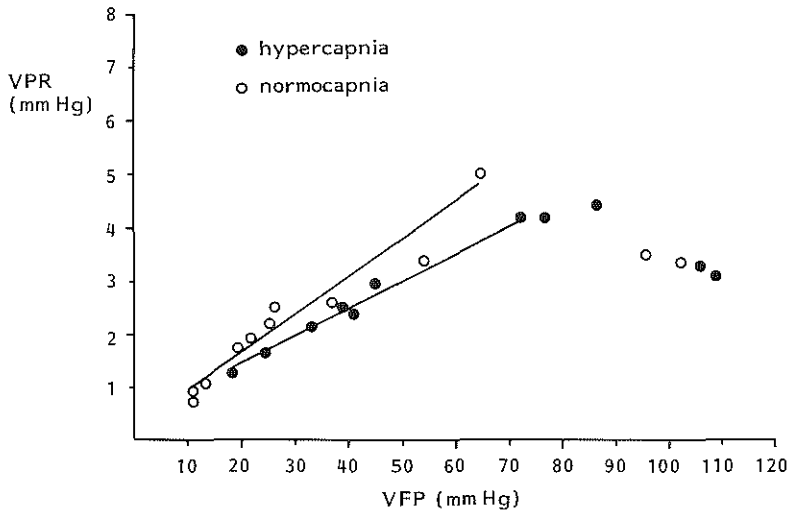


Fig. 39. Plot of volume-pressure response (VPR) against ventricular fluid pressure (VFP) at normocapnia and hypercapnia during cerebral compression in single animal (no 3). Linear relationships ($p < 0.001$) are shown up to breakpoint VFP above which VPR slightly declines. Regression equations are given in Table 11. Slopes were not significantly different (F-test).

Table 11. Relationship between volume-pressure response (VPR) and ventricular fluid pressure during normocapnia and hypercapnia: regression equation, number of datapoints (n), correlation coefficient (r), and elastance coefficient (E_1) below breakpoint, and mean VPR and elastance above breakpoint. Mean values (\pm SD) of arterial carbon dioxide tension (PaCO_2) and systemic arterial pressure (SAP) are given.

Animal no	Below breakpoint				Above breakpoint				
	Regression equation	n	r	E_1 (1/ml)	Mean VPR (mm Hg)	n	Elastance (mm Hg/ml)	PaCO_2 (mm Hg)	SAP (mm Hg)
Normocapnia									
1	$y=0.08x+2.5$	7	0.95	1.5	4.9	3	98	36.3 ± 2.7	126.5 ± 5.0
2	$y=0.10x+1.0$	9	0.97	1.9	5.5	2	110	43.0 ± 2.8	135.1 ± 7.3
3	$y=0.07x+0.3$	10	0.97	1.4	3.4	2	68	43.6 ± 2.9	145.8 ± 7.4
4	$y=0.07x+0.8$	4	0.93	1.4	4.4	4	88	39.7 ± 0.8	132.4 ± 4.0
5	$y=0.06x+1.9$	9	0.85	1.2	4.1	6	82	40.4 ± 1.9	166.3 ± 4.7
6	$y=0.06x+0.4$	6	0.92	1.2	3.8	5	76	42.4 ± 2.4	147.7 ± 2.7
Mean	$y=0.07x+1.2$			1.4	4.4		87	40.9 ± 2.7	142.3 ± 14.3
Hypercapnia									
1	$y=0.07x+2.8$	5	0.95	1.4	5.2	4	104	53.8 ± 5.4	131.2 ± 3.3
2	$y=0.11x+0.7$	8	0.96	2.1	5.7	2	114	61.2 ± 4.0	161.2 ± 10.6
3	$y=0.05x+0.5$	7	0.99	1.0	4.2	4	84	60.7 ± 4.3	155.4 ± 8.1
4	$y=0.05x+1.4$	3	0.96	1.0	4.0	4	80	60.4 ± 3.1	143.8 ± 3.5
5	$y=0.04x+3.2$	6	0.81	0.8	4.7	8	94	55.6 ± 2.5	182.5 ± 5.6
6	$y=0.05x+1.0$	5	0.68	1.0	4.0	4	80	55.3 ± 3.3	152.1 ± 6.1
Mean	$y=0.06x+1.6$			1.2	4.6		93	57.8 ± 3.3	154.4 ± 17.3

In view of the levelling-off phenomenon of the VPR and in accordance with the results of the previous series, the VFP range above the breakpoint was conceived as a pressure range with a constant elastance to which, consequently, a linear volume-pressure model should be applied. The elastance was calculated from the mean VPR of this pressure range (Table 11). In none of the animals did hypercapnia produce a significant change in the high pressure elastance.

A typical example of the effect of hypercapnia on the relationship between CSF pulse pressure and VFP is shown in Figure 40. All the animals behaved in this way. With regard to the analysis of the data the same breakpoints were taken into account as were found in the VPR-VFP relationships. On either side of the breakpoint there was a significant

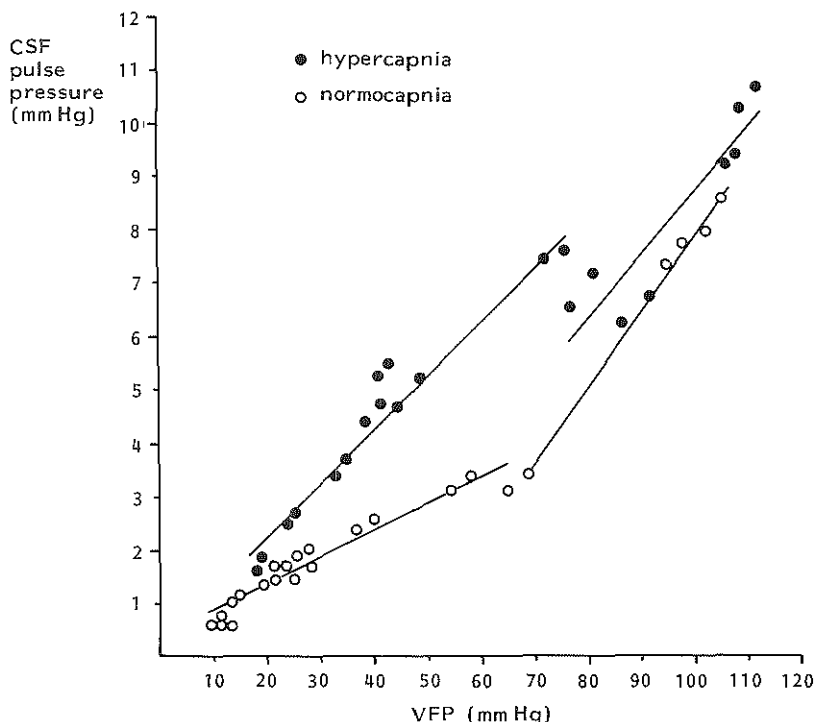


Fig. 40. Effect of hypercapnia on relationship between CSF pulse pressure and ventricular fluid pressure (VFP) during cerebral compression in single animal (no 3). Significant linear relationships ($p < 0.001$) were obtained on either side of breakpoints. Regression equations are given in Table 12. Below breakpoint CSF pulse pressure increased significantly faster during hypercapnia (F-test applied to slopes of regression lines, $p < 0.001$). When slopes of regression lines below and above breakpoints were compared, a significant increase was found during hypercapnia only (F-test, $p < 0.001$).

linear correlation ($p < 0.001$) between CSF pulse pressure and VFP. The regression equations are given in Table 12. Below the breakpoint the gradient of the regression line was always steeper during hypercapnia than during normocapnia. In five animals the difference attained statistical significance (F-test: $p < 0.05$ in one and $p < 0.001$ in four animals). Above the breakpoint, however, the effect of CO_2 on the pulse pressure was less pronounced. In four animals the slope of the 'hypercapnic' relationship was only slightly steeper, in one it was weaker, whereas in the remaining animal there was no difference in slope between hypercapnia and normocapnia. None of these differences was statistically significant.

The breakpoint was also operative in another way. During normocapnia the pulse pressure increased more rapidly above than below the breakpoint in all the animals. The difference between the gradients of the regression lines attained statistical significance in five animals (F-test: $p < 0.05$ in two and $p < 0.001$ in three animals). During hypercapnia the pulse pressure showed a significantly steeper increase above the breakpoint in two animals only (F-test: $p < 0.05$ and $p < 0.001$). These results are summarized in Figure 41 which shows the mean regression lines of the group of animals.

According to the mathematical model, the linear correlations of both VPR and CSF pulse pressure with the VFP imply a constant pulsatile change in CBV below the breakpoint. Using E_1 and the slopes of the CSFPP-VFP regression lines, ΔV_b was calculated, and the results are given in Table 12. Hypercapnia produced a significant increase in ΔV_b in each animal.

The rapid increase in pulse pressure above the breakpoint can only be caused, in view of the constant elastance in this pressure range, by a progressive increase in ΔV_b . The increase in ΔV_b per mm Hg increase in VFP was calculated and the results are given in Table 12, showing no significant differences between the normocapnic and hypercapnic states.

Hypercapnia also produced a slight rise in SAP as well as in ΔSAP (Tables 11 and 12). This should be taken into account when the effects of hypercapnia on both VPR and pulse pressure are to be discussed. The heart rate remained unchanged (Table 12). The difference between these variables on either side of the breakpoint was checked to see if it was significant, but this was not found to be the case.

Table 12. Relationship between CSF pulse pressure and ventricular fluid pressure (VFP) below and above breakpoint during normocapnia and hypercapnia: regression equations, number of datapoints (n), correlation coefficients (r), pulsatile change in cerebral blood volume (ΔV_B), and increase in ΔV_B per mmHg rise in VFP. Mean values (\pm SD) of systemic arterial pressure (SAP) and heart rate (HR) are given.

Animal no	Below breakpoint				Above breakpoint					
	Regression equation	n	r	ΔV_B (ml)	Regression equation	n	r	Increase in ΔV_B (ml/mm Hg VFP)	Δ SAP (mm Hg)	HR (beats/min)
Normocapnia										
1	$y=0.19x-0.9$	12	0.92	0.113	$y=0.23x- 2.1$	8	0.99	0.0023	58.1 ± 4.5	136.7 ± 23.0
2	$y=0.12x+0.7$	17	0.98	0.059	$y=0.16x- 1.3$	5	0.99	0.0015	54.3 ± 6.3	70.7 ± 8.2
3	$y=0.05x+0.4$	20	0.97	0.036	$y=0.14x- 6.3$	5	1.00	0.0021	52.2 ± 5.6	105.8 ± 14.2
4	$y=0.11x+0.0$	7	1.00	0.077	$y=0.15x- 2.4$	8	0.97	0.0017	44.6 ± 5.2	83.3 ± 7.5
5	$y=0.09x+0.6$	17	0.96	0.074	$y=0.23x- 9.2$	13	0.99	0.0028	71.0 ± 3.3	91.0 ± 9.9
6	$y=0.18x-0.7$	12	0.99	0.142	$y=0.36x-10.9$	9	0.91	0.0047	62.1 ± 4.1	87.0 ± 4.2
Mean	$y=0.12x+0.0$			0.084	$y=0.21x- 5.4$			0.0025	57.1 ± 9.0	95.8 ± 23.1
Hypercapnia										
1	$y=0.31x-4.6$	9	0.95	0.200	$y=0.28x- 0.7$	9	0.87	0.0027	65.9 ± 2.8	133.8 ± 19.5
2	$y=0.16x+0.6$	15	0.99	0.071	$y=0.20x- 0.9$	5	0.99	0.0018	65.8 ± 6.2	72.4 ± 5.4
3	$y=0.10x+0.2$	14	0.97	0.098	$y=0.12x- 3.3$	8	0.92	0.0014	57.4 ± 4.7	108.4 ± 7.1
4	$y=0.11x+0.4$	5	1.00	0.107	$y=0.16x- 3.6$	8	0.97	0.0020	47.1 ± 3.9	91.0 ± 6.2
5	$y=0.17x-1.8$	10	0.99	0.200	$y=0.23x- 7.0$	19	0.96	0.0024	77.2 ± 4.1	93.0 ± 8.5
6	$y=0.24x-2.7$	10	1.00	0.220	$y=0.34x- 9.8$	8	0.83	0.0043	63.6 ± 2.9	81.0 ± 3.0
Mean	$y=0.18x-1.3$			0.149	$y=0.22x- 4.2$			0.0024	62.8 ± 10.0	96.6 ± 21.9

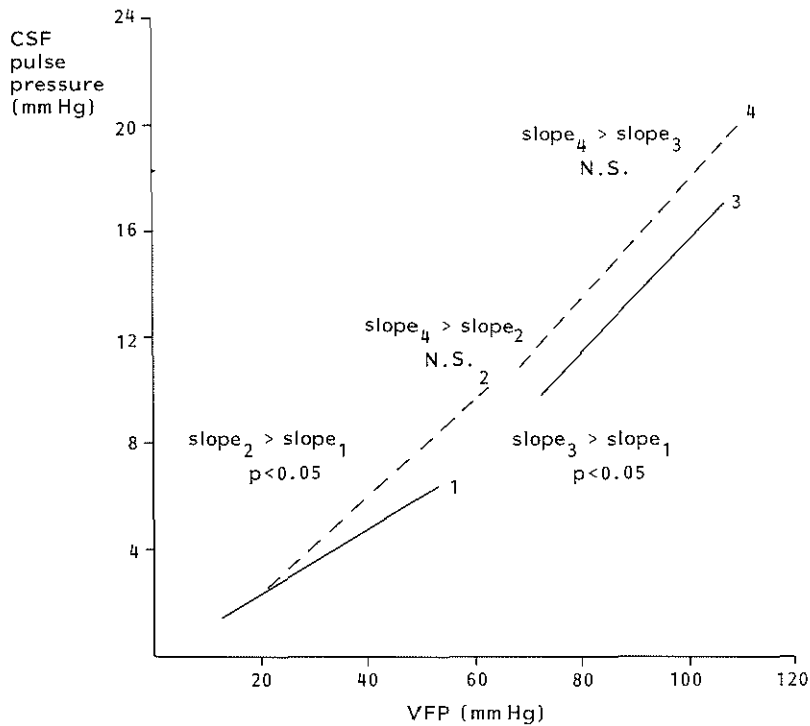


Fig. 41. Summed data of effect of hypercapnia on relationship between CSF pulse pressure and ventricular fluid pressure (VFP) during cerebral compression in six dogs. Mean regression lines during normocapnia (continuous lines) and hypercapnia (dashed lines) are shown on either side of breakpoints. Corresponding regression equations are given in Table 12. Differences between slopes of various regression lines were statistically evaluated by applying Wilcoxon's matched-pairs test to regression lines of individual animals.

Effects of changes in systemic arterial pressure

The hypotensive, normotensive and hypertensive levels of the SAP, Δ SAP and heart rate obtained in the various animals are given in Tables 13 and 14. The last two variables did not significantly differ between the various SAP levels. Typical reactions of the VFP to the administration of trimethaphan and angiotensin are shown in Figure 42. The VFP first moved in the same direction as the SAP, but generally after 10 to 30 seconds the VFP began to move in the opposite direction. This was regarded as the effect of an autoregulatory vasomotor response to the change in cerebral perfusion pressure, consisting of vasodilatation in case of hypotension and vasoconstriction in case of hypertension. So long as this response was effective, the net effect of altering the SAP on the VFP was small, as shown in Figure 43. At a certain level of ICP, however, the response

Table 13. Relationship between volume-pressure response and ventricular fluid pressure at normal, reduced, and raised levels of systemic arterial pressure (SAP): regression equation, number of datapoints (n), correlation coefficient (r), and elastance coefficient (E1) below breakpoint.

Animal no	Regression equation	n	r	E ₁ (1/ml)	SAP (mm Hg)
Normotension					
1	$y=0.07x+0.6$	13	0.94	1.4	129.1 ± 7.8
2	$y=0.04x+0.1$	9	0.89	0.8	132.6 ± 7.4
3	$y=0.05x+0.5$	8	0.95	1.0	140.2 ± 5.6
4	$y=0.10x-0.2$	7	1.00	1.9	145.1 ± 7.0
5	$y=0.10x-0.2$	10	0.96	1.9	133.6 ± 6.0
6	$y=0.09x+0.5$	6	0.99	1.7	132.6 ± 3.6
Mean	$y=0.08x+0.2$			1.5	135.5 ± 5.9
Hypotension					
1	$y=0.07x+0.5$	12	0.85	1.4	87.9 ± 8.7
2	$y=0.03x+1.6$	7	0.55	0.6	86.9 ± 6.0
3	$y=0.05x+0.6$	6	0.95	1.0	90.0 ± 5.4
4	$y=0.07x+0.3$	6	0.96	1.4	96.0 ± 4.5
5	$y=0.07x+0.3$	10	0.98	1.4	92.5 ± 6.2
6	$y=0.04x+1.1$	6	0.94	0.8	80.9 ± 8.4
Mean	$y=0.06x+0.7$			1.1	89.0 ± 5.2
Hypertension					
1	$y=0.12x-0.7$	9	0.96	2.3	175.9 ± 15.1
2	$y=0.06x+0.8$	8	0.95	1.2	164.7 ± 6.1
3	$y=0.08x+0.2$	5	0.98	1.5	174.9 ± 10.1
4	$y=0.09x+0.0$	7	1.00	1.7	190.5 ± 3.6
5	$y=0.13x-0.2$	10	0.95	2.4	178.5 ± 9.6
6	$y=0.08x+0.9$	5	1.00	1.5	167.3 ± 8.0
Mean	$y=0.09x+0.2$			1.8	175.3 ± 9.1

started to decline and finally it disappeared, after which the VFP closely followed the SAP (Fig. 43).

When the VPR was plotted against the VFP, the same type of relationship as in the previous series was found for all three levels of SAP: a significantly linear increase ($p < 0.01$) of the VPR below and a fairly constant VPR above a breakpoint (Fig. 44). The regression equations of the relationships below the breakpoint are given in Table 13. An increase in VPR with rising SAP was observed in all the animals. When the slopes of the regression lines at the various SAP levels were compared, a

Table 14. Relationship between CSF pulse pressure and ventricular fluid pressure at normal, reduced, and raised levels of systemic arterial pressure: regression equation, number of datapoints (n), correlation coefficient (r), and pulsatile change in cerebral blood volume (ΔV_b) below breakpoint. Mean values (\pm SD) of systemic arterial pulse pressure (Δ SAP) and heart rate (HR) are given.

Animal no	Regression equation	n	r	ΔV_b (ml)	Δ SAP (mm Hg)	HR (beats/min)
Normotension						
1	$y=0.13x-1.3$	25	0.96	0.090	46.6 ± 5.9	120.5 ± 15.2
2	$y=0.05x+0.6$	17	0.95	0.062	32.8 ± 4.9	157.3 ± 7.7
3	$y=0.05x+0.4$	15	0.90	0.050	32.2 ± 4.8	138.4 ± 9.0
4	$y=0.11x+0.4$	13	0.99	0.055	54.5 ± 3.0	143.3 ± 9.0
5	$y=0.03x+0.0$	19	0.95	0.016	28.3 ± 2.6	143.1 ± 25.4
6	$y=0.03x+0.1$	11	0.88	0.017	26.5 ± 8.0	135.5 ± 21.6
Mean	$y=0.07x+0.0$			0.048	36.8 ± 11.2	139.7 ± 12.0
Hypotension						
1	$y=0.12x-0.8$	23	0.90	0.084	39.3 ± 6.4	123.3 ± 12.5
2	$y=0.06x+1.3$	14	0.83	0.099	26.3 ± 1.4	143.6 ± 6.6
3	$y=0.14x-0.5$	11	0.95	0.134	28.4 ± 1.8	114.5 ± 4.0
4	$y=0.14x+0.8$	11	0.97	0.097	39.5 ± 2.5	152.0 ± 24.2
5	$y=0.05x+0.2$	19	0.94	0.036	29.1 ± 2.9	124.8 ± 17.0
6	$y=0.05x+0.4$	11	0.84	0.062	24.5 ± 2.9	127.0 ± 10.3
Mean	$y=0.09x+0.2$			0.085	31.2 ± 6.6	130.9 ± 14.0
Hypertension						
1	$y=0.09x-0.2$	17	0.93	0.038	48.7 ± 5.6	98.0 ± 14.7
2	$y=0.03x+0.9$	15	0.90	0.025	27.8 ± 6.3	156.8 ± 13.1
3	$y=0.03x+0.4$	10	0.97	0.019	23.5 ± 4.0	121.8 ± 11.7
4	$y=0.12x+0.0$	10	0.97	0.066	49.9 ± 5.8	129.9 ± 7.7
5	$y=0.02x+0.5$	19	0.55	0.008	29.5 ± 6.0	125.1 ± 14.1
6	$y=0.01x+0.5$	9	0.84	0.006	22.7 ± 3.1	132.0 ± 5.6
Mean	$y=0.05x+0.4$			0.027	33.7 ± 12.4	127.3 ± 18.9

significant difference was found between normotension and hypotension in three animals ($p < 0.01$) and between normotension and hypertension in the other three animals ($p < 0.05$). Only when the extremes, hypotension and hypertension, were compared was a significant change in slope found in all the animals ($p < 0.1$ in one, $p < 0.05$ in two and $p < 0.01$ in the remaining animals).

The elastance coefficients were calculated from the slopes of the regression lines and the results are given in Table 13. Hypertension

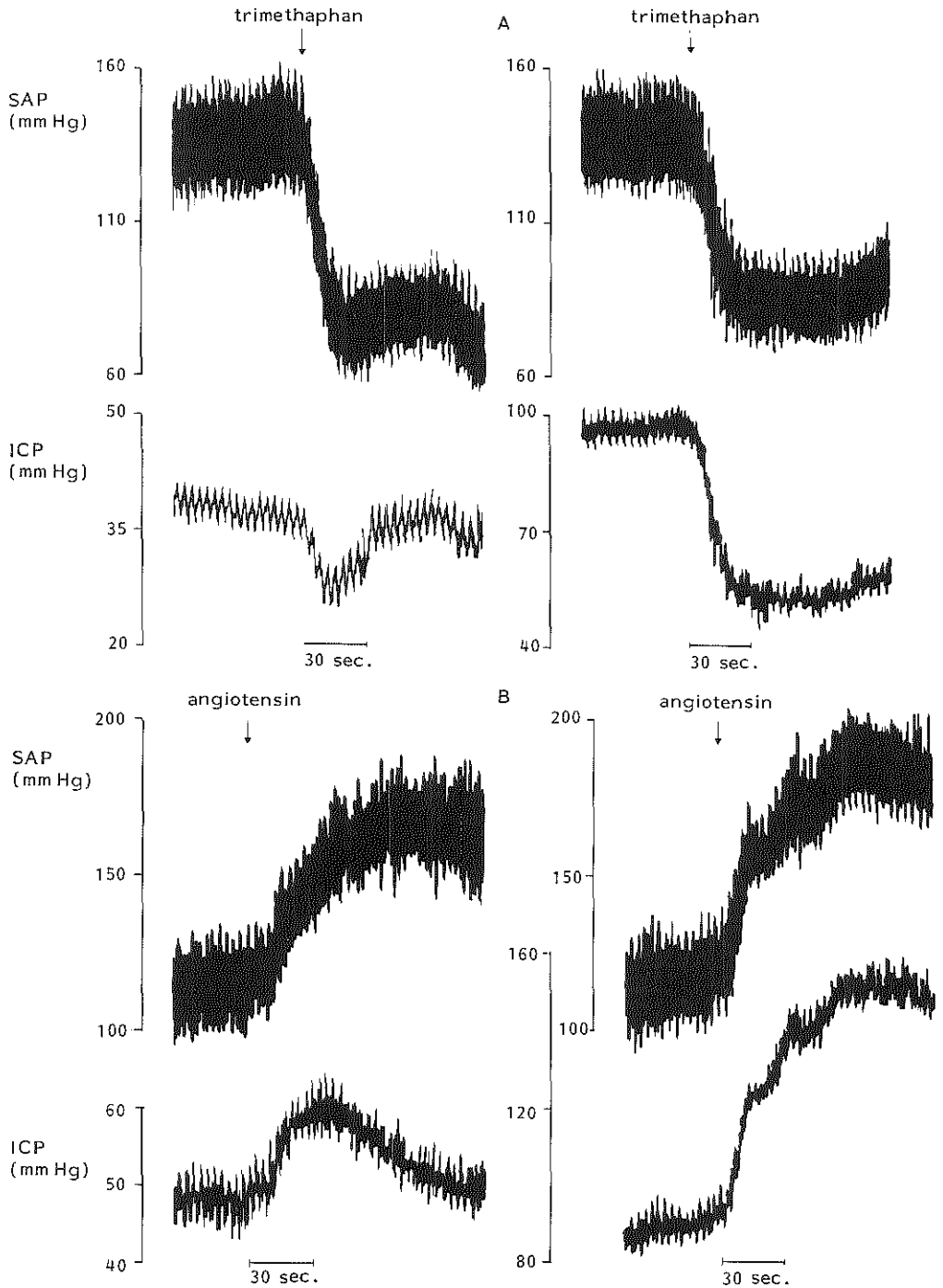


Fig. 42. Tracings of systemic arterial pressure (SAP) and ventricular fluid pressure (VFP) during intravenous administration of trimethaphan (A) and angiotensin (B) before (left) and after (right) breakpoint. Typical response of VFP to change in SAP before breakpoint is believed to reflect cerebro-vascular reactivity, representing intact CBF autoregulation. After breakpoint VFP closely follows SAP, indicating impaired autoregulation.

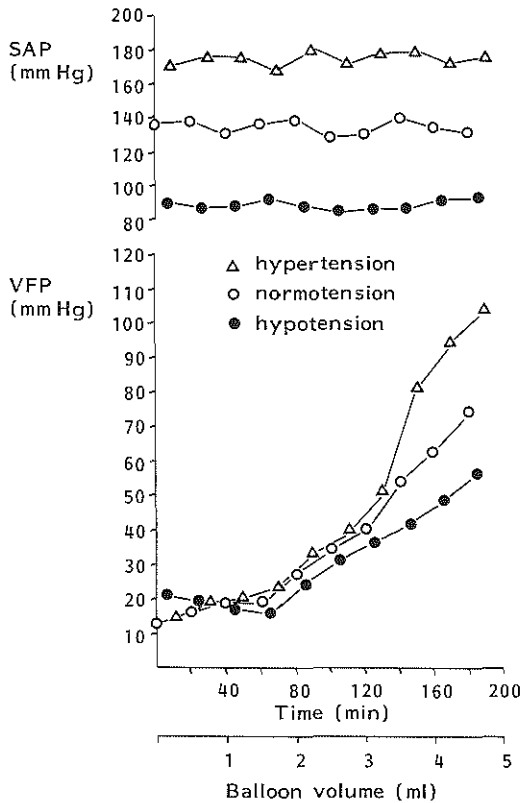


Fig. 43. Composite plots of systemic arterial pressure (SAP) and ventricular fluid pressure (VFP) at arterial normotension and drug induced hypotension and hypertension during steady rate inflation (1 ml/40 min) of extradural balloon in six dogs. Initially, changes in SAP had little effect on VFP. From mean VFP of 55 mm Hg onwards changes in SAP produced significant changes in VFP. In each animal this event coincided with disappearance of vasomotor response as shown in Figure 42 (right), and with breakpoint in relationship between volume-pressure response and VFP.

generally produced an increase in E_1 and hypotension a decrease, implying a steeper and a flatter volume-pressure curve respectively.

The breakpoints occurred at a mean VFP of 45.7 mm Hg for hypotension (range 41.4-48.8 mm Hg), 55.1 mm Hg for normotension (range 38.3-69.6 mm Hg) and 58.3 mm Hg for hypertension (range 45.6-73.8 mm Hg). The breakpoint pressures at the breakpoints were 42.7 mm Hg, 79.6 mm Hg and 119.8 mm Hg. (Wilcoxon matched-pairs test: $p < 0.05$). The corresponding perfusion pressures at the breakpoints were 42.7 mm Hg, 79.6 mm Hg, and 119.8 mm Hg. The breakpoint VFP at normotension corresponded with the VFP at which the autoregulatory vasomotor response disappeared and this was confirmed in each animal.

In this series the VFP range above the breakpoint was not studied

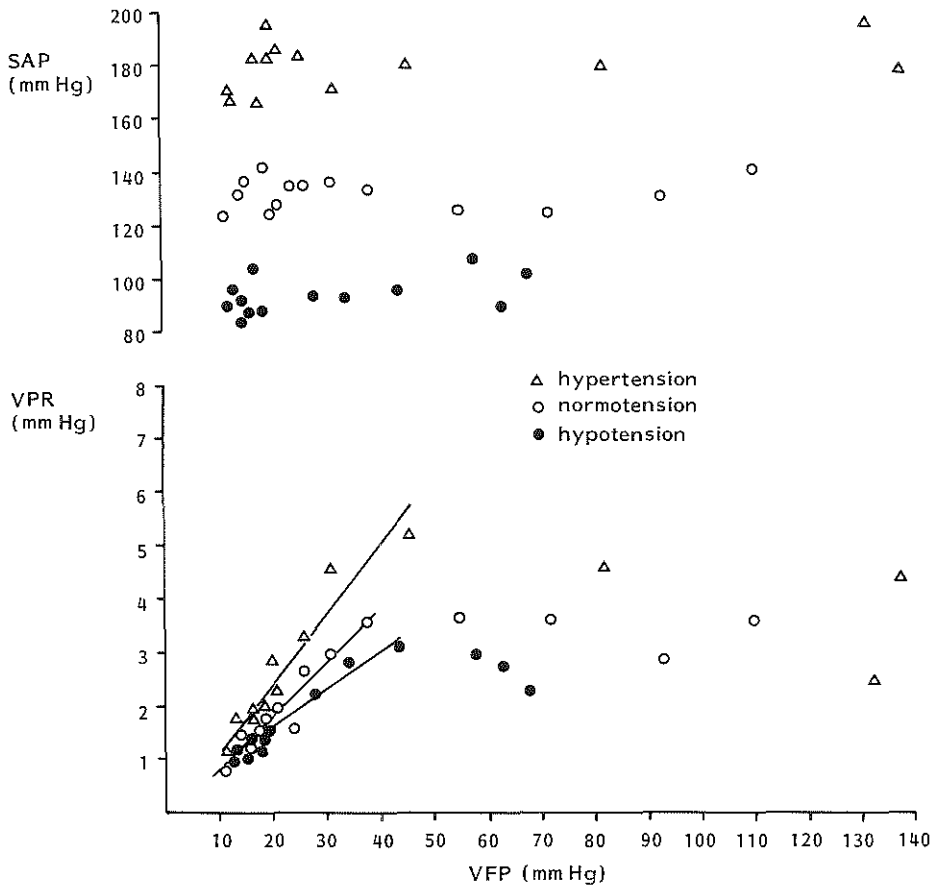


Fig. 44. Effects of systemic arterial hypotension and hypertension, in single animal (no 5), on relationship between volume-pressure response (VPR) and ventricular fluid pressure (VFP) during cerebral compression. Levels of systemic arterial pressure (SAP) are shown. At all three levels of SAP a breakpoint in relationship was observed. Below breakpoint significant linear relationships were obtained ($p < 0.001$). Regression equations are given in Table 13. In this animal there was a significant difference between the slopes of hypotension and normotension and between the slopes of hypotension and hypertension (F-test, $p < 0.01$). Above breakpoints VPR remained constant or decreased slightly.

further; too few data points were available on the whole since the SAP changes caused large fluctuations in VFP.

The plots of CSF pulse pressure against VFP showed linear correlations for each SAP level ($p < 0.01$). Figure 45 shows a typical example in a single animal. The regression equations are given in Table 14. Comparison of the slopes of the regression lines yielded the reverse results to those found in the VPR-VFP plots, i.e., a decrease in slope with increasing SAP level. A significantly weaker slope at hypertension compared with normotension

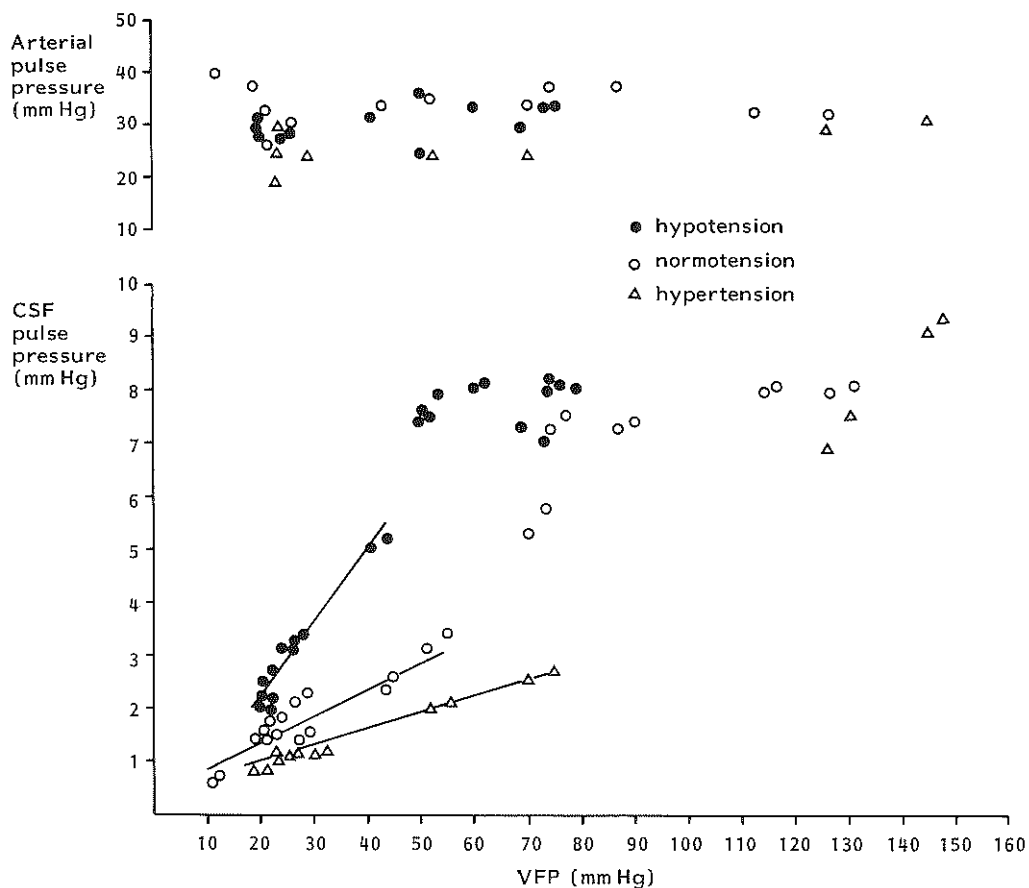


Fig. 45. Effects of systemic arterial hypotension and hypertension on relationship between CSF pulse pressure and ventricular fluid pressure (VFP) during cerebral compression in single animal (no 3). Values of systemic arterial pulse pressure are shown. Only data below breakpoints were analysed. Significant linear relationships were found at all three blood pressure levels ($p < 0.001$); regression equations are given in Table 14. The slopes were significantly different from each other (F-test, $p < 0.01$). Above breakpoints pulse pressures seem to converge.

was found in five animals (F-test: $p < 0.05$). The remaining animal showed a steeper slope at hypertension, but the difference was not statistically significant. Hypotension produced a steeper slope than normotension in all but one animal, but the difference attained statistical significance in only three animals ($p < 0.05$). Only when hypertension was compared with hypotension was a uniform change in slope found in all the animals ($p < 0.05$ in five animals).

The pulsatile change in CBV was calculated for each SAP level from the slopes of the regression lines and E_1 . The results are given in Table 14. Raising SAP caused a decrease in ΔV_b and lowering SAP an increase.

It should be noted that the differences in ΔV_b between the various SAP levels are greater than the differences between the slopes of the regression lines. The reason is that, according to the mathematical model, the slopes are determined by the product of E_1 and ΔV_b , factors which are affected in opposite ways by SAP changes.

Both Δ SAP and heart rate remained fairly constant during alterations in SAP (Table 14) and therefore they cannot account for the differences in ΔV_b . Although the effect of changes in heart rate on the CSF pulse pressure was not studied specifically in these investigations, this effect could be demonstrated in an animal which was rejected from the series due to the development of bradycardia during the infusion of angiotensin. In this case an increase in pulse pressure was observed during hypertension as shown in Figure 46. The reason is that, assuming a constant CBF/min, a decrease in heart rate will result in an increase in CBF per cardiac cycle, which will consequently cause an increase in ΔV_b , as argued

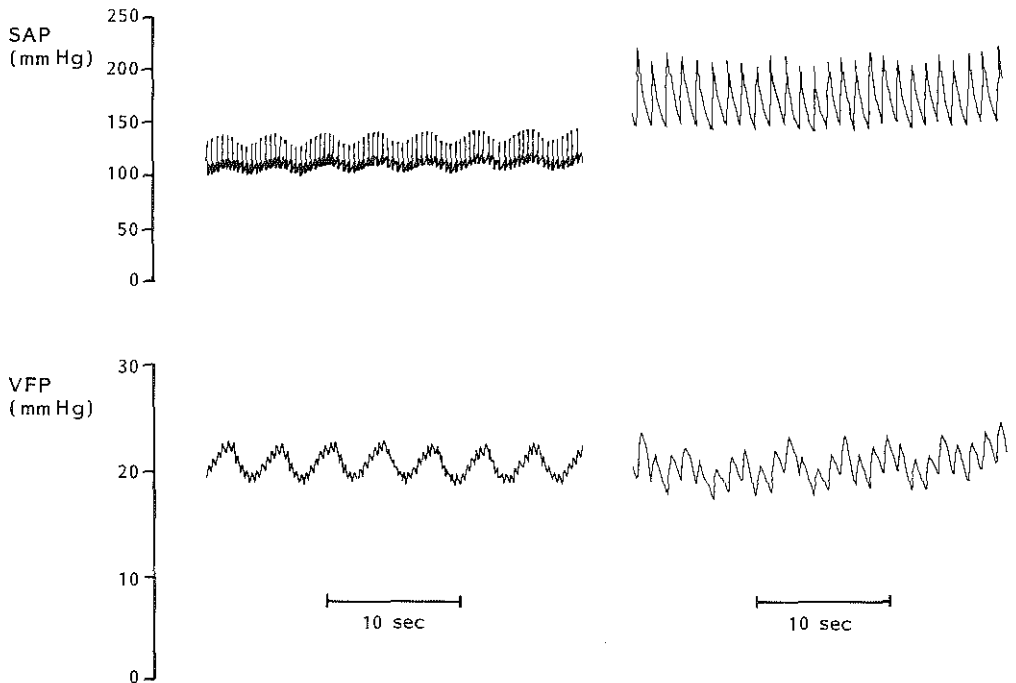


Fig. 46. Experimental run during infusion of angiotensin. Tracings of systemic arterial pressure (SAP) and ventricular fluid pressure (VFP) at normal (left) and raised (right) SAP are shown. Heart rate decreased from 165 beats/min to 54 beats/min. Note marked increase in both arterial and CSF pulse pressure. Due to slowing of heart rate this animal was rejected from series.

in Chapter 3.3. When the pulse pressures were corrected to allow for the slowing in heart rate, using the factor 'heart rate at hypertension divided by mean heart rate at normotension', smaller pulse heights were obtained; these were in accordance with the previous results (Fig. 47).

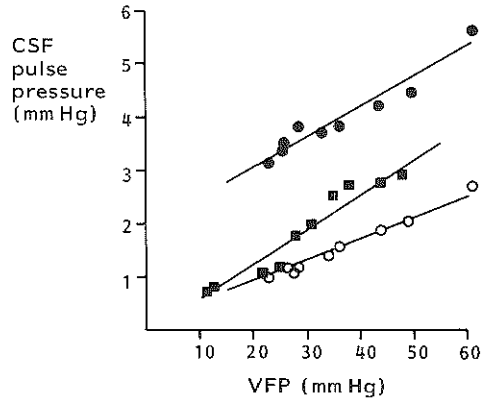


Fig. 47. Effect of change in heart rate, occurring during infusion of angiotensin, on relationship between CSF pulse pressure and ventricular fluid pressure (VFP) in animal rejected from series. See also Figure 46. Systemic arterial pressure was raised from 124 ± 7 mm Hg to 174 ± 12 mm Hg. Heart rate decreased from 155 ± 11 beats/min to 64 ± 8 beats/min. Relationship at normotension is given by squares ($y=0.07x - 0.2$). Note increase in CSF pulse pressure during hypertension (filled circles; $y=0.06x + 1.7$). Correction of CSF pulse pressure at hypertension to allow for slowing in heart rate by factor $155/64$ yields relationship similar to that observed in animals of series (open circles; $y=0.04x + 0.2$).

6.4 Discussion

The results of these investigations lend support to some of the inferences made in the previous experimental study with regard to the relationships of VPR and CSF pulse pressure with the ICP and particularly with regard to the breakpoint in these relationships. This will be discussed first. The more specific effects of hypercapnia and SAP changes will then be considered.

Volume-pressure relationship and CSF pulse pressure

The results obtained at normal levels of PaCO_2 and SAP are consistent with those of the previous study. During cerebral compression by steady rate inflation of an extradural balloon, both VPR and CSF pulse pressure behave

differently on either side of a breakpoint ICP. Their linear relationships with the ICP below the breakpoint confirm the validity of the mathematical model, implying a mono-exponential volume-pressure curve and a constant pulsatile change in CBV. The findings in this study of a constant elastance and a markedly more rapid increase in pulse pressure above the breakpoint support the concept of a linear volume-pressure model and a progressive increase in ΔV_b once the breakpoint ICP is exceeded. The mean breakpoint ICPs of 53.4 mm Hg in the first and 55.1 mm Hg in the second series of the present study do not significantly differ from the previously reported breakpoint pressure of 59.8 mm Hg. The physiological explanation for the occurrence of the breakpoint was derived, as discussed before, from the concepts on the mechanisms underlying the VPR and ΔV_b . It was then suggested that the breakpoint is associated with failure of CBF autoregulation and the onset of cerebral vasoparesis.

This study has yielded arguments in favour of the above explanation. Hypercapnia is known to raise the ICP through an increase in CBV as a result of cerebral vasodilatation (Wolff and Lennox, 1930; Reivich, 1964; Langfitt et al., 1965; Phelps et al., 1973; Grubb et al., 1974). During the initial period of cerebral compression, CO_2 produced increasingly larger rises in ICP (Figs. 37 and 38). Here, two opposite effects are operative. On the one hand, the gradual fall in cerebral perfusion pressure induces autoregulatory vasodilatation and thus reduces the capacity of the cerebral vessels for further dilatation in response to CO_2 stimulus. On the other hand, the CO_2 induced increments in CBV cause progressively larger rises in ICP because of the exponential shape of the volume-pressure curve. The latter effect is apparently the stronger up to a pressure corresponding with the breakpoint ICP (Fig. 38). Above the breakpoint, the CO_2 reactivity of the ICP levels off and finally disappears. In view of the explanation for the breakpoint, two factors can be held responsible for this phenomenon, i.e., the linear nature of the volume-pressure relationship and the gradual loss of CO_2 reactivity of the cerebral vessels due to vasoparesis and, subsequently, vasoparalysis. The finding of some residual CO_2 reactivity beyond the breakpoint is not in conflict with the assumption of failure of autoregulation commencing at the breakpoint, as it has been well documented that some cerebrovascular reactivity to CO_2 is retained when autoregulation is abolished (Langfitt et al., 1965; Häggendal and Johannson, 1965; Ekström-Jodal, 1970). The significantly higher breakpoint ICP during hypercapnia compared with

normocapnia may be related to the increased SAP level during hypercapnia. The autoregulatory constrictor stimulus induced by raised SAP increases the residual vasodilator capacity, thus delaying maximal vasodilatation and consequent loss of autoregulation. The breakpoint seems therefore to be related to the cerebral perfusion pressure rather than to the level of ICP.

Further evidence for attributing the breakpoint in the VPR and pulse pressure versus ICP relationships to failure of autoregulation can be derived from the second series of experiments in which changes in SAP were induced. Below the breakpoint, variations in SAP had little influence on the ICP (Fig. 43). This provides indirect evidence that the cerebrovascular reactivity to changes in perfusion pressure was preserved. The typical shape of the VFP tracings following the induction of SAP changes (Fig. 42) shows that, in spite of the recurrent infliction of systemic arterial hypotension and hypertension, the autoregulatory vasomotor response of the animal preparations remained intact. The absence of response above the breakpoint ICP indicates that the cerebral vessels behaved in a pressure-passive manner to changes in SAP. As a result, the SAP variations produced exaggerated changes in ICP (Fig. 43). These observations are consistent with those made by Langfitt et al. (1965) and Harper (1966). It is interesting to note that the breakpoints at arterial hypotension, normotension and hypertension occurred at successively higher ICPs. Again, the explanation follows from the assumption that the breakpoint is related to disturbance of autoregulation. Since autoregulation is a function of cerebral perfusion pressure, its lower limit is shifted towards a higher ICP if SAP is raised. The perfusion pressures at the breakpoints varied considerably however. The breakpoint at hypertension occurred when the perfusion pressure was still relatively high. This is probably due to damage to the flow regulating structures as cerebral compression progresses.

Effects of hypercapnia

The aim of this study was to examine the effects of changes in PaCO_2 and SAP on the amplitude of the CSF pulse during elevation of ICP. We were mainly interested in the pulsatile ICP variations in so far as they are a measure of intracranial elastance which, in turn, may also be influenced by the variables under investigation. Consequently the craniospinal

volume-pressure relationships had to be studied as well.

Hypercapnia did not significantly alter the elastance coefficient in the individual animals, implying that the shape of the volume-pressure curve was not affected. These results are in line with those of Löfgren (1973) who recorded the volume-pressure curve in dogs by rapid infusion into the cisterna magna. He also found a slight, though not significant decrease in elastance. Both Leech and Miller (1974) and Rowed and co-authors (1975) reported that also *hypocapnia*, induced by hyperventilation, had no effect on the elastance. However, the group results of our study, a reduction of E_1 in five animals, do suggest a slight flattening of the volume-pressure curve. This effect might have been even more pronounced, and perhaps have attained statistical significance, if the SAP with its positive effect on E_1 had not been increased during hypercapnia. In that case the results would have supported those of Cohadon et al. (1975) and Takagi et al. (1980) who did find a decrease in elastance with increasing levels of PaCO_2 . Another reason for our results failing to attain statistical significance may be the relatively small range of PaCO_2 (40.9 \pm 2.7 - 57.8 \pm 3.3 mm Hg) compared with the ranges examined by the authors mentioned above: normocapnia up to 74 \pm 3 mm Hg and 22 to 52 mm Hg respectively. We are therefore inclined to conclude that PaCO_2 and elastance are negatively correlated, but that in the PaCO_2 range encountered clinically the elastance will be little affected.

Some effect of hypercapnia on the VPR could be anticipated from a theoretical point of view, taking into account the physiological basis of the VPR. If CO_2 increases CBV without impeding the efflux of venous blood, the capacity of the venous compartment to accommodate volume increments through the mechanism of spatial compensation will be enlarged. Consequently, the pressure response will decrease.

In this respect it is of interest to note that, in contrast to the findings below the breakpoint, a slight increase in the high pressure elastance was observed during hypercapnia above the breakpoint. In this situation PaCO_2 responsivity of the vessels is lost and CBV is not further increased. This is confirmed by the results of Takagi et al. (1980) who found that PaCO_2 changes did not affect elastance in non-autoregulating animals. The slight increase in elastance in our series can be attributed to the increase in SAP during hypercapnia, as will be discussed later.

In contrast to the effect on the VPR, hypercapnia produced a

significant increase in the amplitude of the CSF pulse. This is in accordance with various other reports (Goldensohn et al., 1951; Hamer et al., 1977). Symon (1968 and 1970) used the ratio of venous to arterial pulse height (pulse index) in the pial circulation within the middle cerebral arterial field for assessing regional vascular reactivity. He found an increased pulse index in response to increased PaCO_2 . Since the venous pulsations in particular are easily transmitted to the CSF, these observations also hold for the CSF pulse.

It follows from the experimental design of the present study that the increased pulse height is purely a CO_2 effect and that it is not related to the CO_2 induced rise in ICP. As E_1 was not significantly affected, the explanation for the increased pulse pressure should be sought in an increase in ΔV_b during hypercapnia. The CO_2 induced cerebral vasodilatation reduces the arterial inflow resistance and thus increases the time lag between the pulsatile inflow and outflow of cerebral blood, with the consequent effect on ΔV_b as discussed in Chapter 3.3. Apart from the timing mechanism, the CO_2 induced increase in CBF *per se* should cause a larger ΔV_b so long as the heart rate remains constant.

These arguments also explain why hypercapnia did not produce a significant effect on the increase in ΔV_b , and consequently on the increase in CSF pulse pressure, above the breakpoint. This is clearly shown in Figure 41. The gradients of the relationships between pulse pressure and VFP above the breakpoint are not significantly different, implying an equal increase in ΔV_b at normocapnia and at hypercapnia. This is because CO_2 gradually loses its vasodilatory action. Moreover, there is almost no breakpoint in the 'hypercapnic' relationships. This is because under hypercapnic conditions the cerebral vessels are almost maximally dilated all the time, and the increase in pulse pressure when autoregulation becomes impaired is therefore less marked than during normocapnia.

The systemic arterial pulse height is determined by vascular compliance and by the maximal pulsatile change in vascular volume. This volume is related to the amplitude of the systemic flow pulse. The systemic flow pattern is modified by cerebrovascular factors to constitute the cerebral arterial inflow profile, which is the major determinant of ΔV_b . ΔSAP may therefore be regarded, in terms of pressure, as reflecting one of the extracranial factors contributing to the formation of ΔV_b . The small rise in ΔSAP during hypercapnia may thus have been a contributory factor to the increase in CSF pulse pressure; it cannot account for the phenomenon

in full however as it was also present in animals with only a minimal difference in Δ SAP (Table 12). Moreover, the simultaneously elevated SAP tends to reduce the CSF pulse pressure and is thus in competition with the effect of Δ SAP. Above the breakpoint, however, the difference in Δ SAP may have been responsible for the constant difference in CSF pulse pressure between normocapnia and hypercapnia. Figure 41 shows the 'hypercapnic' regression line lying above the 'normocapnic' line, which means that the absolute values of ΔV_b were higher during hypercapnia. Another reason for this may have been the increased perfusion pressure during hypercapnia, causing a rise in CBF and, consequently, in ΔV_b in view of the fact that the heart rate remained constant.

Effects of changes in systemic arterial pressure

In contrast to the changes in PaCO_2 , altering the SAP significantly affected the craniospinal volume-pressure relationships. Raising SAP from hypotensive to hypertensive levels caused an increase in E_1 by approximately 50%. This is consistent with the results of Löfgren (1973) who found an elevation of the high pressure elastance by the same percentage if the same range of SAP is considered. Leech and Miller (1974) reported that the VPR increased by approximately 100% with rising SAP, but only at increased levels of ICP. Takagi and co-authors (1980), on the contrary, found that the PVI was not affected by changes in SAP within the relatively small range of 85 to 145 mm Hg. They did find a significant effect of SAP changes on the PVI in non-autoregulating animals however. Looking at each of the animals in our series, it was either hypotension or hypertension as compared with normotension that produced a significant change in E_1 . Only when the extreme levels were compared was a significant difference found in every animal.

Löfgren's hypothesis (1973) provides an explanation for the influence of SAP on elastance. The rapid volume addition to the CSF compartment causes a compression of the venous outflow section and temporarily reduces the egress of blood. Since the inflow remains unaffected, this will result in an augmentation of CBV with a corresponding rise in ICP, i.e., the VPR. In order that the equilibrium between inflow and outflow of blood is restored, the ICP will rise to the extent that the perfusion pressure over the inflow tract is decreased proportionally to the increase in outflow resistance. It can be shown that the magnitude of this rise in pressure

will depend on the magnitude of the pressure gradient over the inflow section of the vascular bed and thus on the SAP. This will be further elaborated in Appendix 4.

The results of the current study show that, in contrast to the effect on the VPR, the level of SAP is inversely related to the height of the CSF pulse (Table 14). The reason for this must be a decrease in ΔV_b with rising SAP since, according to the analogy between VPR and pulse pressure, an increase in pulse height with rising SAP would have been expected. Consequently, during rising SAP two opposing forces affect the amplitude of the CSF pulse, i.e., an increase in E_1 and a decrease in ΔV_b . The latter effect apparently prevails, as in most animals the CSF pulse pressure was significantly reduced when SAP was raised from hypotensive through normotensive to hypertensive levels and vice versa. These findings cannot be explained from changes in ΔSAP which was affected relatively little when SAP was altered (Table 14). Moreover, the small changes that occurred were mostly in the same direction as the SAP, so that their influence on the CSF pulse pressure was contrary to that of the SAP itself. The difference between the mean values of ΔV_b at normal SAP in this series and at normocapnia in the first series may be related to the difference in ΔSAP between the two series, since ΔSAP is the reflection of the systemic arterial flow pulse amplitude.

The explanation of the SAP induced changes in ΔV_b follows the same arguments as previously outlined. The alterations in cerebral perfusion pressure elicit an autoregulatory response of the cerebral resistance vessels, consisting of dilatation during hypotension and constriction during hypertension, thereby affecting the shape of the pulsatile inflow profile and, consequently, the time lag between inflow and outflow. The resulting effect on ΔV_b has been described in Chapter 3.3. Figure 45 shows that the difference in CSF pulse pressure between the various SAP levels tends to disappear above the breakpoints when cerebral vasoreactivity becomes impaired.

Contrary to the results of this study, Hamer et al. (1977) reported an increase in CSF pulse pressure with rising SAP. From their tracings, however, it appears that this was due to a concurrent rise both in ICP and in ΔSAP . Moreover, the rise in SAP probably did not last long enough for the autoregulatory vasoconstrictor response to develop, so that ΔV_b was not negatively influenced.

With regard to the vasomotor response as reflected in the ICP tracings of our study (Fig. 42), it might be argued that this was not a true autoregulatory response, but merely the result of the direct action of angiotensin and trimethaphan on the cerebral vasculature and that, consequently, our results only hold true for drug induced alterations in SAP. This criticism can be answered by referring to the previously mentioned work of Symon (1970) with regard to the arterial and venous pulsations in the middle cerebral field. Lowering the input arterial pressure by exsanguination or temporarily occluding the carotid vessels in the neck caused a reduction in pial artery pressure but a definite increase in pulse transmission from artery to vein. In these cases the CSF pulse pressure can also be assumed to be increased as the pulsations of the veins are easily transmitted through their thin walls to the surrounding CSF.

Furthermore, from comparison between intracarotid and intravenous administration of angiotensin in man, several investigators (Agnoli et al., 1965; Greenfield and Tindall, 1968; Olesen, 1972) have established that the increase in cerebrovascular resistance caused by the drug was secondary to the increase in SAP, representing true autoregulation, and that it was not the result of a direct effect on the cerebral vessels. The same has been demonstrated for trimethaphan by Olesen (1973), who found no CBF change after direct infusion of the drug into the internal carotid artery. Finally, additional evidence for the vasomotor response representing true autoregulation can be found by studying the latency between the change in SAP and the change in ICP in the opposite direction. In the animals in this series, this was always in the order of 10 to 30 seconds, which is consistent with the time intervals reported to be necessary for autoregulation to adjust (Rapela and Green, 1964; Kanzow, 1968; Ekström-Jodal et al., 1970; Symon et al., 1972).

Although we did not study this specifically, the findings during bradycardia confirm the hypothesized effect of the heart rate on the CSF pulse pressure (Chapter 3.3). They are in line with the results of Ikeyama et al. (1980) who also reported an increase in pulse pressure during bradycardia in dogs. The effect of the heart rate on ΔV_b was explained by the increase in CBF per cardiac cycle. In the discussion in Chapter 5 it was argued that an increase in nonpulsatile flow does not necessarily contribute to an increase in ΔV_b , so that generally a rise in CBF/cardiac cycle only causes an increase in ΔV_b if pulsatile flow is increased as well. In the example shown in Figure 46, the assumed increase in pulsatile

flow during bradycardia can be inferred from the increased arterial pulse pressure. In this respect the study made by Greenfield and Tindall (1968) is of interest; in measurements of internal carotid artery blood flow with electromagnetic flowmeters in man, they found less nonpulsatile and more pulsatile flow during slowing of the heart rate.

In conclusion, this study has provided information on the influence of two important clinical variables on the CSF pulse pressure. The ultimate effects were mainly produced through changes in ΔV_b . Consequently, changes in PaCO₂ and SAP occurring during clinical ICP monitoring will seriously interfere with the use of the CSF pulse pressure as a measure of cranio-spinal elastance. However, since these variables are routinely monitored in patients subjected to continuous ICP recording, the quantitative information provided in this study may enable the clinician to interpret changes in the CSFPP-ICP relationship in terms of changes in volume-pressure relationships.

Conclusions

1. This study provided additional evidence that the breakpoint in the relationships of both VPR and CSF pulse pressure to the ICP is related to failure of CBF autoregulation.
2. Hypercapnia produced a slight, though statistically not significant decrease in elastance coefficient.
3. Hypercapnia produced a significant increase in CSF pulse pressure.
4. A positive correlation was found between systemic arterial pressure and elastance coefficient.
5. A negative correlation was found between systemic arterial pressure and CSF pulse pressure.
6. An increase in CSF pulse pressure was observed during bradycardia.
7. The above effects on the CSF pulse pressure were ascribed to changes in the pulsatile change in CBV.

CHAPTER 7

THE PULSATILE CHANGE IN CEREBRAL BLOOD VOLUME IN DOGS ASSESSED BY ELECTROMAGNETIC FLOWMETRY UNDER VARIOUS EXPERIMENTAL CONDITIONS

"The mathematician need not have the skill to conduct a physiological experiment, but he must have the skill to understand one, to criticize one, and to suggest one. The physiologist need not be able to prove a certain mathematical theorem, but he must be able to grasp its physiological significance and to tell the mathematician for what he should look."

N. Wiener (1948)

7.1 Introduction

It has been argued in the preceding chapters that the CSF pulse pressure is determined by two factors: the elastance coefficient of the cranio-spinal system (E_1) and the magnitude of the pulsatile change in CBV (ΔV_b). In the clinical and experimental studies E_1 had actually been measured by rapid volume loading of the system, whereas ΔV_b , as a complementary quantity, had been deduced by application of a mathematical model from E_1 and the slope of the CSFPP-ICP relationship. As a result, alterations in pulse pressure that could not be explained by changes in E_1 were automatically attributed to changes in ΔV_b . A more correct approach would have been to measure both ΔV_b and E_1 independently and to verify whether these results could explain the observations on the CSF pulse pressure.

However, rapid changes in CBV in the order of magnitude of the pulsatile changes, constituting less than 2% of total CBV, are very difficult to assess quantitatively. Since ΔV_b is the resultant of the complex interaction between the pulsatile arterial inflow and venous outflow of blood, it could theoretically be assessed by measurement of all the ingoing and outgoing flow curves. From a practical point of view this does not seem feasible. Flow measurement in major arterial and venous channels, however, might yield a reliable estimate of ΔV_b and, at any rate, provide qualitative information on the direction of changes under various experimental conditions.

Another problem arises with regard to measurement of the flow profile at the venous side of the cerebrovascular bed. The major resistance to outflow lies in the easily compressible subarachnoid veins, probably close to their point of entry into the dural sinuses (Shulman and Verdier, 1967). In the sinuses, which constitute large venous reservoirs, pulsatile flow will be buffered and flow measurement here or in the more distant jugular veins will thus yield a flow profile which is

irrelevant to the formation of ΔV_b . The dynamic venous outflow profile would therefore have to be measured intradurally in the subarachnoid veins, which presents great technical problems. From observations on the CSF pulse pressure during changes in SAP and PaCO_2 (Chapter 6), it was inferred that under these circumstances ΔV_b is mainly determined by the cerebrovascular inflow resistance. It may therefore be expected that measurement of the arterial inflow pattern alone will suffice to explain changes in ΔV_b occurring under such conditions.

In the present series of experiments we measured pulsatile flow electromagnetically in the dog. Measurements were taken in the vertebral artery, which represents a major arterial inflow tract to the cerebral circulation. Assuming a constant, nonpulsatile venous outflow we calculated values for ΔV_b from the arterial inflow curve. As a control, flow was also measured in an arbitrarily chosen vessel contributing to the extracranial circulation. Both the influence of changes in SAP and PaCO_2 and the effect of raised ICP on ΔV_b were investigated.

7.2 Experimental methods

Preparation and Measurements

Seven adult mongrel dogs of either sex weighing from 21 to 26 kg (mean: 23.9 kg) were used. Atropine (0.5 mg) was routinely given as premedication. Anaesthesia was induced with intravenously administered thiopentone (30 mg/kg), maintained with a mixture of nitrous oxide and oxygen (2:1), and supplemented by fentanyl intravenously as needed. The animals were artificially ventilated (Pulmomatt) without the use of muscle relaxants. Body temperature was maintained at about 37° C by heating lamps and a heating pad. Normal saline was slowly infused intravenously throughout the experiment.

Blood flow was measured by means of an electromagnetic flow measuring system (Skalar, Transflow 601). The frequency response of the system was flat up to 100 Hz. The flow probes were provided with a built-in ground reference electrode. Zero flow was determined by immersion of the probes in a cylinder containing normal saline at body temperature and checked

in vivo by occlusion of the vessels distal to their probes. Calibration was done electrically. Dissecting the neck immediately above the first rib and retracting the scapula, the left subclavian artery was exposed. Care was taken not to injure the apex of the pleura. The flowmeter probe was applied to the vertebral artery somewhere between its subclavian origin and its entrance into the foramen transversarium. The size of the probe was chosen so that the vessel was constricted just enough to obtain an adequate signal. Its lumen diameter was usually 2.5 mm. The vertebral artery was chosen for assessment of intracranial flow since, in the dog, it constitutes a greater portion of total CBF than the internal carotid artery (Reivich et al., 1961; Miller et al., 1964). Previous neck dissections had shown that the diameter of the latter vessel was often too small for reliable flow measurements. Moreover, the origin of the internal carotid artery was not always easy to distinguish from that of the occipital artery and many anatomical variations had been observed. We therefore rejected the possible alternative solution, i.e., application of the probe to the common carotid artery with ligation of all the extracranial branches.

For the measurement of extracranial flow, as a control to intracranial flow, a second probe was applied either to the large axillary artery or to one of its smaller branches: internal mammary, thoracic or subscapular artery. This accounts for the large variation in extracranial flow values between the animals reported in the results. The choice was mainly determined by our efforts to ensure an optimal position of the probes without injuring the vessels. The cables from the probes to the flowmeters were attached to muscle and skin in order to avoid kinking of the vessels and the wound was provisionally closed. Both mean flow and pulsatile flow were recorded.

After preparation of the vessels in the neck the animal was placed in a stereotaxic holder in the sphinx position. The VFP was continuously measured from the right lateral ventricle as previously described (Chapter 5.2). The SAP was measured from an aortic catheter introduced via the femoral artery. The pressure transducers (HP 1280; pressure amplifiers: HP 8805B) were placed at the level of the right atrium. Arterial blood samples were drawn at regular intervals for blood gas analysis (Radiometer ABL 1). The readings were corrected for temperature differences between the animal and the recording system (Severinghaus, 1966). Tracheal CO₂ was monitored by an infrared gas analyzer (Beckman

Instruments). The ECG was recorded via needle electrodes placed in the limbs of the animal (HP Biological Amplifier 8811A) and the heart rate was continuously monitored (HP Rate Computer 8812A). All signals were displayed on a multi-channel chart recorder with a time and an event marker (HP Thermal Recording System 7418A).

In some of the animals a needle was percutaneously introduced into the cisterna magna for elevation of the ICP by stepwise infusion of normal saline (Harvard Infusion Pump, Model 975).

Experimental protocol

In each animal four types of experimental runs were performed: hypercapnia, hypocapnia, arterial hypotension and arterial hypertension. The number of runs varied between the animals. If more than one run was performed the results were averaged. The order of the experimental runs was chosen arbitrarily and differed from one animal to the other. The animals were allowed sufficient time for stabilization in between the runs.

Hypercapnia was induced by administration of 5% CO₂ to the inspired gas mixture. Usually after a period of about five minutes the VFP had risen considerably, indicating a significant cerebral vasodilatory effect of CO₂. Hypocapnia was induced by increasing the stroke volume of the ventilator until the VFP had been sufficiently lowered. PaCO₂ was determined before and at the height of each run.

SAP was lowered by intravenous titration of a 0.1% solution of trimethaphan (Arfonad). SAP was increased by continuous infusion of a solution (3 µg/ml) of angiotensin (Hypertensin-CIBA). A CBF autoregulatory response was commonly observed following the change in cerebral perfusion pressure. Data were always collected after this response had been fully established. PaCO₂ was kept within normal limits (37-43 mm Hg) during these runs.

In some of the animals, experimentation was concluded by studying the effects of raised ICP on ΔV_b . For this purpose various levels of intracranial hypertension were obtained by manipulating the speed of a pump infusing normal saline into the cisterna magna. The infusion rates varied from 22.7 to 167.0 ml/hr.

For data collection the speed of the chart recorder was increased to 50 mm/sec, so that both the CSF pulse waves and the flow pulse waves

could be clearly distinguished. The data were compared with those obtained during control runs before each experimental event.

Computation of the pulsatile change in cerebral blood volume

The pulsatile flow of the vertebral artery was read into a computer (PDP 11/34) at a sampling rate of 40/sec using an X-Y tablet (Summagraphics BIT PAD ONE) and analysed for five consecutive R-R intervals of the ECG. The calibration signals of flow and time axes were read into the computer for each separate run. The accuracy of the computer readings was checked by comparing the computed mean value of the flow pulse with the value of the mean flow as read from the recording paper.

The pulsatile change in CBV was computed according to the principles outlined in Chapter 3.3 from the following equations:

$$\Delta V(k) = \sum_{i=n_1}^{n_k} [F_a(i) - F_v(i)] \Delta t(i),$$

where: n_1 = first sample of R-R interval of the ECG,

n_k = k-th sample of the interval,

F_a = arterial inflow function,

F_v = venous outflow function, and

Δt = time interval between two consecutive samples.

Assuming a continuous, nonpulsatile venous outflow curve, the venous outflow can be substituted by the computed mean arterial flow:

$$F_v = \frac{1}{T} \sum_{i=n_1}^{n_2} F_a(i) \Delta t(i),$$

where: T = duration of R-R interval,

$n_2 - n_1$ = number of samples within the R-R interval.

ΔV_b is actually the difference between the maximum and minimum CBV within a cardiac cycle. It was computed from:

$$\Delta V_b = \Delta V(k)_{\max} - \Delta V(k)_{\min}.$$

To improve the reliability of the determination of ΔV_b the average value of five cardiac cycles was taken. The accuracy of this procedure was further checked by analysing known, rectangular test curves. The results for ΔV_b and mean flow were within 5% in agreement with the calculated values.

Figure 48 shows how the change in CBV during a cardiac cycle is computed. The actual magnitude of ΔV_b is given by the maximum amplitude of this change. It is dependent on that part of the flow curve where systolic flow exceeds mean flow, which equals venous outflow if this is assumed to be nonpulsatile. So ΔV_b is not necessarily determined by the peak-to-nadir amplitude of the flow pulse, but rather by the amplitude relative to the mean flow and, furthermore, by the duration of the t_1 - t_2 interval. In Chapter 3.3 we discussed the two mechanisms which determine the magnitude of ΔV_b , i.e., the CBF per cardiac cycle or the pulsatile volume load of blood to the brain and the time lag between the arterial inflow and venous outflow. Both mechanisms may contribute to a change in the amount of systolic flow responsible for ΔV_b by affecting either the amplitude or the duration of the systolic flow pulse. Both may even be affected simultaneously depending on the complex interaction of various extracranial and intracranial haemodynamic factors.

With regard to a change in the pulsatile volume load caused by a change in CBF/min, it can be easily seen that ΔV_b is not influenced if it

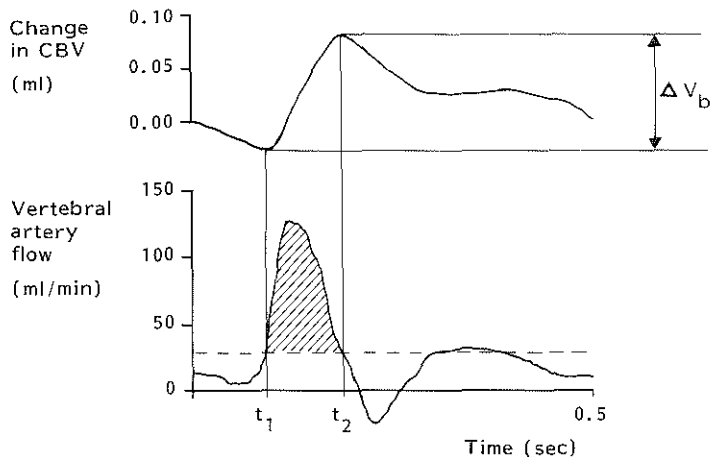


Fig. 48. Vertebral artery blood flow and computed change in cerebral blood volume (CBV) during one cardiac cycle in an experimental animal. Mean flow level, which is equal to venous outflow if this is assumed to be nonpulsatile, is given by dashed line. During time interval t_1 - t_2 , inflow of cerebral blood exceeds outflow, causing an increase in CBV. Magnitude of variation in CBV (ΔV_b) is determined by difference between extreme values of CBV and is thus dependent on shaded area of systolic flow pulse.

takes place only in the continuous portion of flow, as in that case the amplitude of the flow pulse relative to the mean flow is not changed. This was discussed in Chapter 5.4 in an attempt to explain the paradox of a decrease in CBF and an increase in ΔV_b . If the pulsatile volume load is affected by a change in heart rate, the pulsatile component of flow is likely to be always involved. As far as the change in time lag or phase shift between the pulsatile inflow and outflow of cerebral blood is concerned, it will be clear that its effect on the magnitude of ΔV_b is minimized by the assumption of a nonpulsatile venous outflow. In fact, if the change in phase of the inflow curve is such that the area of the systolic flow pulse relative to the mean flow level is not affected, ΔV_b does not change at all. This applies to the situation shown in Figure 11 (Chapter 3.3) where an increase in phase shift was demonstrated by a shift of the arterial and venous peak flows towards the beginning and the end of the cardiac cycle respectively. Although the arterial flow pulse amplitude has increased, the total amount of systolic flow has not changed in this figure. This type of phase shift will thus not give rise to a change in ΔV_b using the method of computing ΔV_b in the present study. However, another situation is conceivable in which the timing or interaction between inflow and outflow is involved, i.e., where there is a shift of flow from diastole to systole or vice versa. In that case the amount of systolic flow is changed at the expense of diastolic flow and, consequently, ΔV_b will change accordingly.

In our view the pulsatile ICP variations are caused by the pulsatile variations in CBV. If this is true, it is clear that the minimum and maximum values of the computed change in CBV and the ICP within a cardiac cycle must be in phase. In the figures that follow, the CSF pulse has therefore been included so that both pulsatile phenomena can be compared.

7.3 Results

Effects of changes in arterial carbon dioxide tension

A total number of eleven and eight runs were performed during hypercapnia and hypocapnia respectively. The results are given in Tables 15 and 16.

Table 15. Effects of raising the arterial carbon dioxide tension (PaCO_2) on vertebral artery blood flow, on flow in an artery supplying the extracranial circulation, on pulsatile volume load through the vertebral artery, on pulsatile change in cerebral blood volume (ΔV_b), on ventricular fluid pressure (VFP), on CSF pulse pressure (CSFPP), on systemic arterial pressure and pulse pressure (SAP and ΔSAP), and on heart rate. C = control; n = number of runs in each animal.

Animal no.	Vertebral artery flow (ml/min)		Extra-cranial flow (ml/min)		Pulsatile volume load (ml)		ΔV_b (ml)		VFP (mm Hg)		CSFPP (mm Hg)		SAP (mm Hg)		ΔSAP (mm Hg)		Heart rate (beats/min)		PaCO_2 (mm Hg)	
	C	C	C	C	C	C	C	C	C	C	C	C	C	C	C	C	C	C	C	
1 (n=1)	25	37	145	145	0.234	0.339	0.193	0.187	6.5	18.9	1.8	5.2	107	105	41	37	107	109	42.1	62.7
2 (n=4)	54	59	64	66	0.528	0.456	0.101	0.094	8.8	28.6	2.3	5.5	104	111	54	51	103	131	40.7	57.5
3 (n=1)	73	95	143	133	0.465	0.601	0.116	0.133	3.9	27.6	2.2	7.7	128	149	47	52	157	158	41.7	56.3
4 (n=2)	27	29	22	20	0.230	0.218	0.103	0.105	8.2	20.4	1.7	5.4	109	106	45	56	118	133	38.8	66.1
5 (n=1)	31	38	19	22	0.274	0.314	0.109	0.130	6.4	21.0	2.1	5.4	99	110	45	60	113	121	35.6	54.3
6 (n=1)	31	53	11	15	0.295	0.424	0.165	0.183	2.0	34.8	0.9	8.5	136	151	65	86	105	125	39.8	74.9
7 (n=1)	19	25	98	114	0.152	0.205	0.065	0.070	7.9	23.2	2.1	4.1	114	120	43	50	125	122	37.3	66.0
Mean	37	48	72	74	0.311	0.365	0.122	0.129	6.2	24.9	1.9	6.0	114	122	49	56	118	128	39.4	62.5
SD	± 19	± 24	± 58	± 57	± 0.136	± 0.140	± 0.043	± 0.044	± 2.5	± 5.7	± 0.5	± 1.5	± 13	± 20	± 8	± 15	± 19	± 15	± 2.4	± 7.2

Table 16. Effects of lowering the arterial carbon dioxide tension (PaCO₂) on vertebral artery blood flow, on flow in an artery supplying the extracranial circulation, on pulsatile volume load through the vertebral artery, on pulsatile change in cerebral blood volume (ΔV_b), on ventricular fluid pressure (VFP), on CSF pulse pressure (CSFPP), on systemic arterial pressure and pulse pressure (SAP and Δ SAP), and on heart rate. C = control; n = number of runs in each animal.

Animal no.	Vertebral artery flow (ml/min)		Extra-cranial flow (ml/min)		Pulsatile volume load (ml)		ΔV_b (ml)		VFP (mm Hg)		CSFPP (mm Hg)		SAP (mm Hg)		Δ SAP (mm Hg)		Heart rate (beats/min)		PaCO ₂ (mm Hg)	
	C	C	C	C	C	C	C	C	C	C	C	C	C	C	C	C	C	C	C	
1 (n=1)	25	18	145	130	0.255	0.177	0.217	0.187	2.1	0.7	1.4	1.3	90	88	46	38	98	102	43.6	30.5
2 (n=2)	53	50	106	106	0.437	0.390	0.107	0.084	7.1	2.6	1.8	1.0	103	108	47	43	120	129	42.0	24.6
3 (n=1)	61	64	155	170	0.386	0.413	0.117	0.125	3.4	0.1	2.2	1.5	139	124	53	44	158	155	40.9	29.1
4 (n=1)	25	32	13	20	0.200	0.241	0.087	0.068	9.1	5.4	2.0	1.3	105	115	44	44	125	133	40.6	28.2
5 (n=1)	31	26	23	23	0.263	0.226	0.104	0.098	5.3	3.4	1.7	1.2	102	94	43	34	118	115	38.6	27.9
6 (n=1)	33	30	12	12	0.320	0.306	0.163	0.154	1.4	1.3	1.7	1.0	136	134	70	70	103	98	41.5	25.1
7 (n=1)	23	22	110	86	0.189	0.180	0.065	0.064	9.4	6.2	1.5	1.5	111	109	42	43	122	120	39.1	27.6
Mean	36	35	81	78	0.293	0.276	0.123	0.111	5.4	2.8	1.8	1.3	112	110	49	45	121	122	40.9	27.6
SD	± 15	± 17	± 63	± 62	± 0.093	± 0.096	± 0.051	± 0.046	± 3.3	± 2.3	± 0.3	± 0.2	± 18	± 16	± 10	± 12	± 19	± 20	± 1.7	± 2.1

Hypercapnia caused an increase both in VFP and in CSF pulse pressure. On the basis of the mean relationship between VFP and pulse pressure found in the experiments described in Chapter 5, an increase in VFP of 18.7 mm Hg would have been expected to have caused an increase in pulse pressure of 2.0 mm Hg. The mean increase in pulse pressure of 4.1 mm Hg found here can thus be regarded as disproportionate to the increase in VFP and must be attributed to the effect of hypercapnia, thereby confirming the results described in Chapter 6.

The decrease in cerebrovascular resistance caused by the vasodilatory action of CO_2 resulted in an increase in vertebral artery blood flow in each animal. The mean increase of 11 ml/min constitutes 30% of mean control flow. Flow in the vessels contributing to the systemic circulation was, on the whole, not significantly altered. As mentioned before, the wide variation in extracranial flow between the animals is due to the fact that vessels of different caliber were used. In contrast to the results of hypercapnia those of hypocapnia did not show a significant reduction in vertebral flow. Extracranial flow was also not significantly changed.

In respect of ΔV_b , the CBF per cardiac cycle or the pulsatile volume load is the important factor, rather than the CBF/min. Since during changes in PaCO_2 , especially during hypercapnia, the heart rates unfortunately changed as well, the values of the pulsatile volume load have been included in the tables so that the changes in ΔV_b can be better appreciated. For example, although during hypercapnia flow increased on average by 30%, the pulsatile volume load increased by only 17%. However, the increase in the pulsatile volume load is still large enough to contrast with the very small to moderate increase in ΔV_b found in most animals. In two animals ΔV_b decreased during hypercapnia. In one of them (no. 2) however the pulsatile volume load decreased proportionally more, so that, relative to the pulsatile volume load, animal no. 1 was actually the only one which did not show an increase in ΔV_b .

Figure 49 shows a typical example of the pulsatile and mean flow changes during hypercapnia. The flow profile did not appear to be significantly altered; the flow increment was evenly distributed over systole and diastole. However, when all the flow curves were closely studied, a slight preference for systolic flow to increase disproportionately to diastolic flow was observed in some animals. Figure 50 shows an example of this in an animal in which the pulsatile

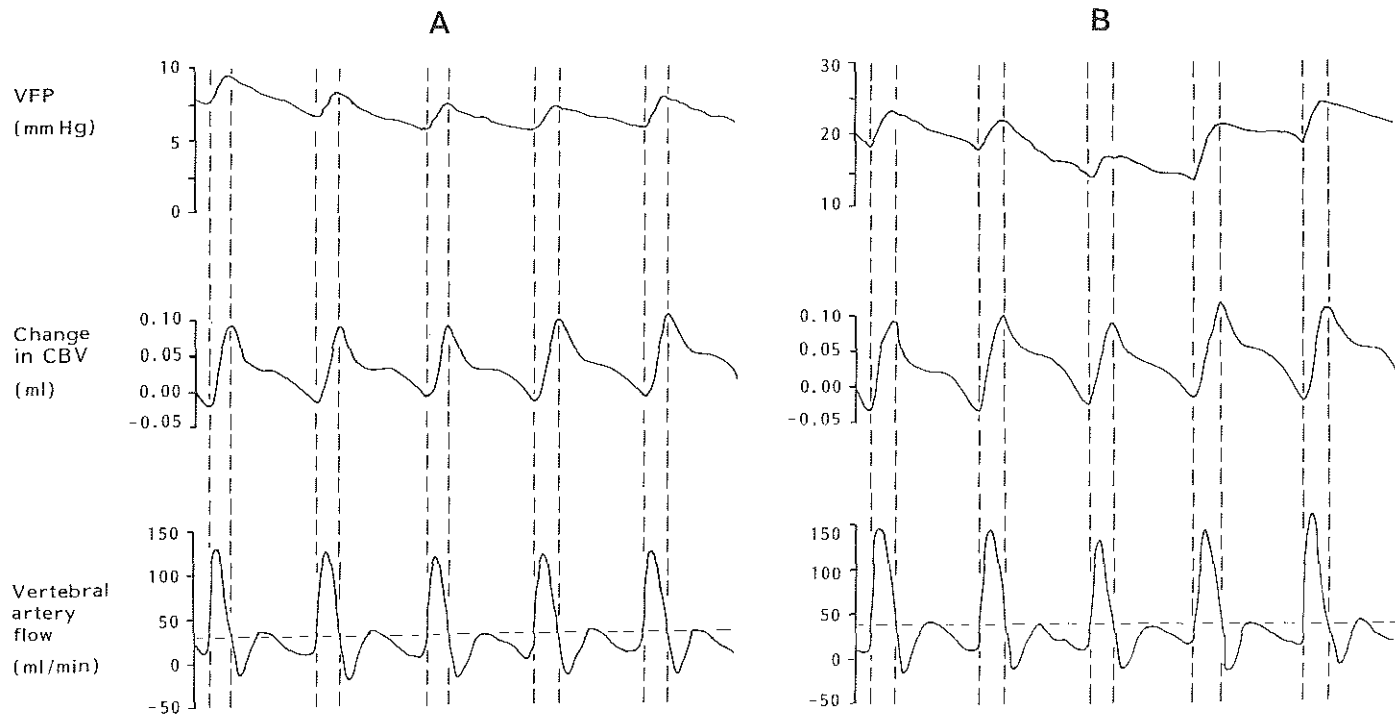


Fig. 49. Computer plot of vertebral artery pulsatile and mean (dashed line) flow, change in cerebral blood volume (CBV) and ventricular fluid pressure (VFP) during five cardiac cycles: A=control (heart rate: 113 beats/min) and B=hypercapnia (heart rate: 121 beats/min). Note increase in mean flow from 31 ml/min to 38 ml/min. Pulsatile flow profile was not significantly affected. Slight increase in peak flow in respect of mean flow level caused an increase in ΔV_B from 0.109 ml to 0.130 ml. Note also coincidence of extreme values of CBV and VFP.

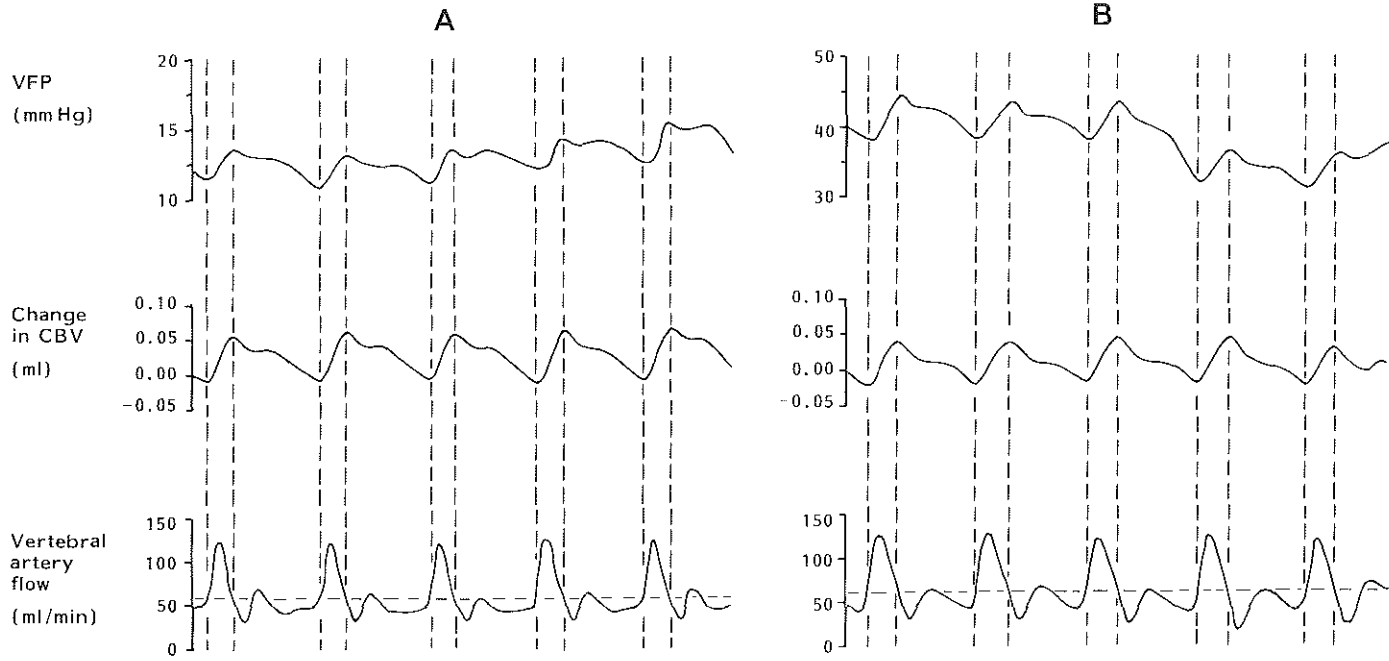


Fig. 50. Computer plot of vertebral artery pulsatile and mean (dashed line) flow, change in cerebral blood volume (CBV) and ventricular fluid pressure (VFP) during five cardiac cycles: A=control and B=hypercapnia. As a result of increase in heart rate from 110 beats/min to 157 beats/min, pulsatile volume load decreased from 0.527 ml to 0.408 ml (23%). As systolic flow increased at the expense of diastolic flow, ΔV_B decreased by only 9% from 0.068 ml to 0.062 ml.

volume load was considerably diminished. Nonetheless, ΔV_b did not decrease correspondingly due to a relative increase in systolic flow.

The results of the hypocapnic states were opposite to those obtained during hypercapnia. A small decrease in ΔV_b was usually found. In the one animal in which ΔV_b increased (no. 3), this was due to an increase in the pulsatile volume load. However, in the other animal in which the volume load increased (no. 4) ΔV_b was nevertheless diminished. Figure 51 shows that the profile of the flow pulse was little affected by hypocapnia.

It is of interest to note that in all the tracings (Figs. 49-51) the extreme values of the change in CBV and the CSF pulse synchronized remarkably well.

In conclusion, the findings suggest a tendency of the pulsatile change in CBV to vary under the influence of PaCO_2 , but the magnitude of the variations does not seem large enough to explain the changes in CSF pulse pressure satisfactorily.

Effects of changes in systemic arterial pressure

The results of changes in cerebral perfusion pressure, produced by increasing and lowering the SAP, were much more consistent than those obtained under the previous experimental conditions. During both arterial hypotension and arterial hypertension 13 runs were conducted, the results of which are given in Tables 17 and 18. The mean results show that the vertebral artery flow was little affected in contrast to the extracerebral flow, suggesting that CBF autoregulation to changes in perfusion pressure was intact in these animal preparations. From a closer study of the individual data some degree of autoregulation also becomes evident. During most of the trimethaphan runs vertebral artery flow remained constant or increased; if flow was reduced, the percentage change was always smaller than that of extracerebral flow.

The VFP was little affected, but the amplitude of the CSF pulse was significantly augmented during arterial hypotension and diminished during hypertension in agreement with previous results (Chapter 6).

In all but one animal (no. 1), lowering the SAP caused a significant increase in ΔV_b with a mean increase of 36%. This one animal was also the

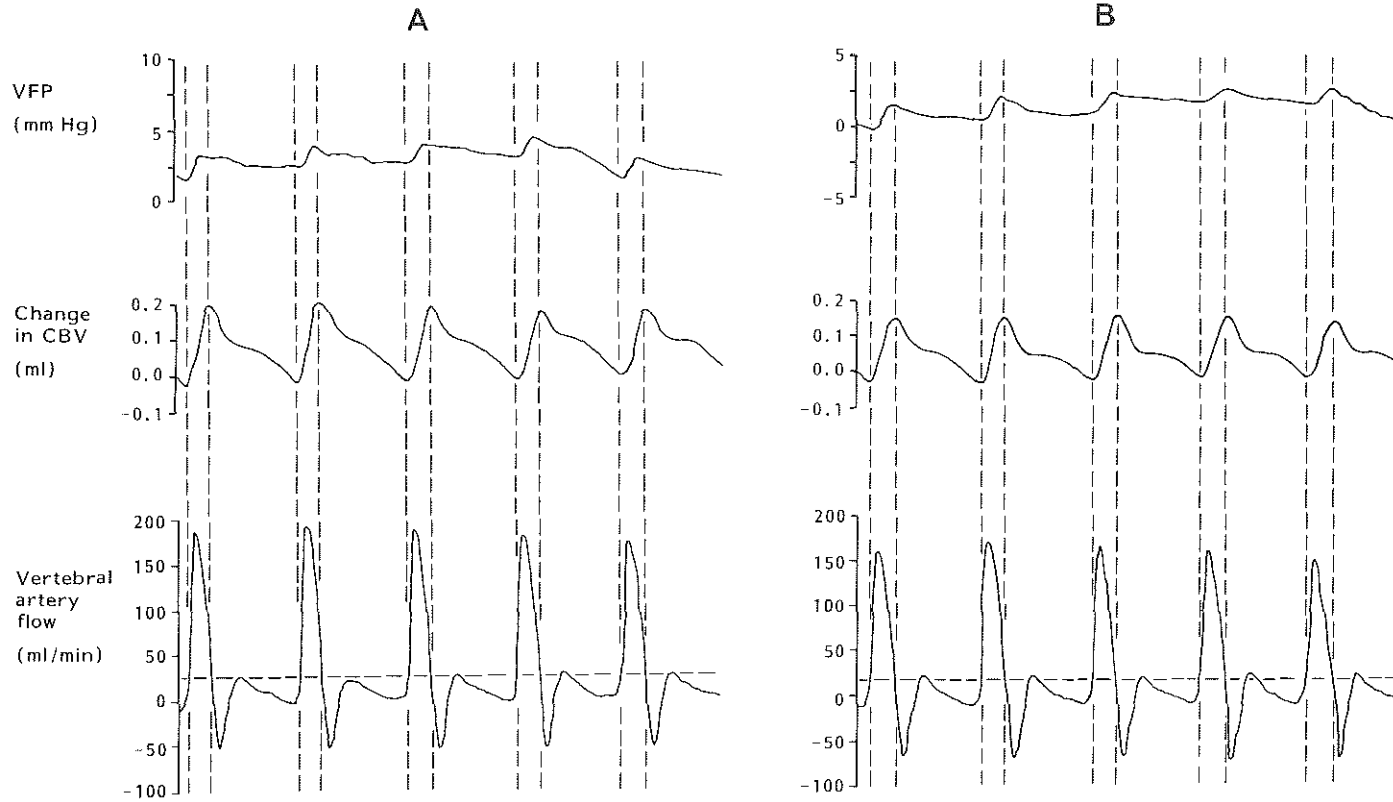


Fig. 51. Computer plot of vertebral artery pulsatile and mean (dashed line) flow, change in cerebral blood volume (CBV) and ventricular fluid pressure (VFP) during five cardiac cycles: A=control (heart rate: 98 beats/min) and B=hypocapnia (heart rate: 102 beats/min). Mean flow decreased from 25 ml/min to 18 ml/min. Distribution of flow between systole and diastole was not significantly affected. Slight decrease in ΔV_b from 0.217 ml to 0.187 ml is caused by decrease in systolic flow relative to mean flow level.

Table 17. Effects of lowering the systemic arterial pressure (SAP) on vertebral artery blood flow, on flow in an artery supplying the extracranial circulation, on pulsatile volume load through the vertebral artery, on pulsatile change in cerebral blood volume (ΔV_B), on ventricular fluid pressure (VFP), on CSF pulse pressure (CSFPP), on systemic arterial pulse pressure (Δ SAP), and on heart rate. C = control; n = number of runs in each animal.

Animal no.	Vertebral artery flow (ml/min)		Extra-cranial flow (ml/min)		Pulsatile volume load (ml)		ΔV_B (ml)		VFP (mm Hg)		CSFPP (mm Hg)		SAP (mm Hg)		Δ SAP (mm Hg)		Heart rate (beats/min)	
	C	C	C	C	C	C	C	C	C	C	C	C	C	C	C	C	C	
1 (n=1)	31	32	165	200	0.188	0.213	0.105	0.108	5.7	3.8	2.2	1.2	113	67	44	35	165	150
2 (n=1)	52	49	185	170	0.400	0.377	0.117	0.210	23.3	22.0	3.5	5.9	109	63	47	38	130	134
3 (n=2)	77	92	195	357	0.501	0.632	0.133	0.204	13.0	9.9	4.1	4.6	122	77	46	42	153	146
4 (n=2)	24	22	16	11	0.167	0.144	0.073	0.090	12.6	12.4	1.8	3.0	116	76	36	30	148	148
5 (n=3)	30	30	22	17	0.278	0.274	0.131	0.179	7.5	8.8	2.3	4.1	97	54	51	51	107	108
6 (n=2)	26	31	13	9	0.248	0.253	0.166	0.201	7.0	8.2	1.6	2.8	130	99	63	49	107	122
7 (n=2)	19	19	90	107	0.155	0.167	0.061	0.075	7.7	8.4	1.7	2.2	113	76	42	40	122	114
Mean	37	39	98	124	0.277	0.294	0.112	0.152	11.0	10.5	2.5	3.4	114	73	47	41	133	132
SD	± 21	± 25	± 83	± 129	± 0.130	± 0.168	± 0.036	± 0.059	± 6.1	± 5.7	± 1.0	± 1.6	± 10	± 14	± 8	± 7	± 23	± 17

Table 18. Effects of raising the systemic arterial pressure (SAP) on vertebral artery blood flow, on flow in an artery supplying the extracranial circulation, on pulsatile volume load through the vertebral artery, on pulsatile change in cerebral blood volume (ΔV_b), on ventricular fluid pressure (VFP), on CSF pulse pressure (CSFPP); on systemic arterial pulse pressure (Δ SAP), and on heart rate. C = control; n = number of runs in each animal.

Animal no.	Vertebral artery flow (ml/min)		Extra-cranial flow (ml/min)		Pulsatile volume load (ml)		ΔV_b (ml)		VFP (mm Hg)		CSFPP (mm Hg)		SAP (mm Hg)		Δ SAP (mm Hg)		Heart rate (beats/min)	
	C	C	C	C	C	C	C	C	C	C	C	C	C	C	C	C	C	
1 (n=2)	33	28	216	175	0.183	0.178	0.125	0.074	6.4	6.3	1.6	1.0	102	171	34	33	184	158
2 (n=1)	43	48	150	180	0.297	0.366	0.105	0.085	14.1	16.4	3.2	2.7	95	154	39	60	145	131
3 (n=2)	56	49	176	160	0.338	0.275	0.125	0.115	3.6	8.1	2.1	2.4	125	174	45	42	166	178
4 (n=2)	23	21	10	15	0.146	0.144	0.067	0.048	12.1	10.2	2.0	1.1	99	165	35	31	157	143
5 (n=2)	35	39	24	23	0.290	0.316	0.135	0.075	7.9	6.8	2.1	1.3	88	142	45	49	120	125
6 (n=3)	29	30	11	11	0.238	0.226	0.150	0.113	8.6	8.4	2.3	1.8	124	158	54	52	121	131
7 (n=1)	21	23	94	41	0.176	0.213	0.064	0.046	7.4	4.5	1.4	1.0	107	166	35	41	119	108
Mean	34	34	97	86	0.238	0.245	0.110	0.079	8.6	8.7	2.1	1.6	106	161	41	44	145	139
SD	± 12	± 11	± 85	± 81	± 0.072	± 0.078	± 0.033	± 0.028	± 3.5	± 3.9	± 0.6	± 0.7	± 14	± 11	± 7	± 10	± 26	± 23

only one in which a decrease in CSF pulse pressure was observed. The combinations of changes in vertebral artery flow and heart rate produced a variable effect on the pulsatile volume load. If the pulsatile volume load was increased, ΔV_b increased proportionally more. If changes in ΔV_b cannot be explained by alterations in the pulsatile volume load, they must originate from the second determinant of ΔV_b : the timing factor as postulated in Chapter 3.3. This was confirmed by the flow curves which during hypotension showed an increase in systolic flow at the expense of diastolic flow. This was effected by an increase in either the amplitude (Fig. 52) or the duration (Fig. 53) of the systolic flow pulse. Even when the pulsatile volume load was reduced, this effect was strong enough to cause an absolute increase in systolic flow (Fig. 53).

The results obtained during hypertension were the reverse of those during hypotension. Irrespective of the change in the pulsatile volume load, a significant reduction in ΔV_b was found in all but one animal with a mean decrease of 28% from control. In animal no. 3 the decrease in ΔV_b was proportionally less than the decrease in the pulsatile volume load. The flow curves during hypertension were characterized by a decreased flow pulse amplitude caused by a shift of flow from systole to diastole (Fig. 54). Even when the pulsatile volume load was increased, systolic flow was reduced so as to cause a significant decrease in ΔV_b (Fig. 55).

Also in these series the extreme values of the change in CBV and the CSF pulse were correlated in time (Figs. 52-55).

Effects of raised ICP

In three animals, the ICP was raised stepwise at the end of the experiment by increasing the speed of a pump infusing normal saline into the cisterna magna. At each pressure plateau the various data were collected. For each variable the same trend of events was observed in each animal but as the absolute values varied considerably, only the mean results are presented and shown in Figure 56.

In spite of a steadily rising SAP the cerebral perfusion pressure was considerably reduced with elevation of the ICP. Nonetheless, vertebral artery blood flow remained constant until the perfusion pressure had fallen below 50 mm Hg. We therefore believe that some degree of auto-

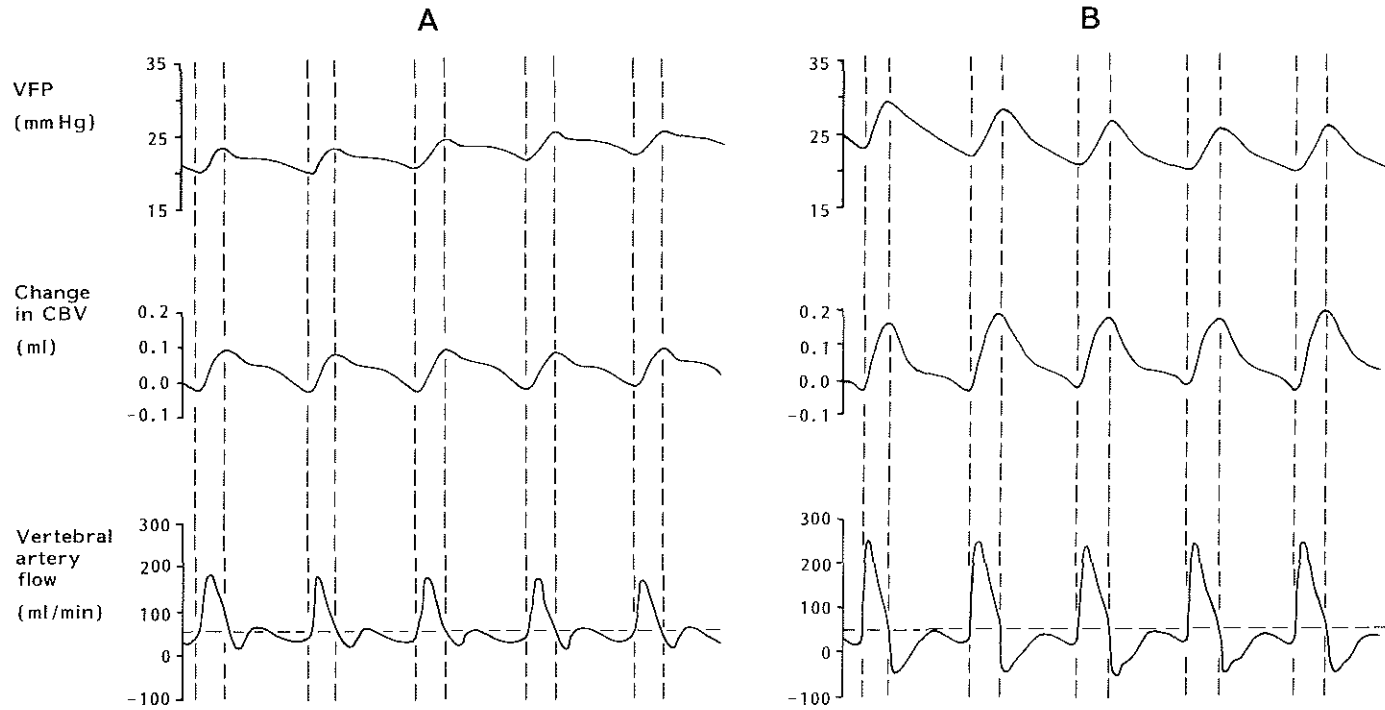


Fig. 52. Computer plot of vertebral artery pulsatile and mean (dashed line) flow, change in cerebral blood volume (CBV) and ventricular fluid pressure (VFP) during five cardiac cycles: A=control (heart rate: 130 beats/min) and B=systemic arterial hypotension (heart rate: 134 beats/min). Note that mean flow is not changed, whereas systolic flow is markedly increased. As a result ΔV_b increased from 0.117 ml to 0.210 ml.

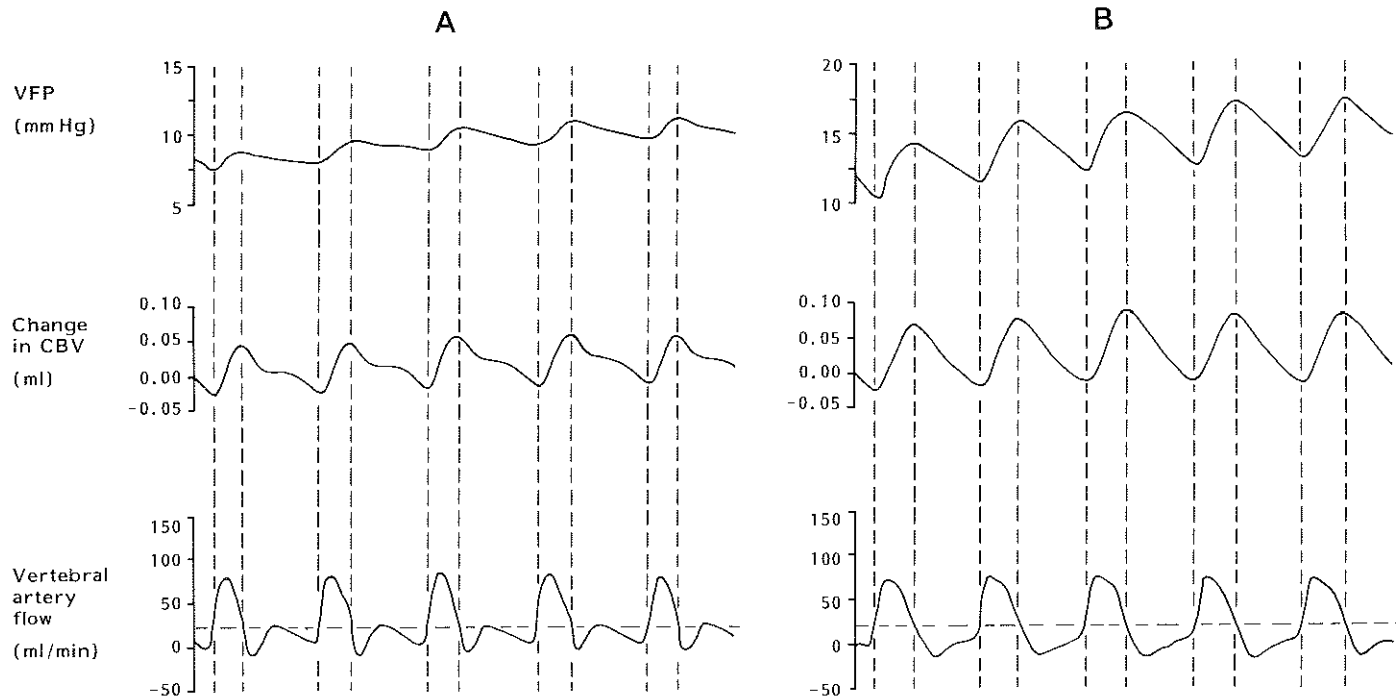


Fig. 53. Computer plot of vertebral artery pulsatile and mean (dashed line) flow, change in cerebral blood volume (CBV) and ventricular fluid pressure (VFP) during five cardiac cycles: A=control (heart rate: 130 beats/min) and B=systemic arterial hypotension (heart rate: 134 beats/min). Due to decrease in mean flow from 23 ml/min to 17 ml/min, pulsatile volume load was reduced from 0.177 ml to 0.127 ml. Nevertheless, ΔV_b increased from 0.075 ml to 0.098 ml because of increase in systolic flow at the expense of diastolic flow.

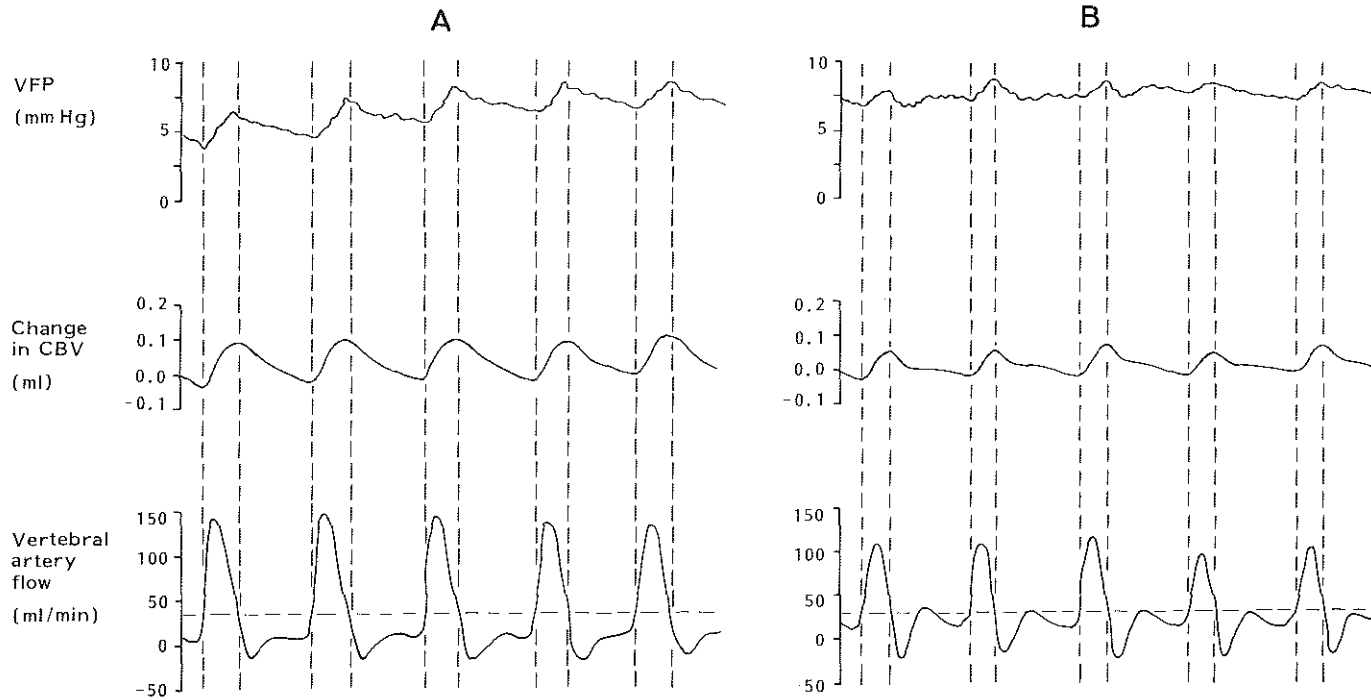


Fig. 54. Computer plot of vertebral artery pulsatile and mean (dashed line) flow, change in cerebral blood volume (CBV) and ventricular fluid pressure (VFP) during five cardiac cycles: A=control (heart rate: 173 beats/min) and B=systemic arterial hypertension (heart rate: 160 beats/min). Pulsatile volume load decreased from 0.197 ml to 0.175 ml due to slight reduction in flow. Change in flow profile can be observed consisting of shift of flow from systole to diastole. As a result ΔV_B decreased from 0.126 ml to 0.079 ml.

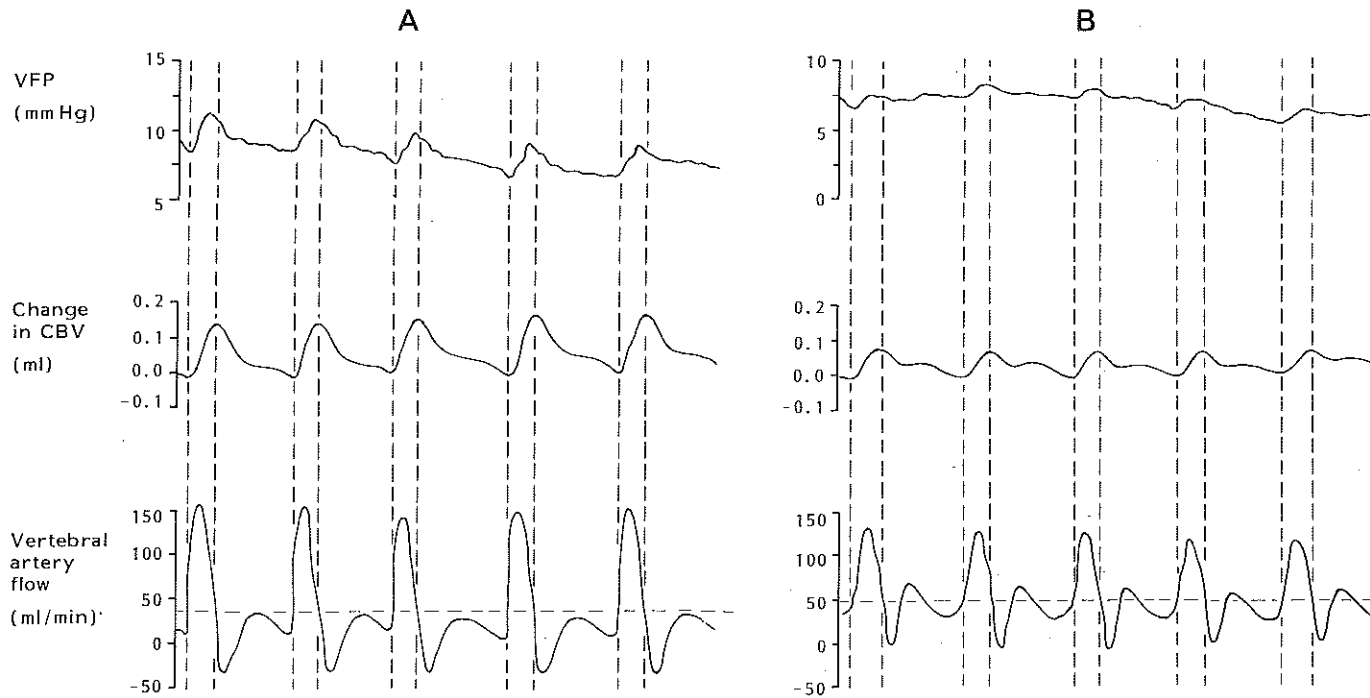


Fig. 55. Computer plot of vertebral artery pulsatile and mean (dashed line) flow, change in cerebral blood volume (CBV) and ventricular fluid pressure (VFP) during five cardiac cycles: A-control (heart rate: 115 beats/min) and B=systemic arterial hypertension (heart rate: 125 beats/min). Due to increased flow, pulsatile volume load increased from 0.313 ml to 0.368 ml. In spite of this, ΔV_B decreased from 0.158 ml to 0.083 ml as a result of diminished systolic flow portion.

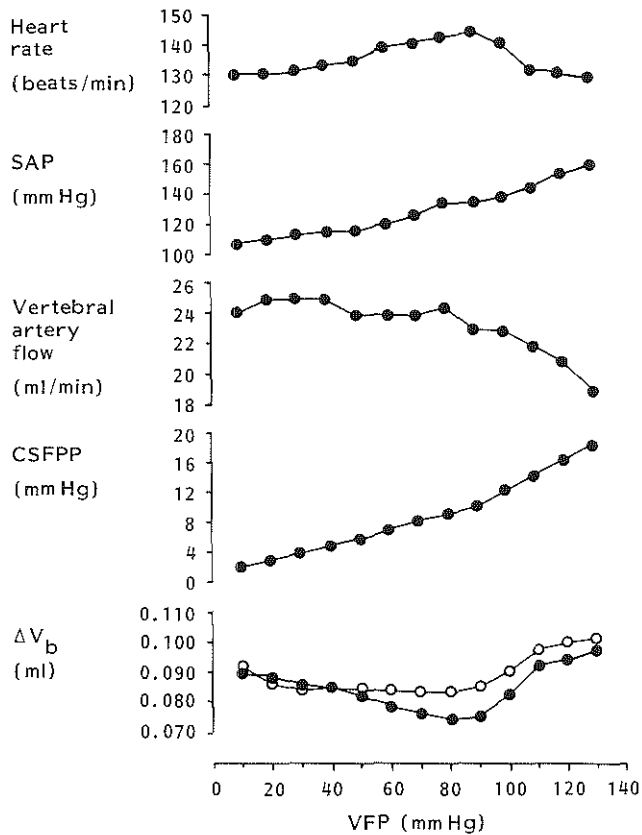


Fig. 56. Combined plot of pulsatile change in cerebral blood volume (ΔV_b , filled circles), ΔV_b corrected proportionally to heart rate (open circles), CSF pulse pressure (CSFPP), vertebral artery blood flow, systemic arterial pressure (SAP), and heart rate versus ventricular fluid pressure (VFP) during continuous infusion into cisterna magna in a group of three animals. Note that above VFP of 90 mm Hg ΔV_b starts to increase, CSFPP increases more rapidly, and blood flow progressively falls.

regulation must have been present in these preparations despite the preceding recurrent experimental inflictions.

The pulsatile change in CBV gradually diminished. However, this may have been the effect of the increase in heart rate which, since CBF remained constant, caused a decrease in the pulsatile volume load to the craniospinal system. When ΔV_b was corrected in proportion to the change in heart rate, it appeared to remain constant. From an ICP of 90 mm Hg onwards ΔV_b began to increase, coinciding with the decrease in vertebral artery flow.

The CSF pulse pressure rose linearly with the ICP. However, in the extremely high range of ICP the pulse amplitude increased more rapidly, coinciding with the increase in ΔV_b as well as with the decrease in vertebral artery flow.

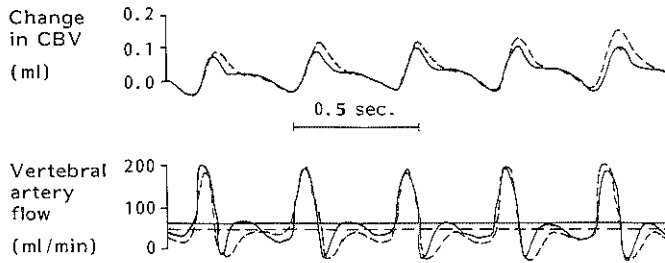


Fig. 57. Computer plot of vertebral artery pulsatile and mean flow and of change in cerebral blood volume (CBV) at extremely elevated ICP (dashed curves), superimposed on the results obtained at normal ICP. Note that at elevated ICP, in spite of reduction in mean flow, ΔV_b increases as a result of shift of flow from diastole to systole.

The paradox of an increase in ΔV_b in spite of a reduced flow can be understood by looking at the flow profiles. Figure 57 shows that in the high ICP range, where flow has started to fall, the reduction in mean flow is mainly caused by a decrease in diastolic flow. The systolic flow pulse remains practically unchanged, so that its amplitude relative to the mean flow level increases. In this case one could speak of a relative shift of flow from diastole to systole.

7.4 Discussion

The purpose of the present series of experiments was to quantify the pulsatile change in CBV empirically and to compare the results with the earlier mathematically derived values for ΔV_b (Chapters 5 and 6). In Chapter 3 the physiological basis of ΔV_b was attributed to the pulsatile volume load of blood to the craniospinal system on the one hand, and to a 'timing' factor governing the interaction between the pulsatile arterial inflow and venous outflow on the other. With regard to the timing factor, great importance was attached to the role of the cerebrovascular resistance in determining the shape of the arterial inflow profile. The validity of this theoretical concept was supported by the experimental verification of the predicted effects of PaCO_2 and SAP changes on the CSF pulse pressure. Furthermore, it was argued that cerebral vasoparalysis caused a breakpoint in the relationship between CSF pulse pressure and ICP by causing an increase in ΔV_b . In the present experiments pulsatile flow in the vertebral artery of the dog was studied, assuming that this

would reflect changes in the cerebrovascular inflow resistance, as the dominant factor in the regulation of blood flow through any artery is the peripheral vascular bed. Venous outflow was deliberately disregarded in the study.

Normal vertebral artery blood flow

On the basis of the overall mean blood flow of 36 ml/min in the left vertebral artery of this group of animals and assuming an equal flow distribution between the two vertebrals, total vertebral artery flow would amount to 72 ml/min, consistent with 70 ml/min found by Reivich et al. (1961) in the same animal species. In order to deduce a figure for total CBF from this value, the distribution of vertebral flow between cerebral and extracerebral flow has to be assessed, as the vertebral artery craniad to the flowmeter probe also supplies branches to the ventral spinal artery, the paravertebral musculature and the occipital artery. On the basis of the findings of Dumke and Schmidt (1943) and those of Symon et al. (1963), albeit in the monkey, we have assumed that 60% of total vertebral artery flow passes through the basilar artery.

Another estimate has to be made for the distribution of flow between the carotid and basilar systems. In dogs the basilar system carries the major proportion of blood to the brain. A ratio of 2:1 at the basilar/internal carotid level seems a reasonable assumption (Reivich et al., 1961). Using the above assumptions, an average total brain flow of 65 ml/min can be deduced for the animals in the present series. The brain weights of the animals were not determined, but taking into account the body and brain weights in the previous experiments a mean brain weight of about 90 g can be estimated. The CBF of 72 ml/100g/min thus obtained compares reasonably well with the CBF range in dogs of 49 to 67 ml/100g/min reported by authors using various methods for measuring CBF (Homburger et al., 1946; Rosomoff and Holaday, 1954; Sagawa and Guyton, 1961; Ekström-Jodal, 1970; Häggendal et al., 1970; Raichle et al., 1970; Hamer et al., 1973). In view of the limitations of electromagnetic flowmetry and of the above assumptions, we do not want to put too much emphasis on the actual value of this figure. We do believe however that it indicates that these flow measurements have been carried out with reasonable accuracy.

The pulsatile change in cerebral blood volume under basal conditions

The overall mean ΔV_b under control conditions of normocapnia and normal SAP was 0.117 ml. Again, if we adopt the assumptions previously made with regard to both the intracranial and extracranial flow distribution of the vertebral arteries and the flow distribution between carotid and basilar systems, a mean ΔV_b of 0.211 ml can be deduced. This figure is considerably higher than that of 0.063 ml which is the average of the values reported in Chapters 5 and 6. Moreover, it should be noted that in the above approximation of ΔV_b the blood flow to the contents of the spinal dural sac has not been taken into account, whereas in the concept of the volume change underlying the CSF pulse pressure the cranial and spinal divisions have always been regarded as belonging to one compartment. Consequently, the actual value of ΔV_b in the dog may be expected to be even higher than the figure reported here.

However, in comparing this empirical value with the earlier mathematically derived values, it is of interest to note that the amplitude of the CSF pulse found in the present series was also considerably larger. The mean value of the control situations was 2.1 mm Hg at a mean ICP of 7.8 mm Hg. According to the relationships between pulse pressure and ICP determined in the previous experimental series, an ICP of 7.8 mm Hg would have yielded a pulsatile amplitude of only 0.6 mm Hg. The larger ΔV_b of the present series is thus consistent with its larger pulse pressure. This may be regarded as indirect evidence of the correctness of the technique used for the computation of ΔV_b .

The reason for the higher values of the present series may be the larger body weights and thus the larger brain weights of these animals, implying a higher CBF/min. Since the heart rates, on average, were not significantly different from the previous series (129 and 127 beats/min respectively), the pulsatile volume load of blood to the brain may have been larger in this series, causing a larger ΔV_b . Slight differences in the anaesthetic technique may have contributed to the supposed difference in CBF, as the experiments were performed in different laboratories. Finally, the generally lower SAP in the present series (112 mm Hg compared to 141 mm Hg in the previous series) may have been another reason for the high values of ΔV_b , as will be discussed subsequently.

Effects of changes in systemic arterial pressure

With regard to the effects of the experimental variables on ΔV_b , those produced by altering the SAP are most conspicuous and will therefore be discussed first. The findings, i.e., an increase in ΔV_b during arterial hypotension and a decrease during hypertension, are consistent with the results described in Chapter 6, where values for ΔV_b were calculated from the CSFPP-ICP relationship and from E_1 . Neither the mean vertebral artery flow nor the heart rate was significantly altered by the variations in SAP. Consequently, the changes in ΔV_b cannot be explained by changes in the pulsatile volume load.

It was clearly shown, on the other hand, that the vertebral artery flow profile was significantly affected, not so much by a shift of the flow pulse towards the beginning of the cardiac cycle, as postulated in Chapter 3.3 (Fig. 11), as by a change in the volume of the flow pulse due to a change in the distribution of flow between systole and diastole. The results obtained during arterial hypertension are consistent with those of Greenfield and Tindall (1968), who found a reduction in pulsatile flow and an increase in nonpulsatile flow in the internal carotid artery during elevation of the SAP in man. The changes in the pulsatile component of flow will affect the transient surplus of cerebral blood within a cardiac cycle which constitutes the underlying volume of the CSF pulse pressure. The ultimate effect on the magnitude of ΔV_b depends, of course, on the changes which may occur simultaneously in the venous outflow profile.

The pulsatile flow changes in the vertebral artery are in our view caused by changes in the peripheral vascular resistance, resulting from dilatation and constriction of the cerebral resistance vessels. In the discussion in Chapter 6 we have already pointed out that the changes in cerebrovascular resistance in response to SAP changes should be attributed to the CBF autoregulatory mechanism and not to the action of the pharmacological agents on the cerebral vasculature.

Because of the difference between the control values of ΔV_b in the present series and in the series described in Chapter 6, it is difficult to compare the quantitative effects of SAP changes in the two series. If the results obtained in one vertebral artery are converted so that they apply to the total CBF, using the assumptions previously made, the absolute

changes are larger in the present series: an increase in ΔV_b of 0.072 ml versus 0.037 ml during arterial hypotension and a decrease in ΔV_b of 0.056 ml versus 0.021 ml during arterial hypertension. Proportionally, the changes in ΔV_b in the present series corresponded remarkably well with the changes in CSF pulse pressure, i.e., 36% versus 36% during hypotension and 28% versus 24% during hypertension. In our view this supports the validity of the method used for the computation of ΔV_b . Furthermore, since in this method only the arterial flow profile was taken into account, it seems probable that the venous flow profile is not significantly influenced by alterations in SAP.

Effects of changes in arterial carbon dioxide tension

The results of variations in PaCO_2 , as opposed to variations in SAP, failed to show a significant effect on ΔV_b , although the small changes that occurred were in the direction which had been expected, i.e., an increase in ΔV_b during hypercapnia and a decrease during hypocapnia. This contradicts the results of the experiments described in Chapter 6 and requires further clarification.

The effect of PaCO_2 changes on ΔV_b would have been expected to be even stronger than the effect of SAP changes, since two mechanisms are operative simultaneously. The CO_2 induced change in the cerebrovascular resistance affects the CBF, and thereby the pulsatile volume load of blood to the brain, as well as the timing of the arterial inflow. With regard to the CBF, however, the increase in heart rate during hypercapnia seriously diminished the effect of the increased CBF in this series by reducing the pulsatile volume load. If this had not occurred, as in the previous series, the increase in ΔV_b might have been much larger.

As far as hypocapnia is concerned, CBF was not significantly reduced on average at all. In some animals a paradoxical increase in flow was observed, whereas in the others flow was only slightly decreased. It should be noted that the induced decrease in PaCO_2 was much smaller than the increase in PaCO_2 during hypercapnia. Furthermore, it has been well documented that the flow change per mm Hg change in PaCO_2 is smallest in the lower range of PaCO_2 because of the S-shaped (Reivich, 1964) or exponential (Olesen et al., 1971) relationship between CBF and PaCO_2 . In this range cerebral hypoxia is probably the factor which further limits

vasoconstriction. Nevertheless, in spite of these arguments, a significant decrease in ICP was observed, also in those animals that showed an increase in flow; this indicates that some degree of vasoconstriction had caused a reduction in CBV. One could therefore wonder whether, especially in those cases, vertebral artery flow truly represented cerebral flow. If CBF had actually been reduced by hypocapnia, a greater proportion of vertebral artery flow could have been diverted through the branches of this artery supplying extracranial structures, the more so as in the same animals extracranial flow was increased (Table 16). So the increase in vertebral flow may not necessarily preclude the possibility of a reduced CBF.

Contrary to what had been predicted (Chapter 3.3), the change in cerebrovascular resistance by altering the PaCO_2 level did not have a significant effect on the pattern of the arterial inflow curve. During hypercapnia, for example, no forwards shift of the flow pulse, as postulated in Figure 11, was observed; nor was any significant increase in systolic flow at the expense of diastolic flow observed, as was the case when the cerebrovascular resistance was reduced by lowering the SAP. So the intriguing question is: why does the cerebrovascular resistance affect the timing of the arterial inflow profile if it is changed as part of an autoregulatory response evoked by altering the SAP, whereas it does not affect the timing if it is changed as a result of the CO_2 reactivity of the vessels? The explanation can be found by considering the main haemodynamic difference between the two situations, i.e., the cerebral perfusion pressure. This pressure, defined as $\text{SAP} - \text{ICP}$, also reflects the transmural pressure of the cerebral arteries. As far as rapid changes are concerned, the transmural pressure is related to the volume of the cerebral arteries in accordance with the pressure-volume relationship of the cerebral arterial system, introducing the concept of vessel compliance. Vessel compliance is defined as change in vessel volume per unit change in intravascular pressure per unit vessel length (Marmarou et al., 1975). It is a function of internal pressure, wall tension and radius. The wall tension in turn is directly proportional to the transmural pressure. Normally, the thick-walled cerebral arteries with their high internal pressure compared to the external pressure, the ICP, are relatively stiff (low compliance). But at low transmural pressures the wall tension is reduced and the arteries thus become more compliant, implying that a rapid increase in vascular pressure causes a larger increase in vascular volume.

It is therefore our view that during arterial hypotension, when the transmural pressure is relatively low, the inflow section of the cerebral vasculature is more compliant than during hypercapnia, when the transmural pressure is not much different from control (see Appendix 5). This has important implications for the pulsatile inflow profile. The rapid, pulsatile increase in intravascular pressure, i.e., the arterial pulse pressure, will cause a greater expansion of the arterial wall if vascular compliance is high. So, during arterial hypotension the decrease in the cerebral arterial inflow impedance allows an increase in the pulsatile component of flow. During hypercapnia the inflow impedance is not significantly changed and the flow increment is evenly distributed over the cardiac cycle without a significant increase in the flow pulse

These considerations make it necessary to reconsider our understanding of the origin of ΔV_b as far as the time lag or phase shift between the pulsatile cerebral inflow and outflow of blood is concerned. It was postulated in Chapter 3.3 that it was the resistance of the inflow and outflow sections of the cerebral vasculature that governed the timing of the pulsatile component of the respective flows. The effects of changes in cerebrovascular resistance on the timing of pulsatile flow were believed to express themselves in a shift of the peak flow in a forward or backward direction. In Figure 11 this shift was accompanied by a change in the height of the peak flow level, but the total amount of flow under the flow pulse was not changed. As previously explained, the magnitude of ΔV_b is not determined by the peak flow value but by the total amount of systolic flow. The shift of the flow pulse was referred to as the timing factor or phase shift. This phenomenon, however, was not observed in the present study. What has been observed, namely during alterations in SAP, was a change in the magnitude of the arterial flow pulse as a result of a change in the distribution of flow between systole and diastole. However, this does not interfere with the timing concept which, on condition that the pulsatile volume load remains constant, implies any disturbance in the synchronization of the arterial inflow and venous outflow which gives rise to a change in the maximum difference between the two flows.

In conclusion, the change in magnitude of the pulsatile component of flow suggests that it is the compliance of the inflow section of the cerebral vascular bed rather than the cerebrovascular resistance which

governs the timing of the arterial inflow. This is confirmed by the finding that during changes in PaCO_2 the pulsatile component is little affected. True, the compliance of the vessels may be influenced to some extent by the active process of vasodilatation and vasoconstriction occurring during hypercapnia and hypocapnia respectively, but not to the same extent as during changes in SAP in which case the transmural pressure of the vessels is also altered.

Why, then, did the changes in PaCO_2 fail to produce a significant change in the magnitude of ΔV_b , whereas the CSF pulse pressure, both in the experiments described in Chapter 6 and in the present study, was changed disproportionately relative to the change in ICP? In view of the foregoing discussion it seems reasonable to assume that under these circumstances the main changes take place at the venous side of the cerebral vascular bed. This possibility had been deliberately neglected in the design of this study, as the main changes had been expected to occur in the arterial inflow tract, which turned out not to be the case.

The egress of cerebral blood is controlled by the perfusion pressure over the outflow tract (subarachnoid venous pressure-venous outflow pressure) and the venous outflow resistance. The venous outflow resistance is dependent on the ICP, which causes the walls of the veins to approximate each other, thus increasing the venous pressure and resistance. This occurs at the vein sinus junction. The cuff constriction mechanism, as it is called (see also Chapter 2.6), ensures that the upstream vascular bed maintains a pressure slightly above the ICP and therefore remains patent in order to be able to transport blood from the capillary bed to the sinus.

Although venous flow is relatively nonpulsatile compared with arterial flow, the presence of venous pulsations (Symon, 1970) indicates that venous flow has a pulsatile component. Since the compliance of the thin-walled subarachnoid veins with their transmural pressure slightly above zero is extremely high under all circumstances, it seems very unlikely that changes in compliance play an important role in influencing the pattern of pulsatile flow through these vessels. We assume instead that pulsatile venous flow is determined by the venous outflow resistance. This resistance, since it is dependent on the ICP, is of a pulsatile nature. It is our view that the arterial inflow of blood causes a pulsatile expansion of the arterial vascular bed which in turn, by means

of the accompanying rise in ICP, causes a pulsatile increase in venous resistance. One could argue that the damping of the arterial pulse wave by venous compression already causes some displacement of venous blood out of the cerebral circulation. But, since the area of compression at the cuff constriction site is relatively small, we believe that the amount of displaced blood is likewise small.

So, in the early phase of the cardiac cycle the venous outflow resistance will gradually increase and a stagnation of venous flow will occur until the perfusion pressure over the outflow tract has risen sufficiently to overcome the outflow resistance, at which point the venous pulse wave develops. In other words, the pulsatile change in outflow resistance causes a pulsatile perfusion pressure which generates a pulsatile outflow. Thus the time lag between the pulsatile inflow and outflow of cerebral blood is caused which, in our view, is ultimately responsible for the origin of the CSF pulse pressure.

Hypercapnia produces an elevation of the ICP by increasing CBV and hence it also causes an increase in the mean pulsatile venous outflow resistance. As shown in Chapter 6, hypercapnia causes an increase in CSF pulse pressure in excess of the increase expected on the basis of the elevation of ICP alone. Therefore, in discussing the effect of hypercapnia proper on the CSF pulse pressure the hypercapnic and normocapnic situations should be compared at the same level of ICP. In that case the mean outflow resistance is the same and, consequently, the increased outflow must be caused by an increased perfusion pressure, i.e., the subarachnoid venous pressure if the venous outflow pressure (dural sinus pressure) is assumed to be zero. According to Shulman (1965), the pressure in the subarachnoid veins is partly due to the collapsing pressure of the surrounding ICP ("vis a latere") and partly due to the pressure of the venous blood delivered by the capillary bed ("vis a tergo"). So, even at the same level of ICP, the subarachnoid venous pressure is greater during hypercapnia due to the larger supply of blood into the venous system. This is consistent with what was stated in Chapter 5.4 in the discussion of craniospinal volume-pressure relationships, namely, that the magnitude of the rise in the upstream vascular pressure resulting from vascular compression is dependent on the amount of flow. The greater transmural pressure of the veins in this situation can be maintained by the increased wall tension of the almost maximally dilated vessels.

However, the fact that the mean outflow resistance during hypercapnia is the same as during normocapnia does not preclude the possibility of a difference in the pulsatile outflow resistance. During hypercapnia, the arterial inflow pulse carries a larger volume of blood, so that the venous outflow tract is temporarily more compressed and the pulsatile component of the outflow resistance is correspondingly higher than during normocapnia. Consequently, during hypercapnia there is more stagnation of venous flow in the early phase of the cardiac cycle. Furthermore, according to the above arguments, the increased pulsatile outflow resistance will give rise to a higher pulsatile perfusion pressure due to the larger supply of venous blood. As a result, the venous flow pulse which finally develops will thus be increased.

It is our view that these are the mechanisms which may be involved in delaying the cerebral outflow of blood during hypercapnia, thus causing an increase in the time lag between arterial inflow and venous outflow of blood with the consequent increase in ΔV_b . For the hypocapnic conditions the reverse argumentation can be applied. We therefore believe that the minor effect of PaCO_2 changes on ΔV_b , found in this study, is due to a methodological error introduced by neglecting the venous outflow profile. Finally, apart from changes in the venous flow profile, the assumption of a nonpulsatile instead of a pulsatile outflow led to an underestimation of the magnitude of ΔV_b . As previously explained, ΔV_b was calculated from the systolic flow pulse in excess of the mean flow level. In the case of a pulsatile venous flow, the outflow during the systolic flow pulse will be less than the mean flow, so that higher values for ΔV_b will be found.

Effects of raised ICP

The results obtained during elevation of the ICP (Figure 56) are consistent with previous experimental findings (Chapter 5). The CSF pulse pressure rose concomitantly with the ICP up to a certain pressure above which the pulse pressure rose more rapidly. The breakpoint pressure coincided with the ICP at which CBF began to fall, confirming our previous contention that the breakpoint in the CSFPP-ICP relationship is related to failure of CBF autoregulation. The breakpoint ICP was higher in the

present series than in the previous one: 90 mm Hg versus 60 mm Hg. This is explained by the difference in technique used to raise the ICP, since it has been established that CBF is better preserved when ICP is elevated by cisterna magna infusion than when it is elevated by balloon inflation (Johnston et al., 1972 and 1973).

The finding of a constant ΔV_b before the breakpoint is in accordance with our mathematical model, implying a constant ΔV_b under the conditions of a linear CSFPP-ICP and an exponential volume-pressure relationship. In view of the previous discussion, however, the constancy of ΔV_b raises two questions. The increase in ΔV_b during arterial hypotension was explained by the reduced transmural pressure of the cerebral arteries, making the arterial system more compliant. Why, then, does ΔV_b not increase when the transmural pressure is lowered by elevating the ICP? Below the breakpoint ICP no significant change in the vertebral artery flow profile was observed, as had indeed been the case during arterial hypotension, namely, an increase in the flow pulse amplitude. This dilemma is not solved by the present study, but a possible explanation may be found in the shape of the cerebral arterial volume-pressure curve. Nornes et al. (1977) described this curve by a steep and almost linear segment (low and constant compliance) with a breakpoint only at extremely low transmural pressures. Below this breakpoint the curve flattens out (high compliance) due to slackening of the arterial wall. This may explain why changing the cerebral perfusion pressure (transmural pressure) by stepwise elevation of the ICP has only little or no effect at all on the magnitude of ΔV_b . In order to verify this explanation the effect of the whole range of SAP, instead of only the extremes, on ΔV_b would have to be examined. On the other hand, the above argument may serve to explain why, both in the series described in Chapter 6 and in the present series, the effect on ΔV_b of arterial hypertension was less than that of arterial hypotension.

In fact, the situation is somewhat more complex. Strictly speaking, the cerebral arterial volume-pressure relationship is represented by the plot of intravascular pressure against vascular volume. The slope of this curve is determined by the physical properties of the vessel wall. Since the wall tension is dependent on the transmural pressure, the slope of the curve thus depends on the ICP. Furthermore, the cerebrovascular motor tone is not only passively, but also actively influenced by the cerebral perfusion pressure as part of the CBF autoregulatory mechanism. So, the

volume-pressure relationship of the arterial system is not represented by a single, uniform curve but by a whole 'family' of curves and their slopes are dependent on the transmural pressure and the integrity of CBF autoregulation.

For example, when the SAP is lowered the system becomes more compliant by shifting downwards along the volume-pressure curve and by moving at the same time to another curve with a weaker slope (autoregulatory vasodilatation). When the ICP is raised, the system becomes more compliant just by shifting to a curve with an extra weak slope due to the accumulative effects of the decrease in transmural pressure and the autoregulatory vasodilatation. It cannot be established beforehand whether these two ways of reducing the cerebral perfusion pressure have the same quantitative effect on ΔV_b . ΔV_b would, however, be expected to increase to some extent during elevation of the ICP.

The second problem with regard to the constancy of ΔV_b during elevation of the ICP is related to the cerebral venous outflow. If, as previously postulated, the timing of the pulsatile venous outflow is determined by the venous outflow resistance, the increase in ICP must have some effect in delaying the venous outflow pulse. This provides a second reason why on theoretical grounds, in contrast to the experimental findings, a gradual increase in ΔV_b is likely to occur during elevation of the ICP.

We claimed in Chapter 5 that the increase in CSF pulse pressure above the breakpoint was due to an increase in ΔV_b . The same applies for the disproportionate increase in pulse pressure observed during plateau waves in patients (Chapter 4). This was inferred from the fact that craniospinal elastance in those circumstances was relatively low. The increase in ΔV_b above the breakpoint found in the present study appears to confirm these results. Again, the increase might have been even more pronounced, if the venous flow pulse had been taken into account. The explanation previously given that the increase in ΔV_b is caused by progressive cerebral vasoparesis is supported by the vertebral artery flow pattern (Figure 57). The loss of cerebral vasomotor tone causes a flattening out of the arterial volume-pressure curve, thus making the vessels highly compliant. Just as during arterial hypotension, this allows an increase in the pulsatile component of flow. The vertebral artery flow profile shows that CBF is reduced at the expense of diastolic flow, so that the flow pulse amplitude is relatively increased.

These findings confirm what was hypothesized in Chapter 5.4. They also agree with the results of Greenfield and Tindall (1965) who measured carotid artery blood flow by means of electromagnetic flowmeters in patients during elevation of the ICP by lumbar infusion. The decrease in flow appeared to occur primarily in its continuous portion without a change in the amplitude of pulsatile flow. The most pronounced changes in the arterial inflow pattern at high ICP were observed by Nornes et al. (1977). By measuring electromagnetic flow in the internal carotid artery in patients, a decrease in mean flow was found accompanied by an increase in pulsatile flow, end-diastolic flow arrest and, finally, negative diastolic flow. The last phenomenon of reverse flow in particular explains the simultaneous occurrence of a decrease in CBF and an increase in ΔV_b . The outstanding example is the situation where the ICP approaches the level of the SAP and CBF ceases completely. In that case we would anticipate a maximum value for ΔV_b , since inflow and outflow, both taking place at the inflow section of the cerebral vascular bed, are completely separated (maximal phase shift).

In conclusion, we are convinced that the results of this study support the concept of ΔV_b as a major determinant of the CSF pulse pressure. Circumstantial evidence in this respect is provided by the finding that the extreme values of the pulsatile ICP variations coincided with the extreme values of the computed pulsatile change in CBV, as shown in the tracings in the various figures in this chapter. The results obtained during changes in PaCO_2 make it necessary for further investigations to be focused on the cerebral venous outflow tract. With regard to the clinical implications, it follows from the results of this study that when the relationship between the ICP and its pulsatile variations is used as a measure of craniospinal volume-pressure relationships, the pulsatile change in CBV should be taken into consideration as an important variable.

Conclusions

1. A method was used in this study by which the magnitude of the pulsatile change in CBV was computed from the pulsatile vertebral artery flow curve.

2. The changes in ΔV_b produced by altering the SAP were consistent with previous results, i.e., an increase in ΔV_b during arterial hypotension and a decrease in ΔV_b during arterial hypertension.
3. These changes were caused by a change in the distribution of flow between systole and diastole, giving rise to an increase and decrease respectively in pulsatile flow.
4. During alterations in PaCO_2 pulsatile vertebral flow was only slightly affected, as a result of which the magnitude of ΔV_b was not significantly changed.
5. Since previous results had shown a significant effect of PaCO_2 on the CSF pulse pressure, disproportionate to the change in ICP, it was inferred that in this case ΔV_b is mainly influenced by changes in the pulsatile cerebral outflow pattern.
6. From the conflicting results of SAP and PaCO_2 changes with regard to their effect on ΔV_b , it was inferred that the cerebral inflow profile is determined by the compliance of the cerebral arteries.
7. During elevation of the ICP, ΔV_b remained constant as long as CBF remained constant. When autoregulation was lost and CBF decreased, ΔV_b started to increase due to a relative increase in pulsatile flow.

CHAPTER 8

GENERAL DISCUSSION OF THE CRANIOSPINAL VOLUME-PRESSURE
RELATIONSHIPS AND THE ROLE OF THE CEREBROSPINAL
FLUID PULSE PRESSURE IN THEIR ASSESSMENT

*Judge: "I have read your case, Mr. Smith, and I am no wiser now than I was when I started."
F.E.S.: "Possibly not, My Lord, but far better informed."*

*From: The life of F.E. Smith, the first Earl of Birkenhead.
Written by his son, the second Earl of Birkenhead.*

8.1 Introduction

The major part of this thesis, dealing with the role of the CSF pulse pressure as a parameter of the craniospinal volume-pressure relationships, will be concluded by a general discussion on the basis of the results of the clinical and experimental investigations described in the previous chapters. At the time these investigations were started, in the early seventies, the foundations of the modern volume-pressure concept had just been laid by Marmarou, Miller, Löfgren and their collaborators. These authors, Miller in particular, had also emphasized the significance of volume-pressure parameters such as the PVI and the VPR in clinical decision making, as discussed in Chapter 2.5. We were among the first to recognize that the pulsatile ICP variations of cardiac origin contained information on the volume-pressure relationships. Inspired by the analogy between CSF pulse pressure and VPR, we developed a method by which this information can be extracted from the ICP signal. The animal experiments designed to elaborate this method further also give rise to some critical remarks about the volume-pressure concept itself and its clinical significance. This will be discussed first, after which the CSF pulse pressure will be considered.

8.2 Craniospinal volume-pressure relationships

Volume compensation versus volume buffering

The problems underlying a clear understanding of craniospinal volume-pressure relationships are contained in the key-words *compensation* on the one hand and *buffering* or *storage* on the other, as was discussed in

Chapter 2.6. Compensation means that a volume load to the craniospinal system is accommodated by a reduction in the volume of one of the normal constituents of the system, in agreement with the original Monro-Kellie principle. Spatial compensatory capacities are mainly determined by the parameters defining CSF absorption. Reduction in the volume of the brain may also occur as, for example, in slowly growing tumours and in hydrocephalus. The CBV does not play an important role in this respect, as the autoregulatory process will not allow a reduction in the volume of cerebral blood. So long as the volume load is fully compensated, the total volume of the system does not increase and ICP does not rise.

In volume buffering no compensation takes place and the craniospinal volume is augmented by the total amount of the volume added. The resulting rise in ICP is solely determined by the magnitude of the volume increment and by the physical properties of the system as mathematically expressed by the volume-pressure relationship. Strictly speaking, in order to avoid pollution of terminology, the term 'volume-pressure relationship' should be reserved for the relationship between the true craniospinal volume, or additions to this volume exclusive of compensation, and the ICP.

However, the separation of volume compensation and volume buffering is artificial, since in the experimental situation and even more in the clinical context both processes occur simultaneously. Langfitt (1972) and Benabid et al. (1980) have suggested that ICP starts to rise when spatial compensation is completely exhausted due to the fact that all available CSF volume has been displaced from the craniospinal compartment. By comparing the volume-pressure curve with the 'volume of intracranial balloon versus ICP curve' in the same experimental animal, we have shown that in the steeply ascending portion of the latter curve accommodation of volume by spatial compensation is still taking place (Chapter 2.6, Fig. 6). Thus the steep section of this curve does not represent true volume-pressure relationships as claimed by the above named investigators. Figure 6 certainly shows that the part of the volume increment to the balloon which is compensated for gradually decreases. However, in the high ICP range this portion still constitutes the major part of the volume increment.

As mentioned before, the spatial compensatory capacity is primarily determined by the CSF dynamics. In the presence of a space-occupying lesion, the functional status of this mechanism is influenced by its

nature, localization and, above all, by its rate of expansion. The occurrence of brain shift, causing disturbance of CSF circulation, is of importance in this respect. In the concept of 'CSF volume available for compensation' used by Langfitt, volume should be conceived as a relative rather than as an absolute term, the amount of which is determined by the above factors.

The important conclusion, therefore, is that volume-pressure parameters are of only limited value in predicting the course of ICP elevation in expanding lesions. Knowledge of the resistance to CSF flow and absorption would be much more worthwhile in this respect. This is clearly demonstrated by the balloon inflation experiments in this study (Chapters 5 and 6). In Figure 58 the elastance coefficients, obtained under conditions of normocapnia and normal blood pressure, have been plotted against the ICP reached when the balloon had been inflated up to a volume of 3 ml. The magnitude of E_1 shows little variation except in the one animal which showed early transtentorial herniation (Chapter 5.4, Table 5). The ICP corresponding with the balloon volume chosen, on the

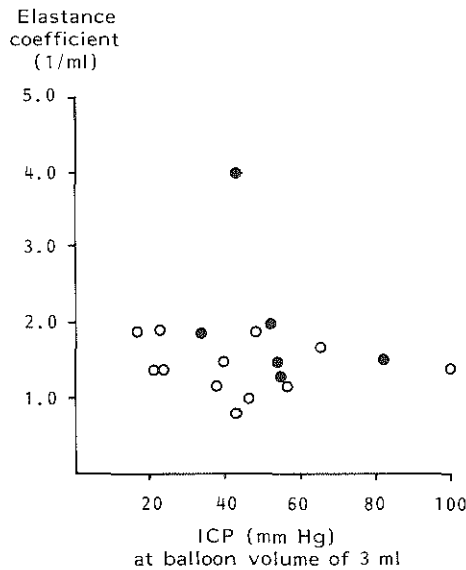


Fig. 58. Plot of elastance coefficient versus intracranial pressure (ICP) reached at balloon volume of 3 ml which was chosen as parameter of spatial compensatory capacity. Data were obtained during inflation of extradural balloons in 18 dogs at constant rates of 1 ml/15 min (filled circles) and 1 ml/40 min (open circles). Note lack of correlation between elastance coefficient and spatial compensatory capacity. Note also that animals with lower expansion rate of balloon show better spatial compensation.

other hand, shows a wide variation and does not appear to have a relationship with E_1 . The animals with the lower balloon inflation rate show a tendency towards better spatial compensation. In other words, volume-pressure parameters do not give information on the ability of an individual to tolerate enlargement of an intracranial mass, as suggested by Miller et al. (1973, 1974 and 1975).

Clinical significance

What is then the clinical value of the assessment of craniospinal volume-pressure relationships? The rate of expansion of most space-occupying lesions encountered in clinical practice is much slower than that in the experimental models. In brain tumours and chronic subdural haematoma, for example, spatial compensatory capacities may cope adequately with the extra volume for a long time without a significant elevation of the ICP (McKissock et al., 1960; Plum and Posner, 1966; Gjerris, 1976). In these patients volume-pressure parameters give no indication of the remaining compensatory capacities.

However, as discussed in Chapter 2.5, there is some evidence that the pathological condition itself may alter the volume-pressure relationship, especially in the presence of brain shift and hydrocephalus (Miller et al., 1973; Miller and Pickard, 1974; Cohadon et al., 1975; Miller and Leech, 1975; Hase et al., 1978; Sklar et al., 1980). In those cases, particularly when the ICP is still within the normal range, volume-pressure testing may give a clue as to whether we are dealing with normal or abnormal intracranial dynamics. Further diagnostic procedures or therapeutic measures can be instituted on this basis. This may apply to the diagnosis of normal pressure hydrocephalus (Granholm and Löfgren, 1975) or to the problem as to whether infantile hydrocephalus needs to be shunted (Shulman and Marmarou, 1971; Shapiro and Marmarou, 1983).

When in the course of a space-occupying lesion the circulation and absorption of CSF become seriously impaired, because of the localization of the mass, its rate of development or the occurrence of brain shift, the spatial compensatory mechanism will begin to fail and the ICP will consequently rise. In a sense, the rise in ICP may be regarded as beneficial, since it restores the circulation and absorption of CSF thus

activating as it were, the compensatory ability. This is consistent with clinical experience that the condition of a patient with a brain tumour may show some improvement as soon as papilloedema appears.

At this stage the volume-pressure relationships come into play, as the volume part in excess of the compensated volume needs to be stored. As previously argued, in the beginning volume buffering plays a subsidiary role, but with further ICP elevation and progressive failure of spatial compensation the volume-pressure function becomes more and more important in setting the level of ICP. This applies particularly to very rapidly expanding mass lesions, such as epidural haematoma and all other complications of a space-occupying nature to which head injury patients are exposed.

Rapid processes, in particular, are the craniospinal volume increments due to bodily activities such as coughing, straining and other Valsalva-manoevres so often observed in critically ill and restless patients. The magnitude both of the rapid ICP fluctuations resulting from such activities, and of the pressure waves associated with cerebro-vasodilatory events and with blood pressure crises in non-autoregulating patients, is primarily determined by the volume-pressure relationship. This relationship is thus important in influencing the daily mean ICP of these patients, whereas the modal or base-line ICP is more a function of the compensatory capacities. This is in agreement with our own observations that patients with a high elastance coefficient show a considerable shift towards the higher pressure classes in their 24-hour pressure histogram. Also in hydrocephalic infants with a normal modal pressure, but with a large E_1 , we have observed an increased right-sided asymmetry of the ICP histogram. This is consistent with the findings of Brock et al. (1976 and 1976) who observed, in patients with brain tumours, a marked reduction in ICP fluctuations and a steepening of the pressure histogram with a narrowing of its base as a result of dexamethasone administration. Since dexamethasone is known to reduce the VPR (Miller and Leech, 1975; Miller et al., 1977), this effect is apparently due to a weakening of the slope of the volume-pressure curve in these patients.

The crucial issue is, of course, whether the craniospinal volume-pressure relationship is sufficiently variable in clinical patients to make its assessment worthwhile. If the volume-pressure function were

a fixed and constant property of the neural axis, showing only minor biological variation and not being influenced by pathological conditions, the only message from the volume-pressure studies worth remembering would be that the pressure response to a rapid volume change will be greater at an elevated ICP. In that case, knowledge of the level of ICP alone would suffice. A variable volume-pressure relationship means that the pressure response varies at the same ICP.

In the heterogenous group of patients described in Chapter 4, E_1 showed considerable variation. This group, admittedly, comprised patients of all age groups and, as previously discussed, the magnitude of E_1 may differ between children and adults by a factor of three to four. The variation in E_1 in the group of clinical patients, however, was much greater. A wide range in the slope of the volume-pressure curve was also found by Cohadon et al. (1975) in a large group of patients (n=144) with various pathological conditions. If one studies the composite plots of VPR versus ICP of Miller et al. (1973), a wide range of VPRs is observed at each pressure level, as in the plot we have presented (Fig. 16). Compartmentation of the craniospinal system, as caused by brain shift and herniation, may also considerably steepen the slope of the volume-pressure curve, as discussed in Chapter 2.3 and demonstrated by the single animal with a high E_1 in the series described in Chapter 5. It seems thus that the volume-pressure function as a feature of abnormal craniospinal dynamics is sufficiently variable to make it worthwhile identifying those patients who are particularly at risk.

The effect of the systemic blood pressure on the volume-pressure relationships, on the other hand, only became manifest at rather extreme levels of this pressure. We do not believe therefore that brain elasticity is significantly affected by the blood pressure variations encountered clinically.

In conclusion, volume-pressure studies have provided most valuable information with regard to a better understanding of the pathophysiology of intracranial hypertension. The value of measuring brain elasticity in the routine management of neurosurgical patients has probably been over-emphasized in the past. The volume-pressure function is just one of the many aspects that matter in the clinical evaluation of elevated ICP.

The exact shape of the volume-pressure curve

In Figure 59 we have plotted, in one graph, a composite volume-pressure curve, constructed from the data of the normocapnic and normotensive experiments described in Chapters 5 and 6 together with various other curves reconstructed from literature data (Löfgren et al., 1973; Marmarou, 1973; Benabid et al., 1975 and 1980; Cohadon et al., 1975; Sullivan et al., 1977). These curves are all different, although four are within a close range. The variety in the shape of the curves can be explained by differences in animal species (cat, dog), type (bolus injection, repetitive bolus injection, infusion) and rate of volume loading. Various techniques for raising the ICP were used (balloon, injection or infusion in the CSF space). Balloon inflation yields steeper volume-pressure curves due to the occurrence of brain shift causing compartmentation of the system, as

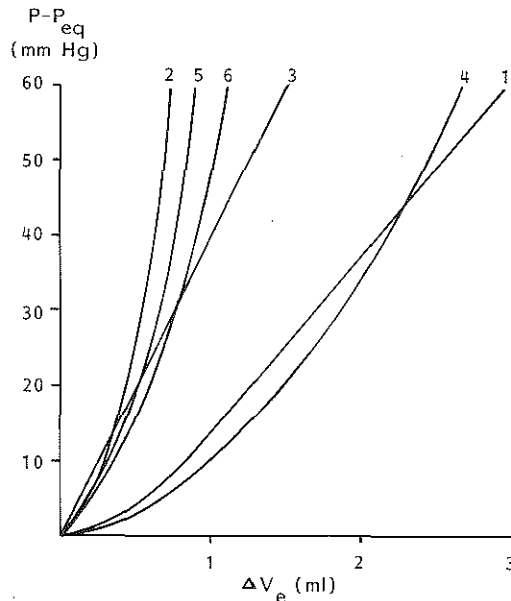


Fig. 59. Volume-pressure curves replotted from literature data. Change in ICP ($P-P_{eq}$) is related to normal equilibrium pressure (P_{eq}) and compared with change in total craniospinal volume (ΔV_e).

1. Löfgren et al. (1973): dog, cisterna magna infusion, 0.25 ml/sec.
2. Marmarou (1973): cat, repetitive ventricular bolus injection with increasing amounts, mean rate 0.1 ml/sec.
3. Benabid et al. (1975): dog, cisterna magna, bolus injection.
4. Cohadon et al. (1975): dog, ventricular infusion, 0.83 ml/sec.
5. Sullivan et al. (1977): cat, ventricular bolus injection of 0.1 ml/sec during balloon inflation.
6. This thesis: dog, ventricular bolus injection of 0.05 ml/sec during balloon inflation.

discussed in Chapter 5.4. The steepest curves were found in the cat, which can be explained by the smaller craniospinal volume of this species.

The exponential shape is predominant in most curves as opposed to the purely linear shape of the curve of Benabid. The major segment of Löfgren's curve, as well as our curve above an ICP of 60 mm Hg are also linear in shape. From our studies we have accumulated considerable evidence that the transition from exponential to linear is related to failure of CBF autoregulation (Chapters 5.4 and 6.4). It was inferred that the exponential shape is related to the autoregulatory process of cerebro-vasodilatation, maintaining a constant CBF. Recording of the volume-pressure curve by bolus injection superimposed on low rate balloon inflation ensures sufficient time for the autoregulatory response to develop. Furthermore, autoregulatory vasodilator responses may also be invoked by bolus injection *per se* as shown by Benabid (1976 and 1980). This may be the case particularly with repetitive injections with increasing amounts of fluid as employed by Marmarou.

If, on the other hand, the volume-pressure curve is recorded by rapid infusion within a very short time interval, as in the case of Löfgren's curve, the autoregulatory response is allowed too little time to become fully established, in which case the curve will take a more linear course. During rapid infusion, CBF and consequently CBV is decreased. Some degree of spatial compensation may thus be involved in the recording of this type of curve and this may partly explain its relatively flat course. With lower infusion rates, as in the curve of Cohadon et al., CBV may increase passively again due to the increased venous outflow resistance, eventually followed, if there is enough time, by an active vasodilatory response. These events may lend Cohadon's curve its exponential shape.

A linear shape of the volume-pressure curve is in agreement with the model of a closed sphere, in which the vascular system is disregarded, as discussed in Appendix 3. Benabid et al. have claimed that 'their' pressure responses were not contaminated by secondary vasomotor responses and their curve seems, therefore, the closest approximation of true craniospinal volume-pressure relationship. One problem is, however, that they have ascribed the linear shape of the curve (constant elastance) to the compliance of the cerebrovascular system. As discussed in Chapter 2.6, vascular compliance implies vascular compression which, in turn, implies

spatial compensation by a reduction in CBV. So the injected volume ΔV_i is no longer equal to ΔV_e , i.e., the 'elastic' volume requiring buffering, but $\Delta V_i = \Delta V_e + \Delta V_c$ (ΔV_c = compensated volume). In this case, the elastance, defined as $\Delta P/\Delta V_e$, is no longer given by $\Delta P/\Delta V_i$. As vascular compression progresses, ΔV_e increases at the expense of ΔV_c . So $\Delta P/\Delta V_e$ is no longer constant and the volume-pressure curve loses its linear shape. Following this line of reasoning one would expect a volume-pressure curve exhibiting a continuously decreasing slope!

The solution to this problem lies in the realization that most authors have meant to describe the volume-pressure relationship of the CSF compartment only. In that case, volume changes occurring in the vascular compartment do not interfere with volume forcing of the CSF space, and the elastic behaviour of the latter compartment can be rightly ascribed to vascular compliance. We have consistently tried to consider the entire craniospinal compartment contained within the dural envelope, including the vascular compartment. In that case, since the system is semi-closed, one has always to reckon with compensatory phenomena mediated through the vascular system.

It may thus be concluded that the discussion on the exact nature of the craniospinal volume-pressure relationships is highly theoretical. The system under consideration is a biological system and changes occurring within it are determined multi-factorially. The interaction between all the factors involved is so complex that studying them in isolation does not necessarily lead to a better understanding of the system as a whole. By studying the various volume-pressure curves reported in the literature one should take into account the definition of volume, the species examined, the technique used, the autoregulatory state of the preparation and many other factors.

From a clinical point of view the exact shape of the volume-pressure curve seems of little significance. The curves are all close together in a relatively small volume range. For man, this volume range, calculated from the mean E_1 of the group of clinical patients (Chapter 4), is in the order of 10 ml in the ICP range of clinical importance, which is less than 1% of the total craniospinal volume. These considerations bring us back to the old theme of the Monro-Kellie hypothesis, the essence of which is that small changes in craniospinal volume produce large changes in ICP.

8.3 CSF pulse pressure

CSF pulse pressure as a volume-pressure parameter

Any pressure response following a rapid volume addition to the craniospinal system is a function of the magnitude of the volume change and the elastic properties of the system as defined by the volume-pressure curve. Both VPR and CSF pulse pressure are such responses. The analogy between the two phenomena led us to consider whether it would be possible to use the CSF pulse pressure, like the VPR, as a volume-pressure parameter. This question was motivated by the problems encountered in the clinical application of the volume-pressure test, as outlined in Chapter 2.6.

The advantages of a method using the pulse pressure are obvious. The pulsatile change in CBV is generated within the system itself, so that there is no need to disturb the system from outside. The risk of intracranial infection is thus avoided. Furthermore, this method makes it possible to assess the craniospinal elastance also when the ICP is measured outside the CSF space. Finally, the pulsatile nature of the pressure response allows for the assessment of elastance on a continuous basis, so that it becomes possible to *monitor* the craniospinal volume-pressure relationships.

Making the most of ICP monitoring, both for routine clinical and for research purposes, requires some form of automatic data processing. This can be achieved by simple, bedside mini-computers which are commercially available. The options with regard to data analysis include mean pressures, pressure histograms either visually displayed or characterized by their modal pressure and right and left standard deviations (Janny et al., 1972; Kullberg, 1972), cerebral perfusion pressure, ICP to blood pressure ratio as an index of the cerebral vasomotor tone (de Rougemont et al., 1976), and other parameters. The time scale for data analysis can be chosen according to clinical requirements. Processing of the CSFPP-ICP relationship can be easily included in such a program.

Both VPR and CSF pulse are recorded in the CSF space. It may be argued that the analogy ceases at the underlying volume changes, since they occur in different compartments, i.e., the CSF and the vascular

compartment respectively. As far as the magnitude of a change in ICP is concerned, one might wonder whether it matters in which subdivision of the craniospinal compartment the volume change takes place. We have dealt with this problem in Chapter 3.4. It should be stressed that our mathematical description of the volume-pressure relationship is meant to apply to the whole craniospinal system and not only to the CSF compartment. This implies that, according to the concept of our volume-pressure model, changes in the volumes of the various craniospinal constituents are only important in so far as they contribute to a change in the total volume of the system. Theoretically, therefore, the pressure response is not compared with the volume change of the compartment in which it was induced, but with the change in total craniospinal volume. This concept was adhered to most consistently in the definition of the volume change underlying the CSF pulse pressure. Essentially, this volume change does not need to originate exclusively from the vascular compartment, but, since simultaneously occurring changes in the volume of CSF may be assumed to be relatively small as discussed in Chapter 3.4, the pulsatile volume change was for practical reasons identified with the change in CBV. As far as the VPR is concerned, this pressure response was only compared with the induced change in CSF volume under the assumption that this volume increment contributed in full to the change in total craniospinal volume. The limitations of this assumption and the consequences for the exact nature of the volume-pressure relationships have been discussed in the previous section.

Elastance is a function of ICP because of the exponential shape of the volume-pressure curve. The volume-pressure function is therefore best characterized by a pressure-independent parameter such as the elastance coefficient. For the same reason, before it can be used as a volume-pressure parameter, the CSF pulse pressure should be related to the ICP. For the purpose of patient monitoring, this can be done by the method described in Chapter 4.2.

If the whole range of ICP is considered, the experimental data are strongly suggestive of an exponential-type relationship between pulse pressure and ICP, as shown in Figure 60. When the volume-pressure relationship is taken into account for the same range of ICP, an exponential CSFPP-ICP relationship implies a progressive increase in ΔV_p . However, the results could also be adequately described by two linear

relationships on either side of a breakpoint. For the area below this point, i.e., the ICP range of clinical importance, this means that ΔV_b can be rightly considered as constant. This was supported by the finding of the highly significant, linear CSFPP-ICP relationships in the clinical study. The slope of this relationship thus becomes a measure of both the volume-pressure relationships and ΔV_b .

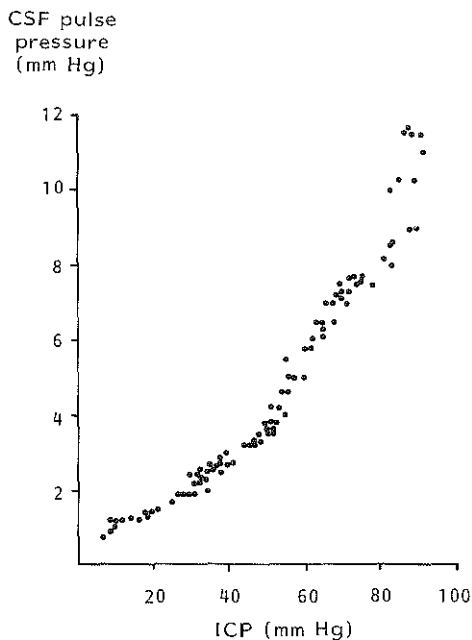


Fig. 60. Plot of CSF pulse pressure against intracranial pressure (ICP) during expansion of extradural balloon in an experimental animal, showing exponential-type relationship.

A rather wide variation in slope index was found in normal patients in the three studies mentioned in Chapter 4.4 (Szcwezykowski et al., 1977; Fridén and Ekstedt, 1980; Godin et al., 1980) with a mean value of 0.38 ± 0.10 . The variability is made up by the biological variation in both E_1 and ΔV_b . This slope index, found in normal patients, does not differ from the value of 0.40 ± 0.16 found in our clinical study, consisting of patients with both arrested and active intracranial pathology. The magnitude of ΔV_b was also found to vary widely in the last study: from 0.36 ml to 4.38 ml. It may thus be inferred that, up to now, it has not been possible to discriminate between the volume-pressure relationships of patients, nor to recognize reliably an abnormal volume-pressure relationship in a single patient, on the basis of the slope index alone.

Before it can be established whether this will ever be possible, it will be necessary to study selected groups of patients with identical intracranial pathology more closely, taking into account all those variables that may affect the pulsatile change in CBV such as: age, heart rate, SAP and PaCO₂. In this respect, it would be most helpful if ΔV_b could be more directly assessed in clinical patients, e.g., by rheo-encephalographic methods or ultrasonic techniques, so that the slope index could be calibrated.

The situation with regard to the clinical application of the slope index as a volume-pressure parameter, as outlined above, is different with regard to individual patient monitoring. Our experimental studies have identified those factors that exert influence, through ΔV_b , on the CSF pulse pressure, among which the SAP, PaCO₂ and heart rate are the most important. So long as these variables remain stable during ICP monitoring, changes in slope index will directly reflect changes in E_1 . Changes in the aforementioned variables can be easily recognized, as they are routinely monitored in the intensive care unit. The slope index can then be corrected, using the qualitative and quantitative information yielded by the experiments described in Chapter 6. How this will work out in clinical practice cannot yet be predicted and will need further, clinical research. Some caution seems needed because of the multi-factorial nature of the phenomena involved, which may complicate routine clinical use. At present, we employ volume-pressure testing at the beginning of each ICP recording to calibrate the slope index and as often afterwards as is indicated by a significant change in the slope of the CSFPP-ICP relationship. Thus we have rationalized the use of the volume-pressure test, thereby minimizing the risk of infection.

CSF pulse pressure and cerebral vasomotor tone

In view of both the relative clinical significance of the assessment of craniospinal volume-pressure relationships, as discussed in the previous section of this chapter, and the dependency of the CSF pulse pressure on the variable pulsatile change in CBV, the role of the pulse pressure as a volume-pressure parameter must await further, clinical research before it can be definitively established. Apart from this aspect of the CSF pulse,

our studies have opened up new perspectives concerning the clinical use of this phenomenon.

It was argued in the discussion in Chapter 7 that the CSF pulse pressure reflects the functional state of the cerebral vasculature as its underlying volume change, ΔV_b , is determined by vascular compliance which, in turn, is a function of intravascular pressure, wall tension and vessel radius. This state is furthermore determined by the cerebral vasomotor tone, which is actively maintained as part of the CBF autoregulatory mechanism. The CSF pulse pressure thus becomes a parameter of the cerebral vasomotor tone and of the ability of the vascular bed to react to changes in perfusion pressure.

This was demonstrated in various situations. When the cerebral perfusion pressure was affected by varying the SAP, it was shown, both by circumstantial evidence (Chapter 6) and by direct flow measurement (Chapter 7), that CBF remained constant. The accompanying change in CSF pulse pressure may thus be ascribed to the effect of the vasomotor tone, changing the cerebrovascular resistance by producing vasoconstriction and vasodilatation respectively. In the individual animal, however, a significant effect could only be demonstrated between the extreme levels of SAP. This is, among other reasons, because the SAP also affects the volume-pressure relationships through which the pulse pressure is influenced in the opposite direction.

When the cerebral perfusion pressure was reduced by raising the ICP, the CSF pulse pressure, as an expression of the cerebral vasomotor tone, did not change significantly so long as CBF remained constant. The reasons for this were discussed at the end of Chapter 7. Furthermore, the range over which the perfusion pressure was changed was much narrower than in the case of SAP variations. Moreover, as previously argued, an exponential analysis of the CSFPP-ICP relationship would allow for a small increase in CSF pulse pressure, that is in relation to the ICP.

A significant increase in pulse pressure was observed when the vasomotor tone was seriously impaired or completely lost. This was demonstrated in the ICP range above the breakpoint, when the autoregulatory mechanism had become completely exhausted, and also in the event of plateau waves occurring in clinical patients. This is even more of clinical interest since under these circumstances a relatively low VPR will be found, which may lead to an underestimation of the patient's

condition. A steep CSFPP-ICP slope will then be the alarm signal to rely on. When brain damage has seriously impaired CBF autoregulation, high slope indices may already be expected at normal levels of ICP.

It would be interesting to investigate the CSFPP-ICP relationship in the presence of B-waves, the origin of which has been ascribed to vasomotor instability (Lundberg, 1960; Obenchain and Stern, 1973). A steep slope in this relationship may, furthermore, have predictive value with regard to the appearance of plateau waves of the type shown in Chapter 4, the origin of which is explained by vasomotor paralysis (Lundberg et al., 1968; Risberg et al., 1969). Finally, the value of an index of brain vasomotor tone in clinical management was extensively studied by de Rougemont et al. (1976) in a series of head injured patients. For this purpose the ratio ICP/SAP was used, which ranged from 0 (complete vasospasm) to 1 (complete vasoparalysis).

In general, a large amplitude of the CSF pulse may be regarded as an ominous sign, since it may indicate a high ICP, a steep volume-pressure relationship, and/or defective cerebral vasomotor tone. However, this statement may not automatically be reversed, as an extremely small amplitude may result from cerebral vasospasm. It seems worthwhile to devote further research to the behaviour of the CSF pulse under various clinical conditions in order to determine the value of pulse pressure monitoring in routine clinical management.

CHAPTER 9

DYNAMICS OF THE CEREBROSPINAL FLUID CIRCULATORY SYSTEM

A mathematical description

"No adequate analysis of cerebrospinal fluid hydrodynamics has been put forth. Many experimental studies have evaluated individual parameters of the CSF circulation, but have not related them to the time course of changes in pressures and flows."

J.E. Guinane (1972)

9.1 Introduction

As discussed in the preceding chapter, the capacity of the craniospinal system to compensate for volume increments seems, from a clinical point of view, to be more important than the storage or buffering capacities. Of all the normal constituents of the system, i.e., brain tissue, blood and CSF, it is the CSF which is particularly capable of compensating for large quantities of volume.

The compensatory capacities of the CSF space and the mechanisms involved in the circulation of CSF were studied by numerous authors (Cushing, 1910; Dandy, 1919; Bering, 1959; Pappenheimer et al., 1961; Davson, 1967; Cserr, 1971; Welch, 1975). Many of these studies were originally aimed at obtaining a better understanding of the pathogenesis and management of hydrocephalus (Bering and Sato, 1963; Hussey et al., 1970; Katzman and Hussey, 1970; Nelson and Goodman, 1971; Portnoy and Croissant, 1976 and 1978; Børgeesen et al., 1979). Since the early seventies, the physiological studies of the CSF circulation have been supported by bio-physical and mathematical models, describing the interaction between formation, storage and absorption of CSF (Agarwal et al., 1969; Benabid, 1970; Guinane, 1972; Moskalenko et al., 1972; Marmarou, 1973; Hofferberth et al., 1975; Bloch and Talalla, 1976; Hakim et al., 1976; Hoffmann, 1980). Although these models were primarily developed to describe the processes involved in the origin of hydrocephalus, they can also be applied to those situations in which there is elevated ICP due to other lesions of a space-occupying nature, such as tumours, haematomas, etc. The model parameters provide information on both the rate of CSF formation and absorption and the storage capacities of the system. The actual values of these parameters, however, depend largely on the assumptions made in the mathematical relationships. In most models, it is assumed that the parameters are not affected by the rate at which volume

changes occur, although the results of a few studies contradict this assumption (Børgesen et al., 1979; Sullivan et al., 1979; Shapiro et al., 1983).

The present study has two aims:

1. to describe the physiological processes of the CSF circulation by a mathematical model, with the ultimate goal of obtaining parameters which are less dependent on the rate of volume disturbance, and
2. to discuss the volume compensatory capacities of the CSF circulation.

The first aim will be pursued by introducing our own concept of the craniospinal volume-pressure relationships (see Chapter 2) into one of the already existing mathematical models of the CSF circulation, namely that of Marmarou (1973, 1975 and 1978).

9.2 CSF formation and absorption

Since the earliest research into the site of CSF formation by Cushing (1910), Dandy (1919) and Howe (1928), it has been generally accepted that the choroid plexus is the main source of CSF formation. However, according to Pollay and Curl (1967) a substantial portion (about one third) of all CSF is produced outside the choroid plexus, i.e., by the brain parenchyma extracellular fluid. From the ventricular system the flow of CSF is directed towards the cranial and spinal subarachnoid spaces. The main portion of CSF is absorbed from the cranial subarachnoid space through the arachnoid villi into the venous blood contained within the dural sinuses. However, other sites of CSF absorption have also been established: the spinal subarachnoid space (Coben and Smith, 1969; Hammerstad et al., 1969) and across the ependyma lining the cerebral ventricles into the brain parenchyma (Bering and Sato, 1963).

Various techniques have been developed to study the effect of physiological variables quantitatively on the CSF formation and absorption rate. They were reviewed by Cserr (1971) and Welch (1975). Among these, the ventriculo-cisternal and ventriculo-lumbar perfusion techniques are the most widely employed (Pappenheimer et al., 1961 and 1962; Heisy et al., 1962). A short survey of this technique will be given here, as the

results will be used for comparison with the data obtained using the mathematical model.

The method involves the infusion of artificial CSF into the ventricular system at a known rate (\dot{V}_i) and with a known concentration of reference material (C_i), and the recovery of the perfusion fluid from the cisterna magna or lumbar region. Both the outflow rate (\dot{V}_o) and the concentration of reference material in the outflow fluid (C_o) are measured. From these data the CSF absorption and formation rates can be calculated using simple equations:

$$\text{Absorption rate: } F_o = \frac{\dot{V}_i C_i - \dot{V}_o C_o}{C_o}, \quad (9.1)$$

$$\text{Formation rate: } F_i = \dot{V}_o - \dot{V}_i + F_o. \quad (9.2)$$

However, these equations are only valid if all fluid formation takes place upstream of the outflow cannula and all fluid absorption downstream. Another prerequisite is that the reference material, which has a large molecular size, can only disappear from the system at the absorption site. In spite of these limitations it is generally believed that the method gives reliable estimates of CSF formation and absorption rates. One disadvantage is that it takes several hours before steady state conditions are reached. For this reason only a restricted number of experimental conditions can be studied in the same animal.

In the context of the present study, the effect of ICP on both formation and absorption rate is of particular interest. Considerable controversy as to the effect of ICP on CSF formation still exists between those authors who claim that CSF production is independent of the level of ICP (Heisy et al., 1962; Bering and Sato, 1963; Rubin et al., 1966; Hochwald and Wallenstein, 1967, Cutler et al., 1968) and those who claim that CSF formation decreases with rising ICP (Calhoun et al., 1967; Sahar et al., 1970; Hochwald and Sahar, 1971). In our view these contradictory conclusions originate from the statistical methods used for the evaluation of the experimental data. The first group of authors have based their conclusions on statistical analysis of group results. However, since the CSF formation rate varies greatly from one animal to the other and since each animal is tested at only one or at the most a few levels

of ICP, the results will produce a scatter of data which do not yield a significant correlation between formation rate and ICP. The second group of authors, on the other hand, have managed to demonstrate the negative correlation between CSF formation rate and ICP in individual animals. We therefore favour the conclusion of the second group of authors that there is some dependency of CSF formation rate on ICP, although the exact relationship has not yet been established.

CSF production is also affected by various pharmacological agents, by the PaCO_2 and by body temperature (Oppelt et al., 1964; Ames et al., 1965; Davson et al., 1970; Snodgras and Lorenzo, 1972). A detailed discussion of these effects is beyond the scope of this study. Whereas these factors may have a direct metabolic effect on choroidal secretory epithelium, it might be argued that they affect CSF production by altering the blood supply to the choroid plexus.

This brings us back to the old question as to whether the mechanism of CSF production is based upon a secretion or a filtration process. The controversy concerning this point has not yet been settled. There is reason to assume that both processes occur in series. Filtration takes place from the capillary lumen to the interstitial spaces of the choroid plexus, the filtrate constituting the fluid from which the secretion is produced by the epithelium. If filtration and blood flow through the choroid plexus play an important role in the formation of CSF, the SAP will be a significant parameter as well. Carey and Vela (1974) found a reduction in CSF production of 39% by lowering mean SAP from 119 to 62 mm Hg, but an exact relationship could not be established. Benabid et al. (1970 and 1975) and Hofferberth et al. (1975) assumed a linear relationship between CSF production and cerebral perfusion pressure minus the blood oncotic pressure, but they did not present experimental data to substantiate these assumptions. According to Welch (1966 and 1975), the role of oncotic pressure gradients in CSF production is negligible.

The process of drainage of CSF is less complex than that of its formation. It is generally accepted that the absorption rate depends on the hydrostatic pressure gradient between the CSF in the subarachnoid space and the venous blood in the dural sinuses. The bulk absorption of fluid was shown to be linearly related to this pressure gradient (Welch and Friedman, 1960; Heisy et al., 1962; Cutler et al., 1968; Davson et al.,

1970). Below an ICP of 5 mm Hg CSF absorption ceases (Cutler et al., 1968). Sahar et al. (1970) showed that this threshold ICP corresponds with the level of the sagittal sinus pressure, thus with a zero pressure difference between subarachnoid space and sagittal sinus. Although the sinus pressure rises to some extent with elevation of ICP, the pressure difference increases, so that the CSF absorption rate also increases (Shulman et al., 1964; Sahar et al., 1970).

The conclusions of most studies are open to some criticism, as they are based on analysis of group results. However, in spite of this, it seems most likely that they also hold true for the individual animal (Sahar et al., 1970; Hochwald and Sahar, 1971).

Under normal, physiological steady state conditions, CSF formation and absorption are in equilibrium. Values for CSF formation at the equilibrium ICP were reported by many investigators using perfusion techniques. The values obtained in the dog and in man are of particular interest to the present study. Mean CSF production in the dog varied between 2.1 and 3.0 ml/hr (Bering and Sato, 1963; Oppelt et al., 1963; Cserr, 1965; Vela et al., 1979) and in man values of 21.0 and 22.2 ml/hr were found (Rubin et al., 1966; Cutler et al., 1968). Since the choroid plexus is regarded as the main source of CSF, it is assumed that, in mammalian species, there is a relationship between the CSF production rate and the total weight of the choroid plexus (Davson, 1967).

9.3 Mathematical CSF circulation model

The basis of the CSF circulation model is given by the equilibrium between CSF formation, CSF absorption and changes in the total volume of CSF. This equilibrium exists under all circumstances within the craniospinal system:

$$F_i - F_o - F_{csf} = 0, \quad (9.3)$$

where: F_i = CSF formation rate,
 F_o = CSF absorption rate, and
 F_{csf} = rate of change in CSF volume.

The model, as shown in the block diagram of Figure 61, will be described in two steps. First, the steady state condition, implying equal CSF formation and absorption rates ($F_{\text{csf}} = 0$), will be studied. Secondly, the dynamic behaviour of the system in response to a disturbance of the equilibrium will be investigated. Furthermore, the significance of the model parameters and their computation from both the steady state and the dynamic relationships will be discussed.

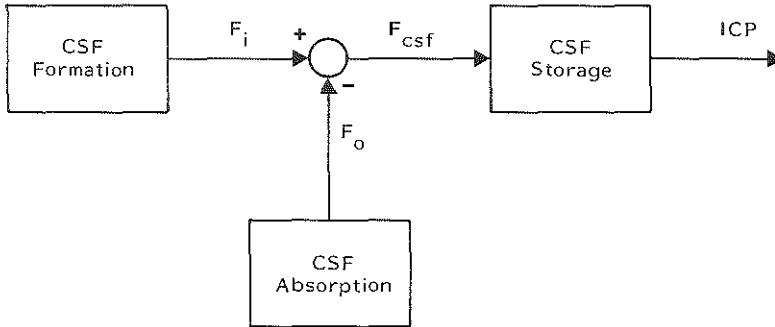


Fig. 61. Block diagram of interrelationship between formation, absorption and storage of CSF.

9.3.1 Steady state conditions

Under physiological steady state conditions the CSF formation rate is balanced by the absorption rate. This implies that the total volume of CSF stored in the system does not change, so that the ICP is maintained at a constant base-line or resting level (P_b), yielding a reduced system equation:

$$F_i - F_o = 0. \quad (9.4)$$

As discussed in the previous section, the exact relationship between CSF formation and the pressure gradient across the choroid plexus is not known. We shall therefore develop the model for two different situations and compare the results:

1. CSF formation is independent of SAP and ICP and takes place at a constant rate, as assumed in most models (Agarwal et al., 1969; Guinane,

1972; Moskalenko et al., 1972; Marmarou, 1973; Bloch and Talalla, 1976):

$$F_i = F_1. \quad (9.5)$$

2. CSF formation is linearly dependent on the pressure gradient between the arteries in the choroid plexus (P_a) and the cerebral ventricles ($P = \text{ICP}$), divided by the resistance to formation or inflow resistance (R_i) which is assumed to be constant (Benabid et al., 1970 and 1975; Hofferberth et al., 1975):

$$F_i = \frac{P_a - P}{R_i}. \quad (9.6)$$

Since the arterial pressure in the choroid plexus is difficult to measure, it is often replaced by the SAP.

The CSF absorption rate, on the other hand, is generally accepted to be linearly related to the pressure difference between the subarachnoid space and the dural sinuses, if and so long as the ICP exceeds the dural sinus pressure (P_d):

$$F_o = \frac{P - P_d}{R_o} \quad \text{for } P \geq P_d, \quad (9.7)$$

and: $F_o = 0 \quad \text{for } P < P_d,$

where: R_o = resistance to absorption of CSF or outflow resistance which is assumed to be constant. Since the dural sinus pressure is not easily accessible to measurement, it is often approximated by the central venous pressure or assumed to be equal to zero. In the following model equations we shall assume that the ICP always exceeds dural sinus pressure.

Pressure-independent CSF formation

For a constant CSF formation rate, independent of SAP and ICP, the equilibrium condition can be derived from Equations 9.4, 9.5 and 9.7:

$$F_1 - \frac{P - P_d}{R_o} = 0.$$

So, the base-line ICP ($P = P_b$) is determined solely by the CSF formation rate, the resistance to outflow and the sinus pressure, as shown in the following equation:

$$P_b = R_o F_1 + P_d. \quad (9.8)$$

The base-line ICP is thus independent of the craniospinal volume-pressure relationship.

The pressure terms of Equation 9.8 can be determined, or at least approximated, by simple, direct measurement. For the calculation of the CSF formation rate and outflow resistance a forcing function has to be applied. When the formation rate increases, the base-line ICP will rise until a new equilibrium is reached. The increase in formation rate can be simulated by infusing artificial CSF at a constant rate into the CSF space (infusion test). If the infusion rate equals F_{in} , Equation 9.4 can be rewritten as:

$$F_i + F_{in} - F_o = 0. \quad (9.9)$$

The new steady state ICP (P_{ss}) can be derived from this equation:

$$P_{ss} = R_o F_1 + R_o F_{in} + P_d, \quad (9.10)$$

or, using Equation 9.8:

$$P_{ss} = R_o F_{in} + P_b, \quad (9.11)$$

According to this equation, the steady state ICP is linearly related to the infusion rate. The outflow resistance can be computed from:

$$R_o = \frac{P_{ss} - P_b}{F_{in}}. \quad (9.12)$$

In this equation, P_{ss} and P_b are the steady state pressures during and before infusion, and F_{in} is given by the speed of the infusion pump. When the outflow resistance is known, the CSF formation rate can be calculated from Equation 9.8 according to:

$$F_1 = \frac{P_b - P_d}{R_o}. \quad (9.13)$$

Since the difference between the base-line ICP and the sinus pressure is often small, the computation of the formation rate is very sensitive to errors in the measurement of these pressures.

The above equations, describing the steady state condition during constant rate infusion, only hold true on condition that the sinus pressure does not change simultaneously with the ICP. There is experimental evidence however that the sagittal sinus pressure is linearly related to the ICP (Shulman et al., 1964; Sahar et al., 1970; Rowan et al., 1972), and the relationship can be described as:

$$P_d = P_{db} + K (P_{ss} - P_b), \quad (9.14)$$

where: P_{db} = the sinus pressure corresponding with the normal base-line ICP, and
 K = a constant.

Applying this equation to the Equations 9.8 and 9.10, the new relationship between the steady state pressure and the infusion rate reads:

$$P_{ss} = R_o F_{in} + P_b + K(P_{ss} - P_b), \quad (9.15)$$

or:

$$P_{ss} = \frac{R_o}{1 - K} F_{in} + P_b. \quad (9.16)$$

Accepting a linear relationship between sinus pressure and ICP, the outflow resistance can be computed from the following equation:

$$R_o = (1 - K) \frac{P_{ss} - P_b}{F_{in}}. \quad (9.17)$$

In the above mentioned reports on the relationship between dural sinus pressure and ICP, established in different species (dog, cat and baboon), values for K were found to vary between 0.1 and 0.5. Consequently, by assuming a constant dural sinus pressure the outflow resistance may be overestimated by 10-50%, resulting in a corresponding underestimation of the CSF formation rate.

Pressure-dependent CSF formation

If the CSF formation rate is assumed to be linearly related to the pressure gradient between the choroidal arterial system and the ventricular system, the Equations 9.8 and 9.10, describing the equilibrium conditions before and during steady state infusion, must be modified by substituting $\frac{P_a - P}{R_i}$ for F_1 (Equation 9.6):

$$P_b = \frac{P_a R_o + P_d R_i}{R_o + R_i}, \quad (9.18)$$

and:

$$P_{ss} = \frac{R_i R_o}{R_i + R_o} F_{in} + P_b. \quad (9.19)$$

So, in this case too, the steady state ICP is linearly related to the infusion rate. From these equations both inflow and outflow resistance can be calculated:

$$R_i = \frac{P_{ss} - P_b}{F_{in}} \cdot \frac{P_a - P_d}{P_b - P_d}, \quad (9.20)$$

and:

$$R_o = \frac{P_{ss} - P_b}{F_{in}} \cdot \frac{P_a - P_d}{P_a - P_b}. \quad (9.21)$$

The inflow resistance in particular is sensitive to small errors in the pressure measurements, as the difference between P_b and P_d is relatively small.

The effect of changes in dural sinus pressure is neglected also in these equations. As with the constant formation rate, it can be seen that alterations in this pressure affect the inflow as well as the outflow resistance by a factor $(1 - K)$; K varies between 0.1 and 0.5:

$$R'_i = (1 - K) R_i, \quad (9.22)$$

and:

$$R'_o = (1 - K) R_o, \quad (9.23)$$

where R'_i and R'_o are the inflow and outflow resistance in the case of an interdependency of ICP and sinus pressure.

Conclusions

It has been shown that the model parameters both for the constant and for the pressure-dependent CSF formation rate can be calculated from simple equations derived from two steady state conditions:

1. the normal, physiological equilibrium between CSF formation and absorption, and
2. the equilibrium resulting from disturbing the system with an external forcing function, i.e., constant rate infusion.

The variables to be measured are physiological entities easily accessible to measurement: ICP, SAP and central venous pressure. It should, however, be realized that SAP and venous pressure are only approximations of the real pressures functioning in the equations.

The problem as to which formation model should be preferred cannot be solved, as the parameters of both models are calculated from the same steady state conditions. To answer this question, a direct measurement of the CSF formation at various levels of ICP would have to be carried out.

The assumption of a constant sagittal sinus pressure, as made in almost all CSF absorption models, may introduce a serious error in the computation of the model parameters (10-50%). Moreover, most models assume a zero sinus pressure, which may produce an even greater error in the calculation of the formation rate. This should be considered when these parameters are compared with values obtained from ventriculo-cisternal and ventriculo-lumbar techniques.

9.3.2 Dynamic behaviour of the CSF circulation

The dynamic behaviour of the CSF circulatory system determines the course of ICP in response to a disturbance of the equilibrium between CSF production and absorption. If more CSF is produced than can be absorbed, the resulting net flow must be stored in the CSF compartment in accordance with Equation 9.3:

$$F_{\text{csf}} = F_i - F_o.$$

The equilibrium can be disturbed by intracranial pathology, interfering with the processes of CSF formation and absorption, or by forcing functions (F_f) externally applied, such as constant rate infusion or the volume-pressure test, in which case the above equation would read:

$$F_{\text{csf}} = F_i - F_o + F_f. \quad (9.24)$$

If the CSF compartment is conceived as a subdivision of the craniospinal compartment, changes in the volume of CSF will contribute to a change in the volume of the total compartment and F_{csf} may be replaced by F_{cs} , which may be defined in terms of flow as the rate of change in the volume of the craniospinal compartment:

$$F_{\text{cs}} = F_i - F_o + F_f. \quad (9.25)$$

F_f may also be understood as a forcing function in the sense of an expanding intracranial mass lesion or a change in the volume of the other craniospinal contents.

The capacity for storing a volume increment resulting from a disturbance in the equilibrium of flows is determined by the volume-pressure relationship of the system. This capacity can generally be described as:

$$F_{\text{cs}} = \frac{dV}{dt} = \frac{dV}{dP} \frac{dP}{dt} = \frac{1}{dP/dV} \frac{dP}{dt}, \quad (9.26)$$

where dP/dV is defined as the elastance of the craniospinal system described by Equation 2.2 (Chapter 2.4) as:

$$dP/dV = E_1(P - P_o).$$

Equation 9.26 can thus be written as:

$$F_{\text{cs}} = \frac{1}{E_1(P - P_o)} \frac{dP}{dt}. \quad (9.27)$$

If P_o is assumed to be equal to zero, this relationship describing the storage capacities is similar to that of the Marmarou model (1973 and 1975). The relations for the storage capacity, CSF formation and CSF

absorption can now be inserted in the system equation, yielding in the case of a constant CSF formation rate:

$$\frac{1}{E_1(P - P_o)} \frac{dP}{dt} = F_1 - \frac{P - P_d}{R_o} + F_f(t) . \quad (9.28)$$

This relationship is shown in a block diagram (Fig. 62). Using Equation 9.8 for the steady state condition of the system, the following non-linear differential equation for the dynamic behaviour can be obtained:

$$\frac{1}{E_1(P - P_o)} \frac{dP}{dt} + C_1(P - P_b) - F_f(t) = 0, \quad (9.29)$$

where: $C_1 = 1/R_o = \text{constant} . \quad (9.30)$

Equation 9.29 also holds true for a pressure-dependent CSF formation model (Fig. 62), in which case:

$$C_1 = \frac{R_o + R_i}{R_o R_i} . \quad (9.31)$$

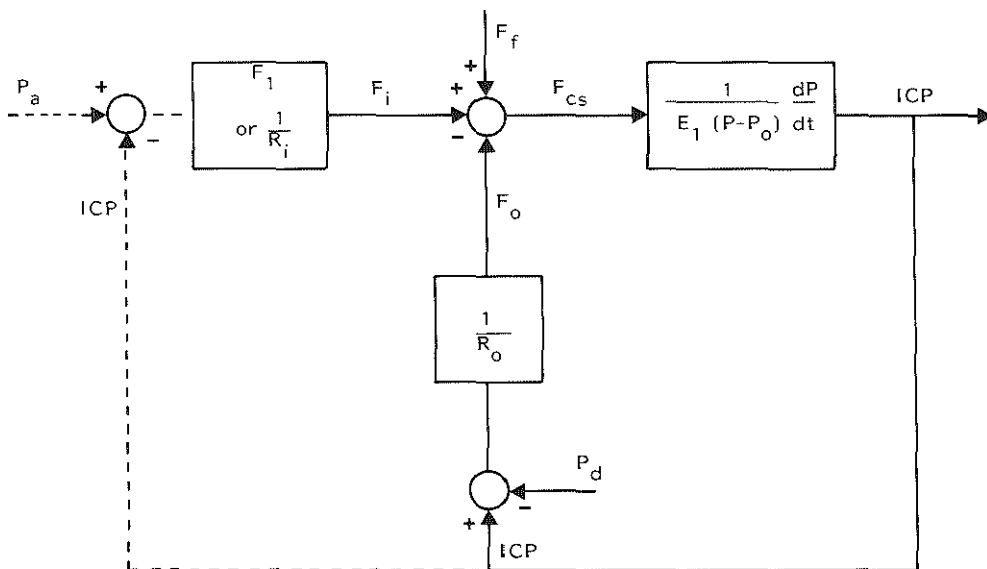


Fig. 62. Block diagram showing relationships between pressures and flows in CSF system. Pressure-dependent CSF formation is represented by dashed line.

This non-linear differential equation can be solved for different external forcing functions as well as for pathological processes. The general solution of the equation and the specific solutions for constant rate infusion (infusion test) and bolus injection (volume-pressure test) are given in Appendix 6.

Infusion test

- When the CSF circulation is disturbed by means of constant rate infusion, the dynamic response of the ICP is given in the following equation (Appendix 6):

$$P(t) = \frac{[F_{in} + C_1(P_b - P_o)][P_b - P_o]}{C_1(P_b - P_o) + F_{in} e^{-E_1[F_{in} + C_1(P_b - P_o)] t}} + P_o . \quad (9.32)$$

So, the ICP as a function of time is dependent on the volume-pressure parameters E_1 and P_o , and on the constant C_1 which contains the outflow resistance; in the case of a pressure-dependent CSF formation, C_1 also contains the inflow resistance. The outflow and inflow resistance are given by the steady state conditions.

In summary, the parameters of the CSF circulation model can be calculated in the following way. The parameters of CSF production (F_1 or F_i , R_1) and of CSF drainage (R_o) can be computed from the steady state equations (9.13, 9.20, and 9.12 or 9.21), whereas the volume-pressure parameters (E_1 and P_o) must be calculated from the dynamic response described in Equation 9.32. The last equation can therefore be rewritten as:

$$E_1 = \frac{1}{[F_{in} + C_1(P_b - P_o)]t} \ln \frac{F_{in}[P(t) - P_o]}{[F_{in} - C_1(P(t) - P_b)][P_b - P_o]} . \quad (9.33)$$

In the Marmarou model P_o is equal to zero, in which case E_1 can be calculated at each instant t from the above equation. In our model however we have assumed that P_o is not necessarily equal to zero; our assumption was based on experimental data. P_o can then be computed by applying the equation at two points of time, t_1 and t_2 , since E_1 at time

t_1 must be equal to E_1 at time t_2 . This results in a simple equation for P_o if the time interval is chosen in such a way that $t_2 = 2t_1$ (Appendix 7):

$$P_o = \frac{P_1^2(P_{ss} - P_2 - P_b) - P_b P_2(P_{ss} - 2P_1)}{P_{ss}(2P_1 - P_2 - P_b) + P_b P_2 - P_1^2}, \quad (9.34)$$

where: $P_1 = P(t_1) = \text{ICP at time } t_1 \text{ after starting the infusion, and}$
 $P_2 = P(t_2) = \text{ICP at time } t_2 = 2t_1.$

When P_o is known, E_1 can be calculated from Equation 9.33. To improve the accuracy of the computation of E_1 and P_o the above procedure can be repeated several times and the average values taken.

Another approach might be to compute the parameters E_1 and P_o by means of an algorithm for least-squares estimation of non-linear parameters (Marquardt, 1963). Theoretically, this may be expected to result in a better fit of the model to the experimental data. The disadvantage of this technique would be that it is more complicated and more time consuming.

Volume-pressure test

The dynamic decay of the ICP following a disturbance of the system by a rapid bolus injection is described by the following equation (Appendix 6):

$$P(t) = \frac{(P_b - P_o) e^{E_1[\Delta V_i + C_1(P_b - P_o)t]}}{1 + e^{E_1 \Delta V_i \left[e^{E_1 C_1(P_b - P_o)t} - 1 \right]}} + P_o, \quad (9.35)$$

where: $\Delta V_i = \text{injected volume.}$

Again, the course of the ICP is dependent on the volume-pressure parameters E_1 and P_o , and on C_1 which is determined by the outflow resistance (R_o) and, in the case of a pressure-dependent CSF formation model, also by the inflow resistance (R_i). The four model parameters can be found by solving four independent equations derived from the volume-pressure relationship, the equilibrium state and the dynamic

behaviour. According to Equation 2.7, E_1 can be written as a function of P_o :

$$E_1 = \frac{1}{\Delta V_i} \ln \frac{P_p - P_o}{P_b - P_o}, \quad (9.36)$$

where: P_p = peak ICP following bolus injection.

Substituting C'_1 for $E_1 C_1$ and Equation 9.36 for E_1 in Equation 9.35, C'_1 can be written as a function of P_o :

$$C'_1 = \frac{1}{(P_b - P_o)t} \ln \frac{[P(t) - P_o][P_p - P_b]}{[P(t) - P_b][P_p - P_o]}. \quad (9.37)$$

In the Marmarou model P_o is equal to zero. In that case E_1 can be calculated from Equation 9.36 and C'_1 , and consequently C_1 , from Equation 9.37 at each instant $t = t_1$. In our model we have assumed that P_o is not necessarily equal to zero. In this case P_o can be computed on condition that $C'_1(t_1) = C'_1(t_2)$ and that $t_2 = 2t_1$. This was carried out in Appendix 8 with as final result:

$$P_o = \frac{P_p P_2 (2P_1 - P_b) - P_1^2 (P_p - P_b + P_2)}{P_b (2P_1 - P_p - P_2) - P_1^2 + P_2 P_p}. \quad (9.38)$$

When P_o is known, E_1 can be calculated from Equation 9.36 and, subsequently, C_1 from Equation 9.37. From C_1 and the equilibrium condition the parameters of CSF formation and absorption can be computed.

In this case too, instead of following the above procedure, C_1 and P_o may be estimated from a least-squares fitting procedure using a Marquardt iteration.

9.4 Discussion

The CSF circulation model has been developed to gain insight into the variables affecting the circulation of CSF. As the volume of CSF is most capable of providing spatial compensation and as the model includes the volume-pressure relationship as well, the model may also be expected to provide knowledge on how and to what extent the ICP is changed, when the normal physiological equilibrium is disturbed by intracranial or extracranial processes. In order to be valid and suitable for clinical

application any model should meet the following requirements:

1. it should accurately describe the changes in ICP occurring with known forcing functions,
2. the model parameters should be stable and reproducible, and
3. the effect of various pathological conditions on the model parameters should be known.

The study of the first two requirements will be the subject of the next chapter. The establishment of the effect of various pathological states on the model parameters requires clinical evaluation of different groups of patients with known pathology and goes beyond the scope of the present study.

We shall briefly discuss here the significance and application of the model parameters, in order to put the abstract information contained in the model equations into a physiological and clinical perspective.

As shown in Equation 9.8, the resting or physiological steady state ICP is determined by the CSF formation rate, the outflow resistance and the dural sinus pressure. Consequently, a change in one of these parameters will always produce a change in the resting ICP. As discussed before, the production of CSF is a complex process, which may be affected by many variables. Among these, the blood supply to the choroid plexus plays a dominant role as the blood is the main source from which the CSF is generated. This implies that physiological factors influencing CBF may ultimately change the resting ICP by affecting CSF production. Obviously, pathology of the choroid plexus may also influence CSF production.

The two remaining parameters defining the steady state ICP are effective in regulating the bulk absorption of CSF. The outflow resistance may be increased by obliteration of the subarachnoid space, as in space-occupying lesions of various nature, infectious processes and subarachnoid haemorrhage, or by pathology involving the arachnoid villi. Obstruction of the CSF pathways away from the site of absorption, as in obstructive hydrocephalus, does not affect the outflow resistance in the strict sense. However, since the model does not provide for parameters governing the transport of CSF from the formation to the absorption site, obstruction of the central CSF pathways will become manifest as an increase in outflow resistance. In this case however a new resistance component has been inserted regulating the transport of CSF. The new steady state ICP is

reached when the ICP has risen sufficiently to restore the flow over the obstruction site, so that CSF formation is again balanced by CSF absorption. In that case the resting pressure is thus determined by the characteristics of the obstructive process.

The dural sinus pressure may be increased by various intracranial conditions causing obstruction of sinus flow or by arterio-venous shunts involving the dural sinuses. Extracranial conditions may also influence the resting ICP by increasing the sinus pressure through the mechanism of the central venous pressure.

Apart from the factors given in the equilibrium condition, it might be argued that other factors too, such as alterations in CBV or in the volume of the brain, may affect the resting ICP. However, such volume alterations will enhance CSF absorption by producing a temporary elevation of the ICP. As a result, the reciprocal changes in CSF volume will cause the system to return to its resting pressure.

It should be noted that under steady state conditions the resting ICP is not dependent on the volume-pressure parameters. Only when spatial compensation is impaired and CSF absorption can no longer cope with CSF production or with the volume of a forcing function, do the volume-pressure relationships come into play. But in that case the steady state is never reached and we are dealing with the dynamic behaviour.

The outflow resistance is often regarded as a measure of the compensatory capacity of the craniospinal system. Accordingly, a low value for the outflow resistance is believed to indicate a large compensatory capacity and vice versa. Strictly speaking, a low outflow resistance only implies that the required increase in absorption rate is established at a lower level of ICP. The benefit of this is, of course, that a smaller pressure rise is needed to cope with a volume increment. The limitations of the compensatory ability, however, are determined more by the quantity of CSF available for compensation, i.e., the size of the CSF space and the patency of the CSF pathways, than by the outflow resistance *per se*. But, as we have pointed out before, obstruction of the CSF circulation will be reflected in the computed outflow resistance, due to the limitations of the model. The outflow resistance may therefore still be regarded as a measure of spatial compensatory capacities. This only holds true, of course, if the forcing function is introduced into the system upstream of

the site of obstruction. In the case of aqueductal stenosis for example, a lumbar infusion test, as opposed to ventricular infusion, will yield a normal outflow resistance.

With a model which assumes a constant dural sinus pressure, the computed values for the outflow resistance may be too high and those for the formation rate may be too low if the sinus pressure increases concomitantly with the ICP. Therefore, on the basis of a high outflow resistance, found with the present model, it is impossible to discriminate between a CSF absorptive defect on the one hand and a CSF circulatory disturbance or a raised sinus pressure on the other.

However, in spite of these limitations, the outflow resistance may be a useful clinical parameter in the diagnosis and management of CSF circulatory disturbances, as has been demonstrated in various forms of hydrocephalus (Hussey et al., 1970; Katzman and Hussey, 1970; Nelson and Goodman, 1971; Trotter et al., 1974; Ekstedt and Fridén, 1976, Hartmann and Alberti, 1977; Portnoy and Croissant, 1978; Tans, 1979; Gessey et al., 1980; Gjerris et al., 1980; Sklar et al., 1980).

Not much attention has been paid, up to now, to the role of CSF formation in the process of spatial compensation. However, if a pressure-dependent CSF production is assumed, it follows from Equation 9.6 that, for instance, an increase in ICP of 20 mm Hg may result, depending on the SAP, in a reduction in formation rate by 20-30%. Therefore, especially at high levels of ICP and with obstruction of the CSF pathways, a decrease in CSF production might play a substantial role in volume compensation.

Another important limitation of the model is the assumption that the external forcing function, whether it is rapid or slow, does not cause changes in craniospinal volume other than those related to CSF formation and absorption. True enough, the general system equation (9.25) allows for such volume changes to occur, but the rate of these changes is unknown, so that artifacts may be introduced in the computation of the system parameters. These volume changes are sure to occur within the cerebrovascular compartment, following both bolus injection and slow rate infusion, as was demonstrated by Benabid et al. (1976 and 1980). They may be incremental as well as decremental to the craniospinal volume. The mechanisms of the changes in CBV were discussed at length in the preceding chapters.

Conclusions

1. A mathematical CSF circulation model was developed, based on the authors' concept of the craniospinal volume-pressure relationship.
2. Theoretically, all model parameters can be analytically computed from a single test by means of simple equations.
3. Both the infusion test and the volume-pressure test should theoretically produce the same results.
4. The assumption of a sinus pressure independent of ICP may result in an overestimation of the outflow resistance by 10-50%.
5. The volumes of cerebral blood and brain are considered constant during the disturbance of the system.

CHAPTER 10

EVALUATION OF THE CEREBROSPINAL FLUID CIRCULATION MODEL

An experimental study in dogs

"Cet enfant a de l'eau dans la tête, dit le vulgaire; cet enfant est hydrocéphale, dit gravement le médecin, répétant littéralement par un mot grec ce que dit l'ignorant dans sa propre langue. Mais quelle est cette eau? d'où vient-elle? Voilà ce dont les médecins auraient dû s'occuper."

F. Magendie (1842)

10.1 Introduction

In the preceding chapter a mathematical model of the CSF circulation was designed, based on experimental data from the literature and describing both the dynamics of CSF formation and absorption and the buffering capacities of the craniospinal system. This model deviates from the Marmarou model on two points:

1. the buffering capacity of the system was derived from an exponential volume-pressure function extended by a constant term (P_0 ; see Chapter 2.4);
2. the model was developed for both a constant rate and a pressure-dependent CSF formation.

Some of the CSF circulation models already described are only of theoretical significance, as they were based on a large number of parameters which could not all be experimentally verified (Agarwal et al., 1969; Moskalenko et al., 1972; Bloch and Talalla, 1976). These models may still have contributed towards a better understanding of CSF dynamics.

Other models were directed more towards clinical applicability and were, therefore, based on a limited set of parameters which could be assessed by simple tests (Benabid et al., 1970 and 1975; Marmarou et al., 1973, 1975 and 1978; Hofferberth et al., 1975; Hoffmann, 1980). It was assumed in these models that the parameters were independent of the rate and nature of volume forcing, the level of ICP and the time at which the parameters were assessed. The forcing functions most commonly used are constant rate infusion and rapid bolus injection. An alternative method is the constant pressure infusion test as first described by Davson et al. (1970) and further elaborated by Ekstedt (1975 and 1977), Portnoy and Croissant (1976) and Sklar et al. (1978). This method was not employed in the present study, since it is technically more complicated and is at

present used only for the computation of CSF formation and CSF outflow resistance.

To the best of our knowledge no studies exist in which all the model parameters were computed from both constant rate infusion and bolus injection and where these parameters were compared for different volume disturbances. Marmarou (1973) computed only the CSF outflow resistance by both methods and found a reasonable agreement between the two techniques. Other investigators (Sullivan et al., 1977; Børgesen et al., 1979; Shapiro et al., 1983), however, found lower values for the outflow resistance by the bolus injection technique as compared with the constant rate infusion method.

We therefore decided to evaluate the CSF circulation model described in Chapter 9 in a series of experiments, with the following objectives in mind:

1. to evaluate the stability of the model parameters for different forcing functions, i.e., constant rate infusion and bolus injection, and to do this at different volume loads;
2. to compare the results of this model with those of the Marmarou model applied to the same data;
3. to compare the parameters obtained using a constant rate CSF formation model with those obtained using a pressure-dependent CSF formation model.

10.2 Experimental methods

Preparation and Measurements

The experiments were performed on six adult mongrel dogs of either sex weighing from 14 to 20 kg. Atropine (0.5 mg) was routinely given as premedication. Anaesthesia was induced with intravenously administered thiopentone (30 mg/kg body weight), maintained with a mixture of nitrous oxide and oxygen (2:1), and supplemented by intravenous infusion of Fentanyl (Janssen). The animals were artificially ventilated (Pulmomatt) under normocapnic conditions (PaCO_2 : 37-43 mm Hg). Pavulon (Organon Teknika), 0.2 mg/kg body weight, was used for muscle relaxation. Body temperature was maintained at about 37°C.

The animals were placed in a stereotaxic frame in the sphinx position. The scalp and temporal muscles were reflected. The methods of continuous recording of VFP, SAP and central venous pressure were described in Chapter 5.2. A needle was percutaneously inserted into the cisterna magna in order to elevate the ICP by infusion of normal saline at various rates (Harvard Infusion Pump, Model 975). The ECG was recorded via needle electrodes placed in the limbs of the animals and the heart rate was continuously monitored. The pressure transducers and amplifiers used for the various physiological signals were the same as those described in Chapter 7.2. All signals were displayed on a multi-channel chart recorder (HP Thermal Recorder System 7418A) and stored on a tape-recorder (Philips Analog 7) for off-line analysis by computer (PDP 11/34). Arterial blood gases were measured at regular intervals (Radiometer ABL1) and corrected for temperature. The tracheal CO₂ concentration was monitored by an infrared gas analyzer (Beckman Instruments).

Experimental protocol and Data collection

In six animals the ICP was raised by continuous infusion of normal saline into the cisterna magna at the following rates: 6.0, 16.2 and 22.7 ml/hr. In four animals an infusion rate of 31.8 ml/hr was also used. In five animals the infusion tests were alternated with bolus injections of 0.1, 0.2 and 0.3 ml into the lateral ventricle. In two animals a volume of 0.4 ml was also used. After the completion of each test the animals were allowed sufficient time to stabilize and the next test was not started until the ICP had returned to its resting level. No special measures were taken to keep the SAP at a constant level, but an experimental run was discarded if the SAP deviated more than 15% from the initial value at the beginning of the experiment.

The model parameters were computed from the ICP course during each experimental run using the equations described in Chapter 9. In the case of the infusion test, the parameters of CSF formation and absorption were calculated from the steady state ICPs before and during infusion using Equations 9.12 and 9.13 for constant rate CSF formation, and Equations 9.12, 9.20 and 9.21 for pressure-dependent CSF formation. The volume-pressure parameters P_0 and E_1 were then calculated in two different ways:

according to the analytic solution contained in Equations 9.33 and 9.34, and by fitting Equation 9.32 to the time course of the ICP using a least-squares fitting procedure (Marquardt, 1963). Finally, the Marmarou model was applied to the experimental data by computing E_1 from Equation 9.33 on the assumption that $P_0 = 0$.

The analytic solution of both our model and the Marmarou model was carried out at nine time intervals in the ICP course, i.e., at 20%, 25%, 30%, 35%, 40%, 50%, 60%, 70% and 80% of the total duration of the test. This was done in order to examine the stability of the parameters, i.e., to determine whether they were affected by the time interval at which they were calculated. This procedure yielded five values for P_0 . The mean value was used to compute E_1 at each point of time.

Hence each experimental run produced three sets of model parameters: those according to the analytic solution, those from the curve fitting procedure and those applying the Marmarou model. The extent to which the model and the experimental data agreed was evaluated from the reduced chi-square of the fit, a lower reduced chi-square value implying a better fit.

In the case of the volume-pressure test, the parameter C'_1 , comprising the parameters for CSF formation and absorption, and the parameter P_0 were computed from the pressure decay after completion of the injection. Again, two different methods of computation were used. An analytic solution applying Equations 9.38 and 9.37 was carried out as with the infusion test. Furthermore, Equation 9.35 was fitted to the ICP decay curve using a least-squares fitting procedure by applying Marquardt's iteration.

The volume-pressure parameter E_1 was subsequently calculated from Equation 9.36. In the case of constant rate CSF formation, the formation and absorption parameters F_1 and R_0 were computed from $C_1 (=C'_1/E_1)$ and Equation 9.8. C_1 and the Equations 9.6 and 9.18 yielded the parameters R_0 , R_i and F_1 for the pressure-dependent CSF formation. The Marmarou model was also applied, in which case, since $P_0 = 0$, E_1 can be calculated directly from Equation 9.36 and C'_1 can be calculated from the decay curve using Equation 9.37.

Consequently, the volume-pressure test also produced three sets of parameters. The results were again evaluated by comparing the reduced chi-square between the models and the experimental data.

Extreme and unrealistic values for P_o were sometimes obtained in the analysis by the curve fit procedure of the ICP decay curve after bolus injection. A restriction was therefore applied in the curve fit procedure with regard to the values which P_o could take. $P_o = -15$ mm Hg was chosen as the lower limit of these values and $P_o = P_b - 0.1$ mm Hg was chosen as the upper limit, since according to Equation 2.7 P_o must always be smaller than the base-line pressure.

10.3 Results

Infusion test

The steady state ICP increased linearly with the infusion rate in all the animals, as shown in Figure 63 for a single animal. This implies that the values for the CSF inflow and outflow resistance and for the CSF formation are within a close range for the various infusion rates (Fig. 63), as can be seen from the Equations 9.11 and 9.19. The mean results are presented in Table 19. It should be noted that the formation rates given for the pressure-dependent CSF formation model are those computed at the base-line ICP. This model always yielded a lower CSF formation

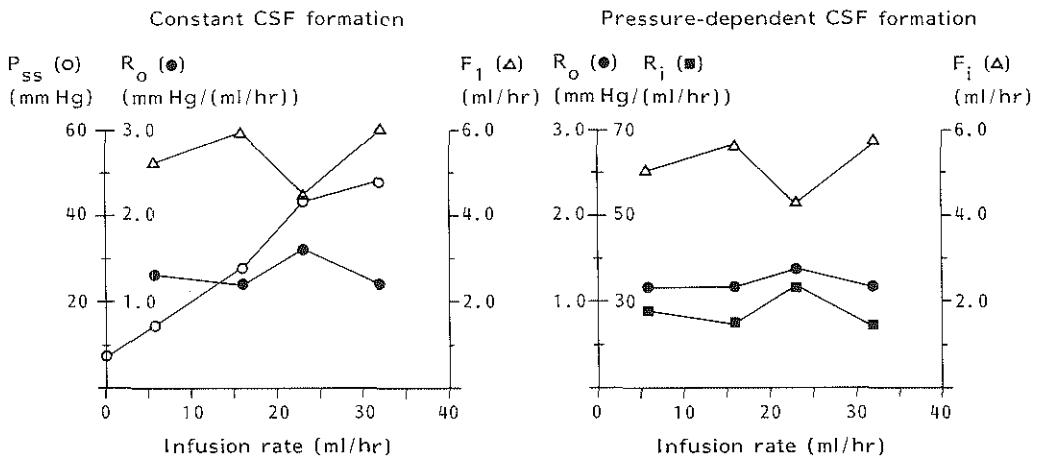


Fig. 63. Parameters of CSF formation and absorption computed for different rates of constant infusion in single animal (no. 1). Left: constant CSF formation and right: pressure-dependent CSF formation. P_{SS} = steady state ICP during infusion, R_o = outflow resistance, F_1 = formation rate, F_i = formation rate at base-line ICP, and R_i = inflow resistance.

Table 19. Parameters of CSF formation and absorption computed from constant rate infusion: formation rate for constant (F_1) and pressure-dependent formation (F_i), CSF inflow resistance (R_i), CSF outflow resistance (R_o), and C_1 . Results of constant rate formation are valid for both the authors' model and the Marmarou model.

Animal no.	Constant CSF formation				Pressure-dependent CSF formation							
	F_1 ml/hr		R_o mm Hg/(ml/hr)		F_i ml/hr		R_i mm Hg/(ml/hr)		R_o mm Hg/(ml/hr)		C_1 (ml/hr)/mm Hg	
	Mean	Range	Mean	Range	Mean	Range	Mean	Range	Mean	Range	Mean	Range
1	5.4	4.4- 6.0	1.3	1.2-1.6	5.1	4.2- 5.7	27.5	24.1-32.6	1.4	1.3-1.7	0.76	0.62-0.82
2	10.5	7.5-13.0	1.4	1.2-1.7	9.3	6.7-10.9	12.4	9.6-16.0	1.6	1.3-1.8	0.73	0.61-0.87
3	10.9	8.5-12.6	1.2	1.0-1.3	9.6	7.8-11.1	11.0	9.7-14.2	1.3	1.1-1.5	0.88	0.76-0.99
4	5.3	4.4- 7.1	1.9	0.8-3.3	4.8	4.3- 5.8	29.0	17.3-36.8	2.1	1.5-3.9	0.76	0.31-1.29
5	8.4	6.8- 9.8	2.0	1.6-2.2	7.2	6.0- 8.5	15.5	11.7-21.1	2.2	1.8-2.5	0.52	0.46-0.64
6	6.7	6.3- 7.3	1.9	1.9-1.9	5.9	5.6- 6.4	16.8	14.8-18.6	2.2	2.1-2.2	0.53	0.52-0.54
Mean	7.9		1.6		7.0		18.7		1.8		0.70	

rate and a higher outflow resistance than the constant rate formation model, but the differences were quite small.

As discussed in Chapter 9, the calculation of formation rate and outflow resistance is strongly affected by the assumption of a constant sagittal sinus pressure which is set to zero in most models. The effect of a constant, non zero sinus pressure of, for instance, 5 mm Hg is shown in Table 20. The CSF formation rate fell by more than 40% and the inflow resistance rose by over 100%. As expected, the outflow resistance did not change in the constant rate formation model and showed only minor changes in the pressure-dependent formation model. Consequently, an accurate estimate of formation rate and inflow resistance can only be obtained if the sinus pressure is monitored.

Table 20. Parameters of CSF formation and absorption computed for a sagittal sinus pressure of 5 mm Hg.

Animal no.	Constant CSF formation		Pressure-dependent CSF formation		
	F_1 ml/hr	R_o mm Hg/(ml/hr)	F_i ml/hr	R_i mm Hg/(ml/hr)	R_o mm Hg/(ml/hr)
1	1.6	1.3	1.6	90.8	1.4
2	6.8	1.4	6.3	18.5	1.5
3	6.4	1.2	6.0	19.5	1.3
4	2.2	1.9	1.9	56.5	2.1
5	5.7	2.0	5.2	21.5	2.2
6	4.0	1.9	3.7	26.9	2.0
Mean	4.5	1.6	4.1	39.0	1.8

The volume-pressure parameters, E_1 and P_o , were generally stable for the various infusion rates, except for the lowest rate of 6.0 ml/hr. The results in a single animal are shown in Figure 64 and the mean results of both the analytical and the curve fit solution are given in Table 21. The results of both methods are in close agreement, but the curve fit solution showed a better fit to the experimental data as shown by the lower reduced chi-square values. The variability of the parameters within each experimental run was also small, except for the lowest infusion rate.

The results of the Marmarou model are also given in Figure 64 and Table 21. In general, the values for E_1 were even more stable than in our model. Because of the positive values for P_o in our model (except in

Table 21. Parameters of storage capacity for the authors' model (E_1 , P_o) and the Marmarou model (E_1) computed from constant rate infusion. Goodness of fit between models and experimental data is given by reduced chi-square values.

Animal no.	Authors' model												Marmarou model			
	Analytical solution						Curve fit solution						E_1 1/ml		Chi-square mm Hg ²	
	E_1 1/ml		P_o mm Hg		Chi-square mm Hg ²		E_1 1/ml		P_o mm Hg		Chi-square mm Hg ²					
Mean	Range	Mean	Range	Mean	Range	Mean	Range	Mean	Range	Mean	Range	Mean	Range	Mean	Range	
1	4.0	3.0-5.2	3.6	0.2- 5.1	0.8	0.2-2.0	6.1	3.3-12.6	5.3	4.8- 5.8	0.5	0.2-1.5	2.7	1.9-5.0	6.8	0.4-18.1
2	2.8	1.9-4.0	9.5	6.6-12.7	0.8	0.3-1.8	3.1	2.3- 4.4	10.6	8.7-13.5	0.7	0.3-1.4	1.3	1.1-1.5	8.1	0.4-21.4
3	4.2	2.7-7.6	7.5	6.7- 8.5	0.5	0.2-0.9	3.0	2.0- 3.7	6.5	-0.7- 9.2	0.4	0.1-0.7	2.1	1.7-2.4	1.3	0.1- 2.8
4	2.7	1.3-4.9	3.3	-1.2- 8.4	0.8	0.1-1.3	1.7	1.5- 1.8	4.5	0.3- 8.7	1.1	0.8-1.3	1.7	1.4-2.1	1.1	0.1- 2.4
5	2.5	2.0-2.8	7.7	4.2- 9.5	0.7	0.1-1.2	3.4	2.7- 5.2	10.3	9.1-12.5	0.5	0.1-0.9	1.7	1.5-1.9	2.8	1.4- 4.7
6	3.3	2.8-3.6	8.1	7.6- 8.4	0.6	0.3-0.8	3.5	2.8- 4.2	8.5	7.7- 9.4	0.5	0.3-0.8	1.7	1.4-2.0	3.5	0.4- 6.3
Mean	3.3		6.6		0.7		3.5		7.6		0.6		1.9		3.9	

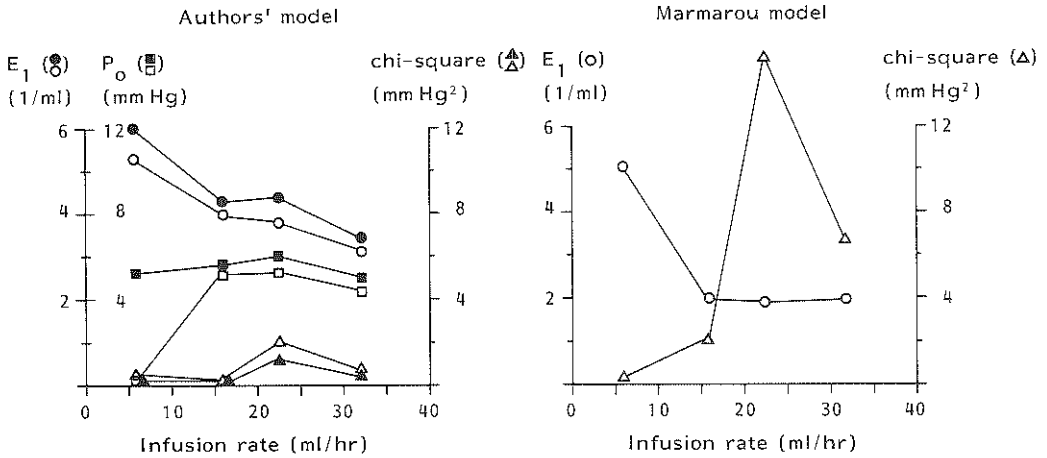


Fig. 64. Parameters of storage capacity of craniospinal system at different rates of constant infusion in single animal (no 1). Left: authors' model; data are given for both analytical (open symbols) and curve fit solution (filled symbols). Right: Marmarou model. E_1 = elastance coefficient and P_0 = constant pressure term. Reduced chi-square values between models and experimental data are shown.

a single run) the Marmarou model always yielded lower values for E_1 in agreement with Equation 9.36.

If both models are compared, two main differences can be observed. Firstly, for both the analytical and the curve fit solution, our model shows a better fit to the data than the Marmarou model; this is shown in Figure 65 and also by the lower reduced chi-square of the fit (Fig. 64 and Table 21). Secondly, the stability of the volume-pressure parameters with regard to the time intervals after which they were determined was better in our model. This is shown in Figure 66. The Marmarou model generally showed an increase in E_1 in the course of time.

Volume-pressure test

One problem with regard to the analytical solution was that P_0 , computed at the different time intervals of the decay curve, showed a very wide variability. This can best be illustrated by the example in Table 22. This table shows that P_0 was very sensitive to the choice which had to be made with regard to the end of the decay curve. Apparently, small changes in the pressures used in Equation 9.38 exert a great influence on the resulting value for P_0 . In the case of the curve fit solution this

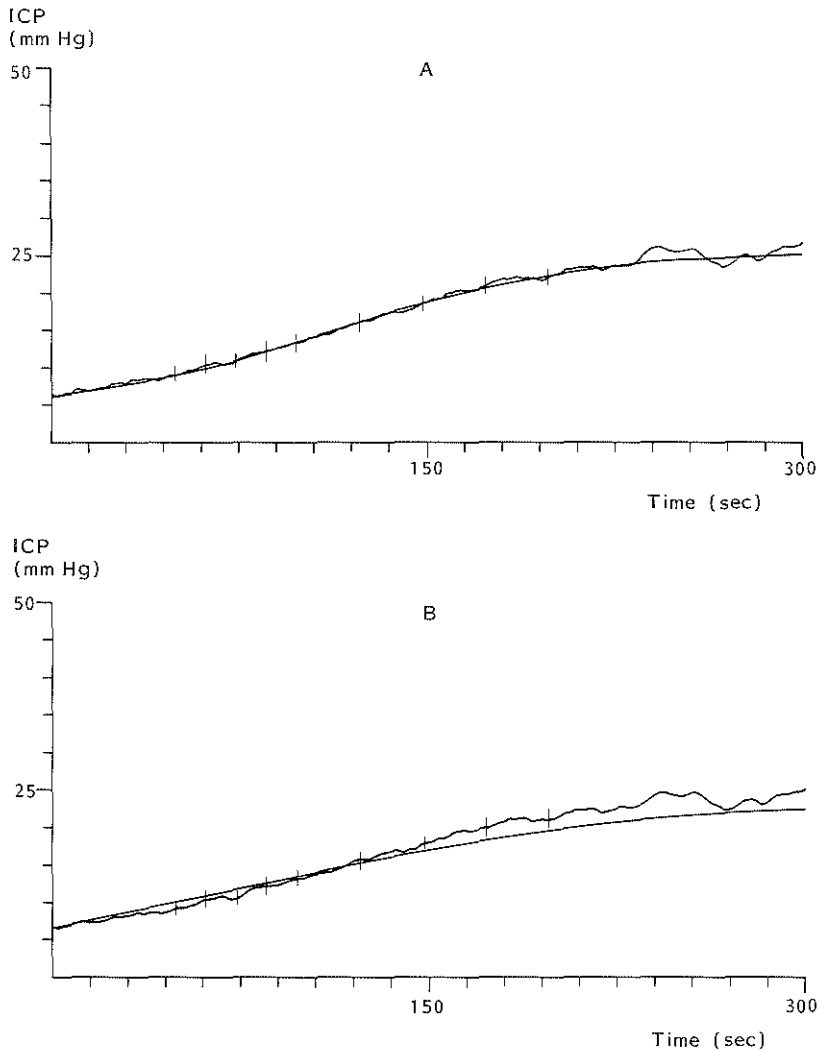


Fig. 65. Computer plot of ICP course in case of constant rate infusion of 16.2 ml/hr and fitted model (animal no. 1). A: authors' model (analytical solution), and B: Marmarou model.

sensitivity of P_o was much smaller. We therefore concluded that the analytical method did not result in reliable model parameters and these results are consequently not presented in the tables.

The mean results of P_o , C_1 and E_1 for the various volume loads are given in Table 23. They varied in each animal; the results from one animal are shown in Figure 67. With regard to the variation in P_o and C_1 for each volume load, it was always observed that this variation decreased with increasing volume loads. The variability of the parameters

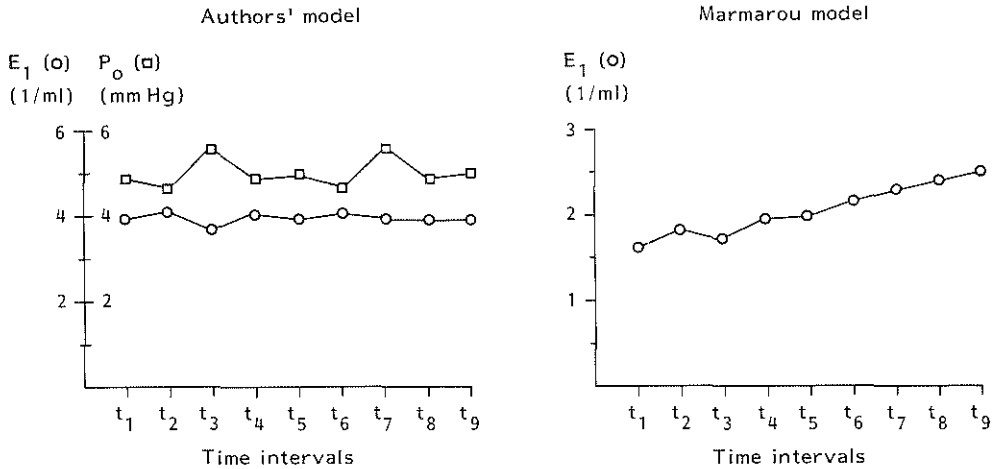


Fig. 66. Volume-pressure parameters for authors' model (left; E_1 and P_0) and Marmarou model (right; E_1) computed at different time intervals after start of infusion test. Results obtained at infusion rate of 16.2 ml/hr in a single animal (no. 1).

Table 22. Effect of three different choices with regard to length of decay curve after bolus injection on constant term P_0 . Note variation in P_0 with respect to both mean value and range in case of analytical solution.

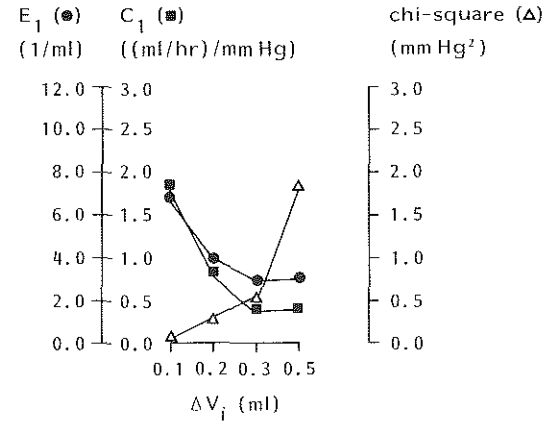
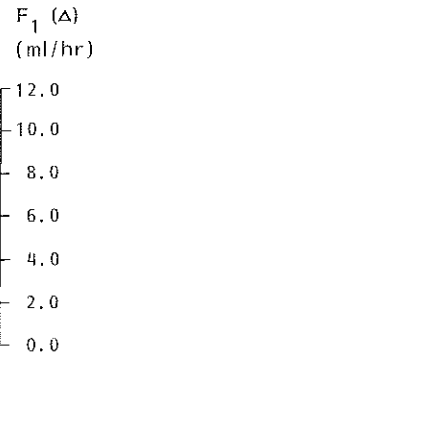
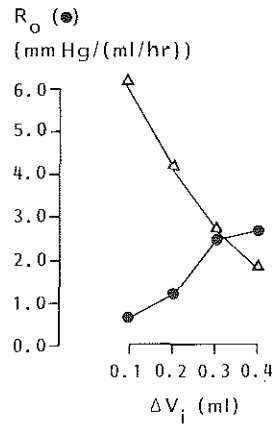
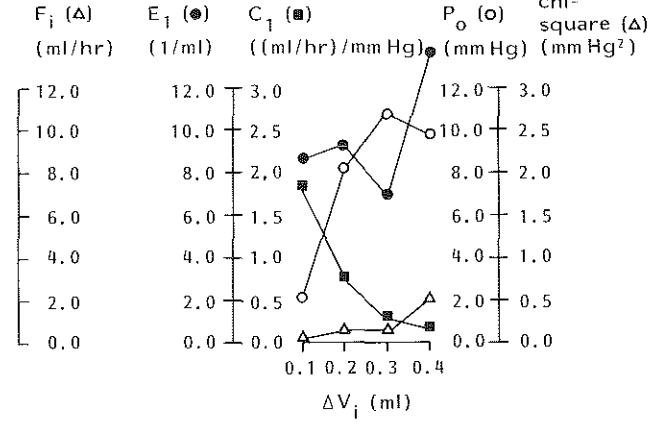
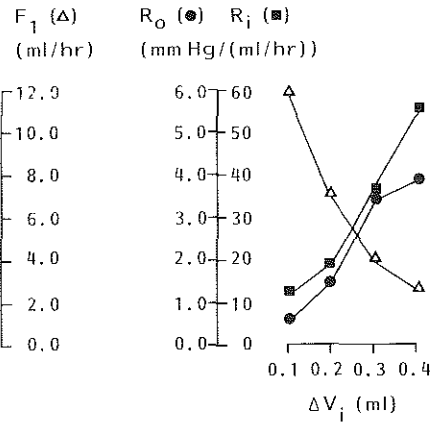
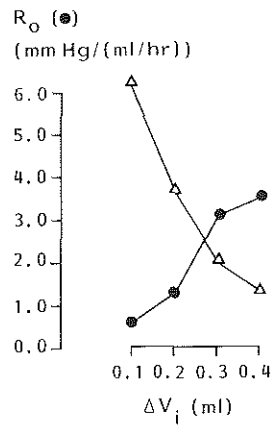
Duration test	Analytical solution		Curve fit solution	
	P_0 mm Hg		P_0 mm Hg	
sec.	Mean	Range	Mean	Range
222	10.6	-26.0 - 44.9	8.2	6.6 - 9.8
232	6.6	-91.0 - 91.0	7.9	6.2 - 9.6
242	29.3	6.3 - 87.7	7.6	5.9 - 9.3

between the various volume loads was also observed in the Marmarou model (Fig. 67; Table 23). The model including P_0 showed the better fit to the experimental data, as appears from the lower reduced chi-square of the fit. An example of the fit of both models is shown in Figure 68.

The parameters describing CSF formation and absorption are also only given for the curve fit solution and for the Marmarou model (Fig. 67; Table 24). They were computed from C_1 and the equilibrium condition before bolus injection. In both models they vary widely between the different volume loads. Since in each animal the Marmarou model yielded a larger C_1 , this model produced a higher CSF formation rate and a lower outflow resistance than our model.

Table 23. Parameters of storage capacity (E_1 , P_0) and C_1 for authors' model (curve fit solution) and the Marmarou model computed from volume-pressure test. Goodness of fit between models and experimental data is given by reduced chi-square values.

Animal no.	Curve fit solution								Marmarou model					
	E_1 1/ml		P_0 mm Hg		C_1 (ml/hr)/mm Hg		Chi-square mm Hg ²		E_1 1/ml		C_1 (ml/hr)/mm Hg		Chi-square mm Hg ²	
	Mean	Range	Mean	Range	Mean	Range	Mean	Range	Mean	Range	Mean	Range	Mean	Range
1	9.4	6.8-13.4	7.5	1.9-10.6	0.75	0.16-1.80	0.21	0.01-0.49	4.1	2.8-6.8	0.85	0.38-1.80	0.64	0.02-1.79
2	5.4	2.0- 7.9	11.9	4.8-18.1	0.57	0.40-0.86	0.17	0.05-0.51	1.7	1.3-2.7	0.65	0.38-1.00	0.23	0.05-0.57
3	6.2	4.1- 8.4	11.9	9.9-14.2	0.60	0.48-0.66	0.39	0.11-0.63	2.5	2.3-2.7	0.68	0.52-0.80	0.44	0.14-0.69
4	8.6	3.9-13.8	36.4	27.4-42.0	0.45	0.22-0.74	1.08	0.52-1.80	1.8	1.4-2.3	0.55	0.25-0.82	1.59	1.14-1.92
5	7.1	5.8- 8.2	15.4	10.3-20.4	0.69	0.50-1.00	0.19	0.10-0.26	1.9	1.2-3.0	0.81	0.66-0.99	0.25	0.12-0.33
Mean	7.3		16.6		0.61		0.41		2.4		0.71		0.63	



A

B

C

Fig. 67. Parameters of authors' model (upper diagrams) and Marmarou model (lower diagrams) for volume-pressure test with different volume loads (ΔV_i) in a single animal (no. 1). A: constant CSF formation, B: pressure-dependent CSF formation, C: volume-pressure parameters and reduced chi-square of the fit.

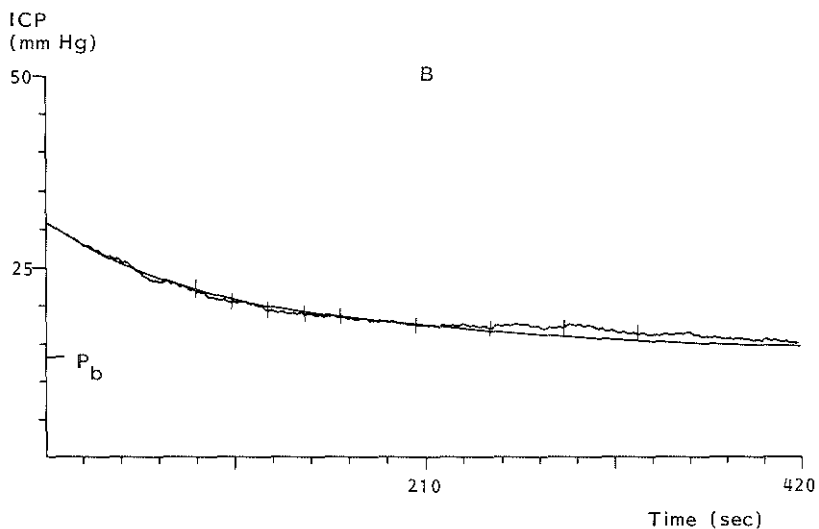
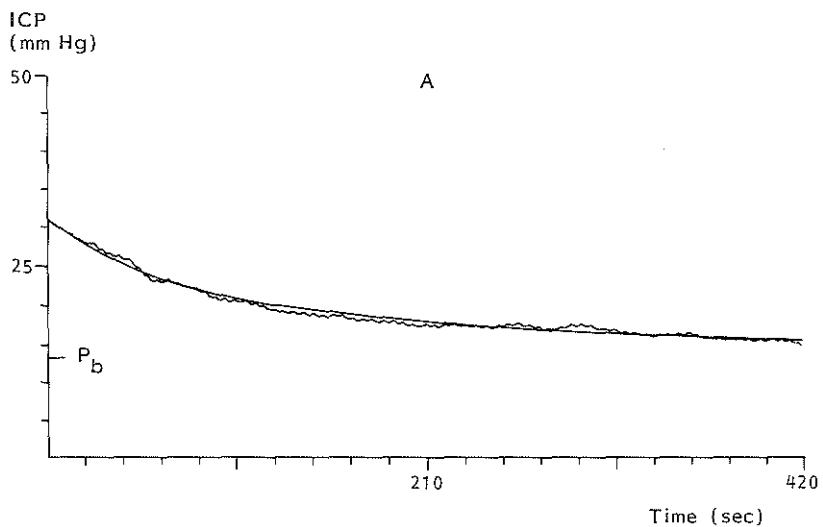


Fig. 68. Computer plot showing fits of authors' model (A) and Marmarou model (B) to ICP decay curve after bolus injection of 0.3 ml (animal no. 1).

Comparison between infusion test and volume-pressure test

Ideally, the mathematical model should yield identical parameters for both tests and under all experimental conditions. The results were therefore evaluated with regard to:

1. the difference between the parameters obtained from both test,
2. the variability of the parameters within each test for different volume disturbances, and

Table 24. Parameters of CSF formation and absorption computed from volume-pressure test: rate of constant (F_1) and of pressure-dependent (F_i) CSF formation, CSF inflow resistance (R_i), and CSF outflow resistance (R_o). Results of Marmarou model are given for constant CSF formation only.

Animal no.	Constant CSF formation								Pressure-dependent CSF formation					
	Curve fit solution				Marmarou model				Curve fit solution					
	F_1 ml/hr		R_o mm Hg/(ml/hr)		F_1 ml/hr		R_o mm Hg/(ml/hr)		F_i ml/hr		R_i mm Hg/(ml/hr)		R_o mm Hg/(ml/hr)	
	Mean	Range	Mean	Range	Mean	Range	Mean	Range	Mean	Range	Mean	Range	Mean	Range
1	6.4	1.5-12.7	2.9	0.5-6.3	7.5	2.6-11.8	1.7	0.6-2.6	6.0	1.5-12.1	41.5	11.8-96.6	3.1	0.6-6.7
2	10.1	6.5-18.1	1.9	1.2-2.5	11.8	6.2-21.7	1.7	1.0-2.6	8.6	5.6-14.9	13.4	6.6-17.7	2.2	1.4-2.9
3	10.5	8.2-12.3	1.7	1.5-2.1	12.0	8.9-15.5	1.5	1.2-1.9	8.9	7.0-10.4	11.7	10.1-14.7	2.0	1.8-2.4
4	19.4	9.3-32.1	2.8	1.4-4.5	24.0	10.7-35.7	2.3	1.2-4.0	13.0	6.0-21.8	8.3	4.2-12.9	4.3	2.0-7.0
5	12.0	8.7-14.3	1.6	1.0-2.0	14.4	11.6-17.3	1.3	1.0-1.5	10.3	7.5-12.8	11.2	9.4-14.4	1.8	1.1-2.3
Mean	11.7		2.2		13.9		1.7		9.4		17.2		2.7	

3. the variability of the parameters within each experimental run. The infusion test always yielded lower values for the elastance coefficient in our model. This is because of the lower P_o found in this test, which automatically results in a lower E_1 . The mean results of the infusion tests showed lower values for CSF formation and outflow resistance and a higher value for the inflow resistance, but the differences between these results and those of the volume-pressure test were not statistically significant.

The parameters of the volume-pressure test varied more between the different volume loads in most animals than was the case in the infusion test. However, the variability of P_o within each volume load in the volume-pressure test was particularly striking, though both the variation in P_o and in C_1 decreased with larger volume loads.

In order to find an explanation for this, we compared the pressure responses caused by the various volume disturbances in both the infusion and the volume-pressure test. As can be seen in Table 25, the infusion test produced much larger pressure responses than the volume-pressure test, except at the lowest rate of 6.0 ml/hr. In this respect, it is of interest to note that, as far as the infusion test is concerned, the lowest rate showed the largest variation in P_o ; this variation was in the same order as we found in the volume-pressure test. We therefore concluded that the assessment of reliable model parameters from the volume-pressure test requires larger volume loads than were used in the present study. The explanation is probably that, with larger volume loads, the computation of the parameters is less disturbed by the contamination of the decay curve with spontaneous ICP fluctuations resulting from changes in CBV.

Table 25. Pressure response for infusion test ($P_{ss} - P_b$) at different infusion rates (F_{in}) and for volume-pressure test ($P_p - P_b$) at different volume loads (ΔV_i).

Infusion test		Volume-pressure test	
F_{in} ml/hr	$P_{ss} - P_b$ mm Hg	ΔV_i ml	$P_p - P_b$ mm Hg
6.0	8.8	0.1	6.6
16.2	25.6	0.2	10.4
22.7	35.4	0.3	15.0
31.8	41.8	0.4	17.3

Comparing the results from the two tests as far as the Marmarou model is concerned, the volume-pressure test produced higher values for CSF formation rate and elastance coefficient in all animals, and for CSF outflow resistance in all but one animal. This model also showed a wide variability of the parameters between the various volume loads in the case of the volume-pressure test. The results obtained at different time intervals in the experimental run also varied widely, as was seen in our model.

10.4 Discussion

The purpose of this series of experiments was to test the stability of the parameters of the CSF circulation model under various conditions. The clinical motive was to examine whether all model parameters could be accurately assessed by a single test. The experimental data were also analyzed according to the frequently used Marmarou model, since our model differs from the former only in the description of the storage capacities of the craniospinal system.

Up till now, most studies have focused on a single aspect of the CSF dynamics, in particular the outflow resistance or a volume-pressure parameter such as the elastance coefficient or the PVI. Consequently, reference values for these parameters can easily be obtained from the literature. With respect to CSF formation and inflow resistance, a comparison can be made with results from ventriculo-lumbar and ventriculo-cisternal perfusion experiments. The last model parameter, P_o , can only be discussed in the light of the results described in the previous chapters.

In this discussion, the subdivisions of the circulation model will be dealt with separately in the following sequence: CSF formation, CSF absorption and storage capacities of the craniospinal system. Special attention will be given to the effect of the type of test (infusion and bolus injection) and the volume load per unit of time on the model parameters. Next the differences between the authors' model and that of Marmarou will be discussed. The chapter will conclude with comments on the clinical significance of the model parameters.

CSF formation

The question as to whether the CSF formation is constant or pressure-dependent in nature can only be solved by direct measurement of the formation rate at various levels of ICP. According to the literature it seems reasonable to assume that the formation rate falls slightly with rising ICP (Calhoun et al., 1967; Sahar et al., 1970; Hochwald and Sahar, 1971). On the other hand, the introduction of an additional model parameter - the inflow resistance - may complicate the evaluation of experimental results. Moreover, the exact nature of the relationship between the pressure drop over the choroid plexus and the formation rate has not yet been definitively established, as the perfusion techniques yield only a few data in a single animal. Therefore, the question as to which model should be preferred remains as yet unanswered.

The mean formation rate found in this study is considerably higher for both tests than the rates reported in the literature, which vary from 2.0 to 3.4 ml/hr in the dog (Frazier and Peet, 1915; Bering, 1958; Bering and Sato, 1963; Oppelt et al., 1963; Cserr, 1965; Weiss and Nulsen, 1970; Sahar, 1972; Carey and Vela, 1974). The difference may be explained by the assumption in the present model of a zero sinus pressure. In the case of the infusion test, the assumption of a sinus pressure of 5 mm Hg caused a fall in formation rate by more than 40%, resulting in 4.5 ml/hr for constant rate formation and 4.1 ml/hr for pressure-dependent formation. The remaining difference may be due to the larger body weights of the animals in the present series.

Values for the inflow resistance could only be derived from the study by Carey and Vela (1974), yielding approximately 45 mm Hg/(ml/hr). The values found in our study were usually lower but, again, at a sinus pressure of 5 mm Hg the results are more similar. Since the sinus pressure is not usually measured and may even increase with rising ICP, it may thus be concluded that the CSF formation rate and inflow resistance cannot be accurately assessed from model equations. However, the assumption of a sinus pressure of 5 mm Hg may give a reasonable approximation of both parameters.

An alternative method for the assessment of CSF formation was applied by Marmarou (1973), who computed the formation rate by rapid

withdrawal of CSF. In this case it is hypothesized that when the ICP falls below a given threshold pressure, the resistance to absorption is infinite and no absorption takes place. The threshold pressure is considered to be the sinus pressure, assuming that CSF is only absorbed if a positive pressure difference exists between the CSF space and the dural sinuses. After E_1 has been calculated from the pressure response, the CSF formation rate can be obtained from the pressure course after withdrawal. However, this technique yields reliable results only if the pressure falls considerably below the sinus pressure, if the sinus pressure remains constant during the procedure and if the formation rate is independent of ICP changes. Furthermore, rapid withdrawal of fluid is somewhat more difficult to achieve than rapid injection and has, therefore, at least the same variability in response as described for the bolus injection technique. Finally, it is questionable whether the mono-exponential volume-pressure model still holds true in this low ICP range (Löfgren et al., 1973).

Still another approach is based on the constant pressure withdrawal technique. The CSF formation rate is here determined by removing CSF at a constant pressure below the sinus pressure and awaiting a constant flow. Since there is no absorption of CSF at this pressure level, the outflow rate of the pump will be equal to the formation rate. In this case the inflow resistance can also be calculated, as the formation rate is determined at a known, constant pressure level.

In spite of their limitations, these alternative methods may result in a more accurate assessment of CSF formation rate and outflow resistance, in which case we would favour the constant pressure withdrawal technique.

CSF absorption

With respect to the absorption model, it is generally accepted that the bulk outflow of CSF is linearly related to the pressure gradient between the subarachnoid space and the dural sinuses. The absorption is therefore characterized by the resistance to outflow.

The values for R_o found in this study are within the range for dogs reported in the literature: 0.71-2.75 mm Hg/(ml/hr) (Bering and Sato, 1963; Oppelt et al., 1964; Benabid et al., 1975; Johnston et al., 1975; Sklar et al., 1978). This range is rather wide, perhaps because of the

differences both in the measuring techniques used and in the body weights of the animals.

In the infusion test, a smaller outflow resistance was found in most animals than in the volume-pressure test. This is in contradiction with Marmarou (1973), who reported similar results for both tests in the cat. However, Sullivan et al. (1979) and Shapiro et al. (1983), in the cat, and Børgesen et al. (1979), in man, found lower values of R_o calculated from bolus injection. There is no generally accepted explanation for these contradictory findings. However, the difference is probably not attributable to physiological processes, but is perhaps due instead to a difference in methodology. R_o calculated from constant rate infusion depends only on two steady state pressure levels and is the result of a simple and straightforward procedure. The computation of R_o from bolus injection, on the other hand, depends on an accurate assessment of the volume-pressure parameters, which is subject to the problems associated with the analysis of the decay curve, as discussed in the previous section. An additional problem is the variability of the pressure response after bolus injection (see Chapter 4). It was argued in Chapter 9 that an increase in sinus pressure concomitantly with rising ICP may result in an overestimation of R_o . However, this would affect both methods equally and cannot therefore explain the results found here.

Many authors have described a linear relationship between steady state pressure and infusion rate, implying a constant R_o (Cutler et al., 1968; Katzman and Hussey, 1970; Ekstedt, 1977; Børgesen et al., 1978; Sklar et al., 1978; Sullivan et al., 1979). The results of the present study are in agreement with these reports. Some authors, however, reported a decrease in R_o with higher infusion rates (Love and Leslie, 1980; Sullivan et al., 1982; Shapiro et al., 1983). They suggested that with rising ICP more and more absorption channels were activated and that, consequently, the maximal absorptive capacity (low outflow resistance) was reached at high ICP. However, these results are open to criticism in so far as it is difficult in animal preparations to completely rule out the leakage of CSF from the craniospinal system under the condition of extremely elevated ICP. This is supported by the conclusion of Sullivan et al. (1982) that their data did not provide justification for preferring either a linear (constant R_o) or a non-linear (decreasing R_o)

absorption model. In the light of these considerations we still consider a linear model to be a valid approximation of CSF absorption.

Storage capacities of the craniospinal system

The storage capacities of the craniospinal system are derived from the volume-pressure relationship. The discussion as to the exact nature of this relationship was given in Chapter 8. Our contribution consisted of the extension of the exponential volume-pressure model by a constant pressure term P_o (see Chapter 2.4).

As far as the infusion test is concerned, the mean results of E_1 and P_o computed by the analytical and the curve fit solution are in agreement. However, they differ significantly from the results which were obtained in Chapter 5 from the VPR-ICP relationship: 3.3 and 3.5 l/ml versus 2.0 l/ml. The difference can be wholly attributed to the difference in P_o between the two series since, according to Equation 2.7, a larger P_o will result in a higher value for E_1 . Consequently, the discussion should be focused on the cause of the difference in P_o : 6.6 and 7.6 mm Hg versus -3.5 mm Hg.

It was explained in Chapter 5 that the leveling-off phenomenon of the VPR, before it became constant, led to an underestimation of the slope of the VPR-ICP relationship. As a result, the intercept of the relationship with the pressure axis, which is equal to P_o , fell in the negative ICP range. It seems reasonable therefore to assume that P_o , and consequently also E_1 , were underestimated in Chapter 5. The P_o in Chapter 5 obtained from the CSFPP-ICP relationship was 6.3 mm Hg, which is much more consistent with the values found here. On the other hand, it was argued that the slope of that relationship might have been *overestimated*, resulting in an overestimation of P_o . Nevertheless, the difference between the results of the present and the previous series may ultimately turn out to be small.

The results obtained from the volume-pressure test are more of a problem. The analytical solution of our model yielded such unstable values for P_o within each test that the results had to be rejected. We suggested in the previous section that this may be due to the fact that the volumes used were too small.

The value for P_o resulting from the curve fit procedure was

considerably higher than that obtained by means of the infusion test: 16.6 mm Hg versus 7.6 mm Hg. However, this difference becomes insignificant if it is considered that the reduced chi-square of our model is not very different from that of the Marmarou model which assumes that P_o equals zero. This implies that P_o may vary between 0 and 16.6 mm Hg without having a significant effect on the fit of the experimental data. Apparently we are dealing with a parameter optimization problem. This hypothesis was checked by computing the reduced chi-square for different values of P_o and C_1 . It was found that the reduced chi-square decreased gradually over the pressure range of 0-16 mm Hg.

It may thus be concluded that, as far as the volume-pressure parameters are concerned, the results of the infusion experiments are more consistent with the prerequisites of the circulation model, i.e., constant model parameters, than are the results of the volume-pressure test.

Comparison with the Marmarou model

The CSF circulation model under consideration and the Marmarou model are based on the same assumptions with respect to CSF formation and absorption. The only difference between the models is in the description of the storage capacities. Our model is based on two volume-pressure parameters (E_1 and P_o), whereas that of Marmarou has only one parameter (E_1).

Due to the positive values for P_o in our model, the Marmarou model resulted in lower values for E_1 : 1.9 l/ml and 2.4 l/ml in the case of the infusion and volume-pressure test respectively. The Marmarou model produced a higher CSF formation rate and a slightly lower outflow resistance in the case of the volume-pressure test, as did our model. As in our model, the formation rate varied considerably between the various volume loads in the volume-pressure test.

Since in the case of the infusion test the volume-pressure relationship is not involved in the computation of the parameters of CSF formation and absorption, the results of our model are identical to those of Marmarou's. With regard to the storage capacity two differences could be observed. Firstly, in the Marmarou model, E_1 increased with the length

of the time interval after the start of the infusion, whereas in our model the parameters were independent of the time at which they were determined. Secondly, our model showed a considerably better fit to the experimental data than the Marmarou model.

A disadvantage of our model is that the equations for the computation of the volume-pressure parameters are more complex. However, since both methods of computation, analytical and curve fit solution, produced comparable results, the parameters can still be computed analytically at the bedside using a simple calculator.

The results of the volume-pressure test are less in favour of our model. In most cases the analytical computation of the parameters yielded highly unstable results. Furthermore, the curve fit solution resulted in values for P_0 and E_1 which were considerably larger than those obtained from the infusion test or those reported in Chapters 5 and 6. In the Marmarou model the values of E_1 were much more consistent with those found in the infusion test. However, in both models the parameters varied with the volume of the injections, although the variation was less in the Marmarou model than in ours.

The parameters of CSF formation and absorption are computed from C_1 , which in turn is calculated from the pressure decay curve, and the equilibrium condition before injection. Since in our model C_1 is dependent on P_0 , it may be expected that the variability of P_0 is reflected in C_1 and therefore also in the CSF formation and absorption parameters. In the Marmarou model, however, in which P_0 is assumed to be equal to zero, the parameters showed the same variability. The instability of the parameters in our model is thus not caused by the introduction of P_0 .

It may be concluded that our model shows a better fit to the data in the case of the infusion test and, to a lesser extent, also in the case of the volume-pressure test. Our model also fulfils the requirements of the circulation model better, i.e., constant parameters for different infusion rates. On the other hand, as far as the analytical method is concerned, the extra parameter is the main cause of unstable results in the bolus injection test. Leaving aside the volume-pressure test, with respect to which both models perform rather poorly, we would therefore favour our model, particularly as the experiments described in Chapters 5 and 6 have yielded realistic values for P_0 . Tans and Poortvliet (1982),

comparing various volume-pressure models in a clinical study, also found that the model with a constant term fitted the data best. However, a physiological basis of P_o is still lacking. Theoretical as well as practical considerations for the introduction of the constant term were given in Chapter 2.4. It was then suggested that P_o may be related to the factors which determine the equilibrium conditions of the craniospinal system. Considering the model equations which describe these equilibrium conditions and considering the values taken by P_o , the factor most likely to be involved is the dural sinus pressure.

Clinical significance

CSF circulation models have been developed to gain insight into the physiological variables governing the circulation of CSF. The clinical significance of volume-pressure parameters was discussed extensively in Chapter 8. The following discussion will therefore focus on the compensatory capacities of the craniospinal system in which the CSF plays a major role. As discussed in Chapter 9, the compensatory capacities of the system are determined by the quantity of CSF available, the patency of the CSF pathways and the parameters of CSF formation and absorption.

The CSF outflow resistance is usually regarded as the main parameter of the compensatory capacity, a low outflow resistance indicating a large capacity and vice versa. Sometimes the inverse parameter, conductance, is used. Up to now, this parameter has been applied mainly in the selection of patients with various types of hydrocephalus who are to be considered for a CSF shunting procedure. It was found that if the outflow resistance was above a critical level, the vast majority (over 90%) of patients improved after shunting. A review of the clinical studies reported in the literature shows this critical level to be remarkably constant: Martins (1973): 13.2, Gjerris et al. (1980): 13.3, Lamas et al. (1980): 14.4, Costabile et al. (1983): 12.3, and Tans and Poortvliet (1983): 13.0 mm Hg/(ml/hr). The infusion rates used in these studies varied between 45 and 120 ml/hr.

In the case of hydrocephalus it is the CSF volume itself which acts as a space-consuming lesion and the problem of compensation is therefore not related to the available volume, but merely to the obstruction of the circulation and outflow pathways. As discussed in Chapter 9, an obstruction in the flow of CSF from the site of formation to the site of

absorption will manifest itself, in the present model, by an increase in outflow resistance.

To the best of our knowledge no studies exist in which the CSF outflow has been systematically studied in the presence of processes of a space-occupying nature other than hydrocephalus, such as traumatic mass lesions or brain tumours. In the early phase of their development volume compensation will depend on the amount of CSF available. It is common clinical experience that elderly patients with an enlarged CSF space due to cerebral atrophy may tolerate large masses without significant elevation of the ICP. However, as soon as these processes start to encroach on the CSF pathways and thereby interfere with the free flow of CSF, the ICP will rise. Evidence was presented in Chapter 2.6 that, even at the advanced stage of intracranial hypertension, volume compensation by absorption of CSF still takes place. This seems to support the hypothesis that intracranial hypertension always implies impairment of CSF circulation and/or absorption (van Crevel, 1979). Measurement of the outflow resistance under these circumstances would make it possible to assess the severity of the CSF circulatory disturbance and thereby give a clue as to the reserve compensatory capacity. This would finally give the clinician the kind of information that volume-pressure parameters cannot provide.

The role of CSF formation in the process of spatial compensation is usually not considered. However, from the results of the pressure-dependent formation model it can be inferred that CSF production falls by more than 30% when the ICP is raised to 50 mm Hg.

Which test is preferable from a clinical point of view? The ideal test should be safe and simple, yield stable and reliable parameters and should require no cooperation from the patient. The infusion method, which is the better method from a mathematical viewpoint, is technically more complicated and time consuming and calls on the cooperation of the patient. It is therefore not easily repeatable. Depending on the intracranial pathology, either the lumbar or the ventricular route will have to be chosen. Furthermore, since large volumes are infused, the ICP and the clinical condition of the patient must be carefully monitored. This applies in particular to patients with already elevated ICP.

The bolus injection method can be easily used in patients whose ICP is recorded through a ventricular catheter. Unfortunately, its results are less reliable. Restlessness of the patient may further complicate the analysis of the ICP decay curve. The pressure response to bolus injection may also vary, as was shown in the clinical study described in Chapter 4. It remains to be seen, however, to what extent the results can be improved by using larger volumes, although the problem with larger volumes is that they may provoke vasodilatation. In order to improve the reliability of the test-results, it may therefore be advisable to carry out a number of tests and take the mean results.

In conclusion, there is as yet no single test available which fulfils all the requirements, from both a clinical and a mathematical viewpoint, for reliable assessment of the parameters of craniospinal dynamics. The most suitable test has to be chosen on each occasion according to clinical needs. If one-time assessment is required, as in the diagnosis of normal pressure hydrocephalus for instance, we consider that the infusion test is most suitable. The safest method is probably the constant pressure infusion test mentioned earlier (Davson et al., 1970; Ekstedt, 1975), as the ICP will never rise above a level fixed in advance. However, this test requires more sophisticated equipment and it must still be proven that the test produces reliable results for all model parameters. If, on the other hand, the parameters have to be assessed repeatedly during ICP monitoring, bolus injection is the obvious method to choose.

Conclusions

1. The constant rate infusion test yielded model parameters which were independent of the rate of volume disturbance.
2. With respect to the infusion test, the authors' model yielded parameters which were independent of the time interval at which they were determined. This was not true of the Marmarou model.
3. With respect to the infusion test, the authors' model showed a better fit to the experimental data than that of Marmarou.
4. With respect to the infusion test, the results of the analytical solution were in agreement with those of the curve fit solution.

5. With respect to the volume-pressure test, the analytical solution failed to produce reliable results.
6. The parameters of both models under investigation showed in every respect a large variability in the case of the volume-pressure test.

CONCLUDING REMARKS AND RECOMMENDATIONS FOR FURTHER RESEARCH

The aim of this study was originally to investigate whether the CSF pulse pressure could be used as a measure of craniospinal elastance. We argued that the pulse pressure is not only dependent on the elastance, but also on the pulsatile change in CBV. Since this cannot be measured in clinical patients, an accurate assessment of the volume-pressure relationships always requires volume loading of the CSF compartment, either by bolus injection or by infusion.

Hence we still prefer recording of the ventricular fluid pressure to recording of the epidural pressure as a method for monitoring ICP in clinical patients, particularly as volume loading also yields the other parameters of CSF dynamics. Of these, the resistance to outflow of CSF is especially significant, since this is an important parameter of the craniospinal spatial compensatory capacity. It has been shown in this study that the assessment of this capacity is more valuable from a clinical point of view than the assessment of the elastance. The significance of the information derived from volume disturbance may thus outweigh the disadvantages associated with the invasive nature of ICP measurement in the CSF space.

This does not mean that the CSF pulse pressure has become irrelevant. Once the volume-pressure relationship has been established, the pulse pressure can be used to monitor changes in the relationship. This is possible because the results of this study have quantified the effect of various physiological variables on the pulsatile change in CBV; the invasive volume loading tests can thus be applied more rationally. Moreover, the pulse pressure may prove to be a useful parameter of cerebral vasomotor tone.

Scientific research not only provides answers to questions but also

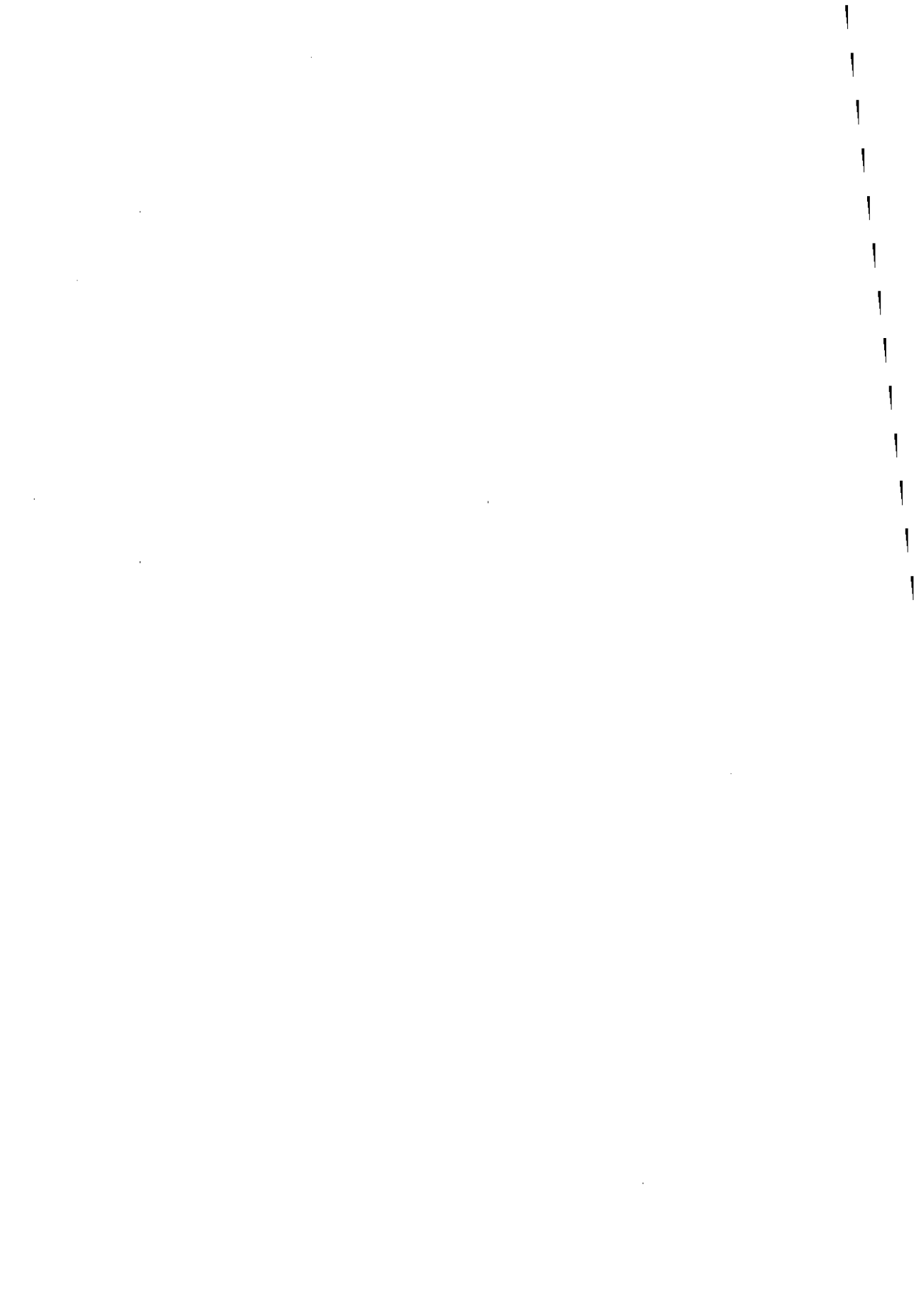
raises new questions. This thesis is no exception to this rule. We should therefore like to make some suggestions for further investigations which might solve some of the remaining problems.

1. The volume-pressure model developed here is differentiated from other volume-pressure models by the constant term P_0 . The physiological meaning of this term is not yet clear. It was argued that P_0 may be related to those factors that determine the normal resting ICP, possibly the dural sinus pressure. This can be verified by examining the volume-pressure relationships in experimental animals at various levels of the sinus pressure produced, for example, by altering the central venous pressure.
2. The effect of changes in PaCO_2 on the pulsatile change in CBV could not be entirely explained by changes in the cerebral arterial inflow profile. The hypothesis that this effect is mainly due to changes occurring at the venous side of the cerebral vascular bed needs to be verified by direct measurement of the venous flow profile.
3. Clinical studies should be initiated on the basis of the results of this study to examine further both the volume-pressure relationship and the CSFPP-ICP relationship. The feasibility of monitoring craniospinal elastance by means of the CSF pulse pressure should be investigated in patients subjected to continuous ICP recording as part of their management. Furthermore, the CSFPP-ICP relationship should be examined in selected groups of patients with identical pathology to establish the normal and pathological ranges of this relationship.
4. If the pulsatile change in CBV could be assessed in clinical patients by more direct measurement, preferably on a continuous basis, this would be most useful. The development of such a method deserves particular attention.
5. The clinical value of the assessment of craniospinal compensatory capacities should be examined by measuring CSF outflow resistance under various clinical conditions.

6. Since bolus injection is the simplest method of acquiring the parameters of the CSF circulation model, it would be worth investigating whether one could produce more reliable and stable results by using larger volumes than were used in this study.

7. Both the influence of the dural sinus pressure on the model parameters and the validity of the ICP-dependent CSF formation model could be studied further, by comparing, in the same animal preparation, the direct measurements of CSF formation and outflow resistance with the results calculated from model equations.

APPENDICES



APPENDIX 1

FREQUENCY ANALYSIS OF THE ICP MEASURING SYSTEM

Introduction

An accurate measurement of the dynamic component of ICP depends on the frequency response of the measuring system. The measuring system used in the present studies consisted of a pressure transducer, a distensible fluid filled manometer line and a needle. In the animal experiments the needle was inserted directly into the lateral ventricle. In the patient study the needle was percutaneously inserted into the Rickham reservoir (Rickham and Penn, 1965) of a ventricular catheter.

It is obviously important that pressure recordings should be obtained with as little distortion as possible. One problem in this respect is that the frequency response of the measuring system is often not known. Another problem concerns the enclosure of small air-bubbles in the system, which seriously affects the frequency characteristics.

Methods

Theoretically, a catheter-manometer system can be simply approximated by a second order system (Vierhout, 1966; Wesseling and Beneken, 1970). The transfer function of the systems used was measured by means of a fluid filled pressure chamber (Millar Instruments, flat frequency response up to 200 Hz). The frequency of the pressure pulse generated inside the pressure chamber was automatically shifted from 1 to 100 Hz. The amplitude of the pulse was measured and the transfer ratio (outgoing pulse amplitude divided by ingoing pulse amplitude) was plotted against the logarithm of the frequency.

Several types of needle to manometer systems were tested, containing either a 21G butterfly needle (Abbott; internal radius: 0.045 cm) inserted into the Rickham reservoir of a ventricular catheter, as used in the clinical situation, or a ventricular needle of the type used in the laboratory (internal radius: 0.075 cm). Manometer lines (internal radius: 0.075 cm) of varying length up to 100 cm were used. The pressure transducers used were Statham P37 and Hewlett Packard 1280.

Results

The amplitude frequency response of these systems was generally flat up to 15-20 Hz with a resonance frequency of about 50 Hz. This implies that the 8th to 10th harmonic of the basic frequency of the CSF pulse, i.e., the heart rate, is not distorted by the measuring system. This result guarantees an accurate measurement of the CSF pulse amplitude. Typical examples of transfer functions of the butterfly and ventricular needle systems are shown in Figures A.1 and A.2. The deterioration in the frequency response when air-bubbles were present inside the system is shown in Figure A.3. The resonance frequency decreased with increasing length of the manometer lines, but this effect was small compared to the effect of air-bubbles in the system.

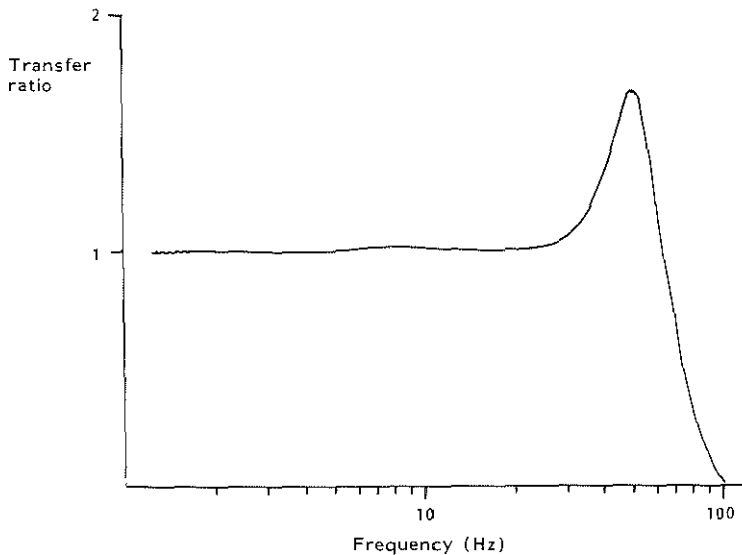


Fig. A.1. Frequency response of ICP measuring system used in clinical study, consisting of ventricular catheter, Rickham reservoir, 21G butterfly needle, manometer line (length: 60 cm, internal width: 0.15 cm), and pressure transducer (HP 1280). Note flat response up to 20 Hz.

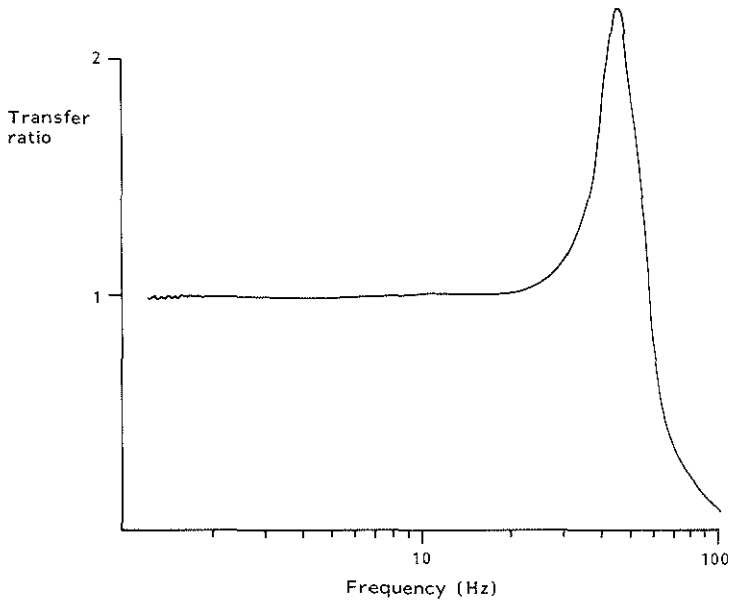


Fig. A.2. Frequency response of ICP measuring system used in experimental studies, consisting of ventricular needle (internal width: 0.15 cm), manometer line (length: 100 cm, internal width: 0.15 cm), and pressure transducer (HP 1280). Response is flat up to 20 Hz.

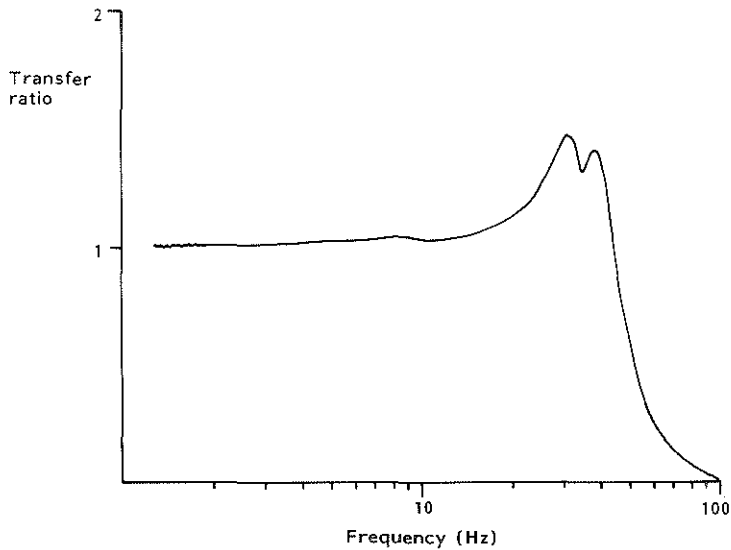


Fig. A.3. Effect of small air-bubble in the measuring system of Figure A.2 on its frequency response. Response is flat up to 10 Hz only and resonance frequency is decreased.

APPENDIX 2

RELATIONSHIP BETWEEN CSF PULSE PRESSURE AND ICP: COMPARISON BETWEEN PLOTTING PULSE PRESSURE AGAINST MEAN ICP AND AGAINST DIASTOLIC ICP

Both CSF pulse pressure and VPR are pressure responses to increments in craniospinal volume. Consequently, an analogy between the CSFPP-ICP and the VPR-ICP relationships will only exist if both pressure responses are compared with corresponding base-line pressures. However, both in the computer analysis described in Chapter 4 and in the analysis of the experimental data, CSF pulse pressure was always plotted against mean ICP, whereas VPR was plotted against resting ICP prior to volume loading. In this Appendix the effect of plotting CSF pulse pressure against mean ICP instead of against diastolic ICP on the slope of the relationship will be assessed.

The relationship between pulse pressure and ICP is given by Equation 3.1:

$$\text{CSFPP} = (P - P_o) (e^{E_1 \Delta V_b} - 1). \quad (\text{A2.1})$$

Since we have plotted the pulse pressure against mean ICP the relationship may be rewritten as:

$$\text{CSFPP} = A_1 P_m - A_2, \quad (\text{A2.2})$$

where: $A_1 = e^{E_1 \Delta V_b} - 1,$

$$A_2 = P_o (e^{E_1 \Delta V_b} - 1), \text{ and}$$

P_m = mean pulsatile ICP.

A_1 and A_2 are constant so long as E_1 , ΔV_b and P_o are constant.

Using the usual, practical calculation of mean pulsatile ICP from diastolic pressure plus one third of the pulse pressure:

$$P_m = P_{diast} + 1/3 \text{ CSFPP}, \quad (\text{A2.3})$$

Equation A2.2 can be rewritten as:

$$\text{CSFPP} = A_1(P_{diast} + 1/3 \text{ CSFPP}) - A_2, \quad (\text{A2.4})$$

or:

$$\text{CSFPP} = \frac{3A_1}{3-A_1} P_{diast} - \frac{3A_2}{3-A_1}. \quad (\text{A2.5})$$

Consequently, the slope of the CSFPP-ICP relationship changes from A_1 to $3A_1/(3-A_1)$, if the diastolic pressure is used as the reference pressure instead of P_m . It can thus be calculated that the mean slope value of 0.40 ($=A_1$) found in the clinical study (Table 3) would have been 0.46, if the pulse pressure had been plotted against diastolic ICP, implying an increase of 15%. This mathematically derived value accords remarkably well with the difference of 16% actually found by Godin et al. (1980) who compared both types of relationship in a group of clinical patients. The effect on the much lower slope values of the animal studies (Chapters 5 and 6) is less significant. From a mean slope of 0.110 (Table 9) a value of 0.114 can be derived for the slope of CSF pulse pressure versus diastolic ICP, i.e., an increase of less than 4%.

APPENDIX 3

RELATIONSHIP BETWEEN VOLUME AND PRESSURE WITHIN A CLOSED SPHERE

In this Appendix the volume-pressure relationship of the craniospinal system is described by comparing the system to a closed sphere to which the laws of Laplace and Hooke can be applied.

The relationship between the stress in the wall and the pressure inside the sphere is given by:

$$\sigma 2\pi R d = \pi R^2 P, \quad (\text{Laplace})$$

where: σ = stress,

R = radius,

d = thickness of the wall, and

P = pressure,

or:
$$\sigma = \frac{PR}{2d} . \quad (\text{A3.1})$$

When its volume is loaded with an incremental volume (ΔV), the wall of the sphere will be stretched. Strain is defined as:

$$\epsilon = \frac{\ell - \ell_0}{\ell_0},$$

where: ℓ_0 = original length, and

ℓ = length after stretching.

For the wall of a sphere this equation can be written as:

$$\epsilon = \left(\frac{V}{V_0} \right)^{1/3} - 1 , \quad (\text{A3.2})$$

where: V_0 = original volume, and

V = volume after volume loading = $V_0 + \Delta V$.

The relationship between the stress and strain of the wall is given by Hooke's law:

$$\sigma = E \varepsilon , \quad (A3.3)$$

with: E = modulus of elasticity.

The relationship between the volume and pressure within the sphere can now be derived from Equation A3.1, A3.2 and A3.3:

$$\Delta P = K_1 \left[\left(\frac{V}{V_0} \right)^{1/3} - 1 \right] , \quad (A3.4)$$

where: $\Delta P = P$ from Equation A3.1, i.e., change in pressure in respect of the original pressure (P_0), and

$K_1 = 2dER$, which is constant in the case of small volume changes.

Applying the Taylor-MacLaurin series on Equation A3.4, it can be written as:

$$\Delta P = K_1 \left[1/3 \frac{\Delta V}{V_0} - 1/9 \left(\frac{\Delta V}{V_0} \right)^2 + 5/81 \left(\frac{\Delta V}{V_0} \right)^3 \dots \right] \quad (A3.5)$$

In man V_0 is in the order of 2000 ml, whereas ΔV is generally smaller than 30 ml as can be derived from the volume-pressure relationships in patients (Chapter 4), which is in the order of 1 to 2% of total craniospinal volume. The relationship described by Equation A3.5 may therefore be regarded as a linear function, since the higher order terms do not contribute significantly to the pressure. The equation may thus be reduced to:

$$\Delta P = 1/3 K_1 \frac{\Delta V}{V_0} ,$$

or:
$$P = P_0 + 1/3 K_1 \frac{\Delta V}{V_0} . \quad (A3.6)$$

In conclusion, if the craniospinal system were comparable with a closed, elastic sphere the relationship between volume and pressure could be approximated by a linear function.

APPENDIX 4

EFFECT OF SYSTEMIC ARTERIAL PRESSURE ON THE CRANIOSPINAL VOLUME-PRESSURE RELATIONSHIP

In the experimental series of Chapter 6 a positive correlation was found between the level of SAP and E_1 . In this Appendix a mathematical basis is offered for the explanation of this finding. According to the law of Poiseuille the relationship between pressure and flow is given by:

$$P_2 - P_1 = F R,$$

where: $P_2 - P_1$ = pressure gradient over the flow tract,
F = flow, and
R = resistance to flow.

When this relationship is applied to the CBF, it can be rewritten

1. for the inflow tract as:

$$SAP - SAVP = CBF_i R_{bi},$$

where: SAP = systemic arterial pressure,
SAVP = subarachnoid venous pressure,
 CBF_i = inflow of CBF, and
 R_{bi} = inflow resistance.

Since SAVP accurately reflects changes in ICP (Shulman, 1965; Shulman and Verdier, 1967), it can be replaced by the latter:

$$SAP - ICP = CBF_i R_{bi}. \quad (A4.1)$$

2. for the outflow tract as:

$$ICP - JVP = CBF_o R_{bo} \quad (A4.2)$$

where: JVP = jugular venous pressure,

CBF_o = outflow of blood which, under steady state conditions,
is equal to CBF_i , and

R_{bo} = outflow resistance.

In this equation ICP has already been substituted for SAVP.

When a volume-pressure test is carried out, the volume added causes an increase in total craniospinal volume and at the same time a compression of the distal venous vascular bed (cuff constriction), as discussed in Chapters 2.6 and 5.4. The latter effect increases the resistance to outflow by a factor k , so:

$$R'_{bo} = k R_{bo}, \quad k > 1.$$

Consequently, the new venous outflow of blood (CBF'_o) is given by:

$$CBF'_o = \frac{ICP - JVP}{k R_{bo}} = \frac{CBF_o}{k}, \quad (A4.3)$$

or, since prior to the volume-pressure test CBF_o equals CBF_i :

$$CBF'_o = \frac{SAP - ICP}{k R_{bi}}. \quad (A4.4)$$

Initially, the inflow remains unaltered, resulting in an increase in CBV and consequently in ICP. The effect of the elevation of ICP, substituted for SAVP, will be twofold. The outflow is partly restored as a result of the increased pressure gradient over the outflow tract and secondly, the inflow is reduced on account of the decreased perfusion pressure over the inflow tract. This will result in a new equilibrium between inflow and outflow (CBF_n) at an elevated level of ICP (ICP_n), which can be described by:

$$CBF_n = CBF'_o + x(CBF_o - CBF'_o), \quad x < 1.$$

Since prior to the volume-pressure test inflow and outflow are in equilibrium, the equation can be rewritten as:

$$CBF_n = CBF'_o + x(CBF_i - CBF'_o),$$

or:
$$CBF_n = (1 - x)CBF'_o + x CBF_i. \quad (A4.5)$$

Application of the Equations A4.1 and A4.4 yields:

$$\frac{SAP - ICP_n}{R_{bi}} = (1 - x) \frac{SAP - ICP}{k R_{bi}} + x \frac{SAP - ICP}{R_{bi}}. \quad (A4.6)$$

This results in the following relationship for the increase in ICP:

$$ICP_n - ICP = \frac{(1 - x)(k - 1)}{k}(SAP - ICP). \quad (A4.7)$$

This equation shows that the portion of the VPR related to venous compression and disturbance of flow ($ICP_n - ICP$) is dependent on the cerebral perfusion pressure and thus on the SAP. The elastance coefficient which is calculated from the VPR will thus be positively correlated with the SAP.

Finally, the original CBF will be restored by an autoregulatory response which may lead to a further increase in CBV and a secondary rise in ICP. But, because of the time factor involved in the development of this response, this does not interfere with the direct pressure response to bolus injection.

APPENDIX 5

STRAIN IN THE CEREBRAL ARTERIAL WALL DURING CHANGES IN SYSTEMIC ARTERIAL PRESSURE AND ARTERIAL CARBON DIOXIDE TENSION

Under steady state conditions the transmural pressure of the cerebral arterial wall is balanced by the strain in the wall according to:

$$[SAP - ICP]2r\ell = 2\sigma d\ell ,$$

or:
$$\frac{\sigma d}{r} = SAP - ICP,$$

where: σ = strain in the vessel wall,
 d = thickness of the wall,
 r = vessel radius,
 ℓ = vessel length, and
 $SAP - ICP$ = transmural pressure.

The transmural pressure can be assumed to be equal to the cerebral perfusion pressure (CPP):

$$\frac{\sigma d}{r} = CPP. \tag{A5.1}$$

The blood flow through the arteries is determined by the CPP and the hydraulic resistance of the vessels according to:

$$CBF = \frac{CPP}{R}, \tag{A5.2}$$

in which the hydraulic resistance R can be replaced by the Poiseuille resistance:

$$CBF \frac{8\mu\ell}{\pi r^4} = CPP, \tag{A5.3}$$

where: μ = viscosity of blood.

It is assumed that the volume of the arterial wall (V_w) remains constant during changes in SAP and $PaCO_2$:

$$V_w = 2\pi r \ell d = \text{constant.} \quad (\text{A5.4})$$

The relationship between strain in the wall, the CBF and the vessel radius follows from the Equations A5.1, A5.3 and A5.4.

$$\sigma = K_1 \frac{\text{CBF}}{r^2}, \quad (\text{A5.5})$$

where: $K_1 = \frac{16\mu}{V_w} = \text{constant.}$

During arterial hypotension CBF will remain unchanged as a result of vasodilatation caused by the autoregulatory mechanism. The increase in the arterial radius will therefore, according to Equation A5.5, result in a decrease in the strain in the arterial wall. The opposite effect will result from arterial hypertension.

The effect of changes in PaCO_2 on the strain in the wall is more difficult to establish, since, during hypercapnia for instance, the vasodilatory response of the arteries results in a concomitant rise in CBF. Therefore, the effect on the strain in the wall cannot easily be predicted from Equation A5.5. However, a relationship between strain, the CPP and the radius can be derived from Equation A5.1 and A5.4:

$$\sigma = K_2 \text{CPP } r^2, \quad (\text{A5.6})$$

where: $K_2 = \frac{2\pi \ell}{V_w} = \text{constant.}$

The CPP remains almost constant during hypercapnia. Vasodilatation during hypercapnia will thus result in a rise in the strain of the arterial wall.

APPENDIX 6

SOLUTION OF THE NON-LINEAR DIFFERENTIAL EQUATION DESCRIBING THE DYNAMIC BEHAVIOUR OF THE CEREBROSPINAL FLUID SYSTEM

In Chapter 9.3.2 the dynamic behaviour of the craniospinal system was described by the following non-linear differential equation (9.29):

$$\frac{1}{E_1(P - P_o)} \frac{dP}{dt} + C_1(P - P_b) - F_f(t) = 0. \quad (A6.1)$$

This equation can be reduced to a linear differential equation by two subsequent substitutions:

1. $x = P - P_o$ and $\frac{dx}{dt} = \frac{dP}{dt}$,

resulting in:

$$\frac{dx}{dt} + E_1 C_1 x^2 + E_1 [C_1(P_o - P_b) - F_f(t)] x = 0. \quad (A6.2)$$

2. Substitution according to the method of Bernouilly:

$$x = \frac{1}{y} \quad \text{and} \quad \frac{dx}{dt} = -\frac{1}{y^2} \frac{dy}{dt},$$

resulting in:

$$\frac{dy}{dt} + E_1 [F_f(t) + C_1(P_b - P_o)] y = E_1 C_1. \quad (A6.3)$$

If:

$$F(t) = E_1 [F_f(t) + C_1(P_b - P_o)],$$

Equation A6.3 can be reduced to:

$$\frac{dy}{dt} + F(t) y = E_1 C_1. \quad (A6.4)$$

This equation can be solved using the method of Lagrange, yielding:

$$y = C(t) e^{-\text{Pr} \{F(t)\}}, \quad (A6.5)$$

where: $\Pr \{F(t)\} = \int_0^t F(t)dt$, and

$$C(t) = E_1 C_1 \int_0^t e^{-\Pr \{F(t)\}} dt + \frac{1}{P_b - P_o} .$$

Equation A6.5 is here solved for two forcing functions:

1. Constant rate infusion, implying:

$$F(t) = E_1 [F_{in} + C_1 (P_b - P_o)] . \quad (A6.6)$$

Equation A6.5 can now be solved:

$$P(t) = \frac{[F_{in} + C_1 (P_b - P_o)] [P_b - P_o]}{C_1 (P_b - P_o) + F_{in} e^{-E_1 [F_{in} + C_1 (P_b - P_o)] t}} + P_o . \quad (A6.7)$$

This equation results in $P(0) = P_b$ for $t = 0$, and in $P(\infty) = P_{ss}$ (steady state ICP) for $t = \infty$

2. Volume-pressure test

The bolus injection may be regarded as an infusion at a constant speed within a short interval. For this reason, the bolus injection can be described as a flow pulse or, if the injection time is short compared to the time constant of the system, as an impulse flow function, implying:

$$F(t) = E_1 [\Delta V_i \delta_o(t) + C_1 (P_b - P_o)] , \quad (A6.8)$$

where: $\delta_o(t) =$ Dirac function.

Equation A6.5 can now be solved for the volume-pressure test:

$$P(t) = \frac{(P_b - P_o) e^{-E_1 [\Delta V_i + C_1 (P_b - P_o) t]}}{1 + e^{-E_1 \Delta V_i} \left[\frac{E_1 C_1 (P_b - P_o) t}{e^{-E_1 C_1 (P_b - P_o) t} - 1} \right]} + P_o . \quad (A6.9)$$

The pressure immediately after injection (P_p) and at infinity can be calculated from this equation:

$$P(0^+) = (P_b - P_o) e^{E_1 \Delta V_i} + P_o ,$$

or:

$$(P_p - P_o) = (P_b - P_o) e^{E_1 \Delta V_i} ,$$

or:

$$E_1 = \frac{1}{\Delta V_i} \ln \frac{P_p - P_o}{P_b - P_o} .$$

This is the equation for E_1 as it was also derived directly from the craniospinal volume-pressure relationship (Chapter 2.4). At infinity the pressure has returned to the initial equilibrium pressure: $P(\infty) = P_b$.

APPENDIX 7

COMPUTATION OF THE MODEL PARAMETERS P_0 AND E_1 FROM THE CONSTANT RATE INFUSION TEST

From the dynamic response of the ICP following a disturbance of the CSF circulation by a constant rate infusion (Equation 9.32) E_1 can be derived as a function of P_0 (Equation 9.33), since the third parameter, C_1 , is given by the steady state conditions:

$$C_1 = \frac{F_{in}}{P_{ss} - P_b} .$$

If it is assumed that the model parameters are stable with rising ICP, E_1 must be constant at each instant t :

$$E_1(t_1) = E_1(t_2), \tag{A7.1}$$

with:

$$ICP(t_1) = P_1, \text{ and}$$

$$ICP(t_2) = P_2 .$$

E_1 at both instants (t_1 and t_2) is given by the following equations:

$$E_1(t_1) = \frac{[P_{ss} - P_b]}{F_{in}[P_{ss} - P_0]t_1} \ln \frac{[P_1 - P_0][P_{ss} - P_b]}{[P_b - P_0][P_{ss} - P_1]}, \tag{A7.2}$$

and:

$$E_1(t_2) = \frac{[P_{ss} - P_b]}{F_{in}[P_{ss} - P_0]t_2} \ln \frac{[P_2 - P_0][P_{ss} - P_b]}{[P_b - P_0][P_{ss} - P_2]}, \tag{A7.3}$$

If $t_2 = 2t_1$, E_1 can be eliminated from the above equations:

$$\ln \left[\frac{[P_1 - P_0][P_{ss} - P_b]}{[P_b - P_0][P_{ss} - P_1]} \right]^2 = \ln \frac{[P_2 - P_0][P_{ss} - P_b]}{[P_b - P_0][P_{ss} - P_2]}, \tag{A7.4}$$

or:

$$(P_1 - P_o)^2 (P_{ss} - P_b)(P_{ss} - P_2) - (P_{ss} - P_1)^2 (P_b - P_o)(P_2 - P_o) = 0.$$

This represents a quadratic equation of the parameter P_o , which can be simplified since one of its roots is: $P_o = P_{ss}$. This root is not relevant, as $P_o < P_b < P_{ss}$.

Equation 7.4 can now be reduced to:

$$P_o \left[P_{ss} (2P_1 - P_2 - P_b) + P_2 P_b - P_1^2 \right] - P_1^2 (P_{ss} - P_2 - P_b) + P_2 P_b (P_{ss} - 2P_1) = 0.$$

P_o can now be solved:

$$P_o = \frac{P_1^2 (P_{ss} - P_2 - P_b) - P_b P_2 (P_{ss} - 2P_1)}{P_{ss} (2P_1 - P_2 - P_b) + P_b P_2 - P_1^2}. \quad (A7.5)$$

If P_o is known, E_1 can be calculated from Equation A7.2 or A7.3.

APPENDIX 8

COMPUTATION OF THE MODEL PARAMETERS P_o , E_1 AND C_1 FROM THE VOLUME-PRESSURE TEST

The dynamic course of the ICP following a disturbance of the CSF circulation by a volume-pressure test is given by Equation 9.35. Substituting C'_1 for $E_1 C_1$, this equation can be written as:

$$P(t) = \frac{(P_b - P_o)e \left[E_1 \Delta V_i + C'_1 (P_b - P_o) t \right]}{1 + e E_1 \Delta V_i \left[e^{C'_1 (P_b - P_o) t} - 1 \right]} + P_o, \quad (A8.1)$$

where:
$$E_1 = \frac{1}{\Delta V_i} \ln \frac{P_p - P_o}{P_b - P_o} \quad (\text{Equation 9.36}). \quad (A8.2)$$

Assuming that the model parameters are constant with rising ICP, C'_1 must be constant at each instant t :

$$C'_1(t_1) = C'_1(t_2),$$

with:
$$\begin{aligned} \text{ICP}(t_1) &= P_1, \text{ and} \\ \text{ICP}(t_2) &= P_2. \end{aligned}$$

C'_1 at both instants (t_1 and t_2) is given by the following equations:

$$C'_1(t_1) = \frac{1}{[P_b - P_o] t_1} \ln \frac{[P_1 - P_o][P_p - P_b]}{[P_1 - P_b][P_p - P_o]}, \quad (A8.3)$$

and:

$$C'_1(t_2) = \frac{1}{[P_b - P_o] t_2} \ln \frac{[P_2 - P_o][P_p - P_b]}{[P_2 - P_b][P_p - P_o]}. \quad (A8.4)$$

If t_2 is chosen so that $t_2 = 2t_1$, C'_1 can be eliminated according to:

$$\ln \left[\frac{[P_1 - P_o][P_p - P_b]}{[P_1 - P_b][P_p - P_o]} \right]^2 = \ln \frac{[P_2 - P_o][P_p - P_b]}{[P_2 - P_b][P_p - P_o]}.$$

This results in a quadratic equation for P_o :

$$\begin{aligned} &P_o^2 [P_2(P_p - P_b) - P_p P_b - P_1(P_1 - 2P_b)] + \\ &P_o [P_1^2(P_2 + P_p) - 2P_1 P_2 P_p + P_b^2(P_2 + P_p - 2P_1)] + \\ &P_2 P_b P_p (2P_1 - P_b) - P_1^2 P_b (P_2 + P_p - P_b) = 0. \end{aligned} \quad (A8.6)$$

One of the roots of this equation is: $P_o = P_b$. This root is not relevant, as $P_o < P_b$. Consequently, Equation A8.6 may be reduced to the following equation for P_o :

$$P_o = \frac{P_2 P_p (2P_1 - P_b) - P_1^2 (P_2 + P_p - P_b)}{P_b (2P_1 - P_2 - P_p) - P_1^2 + P_2 P_p}. \quad (A8.7)$$

Now that P_o is known, E_1 can be solved from Equation A8.2 and C_1' from Equation A8.3 or A8.4, after which C_1 can be calculated from E_1 and C_1' .

SUMMARY

In the first part of this thesis (Chapters 2-8) a new method is developed for the continuous assessment of the craniospinal volume-pressure relationships. This method uses the amplitude of the pulsatile ICP variations, i.e., the CSF pulse pressure, as a measure of craniospinal elastance. In the second part (Chapters 9 and 10) a mathematical model of the CSF dynamics is presented and experimentally verified.

CHAPTER 1 gives a general introduction and summarizes the aims. The level of ICP does not always correlate with the clinical condition of the patient. The level of ICP should therefore be considered not in isolation but in conjunction with many other aspects of intracranial hypertension. The volume-pressure relationship is one of these aspects and may be particularly important from a clinical viewpoint, as it determines the volume buffering capacities of the craniospinal system.

The volume-pressure relationship is assessed from the response in ICP (VPR) resulting from rapid volume loading of the CSF space. This procedure has several disadvantages due to its invasive nature. The CSF pulse pressure is also a pressure response to a rapid volume load, namely the volume load of cerebral blood during a cardiac cycle. Craniospinal volume-pressure relationships can thus be assessed on a continuous and non-invasive basis by means of the CSF pulse pressure. The main aim of this thesis has been to investigate this idea.

Rapid volume increments encroach on the buffering capacities of the craniospinal system; however, in more slowly expanding lesions, as are usually encountered in the clinical situation, volume compensation by absorption of CSF plays a major role. This observation led to the development of a mathematical model of the CSF dynamics, with which the parameters of CSF formation and absorption can be computed.

CHAPTER 2 deals with the craniospinal volume-pressure relationships.

A short description of the craniospinal system is given. Furthermore, a historical survey is given starting from the Monro-Kellie doctrine which postulates that the total craniospinal volume is constant. The idea was finally accepted that this volume is variable, mainly due to the distensibility of the spinal dural sac. In true volume-pressure relationships the changes in ICP occurring with changes in total craniospinal volume are considered.

The first volume-pressure models were of a linear nature. Most of the present models are based on an exponential relationship. In this chapter we have also developed an exponential model, which is characterized by two parameters: the elastance coefficient (E_1) determining the slope of the volume-pressure curve, and a constant pressure term (P_0). P_0 is unique to our model and was introduced for several reasons, both mathematical and physiological. If it is assumed that P_0 equals zero, our model is similar to that of Marmarou. It follows directly from the exponential nature of the model that the relationship between the ICP and the pressure response resulting from a rapid and uniform volume increment (VPR) is of a linear nature. Both model parameters are given by this relationship: E_1 by the slope and P_0 by the intercept with the pressure axis.

The clinical significance of the volume-pressure relationships and the difference between volume buffering and volume compensation are discussed. So long as the volume of an expanding mass lesion is completely compensated for and the volume buffering capacities are not encroached on, the ICP does not rise. When volume compensation becomes impaired, the ICP starts to rise and the course of ICP elevation also becomes dependent on the buffering capacities as determined by the volume-pressure relationships. It is shown that even when the ICP is considerably elevated, volume compensation is still effective. In intracranial hypertension encountered clinically, both mechanisms are thus always operative simultaneously.

In CHAPTER 3 the relationship between CSF pulse pressure and ICP is mathematically described by substituting the pulse pressure for the VPR, and the pulsatile change in CBV (ΔV_b) for the volume of bolus injection, in the equations of the volume-pressure model. Thus, it follows that the CSF pulse pressure at a given ICP is dependent on E_1 and on the magnitude of ΔV_b . This means that the pulse pressure can only be a measure of the elastance if the magnitude of ΔV_b is known. It can also be derived that

the CSFPP-ICP relationship is linear so long as ΔV_b is constant, in which case changes in the slope of the relationship reflect changes in E_1 .

The pulsatile change in CBV is by definition the volume change underlying the CSF pulse pressure. It is caused by the interaction of the pulsatile inflow and outflow of cerebral blood during a cardiac cycle. The magnitude of ΔV_b is determined by the pulsatile volume load of blood to the craniospinal system and by the phase shift or time lag between the arterial inflow and venous outflow curves. The pulsatile volume load is dependent on the CBF and the heart rate. The cerebral arterial and venous flow profiles are determined by the impedances of the respective vascular beds. The inflow impedance is largely controlled by the vasomotor tone of the cerebral resistance vessels. CBF autoregulation may therefore be expected to exert influence on the magnitude of ΔV_b .

The clinical study described in CHAPTER 4 comprises 58 patients who underwent continuous ICP recording as part of their diagnostic investigations. The aims of the study were to examine the nature of the CSFPP-ICP relationship in clinical patients and to compare this relationship with the volume-pressure relationship. A method is described for automatic processing of the CSFPP-ICP relationship by means of a computer. Linear relationships with high correlation coefficients were always found. This means, according to the mathematical model, that ΔV_b remained constant within the ICP ranges examined.

The volume-pressure parameter E_1 was determined by bolus injection in the lateral ventricle and computed from the VPR and the P_0 of the CSFPP-ICP relationship. The mean E_1 was 0.26 ± 0.17 l/ml. The slope of the CSFPP-ICP relationship showed a significant correlation with E_1 . ΔV_b was computed from the slope of the CSFPP-ICP relationship and from E_1 ; it was found to vary between 0.36 and 4.38 ml with a mean value of 1.67 ml.

A breakpoint in the CSFPP-ICP relationship was found during plateau waves above which the CSF pulse pressure increased more rapidly. At the same time a relative decrease in elastance was found. It is therefore concluded that the disproportionate increase in CSF pulse pressure during plateau waves is due to an increase in ΔV_b , caused by vasoparalysis.

The experiments described in CHAPTER 5 were designed to compare the CSF pulse pressure with the VPR systematically for the whole range of ICP. The experimental animal was the dog and the ICP was raised by means

of continuous inflation of an extradural balloon causing cerebral compression. Both the pulse pressure and the VPR were found to increase linearly with the ICP up to a breakpoint at an ICP of about 60 mm Hg, above which the pulse pressure rose more rapidly and the VPR remained constant. From these results it is inferred that ΔV_b remains constant in the ICP range below the breakpoint, whereas it increases progressively above the breakpoint. Furthermore, the concept of a mono-exponential volume-pressure relationship is only valid in the ICP range below the breakpoint. Above the breakpoint the volume-pressure relationship is linear in nature. Due to the variation in ΔV_b , no correlation was found between the slope of the CSFPP-ICP relationship and E_1 below the breakpoint ICP.

It is argued that the breakpoint in both relationships is caused by loss of CBF autoregulation. The craniospinal volume-pressure curve derives its exponential shape from cerebrovascular reactivity. When vasoparalysis exists, the system behaves like a closed elastic sphere with a linear volume-pressure relationship. It is further hypothesized that cerebral vasoparalysis causes a marked decrease in the cerebral arterial inflow resistance. This results in a change in the pulsatile inflow of blood consisting of a shift of flow from diastole to systole. The phase shift between inflow and outflow of cerebral blood during a cardiac cycle is thereby increased, causing an increase in the magnitude of ΔV_b .

The experimental model used in CHAPTER 6 is similar to that described in Chapter 5. In this series the effects of hypercapnia and of drug induced systemic arterial hypotension and hypertension on both CSF pulse pressure and the VPR were examined during elevation of the ICP. Hypercapnia did not significantly affect the volume-pressure relationship, but it did cause an increase in CSF pulse pressure. Changing the SAP produced opposite effects on pulse pressure and VPR. Lowering the SAP caused an increase in CSF pulse pressure and a decrease in E_1 , whereas raising the SAP produced the reverse results.

The discrepancies between pulse pressure and VPR were attributed to the influence of the variables under examination on ΔV_b . Dilatation of the cerebral resistance vessel, provoked by CO_2 and by the autoregulatory response elicited by lowering the SAP, causes ΔV_b to increase.

Autoregulatory vasoconstriction resulting from raising the SAP causes a decrease in ΔV_b .

This series provided further evidence for relating the breakpoints in the CSFPP-ICP and VPR-ICP relationships to the failure of CBF autoregulation, as the above effects disappeared beyond the breakpoint.

The purpose of the experimental series in the dog described in CHAPTER 7 was to assess by more direct measurement the changes in ΔV_b which occur when the SAP and the PaCO_2 are altered and when the ICP is elevated. This was done by computation of ΔV_b from the electromagnetically measured flow profile in the vertebral artery, on the assumption of a nonpulsatile and constant cerebral venous outflow.

The results are consistent with those of the previous two chapters except for the results of changes in PaCO_2 . The increase in ΔV_b during arterial hypotension was caused by an increase in pulsatile flow due to a shift of flow from diastole to systole, whereas the mean flow was not significantly affected. The reverse phenomenon was observed when the SAP was raised, and this was responsible for a decrease in ΔV_b . When the ICP was raised above the breakpoint pressure (see Chapter 5), it was observed that the fall in CBF was mainly due to a decrease in diastolic flow. The systolic flow pulse relative to the mean flow level was increased and this caused an increase in ΔV_b . Pulsatile flow was little affected by changing the PaCO_2 . The changes in total flow that were found were evenly distributed over the cardiac cycle. ΔV_b was consequently not significantly affected, although the CSF pulse pressure was considerably changed.

The underlying mechanisms of the changes in pulsatile flow are discussed extensively. It is argued that the cerebral arterial inflow profile is largely determined by the compliance of the vascular bed. Vascular compliance is significantly altered by changes in SAP and ICP since they affect the transmural pressure of the vessels, whereas this is not the case during changes in PaCO_2 .

CHAPTER 8 gives a general discussion of the first part of the thesis dealing with the CSF pulse pressure and the craniospinal volume-pressure relationship. It is argued that, from a clinical point of view, the volume compensatory capacities are more important than the volume buffering capacities. The former capacities determine the long-term

course of the ICP during expansion of intracranial masses, whereas the latter capacities determine the response of the ICP to rapid volume changes. The exact shape of the volume-pressure curve is discussed and the various curves reported in the literature are compared. It is concluded that the answer to the question as to whether the curve is exponential or linear in shape depends on the extent to which changes in CBV are involved in the recording of the curve.

It is furthermore concluded that the volume-pressure relationship cannot be accurately assessed on the basis of the CSF pulse pressure alone, since the pulse pressure is also dependent on the pulsatile change in CBV, the magnitude of which is not known in clinical patients. However, so long as the pulsatile change in CBV remains constant, changes in the slope of the CSFPP-ICP relationship will accurately reflect changes in the volume-pressure relationship. This study has revealed the influence of several physiological variables on the pulsatile change in CBV, so that the CSF pulse pressure may still be a useful guide to craniospinal elastance during ICP monitoring in clinical patients. In any case, the volume-pressure test can be applied more rationally. The fact that the pulse pressure is a reflection of the cerebral vasomotor tone provides an additional argument in favour of CSF pulse pressure monitoring.

A mathematical model is introduced in CHAPTER 9 which describes the dynamics of the CSF circulatory system: CSF formation and absorption, and the storage capacities of the system. A brief survey of the literature is given. The model is described for both a constant and a pressure-dependent CSF formation. The base-line (resting) ICP is determined by the formation rate, the resistance to outflow of CSF and the dural sinus pressure. The parameters of CSF formation and absorption can be calculated from the equations describing both the normal equilibrium condition and the the equilibrium condition resulting from constant rate infusion into the CSF space.

In describing the dynamic behaviour of the system, the storage capacity as given by the volume-pressure relationship has also to be considered. The ICP as a function of time is thus dependent on both the volume-pressure parameters and the parameters of CSF formation and absorption. The equations from which these parameters can be computed are derived for both constant rate infusion and the volume-pressure test.

The clinical significance of the model parameters is discussed.

CHAPTER 10 describes a series of experiments in the dog which were designed to evaluate the mathematical CSF circulation model. The parameters were calculated from the model equations and the results were compared in several ways: constant rate infusion with bolus injection, two methods of computation (analytical and curve fit solution), the computation of the parameters at different time intervals after the start of the test, the use of different volume loads, the pressure-independent with the pressure-dependent CSF formation model and, finally, the model of the authors with that of Marmarou.

The infusion test produced more stable and reliable results in every respect than the volume-pressure test. The curve fit solution showed a better fit to the experimental data than the analytical method of computation. In the volume-pressure test the analytical method did not produce reliable results at all. However, the reliability of the model parameters improved in the volume-pressure test with increasing volume loads. The values for the outflow resistance found in this series are within the range reported in the literature. The CSF formation rate, on the contrary, was considerably higher than the values of 2.0-3.4 ml/hr reported in the literature. However, if a dural sinus pressure of 5 mm Hg is assumed, the formation rate is closer to that of the literature (4.5 ml/hr for constant rate and 4.1 ml/hr for pressure-dependent CSF formation).

Our model showed a better fit to the experimental data than that of Marmarou. This was most significant in the infusion test. Moreover, as opposed to the Marmarou model, our model yielded stable results for the parameters computed at different time intervals after the start of the test.

SAMENVATTING

In het eerste gedeelte van dit proefschrift (Hoofdstukken 2-8) wordt een nieuwe methode ontwikkeld ter bepaling van de craniospinale volume-druk relatie. Deze methode houdt in, dat de amplitude van de liquorpulsaties wordt gehanteerd als een maat voor de craniospinale elastantie. In het tweede gedeelte (Hoofdstukken 9 en 10) wordt een mathematisch model van de liquorcirculatie ontwikkeld en dit model wordt getest in het dier-experiment.

HOOFDSTUK 1 bevat een algemene inleiding en geeft een opsomming van de doelstellingen van het onderzoek. Gesteld wordt, dat de hoogte van de intracraniële druk niet altijd overeenkomt met de ernst van de klinische toestand van de patiënt. De hoogte van de druk moet daarom altijd worden geïnterpreteerd in samenhang met talrijke andere aspecten van intracraniële drukverhoging. Eén van deze aspecten is de verhouding tussen het volume van en de druk binnen de craniospinale ruimte. Deze verhouding kan voor de kliniek van groot belang zijn, omdat zij de mate bepaalt waarin de druk stijgt, wanneer het craniospinale volume toeneemt (volume-opslag-capaciteit).

De volume-druk relatie kan worden berekend uit de drukstijging die ontstaat na een snelle injectie van een bepaalde hoeveelheid fysiologisch zout in de liquorruimte (volume-druk respons). Aan deze methode kleven echter, vanwege haar invasieve karakter, verschillende nadelen. De liquorpulsaties zijn eveneens het gevolg van snelle veranderingen in het craniospinale volume, zij het dat deze niet plaatsvinden in de liquorruimte maar in het vasculaire compartiment. Deze analogie biedt dus de mogelijkheid om de volume-druk relatie te bepalen uit de liquorpulsaties. Het voordeel hiervan is, dat deze bepaling kan geschieden op een continue en niet-invasieve wijze. De uitwerking van dit idee vormt het voornaamste onderwerp van dit proefschrift.

Het zijn vooral snel optredende volumetoenemingen die een beroep doen op de opslagcapaciteit van het craniospinale systeem. In de kliniek hebben we echter meestal te maken met ruimtebenemende processen die betrekkelijk langzaam in volume toenemen. Daarbij speelt volume-compensatie door absorptie van liquor een belangrijkere rol dan de opslagcapaciteit. Dit vormt de reden voor de ontwikkeling van een mathematisch model van de liquorcirculatie waarmee de parameters van liquorproductie en liquor-absorptie berekend kunnen worden.

HOOFDSTUK 2 behandelt de craniospinale volume-druk relatie. Na een korte beschrijving van de craniospinale ruimte wordt een historisch overzicht gegeven, beginnend bij de Monro-Kellie doctrine die stelt, dat het volume van de ruimte constant is. Tenslotte kwam men tot het inzicht, dat dit volume variabel is vanwege de rekbaarheid van de duraalzak in het wervelkanaal. Het gaat bij de volume-druk relatie om een vergelijking van veranderingen in de druk met veranderingen in het totale craniospinale volume.

De eerste volume-druk modellen gingen uit van een lineaire relatie. De meeste van de huidige modellen zijn gebaseerd op een exponentiële functie. Het model dat hier wordt beschreven is ook exponentieel en wordt gekenmerkt door twee parameters: de elastantie-coëfficiënt (E_1) en een constante term (P_0). E_1 bepaalt de helling van de volume-druk curve. P_0 is uniek voor ons model en werd om verschillende redenen, zowel mathematische als fysiologische, geïntroduceerd. Ons model komt overeen met dat van Marmarou, indien wordt aangenomen dat P_0 gelijk is aan nul. Uit de exponentiële relatie kan worden afgeleid, dat de relatie tussen de intracraniële druk en de drukstijging tengevolge van een snelle en uniforme volumetoeneming lineair is. Beide modelparameters worden uit deze lineaire relatie bepaald: E_1 uit de helling en P_0 uit het snijpunt met de druk-as.

De klinische betekenis van de volume-druk relatie alsmede het verschil tussen volume-opslag en volume-compensatie worden besproken. De intracraniële druk zal niet stijgen, zolang als het volume van een ruimtebenemend proces volledig wordt gecompenseerd. Wanneer dit niet langer mogelijk is, begint de druk te stijgen en wordt het drukverloop mede bepaald door de opslagcapaciteit welke kan worden afgeleid uit de volume-druk relatie. Het wordt aangetoond, dat zelfs wanneer de intracraniële druk aanzienlijk verhoogd is, compensatie van volume nog steeds

plaatsvindt. Bij aandoeningen die gepaard gaan met intracraniële hypertensie zijn beide mechanismen dus steeds gelijktijdig werkzaam.

In HOOFDSTUK 3 wordt de relatie tussen de amplitude van de liquorpulsaties en de intracraniële druk beschreven door gebruik te maken van de overeenkomst tussen de amplitude en de volume-druk respons. Daartoe worden in het volume-druk model de amplitude van de liquorpulsaties en de pulsatieve verandering in het cerebrale bloedvolume (ΔV_b) gesubstitueerd voor respectievelijk de volume-druk respons en het volume van de bolus injectie in de liquorruimte. De amplitude van de bij een bepaalde intracraniële druk behorende pulsatie is dus afhankelijk van E_1 en van de grootte van ΔV_b . Dit betekent, dat de polsdruk alleen een maat voor de elastantie kan zijn, indien de grootte van ΔV_b bekend is. Het kan gemakkelijk worden ingezien, dat de relatie tussen polsdruk en intracraniële druk lineair is, zolang ΔV_b constant blijft. In dat geval corresponderen veranderingen in de helling van deze relatie met veranderingen in E_1 .

De pulsatieve verandering in het cerebrale bloedvolume is per definitie de volumeverandering die ten grondslag ligt aan de amplitude van de liquorpulsaties. Deze wordt veroorzaakt door de wisselwerking van de pulsatieve instroom en uitstroom van het hersenbloed tijdens een hartcyclus. De grootte van ΔV_b wordt bepaald door het pulsatieve aanbod van bloed aan het craniospinale systeem enerzijds en door het fase-verschil of het tijdsverschil tussen de instroom- en uitstroomprofielen anderzijds. Het aanbod van bloed is afhankelijk van de bloedstroom naar de hersenen en van de hartfrequentie. De arteriële en veneuze stroomprofielen worden weer bepaald door de impedanties van de betrokken vaatgebieden. De instroomimpedantie wordt grotendeels gecontroleerd door de tonus van de zg. cerebrale weerstandsvaten. Het ligt daarom in de verwachting, dat het fenomeen van de autoregulatie van de cerebrale bloeddoodstroming de grootte van ΔV_b kan beïnvloeden.

In HOOFDSTUK 4 wordt een klinisch onderzoek beschreven dat tot doel had de aard van de relatie tussen de amplitude van de liquorpulsaties en de intracraniële druk te onderzoeken bij patiënten en deze te vergelijken met de volume-druk relatie. Het onderzoek bevatte 58 patiënten die in het kader van het diagnostisch onderzoek een continue ventrikeldrukmeter ondergingen. Een methode wordt beschreven voor de automatische bepaling

van de relatie tussen polsdruk en intracraniële druk met behulp van een computer. Deze relatie bleek bij de onderzochte patiënten steeds lineair te zijn met een hoge correlatie-coëfficiënt. Dit betekent volgens het mathematisch model, dat ΔV_b constant was in het drukgebied dat werd onderzocht.

De volume-druk parameter E_1 werd bepaald door middel van bolus injectie van 1 ml in de laterale ventrikel en werd berekend uit de volume-druk respons en de P_o van de relatie tussen de amplitude van de liquorpols en de intracraniële druk. E_1 bedroeg gemiddeld 0.26 ± 0.17 l/ml. De helling van de polspulsaties tegen de druk toonde een significante correlatie met E_1 . ΔV_b werd berekend uit de helling en uit E_1 ; ΔV_b varieerde tussen 0.36 en 4.38 ml met een gemiddelde waarde van 1.67 ml.

Tijdens plateau golven vertoonde de relatie een steilere helling, d.w.z.: de amplitude van de pulsaties nam meer toe met de druk tijdens dan buiten de plateau golven. Tegelijkertijd werd een relatieve afnemning van de volume-druk respons gevonden. Hieruit wordt de conclusie getrokken, dat de disproportionele toeneming van de liquorpulsaties tijdens plateau golven veroorzaakt wordt door een toeneming van ΔV_b tengevolge van cerebrale vasoparalyse.

In HOOFDSTUK 5 wordt een serie experimenten met honden beschreven waarin de amplitude van de liquorpulsaties systematisch wordt vergeleken met de volume-druk respons voor een intracraniële drukverhoging tot aan het niveau van de bloeddruk. De druk werd verhoogd door middel van geleidelijke vulling van een intracraniële extradurale ballon. Zowel de amplitude van de liquorpols als de volume-druk respons namen lineair toe met de druk tot aan een breekpunt bij een druk van ongeveer 60 mm Hg. Daarboven nam de polsdruk nog sterker toe, maar de volume-druk respons bleef gelijk. Uit de resultaten kan worden afgeleid, dat ΔV_b onder het breekpunt constant is, maar daarboven progressief toeneemt. Met betrekking tot de volume-druk relatie kan worden gesteld, dat deze onder het breekpunt een exponentieel en boven het breekpunt een lineair karakter heeft. Onder het breekpunt bleek er geen verband te bestaan tussen de helling van de relatie tussen polsdruk en intracraniële druk enerzijds en E_1 anderzijds. De verklaring hiervoor kan worden gevonden in het feit dat de waarde van ΔV_b aanzienlijk verschilde tussen de proefdieren.

De oorzaak van het breekpunt wordt toegeschreven aan het verloren gaan van het autoregulerend vermogen van de hersenen met betrekking tot

hun bloedvoorziening. De volume-druk relatie ontleent haar exponentiële vorm aan de reaktiviteit van het cerebrale vaatbed. Wanneer deze reaktiviteit verloren gaat (vasoparalyse), gedraagt het systeem zich als een gesloten elastische bol waarvan de volume-druk relatie benaderd kan worden door een lineaire functie. Vasoparalyse veroorzaakt een verlaging van de instroomweerstand. Hierdoor treedt er een verandering op in de pulsatieve instroom van bloed bestaande uit een verschuiving in de bloedstroom van diastole naar systole. Dit heeft tot gevolg, dat het fase-verschil tussen de instroom en uitstroom van hersenbloed tijdens een hartcyclus toeneemt, hetgeen een toeneming van ΔV_b veroorzaakt.

In HOOFDSTUK 6 worden de effecten van hypercapnie alsmede van een verlaging en een verhoging van de bloeddruk nagegaan op de amplitude van de liquorpulsaties en op de volume-druk respons. Het experimentele model is hetzelfde als dat beschreven in Hoofdstuk 5. Hypercapnie had geen significante invloed op de volume-druk relatie, maar veroorzaakte wel een toeneming van de liquorpulsaties. Het veranderen van de bloeddruk had tegengestelde effecten op de polsdruk en de volume-druk respons. Bloeddrukverlaging veroorzaakte een toeneming van de liquorpulsaties tegenover een afname van E_1 . De omgekeerde resultaten werden bereikt, wanneer de bloeddruk werd verhoogd.

Het verschillend gedrag van de liquorpulsaties en de volume-druk respons wordt toegeschreven aan de invloed van CO_2 en de bloeddruk op ΔV_b . Zowel CO_2 als bloeddrukverlaging veroorzaken een verwijding van de hersenvaten, tenminste zolang als de reaktiviteit van de vaten intact is. Bloeddrukverhoging veroorzaakt een autoregulatorische vernauwing van de cerebrale weerstandsvaten. In het eerste geval veroorzaakt de verlaging van de instroomweerstand een vergroting van ΔV_b , terwijl in het tweede geval ΔV_b afneemt als gevolg van een verhoging van de instroomweerstand.

Deze experimenten verschaften aanvullend bewijsmateriaal om de breekpunten in de relaties van zowel de liquorpulsaties als de volume-druk respons met de intracraniële druk toe te schrijven aan het verloren gaan van de cerebrale autoregulatie. De bovengenoemde effecten verdwenen namelijk, wanneer de druk verhoogd was tot boven het niveau van het breekpunt.

In HOOFDSTUK 7 wordt verslag gedaan van een serie experimenten waarin getracht werd op een meer directe wijze veranderingen in ΔV_b te

meten. Hiertoe werd de bloedstroom in de arteria vertebralis van de hond gemeten met behulp van electromagnetische stroommeters. ΔV_b werd berekend uit het pulsatieve stroomprofiel aannemende dat de veneuze uitstroom niet pulsatief maar constant was. Onderzocht werden de effecten van veranderingen in de arteriële CO_2 spanning ($PaCO_2$) en de bloeddruk en de effecten van intracraniële drukverhoging.

De resultaten komen overeen met die van de voorafgaande twee hoofdstukken met uitzondering van die van veranderingen in $PaCO_2$. De toeneming van ΔV_b als gevolg van bloeddrukverlaging werd veroorzaakt door een toeneming van de pulsatieve bloedstroom tengevolge van een stroomverplaatsing van diastole naar systole, terwijl de gemiddelde bloedstroming niet significant werd beïnvloed. Het tegenovergestelde fenomeen werd waargenomen tijdens bloeddrukverhoging, waardoor ΔV_b afnam. Wanneer de intracraniële druk zo sterk verhoogd was dat de cerebrale bloeddorstrooming afnam, bleek deze afneming vooral op rekening te komen van de diastole stroom. De systole bloedstroom verminderde niet en nam dus relatief, d.w.z. ten opzichte van de gemiddelde bloedstroom, toe. Als gevolg hiervan nam ΔV_b toe ondanks een vermindering van de gemiddelde bloeddorstrooming.

De pulsatieve bloedstroom werd nauwelijks beïnvloed door de veranderingen aangebracht in de $PaCO_2$. De totale bloedstroom veranderde wel, maar de toeneming of afneming was gelijkmatig verdeeld over de gehele hartcyclus. Hierdoor traden er geen significante veranderingen op in ΔV_b , hoewel deze wel optraden in de hoogte van de liquorpulsaties.

De oorzaken die ten grondslag liggen aan de waargenomen veranderingen in de pulsatieve bloedstroom worden uitvoerig besproken. De voornaamste conclusie is, dat het arteriële instroomprofiel eerder wordt bepaald door de compliantie van het arteriële vaatbed dan door de instroomweerstand. Deze compliantie is afhankelijk van de bloeddruk en de intracraniële druk, omdat deze factoren de transmurale druk van de vaten beïnvloeden. Bij veranderingen in de $PaCO_2$ blijft de transmurale druk vrijwel constant.

HOOFDSTUK 8 geeft een samenvattende bespreking van het eerste deel van het proefschrift. Er wordt op gewezen, dat het vermogen van het craniospinale systeem om volume te compenseren vanuit een klinisch standpunt belangrijker is dan het vermogen om volume op te slaan. De eerstgenoemde eigenschap bepaalt het verloop van de intracraniële druk op langere termijn tijdens de evolutie van een intracraniëel ruimtebenemend proces. De tweede eigenschap bepaalt de drukstijging tengevolge

van snelle volumeveranderingen. De exacte vorm van de volume-druk curve wordt besproken en verschillende curven uit de literatuur worden met elkaar vergeleken. Hieruit wordt de conclusie getrokken, dat de vorm van de curve (exponentieel of lineair) afhankelijk is van de mate waarin veranderingen in het cerebrale bloedvolume optreden tijdens de experimentele registratie van de curve.

De volume-druk relatie kan niet nauwkeurig worden bepaald op grond van de liquorpulsaties alleen. Deze zijn namelijk ook afhankelijk van de pulsatieve verandering in het cerebrale bloedvolume. Helaas kan deze verandering bij patiënten niet exact worden gemeten. Zolang ΔV_b echter constant blijft, kan de helling van de relatie tussen liquorpulsaties en intracranieële druk worden opgevat als een relatieve maat van de elastantie-coëfficiënt. Deze studie heeft inzicht verschaft in de effecten, zowel in kwalitatieve als in kwantitatieve zin, van verschillende physiologische variabelen op ΔV_b . Met behulp van deze kennis kan de amplitude van de liquorpulsaties worden gecorrigeerd voor veranderingen in ΔV_b . Dit biedt derhalve alsnog de mogelijkheid om bij patiënten de volume-druk relatie te 'bewaken' door middel van een continue analyse van de relatie tussen de amplitude van de liquorpols en de intracranieële druk.

In HOOFDSTUK 9 wordt een mathematisch model geïntroduceerd dat de dynamica van de liquorcirculatie beschrijft: liquorproductie, liquorabsorptie en de opslagcapaciteit van het systeem. De literatuur over dit onderwerp wordt in het kort besproken. Het model wordt uitgewerkt voor zowel een constante als een druk-afhankelijke liquorproductie. De normale intracranieële evenwichtsdruk wordt bepaald door de produktiesnelheid, de absorptieweerstand en de druk in de sinus sagittalis. Door middel van een infusie van fysiologisch zout in de liquorruimte met een constante snelheid wordt een nieuw evenwicht bereikt. Uit de vergelijkingen die beide evenwichtstoestanden beschrijven kunnen de parameters van liquorproductie en liquorabsorptie worden berekend.

Bij de beschrijving van het dynamisch gedrag van het systeem moet rekening worden gehouden met de opslagcapaciteit welke bepaald wordt door de volume-druk relatie. De intracranieële druk als een functie van de tijd is dus afhankelijk zowel van de volume-druk parameters als van de parameters van liquorproductie en liquorabsorptie. De vergelijkingen waaruit deze parameters kunnen worden berekend worden zowel voor de

infusietest als voor de volume-druk test afgeleid. De klinische betekenis van de modelparameters wordt besproken.

In HOOFDSTUK 10 wordt een serie experimenten met honden beschreven die tot doel had het mathematische model van de liquorcirculatie te evalueren. De parameters werden berekend uit de modelvergelijkingen en de resultaten werden op verschillende manieren met elkaar vergeleken. De resultaten van de infusietest werden vergeleken met die van de volume-druk test. De resultaten van een analytische berekeningswijze werden vergeleken met die van een 'curve-fit' oplossing. De parameters werden berekend op verschillende tijdstippen na het begin van de test en de uitkomsten werden met elkaar vergeleken. Verschillende volumina werden gebruikt, zowel bij de infusie test als bij de volume-druk test, en het effect hiervan op de modelparameters werd nagegaan. Tenslotte werd ook nog het model van de auteurs vergeleken met dat van Marmarou.

De infusietest leverde in ieder opzicht meer stabiele en betrouwbare uitkomsten op dan de volume-druk test. De 'curve-fit' oplossing leverde een nauwkeuriger benadering van het intracraniële drukverloop op dan de analytische methode. Bij de volume-druk test leverde de analytische berekening zelfs uitkomsten op die in het geheel niet betrouwbaar waren. De betrouwbaarheid nam toe met het gebruik van grotere volumina.

De waarden van de absorptieweerstand kwamen overeen met die van de literatuur. De liquorproductie daarentegen was aanzienlijk hoger dan de waarden van 2.0 tot 3.4 ml/uur gepubliceerd in de literatuur. Als men echter een sinusdruk van 5 mm Hg aanneemt, dan komt de liquorproductie beter overeen met de literatuurgegevens (4.5 ml/uur voor een constante liquorproductie en 4.1 ml/uur voor een druk-afhankelijke liquorproductie).

Ons model beschreef het verloop van de intracraniële druk nauwkeuriger dan het Marmarou model. Dit was vooral het geval bij de infusietest. Bovendien leverde ons model stabielere uitkomsten op voor de berekening van de parameters op verschillende tijdstippen na het begin van de test.

REFERENCES

- ADOLPH RJ; FUKUSUMI H; FOWLER NO: Origin of cerebrospinal fluid pulsations. Am. J. Physiol., 212, 840-846, 1967.
- AGARWAL GC; BERMAN BM; STARK L: A lumped parameter model of the cerebrospinal fluid system. IEEE Trans. Biomed. Eng., 16, 45-53, 1969.
- AGNOLI A; BATTISTINI N; BOZZAO L; FIESCHI C: Drug action on regional cerebral blood flow in cases of acute cerebro-vascular involvement. Acta Neurol. Scand., 41, Suppl. 14, 142-144, 1965.
- AMES A III; HIGASHI K; NESBETT FB: Effects of P_{CO_2} , acetazolamide and ouabain on volume and composition of choroid-plexus fluid. J. Physiol., 181, 516-524, 1965.
- ANTONI N: Variations in respiratory and pulse pressure in spinal subarachnoid space, and their importance in subarachnoid spinal block, Svenska Läk.-Sällsk. Förhandl., 57, 119-166, 1931.
- ANTONI N: Pressure curves from the cerebrospinal fluid. Acta Med. Scand., Suppl. 170, 439-462, 1946.
- AYALA G: Über den diagnostischen Wert des Liquordruckes und einen Apparat zu seiner Messung. Z. ges. Neurol. Psychiat., 84, 42-95, 1923.
- AYALA G: Die Physiopathologie der Mechanik des Liquor cerebrospinalis und der Rachidealquotient. Mschr. Psychiat. Neurol., 58, 65-101, 1925.
- BARNES RW; MCGRAW CP: A new on-line portable ICP data processor. In: Intracranial Pressure II eds. N Lundberg, U Pontén, M Brock, Springer-Verlag, Berlin-Heidelberg-New York, 389-390, 1975.
- BARRÉ JA; SCHRAPP R: Sur la pression du liquide céphalo-rachidien. Bull. méd. Paris, 35, 63, 1921.
- BECHER E: Über photographische registrierte Hirnbewegungen. Mitt. Grenzgeb. Med. Chir., 35, 329-342, 1922.
- BEDFORD THB: The effect of variations in the subarachnoid pressure on the venous pressure in the superior longitudinal sinus and in the torcular of the dog. J. Physiol., 101, 362-368, 1942.

- BENABID AL: Contribution à l'étude de l'hypertension intracrânienne modèle mathématique, MD Thesis, Grenoble University, 1970.
- BENABID AL; ROUGEMONT J de; BARGE M: CSF dynamics: A mathematical approach. In: Intracranial Pressure II eds. N Lundberg, U Pontén, M Brock, Springer-Verlag, Berlin-Heidelberg-New York, 54-60, 1975.
- BENABID AL; PERSAT JC; PIQUARD JF; BARGE M; CHIROSSEL JP: Rheographic assessment of cerebral blood volume and correlations with changes in intracranial pressure. *Acta Neurochir. (Wien)*, 34, 287-294, 1976.
- BENABID AL; ROUGEMONT J de; CHIROSSEL JP; BARGE M: Does the pressure-volume relationship exist? In: Intracranial Pressure IV eds. K Shulman, A Marmarou, JD Miller, DP Becker, GH Hochwald, M Brock, Springer-Verlag, Berlin-Heidelberg-New York, 60-65, 1980.
- BERING EA; INGRAHAM FD: The arterial pulsation of the cerebrospinal fluid. *Tr. Am. Neurol.*, 78, 49-54, 1953.
- BERING EA: Choroid plexus and arterial pulsation of cerebrospinal fluid. *Arch. Neurol. Psychiat.*, 73, 165-172, 1955.
- BERING EA: Problems of the dynamics of the cerebrospinal fluid with particular reference to the formation of cerebrospinal fluid and its relationship to cerebral metabolism. *Clin. Neurosurg.*, 5, 77-97, 1958.
- BERING EA: Cerebrospinal fluid production and its relationship to cerebral metabolism and cerebral blood flow. *Am. J. Physiol.*, 197, 825-828, 1959.
- BERING EA: Circulation of the cerebrospinal fluid. *J. Neurosurg.*, 19, 405-413, 1962.
- BERING EA; SATO O: Hydrocephalus: Changes in formation and absorption of cerebrospinal fluid within the cerebral ventricles. *J. Neurosurg.*, 20, 1050-1063, 1963.
- BLOCH R; TALALLA A: A mathematical model of cerebrospinal fluid dynamics. *J. Neurol. Sci.*, 27, 485-498, 1976.
- BØRGESEN SE; GJERRIS F; SØRENSEN SC: The resistance to cerebrospinal fluid absorption in humans. *Acta Neurol. Scand.*, 57, 88-96, 1978.
- BØRGESEN SE; GJERRIS F; SØRENSEN SC: Intracranial pressure and conductance to outflow of cerebrospinal fluid in normal-pressure hydrocephalus. *J. Neurosurg.*, 50, 489-493, 1979.
- BØRGESEN SE; GJERRIS F; SØRENSEN SC: Cerebrospinal fluid conductance and compliance of the craniospinal space in normal-pressure hydrocephalus. *J. Neurosurg.*, 51, 521-525, 1979.

- BOULAY GH du: Pulsatile movements in the CSF pathways. Br. J. Radiol., 39, 255-262, 1966.
- BOULAY GH du; EL GAMMAL T: The classification, clinical value and mechanism of sella turcica changes in raised intracranial pressure. Br. J. Radiol., 39, 422-442, 1966.
- BROCK M; DIEFENTHALER K; ZYWIETZ C; PÖLL W; MOCK P; DIETZ H: Amplitude analysis of intracranial pressure recordings. In: Intracranial Pressure II eds. N Lundberg, U Pontén, M Brock, Springer-Verlag, Berlin-Heidelberg-New York, 391, 1975.
- BROCK M; ZILLIG C; WIEGAND H; ZYWIETZ C; MOCK P; DIETZ H: The effect of dexamethasone on intracranial pressure in patients with supratentorial tumors. In: Brain Edema. Formation and Resolution. eds. H Pappius, W Feindel, Springer-Verlag, Berlin-Heidelberg-New York, 330-336, 1976.
- BROCK M; ZILLIG C; WIEGAND H; ZYWIETZ C; MOCK P: The influence of dexamethasone therapy on ICP in patients with tumors of the posterior fossa. In: Intracranial Pressure III eds. JWF Beks, DA Bosch, M Brock, Springer-Verlag, Berlin-Heidelberg-New York, 236-246, 1976.
- BROCK M; ZYWIETZ C; MOCK P; WIEGAND H; ZILLIG C; TAMBURUS WM: Reliability and reproduceability of ICP frequency analysis. In: Intracranial Pressure III eds. JWF Beks, DA Bosch, M Brock, Springer-Verlag, Berlin-Heidelberg-New York, 288-294, 1976.
- BURROWS G: Disorders of the cerebral circulation, Longman, London, 1846.
- BURTON AC: Relation of structure to function of the tissues of the wall of blood vessels. Physiol. Rev., 34, 619-642, 1954.
- CALHOUN MC; HURT HD; EATON HD; ROUSSEAU JE; HALL RC: Rates of formation and absorption of cerebrospinal fluid in holstein male calves. Bull. 401, Storrs Agricultural Experiment station. The University of Connecticut, Storrs, 1967.
- CAREY ME; VELA AR: Effect of systemic arterial hypotension on the rate of cerebrospinal fluid formation in dogs. J. Neurosurg., 41, 350-355, 1974.
- CASTEL JP; COHADON F: The pattern of cerebral pulse: Automatic Analysis. In: Intracranial Pressure III eds. JFW Beks, DA Bosch, M Brock, Springer-Verlag, Berlin-Heidelberg-New York, 303-307, 1976.
- COBEN LA; SMITH KR: Iodide transfer at four cerebrospinal fluid sites in the dog: evidence for spinal iodide carrier transport. Exp. Neurol., 23, 76-90, 1969.
- COHADON F; CASTEL JP; NOUILLANT A; VANDENDRIESSCHE M: Volume pressure relationship in clinical and experimental conditions of raised ICP.

- In: Intracranial Pressure II eds. N Lundberg, U Pontén, M Brock, Springer-Verlag, Berlin-Heidelberg-New York, 107-112, 1975.
- CORBIN SD; REAM AK; SCHMIDT EV; SILVERBERG GD; FRYER TB: Data display for intracranial pressure monitoring. In: Intracranial Pressure IV eds. K Shulman, A Marmarou, JD Miller, DP Becker, GM Hochwald, M Brock, Springer-Verlag, Berlin-Heidelberg-New York, 426-428, 1980.
- COSTABILE GV; PROBST Ch; SCHÖNHOLZER AM: Further experiences with the intrathecal infusion test in the management of the communicating hydrocephalus In: Intracranial Pressure V, in press 1983.
- CREVEL H van: Papilloedema, CSF pressure, and CSF flow in cerebral tumours. J. Neurol. Neurosurg. Psychiat., 42, 493-500, 1979.
- CSERR HF: Potassium exchange between cerebrospinal fluid, plasma and brain. Am. J. Physiol., 209, 1219-1226, 1965.
- CSERR HF: Physiology of the choroid plexus. Physiol. Rev., 51, 273-311, 1971.
- CUSHING H: Some experimental and clinical observations concerning states of increased intracranial tension. Am. J. Med. Sci., 124, 375-400, 1902.
- CUSHING H; GOETSCH E: Concerning the secretion of infundibular lobe of the pituitary body and its presence in the cerebrospinal fluid. Am. J. Physiol., 27, 60-86, 1910.
- CUSHING H: Studies in intracranial physiology and surgery. London, Oxford University Press, 1925.
- CUTLER RWP; PAGE L; GALICICH J; WATTERS CV: Formation and absorption of cerebrospinal fluid in man. Brain, 91, 707-720, 1968.
- DANDY WE: Experimental hydrocephalus. Ann. Surg., 70, 129-142, 1919.
- DARDENNE G; DEREYMAEKER A; LACHERON JM: Cerebrospinal fluid pressure and pulsatility. Europ. Neurol., 2, 193-216, 1969.
- DAVSON H: Physiology of the cerebrospinal fluid. Churchill, London, 1967.
- DAVSON H; HOLLINGSWORTH G; SEGAL MB: The mechanism of drainage of the cerebrospinal fluid. Brain, 93, 665-678, 1970.
- DEREYMAEKER A; STEVENS A; ROMBOUTS JJ; LACHERON JM; PIERQUIN A: Study on the influence of the arterial pressure upon the morphology of cisternal CSF pulsations. Europ. Neurol., 5, 107-114, 1971.
- DI ROCCO C; DI TRAPANI G; PETTOROSSO VE; CALDARELLI M: On the pathology of experimental hydrocephalus induced by artificial increase in endoventricular CSF pulse pressure. Child's Brain, 5, 81-95, 1979.
- DIXON WE; HALLIBURTON WD: The cerebrospinal fluid. II Cerebrospinal pressure. J. Physiol., 48, 128-153, 1914.

- DUMKE PR; SCHMIDT CF: Quantitative measurements of cerebral blood flow in the macaque monkey. *Am. J. Physiol.*, 13, 421-431, 1943.
- DUNBAR HS; GUTHRIE TC; KARPELL B: A study of the cerebrospinal fluid pulse wave. *Arch. Neurol.*, 14, 624-630, 1966.
- EKSTEDT J: CSF hydrodynamics studied by means of constant pressure infusion technique. In: *Intracranial Pressure II* eds. N Lundberg, U Pontén, M Brock, Springer-Verlag, Berlin-Heidelberg-New York, 35-41, 1975.
- EKSTEDT J; FRIDEN H: CSF hydrodynamics especially in the adult hydrocephalus syndrome. In: *Intracranial Pressure III* eds. JWF Beks, DA Bosch, M Brock, Springer-Verlag, Berlin-Heidelberg-New York, 177-185, 1976.
- EKSTEDT J: CSF hydrodynamic studies in man. 1. Method of constant pressure CSF infusion. *J. Neurol. Neurosurg. Psychiat.*, 40, 105-119, 1977.
- EKSTRÖM-JODAL B: On the relation between blood pressure and blood flow in the canine brain with particular regard to the mechanism responsible for cerebral blood flow autoregulation. *Acta Physiol. Scand.*, Suppl. 350, 1-28, 1970.
- EKSTRÖM-JODAL B; HÄGGENDAL E; NILSSON NJ: Cerebral venous oxygen saturation during rapid changes in the arterial blood pressure. An oxymetric study in dogs. *Acta Physiol. Scand.*, Suppl. 350, 43-50, 1970.
- EVANS JP; ESPEY FF; KRISTOFF FV; KIMBELL FD; RYDER HW: Experimental and clinical observations on rising intracranial pressure. *Arch. Surg.*, 63, 107-114, 1951.
- EVANS JP: Increased intracranial pressure. Its physiology and management. *Surg. Clin. N. Am.*, 36, 233-242, 1956.
- FITCH W; BARKER J; McDOWALL DG; JENNETT WB: The effect of methoxyflurane on cerebrospinal fluid pressure in patients with and without intracranial space-occupying lesions. *Br. J. Anaesth.*, 41, 564-573, 1969.
- FLEXNER LB; CLARK JH; WEED LH: The elasticity of the dural sac and its contents. *Am. J. Physiol.*, 101, 292-303, 1932.
- FLEXNER LB; WEED LH: Factors concerned in positional alterations of intracranial pressure. *Am. J. Physiol.*, 104, 681-692, 1933.
- FOG M: Influence of intracranial hypertension upon the cerebral circulation. *Arch. Psychiat. (Kbh)*, 8, 191-198, 1933.
- FOG M: Om piaarteriernes vasmotoriske reaktioner. Et bidrag til hjernes kredsløbsfysiologi. *Disputats Levin og Munksgaard, Copenhagen*, 1934.
- FOLDES FF; KEUTMAN E; HUNT RD: The effect of continuous removal of cerebrospinal fluid on cerebrospinal fluid pressure. *Anesthesist.*, 7, 261-265, 1958.

- FRAZIER CH; PEET MM: The action of glandular extracts on the secretion of cerebrospinal fluid. *Am. J. Physiol.*, 36, 464-487, 1915.
- FRIDÉN H; EKSTEDT J: CSF pressure-volume relation and pulse related CSF pressure variations in man. In: *Intracranial Pressure IV* eds. K Shulman, A Marmarou, JD Miller, DP Becker, GM Hochwald, M Brock, Springer-Verlag, Berlin-Heidelberg-New York, 93-96, 1980.
- FURESE M; HASUO M; BROCK M; DIETZ H: The role of CSF resorption on the intracranial pressure/volume relationship. In: *Intracranial Pressure III* eds. JWF Beks, DA Bosch, M Brock, Springer-Verlag, Berlin-Heidelberg-New York, 20-24, 1976.
- GARDNER WJ: Hydrodynamic mechanisms of syringomyelia: Its relationship to myelocoele. *J. Neurol. Neurosurg. Psychiat.*, 28, 247-259, 1965.
- GERLACH J: Zerebraler Grenzdruk und Hirnpuls. *Klinische Untersuchungen und Ergebnisse. Acta Neurochir.*, 120-158, 1952.
- GESSEY G; BAKER P; WHITE A; FIRTH JL: Lumbar sac infusion test revisited. In: *Intracranial Pressure IV* eds. K Shulman, A Marmarou, JD Miller, DP Becker, GM Hochwald, M Brock, Springer-Verlag, Berlin-Heidelberg-New York, 456-459, 1980.
- GILLAND O: CSF dynamic diagnosis of spinal block II. The spinal CSF pressure-volume curve. *Acta Neurol. Scand.*, 41, 487-496, 1965.
- GJERRIS F: Intraventricular pressure in patients with chronic subdural hematomas before and after evacuation of the hematoma. In: *Intracranial Pressure III* eds. JWF Beks, DA Bosch, M Brock, Springer-Verlag, Berlin-Heidelberg-New York, 85-87, 1976.
- GJERRIS F; BØRGESEN SE; SØRENSEN SC: Predicting the results of ventricular shunting in normal pressure hydrocephalus by lumbo-ventricular perfusion test. In: *Intracranial Pressure IV* eds. K Shulman, A Marmarou, JD Miller, DP Becker, GM Hochwald, M Brock, Springer-Verlag, Berlin-Heidelberg-New York, 494-497, 1980.
- GODIN D; STEVENAERT A; LHOMMEL R: Study of the CSF pulsation transfer: Application to the frequency analysis. In: *Intracranial Pressure IV* eds. K Shulman, A Marmarou, JD Miller, DP Becker, GM Hochwald, M Brock, Springer-Verlag, Berlin-Heidelberg-New York, 191-194, 1980.
- GOLDENSOHN ES; WHITEHEAD RW; PARRY TM; SPENCER JN; GROVER RF; DRAPER WB: Studies on diffusion respiration. IX. Effect of diffusion respiration and high concentrations of CO₂ on cerebrospinal fluid pressure of anesthetized dogs. *Am. J. Physiol.*, 165, 334-340, 1951.
- GRAHAM SH; HACKENBERRY LE; REA G; MINER ME: A microcomputer system for

- ICP analysis. In: Intracranial Pressure IV eds. K Shulman, A Marmarou, JD Miller, DP Becker, GM Hochwald, M Erock, Springer-Verlag, Berlin-Heidelberg-New York, 409-412, 1980.
- GRANHOLM L; LOFGREN J: A discussion of the intracranial pressure-volume relationship in normal pressure hydrocephalus. In: Intracranial Pressure II eds. N Lundberg, U Pontén, M Brock, Springer-Verlag, Berlin-Heidelberg-New York, 137-140, 1975.
- GREENFIELD JC; TINDALL GT: Effect of acute increase in intracranial pressure on blood flow in the internal carotid artery of man. *J. Clin. Invest.*, 44, 1343-1351, 1965.
- GREENFIELD JC; TINDALL GT: Effect of norepinephrine, epinephrine, and angiotension on blood flow in the internal carotid artery of man. *J. Clin. Invest.*, 47, 1672-1684, 1968.
- GRUBB RL; RAICHLE ME; EICHLING JO; TER-POGOSSIAN MM: The effects of changes in PaCO₂ on cerebral blood volume, blood flow and vascular mean transit time. *Stroke*, 5, 630-639, 1974.
- GRUBB RL; RAICHLE ME; PHELPS ME; RATCHESON RA: Effects of increased intracranial pressure on cerebral blood volume, blood flow, and oxygen utilization in monkeys. *J. Neurosurg.*, 43, 385-398, 1975.
- GUILLAUME J; JANNY P: Manométrie intracrânienne continue. Intérêt de la méthode et premiers résultats. *Rev. Neurol.*, 84, 131-142, 1951.
- GUINANE JE: An equivalent circuit analysis of cerebrospinal fluid hydrodynamics. *Am. J. Physiol.*, 223, 425-430, 1972.
- GUINANE JE: Cerebrospinal fluid resistance and compliance in subacutely hydrocephalic cats. *Neurology*, 24, 138-142, 1974.
- GUINANE JE: Cerebrospinal fluid pulse pressure and brain compliance in adult cats. *Neurology*, 25, 559-564, 1975.
- HAGGENDAL E; JOHANSSON B: Effects of arterial carbon dioxide tension and oxygen saturation on cerebral blood flow autoregulation in dogs. *Acta Physiol. Scand.*, 66, Suppl. 258, 27-53, 1965.
- HAGGENDAL E; LOFGREN J; NILSSON NJ; ZWETNOW NN: Effects of varied cerebrospinal fluid pressure on cerebral blood flow in dogs. *Acta Physiol. Scand.*, 79, 262-271, 1970.
- HAKIM S; VENEGAS JG; BURTON JD: The physics of the cranial cavity, hydrocephalus and normal pressure hydrocephalus. *Surg. Neurol.*, 5, 187-210, 1976.
- HAMER J; HOYER S; STOECKEL H; ALBERTI E; WEINHARDT F: Cerebral blood flow

- and cerebral metabolism in acute increase of intracranial pressure. *Acta Neurochir.*, 28, 95-110, 1973.
- HAMER J; ALBERTI E; HOYER S; WIEDEMANN K: Influence of systemic and cerebral vascular factors in the cerebrospinal fluid pulse waves. *J. Neurosurg.*, 46, 36-45, 1977.
- HAMIT HF; BEALL AC; DE BAKEY ME; Hemodynamic influences upon brain and cerebrospinal fluid pulsations and pressures. *J. Trauma*, 5, 174-184, 1965.
- HAMMERSTAD JP; LORENZO AV; CUTLER RWP: Iodide transport from the spinal sub-arachnoid fluid in the cat. *Am. J. Physiol.*, 216, 353-358, 1969.
- HARPER AM: Autoregulation of cerebral blood flow: Influence of arterial blood pressure on the blood flow through the cerebral cortex. *J. Neurol. Neurosurg. Psychiat.*, 29, 398-403, 1966.
- HARTMANN A; ALBERTI E: Differentiation of communicating hydrocephalus and presenile dementia by continuous recording of cerebrospinal fluid pressure. *J. Neurol. Neurosurg. Psychiat.*, 40, 630-640, 1977.
- HARTMANN A: Continuous monitoring of CSF pressure in acute subarachnoid hemorrhage. In: *Intracranial Pressure IV* eds. K Shulman, A Marmarou, JD Miller, DP Becker, GM Hochwald, M Brock, Springer-Verlag, Berlin-Heidelberg-New York, 220-228, 1980.
- HASE U; REULEN HJ; MEINIG G; SCHÜRMAN K: The influence of the decompressive operation on the intracranial pressure and the pressure-volume relation in patients with severe head injuries. *Acta Neurochir.*, 45, 1-13, 1978.
- HEDGES TR; WEINSTEIN JD; KASSELL N; STEIN S: Cerebrovascular responses to increased intracranial pressure. *J. Neurosurg.*, 21, 292-297, 1964.
- HEISY SR; HELD D; PAPPENHEIMER JR: Bulk flow and diffusion in the cerebrospinal fluid system of the goat. *Am. J. Physiol.*, 203, 775-781, 1962.
- HILL L: *The physiology and pathology of the cerebral circulation.* Churchill, London, 1896.
- HIRSCH H; KORNER K: Über die Druck-Durchblutungs-Relation der Gehirngefäße. *Pflügers Arch. ges. Physiol.*, 280, 316-325, 1964.
- HOCHWALD GM; WALLENSTEIN M: Exchange of albumin between blood, cerebrospinal fluid and brain in the cat. *Am. J. Physiol.*, 212, 1199-1204, 1967.
- HOCHWALD GM; SAHAR A: Effect of spinal fluid pressure on cerebrospinal fluid formation. *Exp. Neurol.*, 32, 30-40, 1971.
- HOFFERBERTH B; MATAKAS F; FRITSCHKA E: A computer model of CSF dynamics. In: *Intracranial Pressure II* eds. N Lundberg, U Pontén, M Brock, Springer-Verlag, Berlin-Heidelberg-New York, 61-66, 1975.

- HOFFMANN O: Mathematische Modelle zur Untersuchung der Liquor Dynamik.
PhD Thesis, Justus Liebig Universität Giessen, 1980.
- HOMBURGER E; HIMWICH WA; ETSTEN B; YORK G; MARESCA R; HIMWICH HE: Effect of pentothal anesthesia on canine cerebral cortex. *Am. J. Physiol.*, 147, 343-345, 1946.
- HOWE HS: Physiologic mechanism for the maintenance of intracranial pressure. *Arch. Neurol. Psychiat.*, 20, 1048-1064, 1928.
- HULME A; COOPER R: Multi-channel data acquisition and analysis in clinical practice. In: *Intracranial Pressure II* eds. N Lundberg, U Pontén, M Brock, Springer-Verlag, Berlin-Heidelberg-New York, 387-388, 1975.
- HUSSEY F; SCHANZER B; KATZMAN R: A simple constant-infusion manometric test for measurement of CSF absorption. II. Clinical studies. *Neurology*, 20, 665-680, 1970.
- IKEYAMA A; NAKAYA T; TERAOKA M; HASUO M; MEADA S; KUCHIWAKI H; FURESE M; NAGAI H: Blood pressure factors causing raised ICP. In: *Intracranial Pressure IV* eds. K Shulman, A Marmarou, JD Miller, DP Becker, GM Hochwald, M Brock, Springer-Verlag, Berlin-Heidelberg-New York, 195-197, 1980.
- JANNY P: La pression intra-crânienne chez l'homme. Méthode d'enregistrement, étude de ses variations et des rapports avec des signes cliniques et ophtalmologiques. Thèse, Clermont-Ferrand reproduction, Paris, 1950.
- JANNY P; JOUAN JP; JANNY L; GOURGAND M; GUEIT UM: A statistical approach to long-term monitoring of intracranial pressure. In: *Intracranial pressure* eds. M Brock, H Dietz, Springer-Verlag, Berlin-Heidelberg-New York, 59-64, 1972.
- JANNY P: La surveillance de la pression intra-crânienne en neurochirurgie. *Neurochir.*, 521-554, 1974.
- JENNETT WB; BARKER J; FITCH W; McDOWALL DG: Effect of anaesthesia on intracranial pressure in patients with space-occupying lesions. *Lancet*, 1, 61-64, 1969.
- JENNETT B: Importance of ICP monitoring in clinical management of patients with intracranial lesions. Chairman's Comments. In: *Intracranial Pressure II* eds. N Lundberg, U Pontén, M Brock, Springer Verlag, Berlin-Heidelberg-New York, 493-495, 1975.
- JENNETT B: Closing Comments. In: *Intracranial Pressure III* eds. JWF Beks, DA Bosch, M Brock, Springer-Verlag, Berlin-Heidelberg-New York, 343-346, 1976.
- JOHNSTON IH; ROWAN JO; HARPER AM; JENNETT WB: Raised intracranial pressure and

- cerebral blood flow: 1. Cisterna magna infusion in primates. *J. Neurol. Neurosurg. Psychiat.*, 35, 285-296, 1972.
- JOHNSTON IH; ROWAN JO; HARPER AM; JENNETT WE: Raised intracranial pressure and cerebral blood flow: 2. Supratentorial and infratentorial mass lesions in primates. *J. Neurol. Neurosurg. Psychiat.*, 36, 161-170, 1973.
- JOHNSTON IH; GILDAY DL; PATERSON A; HENDRICK EB: The definition of a reduced CSF absorption syndrome: Clinical and experimental studies. In: *Intracranial Pressure II* eds. N Lundberg, U Pontén, M Prock, Springer-Verlag, Berlin-Heidelberg-New York, 50-53, 1975.
- KANZOW E: Diskussion in Pharmakologie der lokalen Gehirndurchblutung: Messmethoden und Ergebnisse. In: *Ein internationales Symposium, Bonn: Aertzliche Forschungen* eds. E Betz, R Wüllenweber, Beiheft, 177-178, 1968.
- KATZMAN R; HUSSEY F: A simple constant infusion manometric test for measurement of CSF absorption. *Neurology*, 20, 534-544, 1970.
- KAUFMAN B: The "empty" sella turcica - a manifestation of the intrasellar subarachnoid space. *Radiology*, 90, 931-941, 1968.
- KELLIE G: An account of the appearances observed in the dissection of two of three individuals presumed to have perished in the storm of the 3D, and whose bodies were discovered in the vicinity of Leith on the morning of the 4th, November 1821, with some reflections on the pathology of the brain. *Trans. Med.-Chir. Soc. Edinb.*, 1, 84-169, 1824.
- KETY S: Remarks. In: *Cerebral Vascular Diseases. Transactions of the Fourth Conference, Princeton, N.J.*, eds. CH Millikan, RG Siekert, JP Whisnant, Grune and Stratton, New York, 83, 1964.
- KEY G; RETZIUS A: *Anatomie des Nervensystems und des Bindegewebes*. Stockholm, 1875.
- KING AL; LAWTON RW: The elasticity of soft body tissues. *The Scientific Monthly*, 71, 258-260, 1950.
- KNOLL Ph: *Über die Druckschwankungen in der Cerebrospinal Flüssigkeit und den Wechsel in der Blutfülle des centralen Nervensystems*. Sitzungsberichte der Kaiserlichen Akademie der Wissenschaften, 93, 217-246, 1886.
- KOGURE K; SCHEINBERG P; FUJISHIMA M; BUSTO R; REINMUTH OM: Effects of hypoxia on cerebral autoregulation. *Am. J. Physiol.*, 219, 1393-1396, 1970.
- KULLBERG G; WEST KA: Influence of corticosteroids on the ventricular fluid pressure. *Acta Neurol. Scand.*, 41, Suppl. 13, 445-452, 1965.
- KULLBERG G: A method for statistical analysis of intracranial pressure recordings. In: *Intracranial Pressure* eds. M Brock, H Dietz, Springer-Verlag, Berlin-Heidelberg-New York, 65-69, 1972.

- KULLBERG G; SUNDBÄRG G: Reduction of raised intracranial pressure following infusion of mannitol. A review of clinical pressure recordings. In: Intracranial Pressure III eds. JWF Beks, DA Bosch, M Brock, Springer-Verlag, Berlin-Heidelberg-New York, 224-227, 1976.
- LAMAS E; LOBATO RD; ESPARZA J: Long term intraventricular pressure measurement in chronic communicating hydrocephalus. In: Intracranial Pressure IV eds. K Shulman, A Marmarou, JD Miller, DP Becker, GM Hochwald, M Brock, Springer-Verlag, Berlin-Heidelberg-New York, 505-510, 1980.
- LANGÉ SA de; DERNIER VAN DER GON JJ; VLIÉGER M de: Preliminary study on the ventricular pressure in hydrocephalic patients. *Psychiat. Neurol. Neurochir.*, 71, 267-273, 1968.
- LANGÉ SA de; DERNIER VAN DER GON JJ; VLIÉGER M de: Ventricular CSF pressure in relation to the body position in hydrocephalic patients. In: Third European Congress of Neurosurgery, Excerpta Medica Foundation, Amsterdam, 148, 1967.
- LANGFITT TW; WEINSTEIN JD; KASSEL NF: Cerebral vasomotor paralysis produced by intracranial hypertension. *Neurology*, 15, 622-641, 1965.
- LANGFITT TW; KASSEL NF; WEINSTEIN JD: Cerebral blood flow with intracranial hypertension. *Neurology*, 15, 761-773, 1965.
- LANGFITT TW; WEINSTEIN JD; KASSEL NF: Vascular factors in head injury: contribution to brain swelling and intracranial hypertension. In: Head Injury: Proc. of the Conference, JB Lippincott, Philadelphia, 172-194, 1966.
- LANGFITT TW; WEINSTEIN JD; KASSEL NF; GAGLIARDI LJ; SHAPIRO HM: Compression of cerebral vessels by intracranial hypertension. I. Dural sinus pressures. *Acta Neurochir.*, 15, 222-233, 1966.
- LANGFITT TW: Increased intracranial pressure. *Clin. Neurosurg.*, 16, 436-471, 1969.
- LANGFITT TW: Pathophysiology of increased ICP. In: Intracranial Pressure eds. M Brock, H Dietz, Springer-Verlag, Berlin-Heidelberg-New York, 361-364, 1972.
- LANGFITT TW: Intracranial volume-pressure relationship. In: Intracranial Pressure II eds. N Lundberg, U Pontén, M Brock, Springer-Verlag, Berlin-Heidelberg-New York, 69-76, 1975.
- LEECH P; MILLER JD: Intracranial volume-pressure relationships during experimental brain compression in primates. 1. Pressure responses to changes in ventricular volume. 2. Effect of induced changes in systemic arterial pressure and cerebral blood flow. 3. Effect of mannitol and

- hyperventilation. *J. Neurol. Neurosurg. Psychiat.*, 37, 1093-1111, 1974.
- LEYDEN E: Beiträge und Untersuchungen zur Physiologie und Pathologie des Gehirns. Über Hirndruck und Hirnbewegungen. *Arch. für Pathologische Anatomie und Physiologie und für Klinische Medizin*, 37, 519-559, 1866.
- LIM ST; POTTS DG; DEONARINE V; DECK MDF: Ventricular compliance in dogs with and without aqueductal obstruction. *J. Neurosurg.*, 39, 463-473, 1973.
- LÖFGREN J: Pressure-volume relationships of the cerebrospinal fluid system. Thesis, University of Göteborg, 1973.
- LÖFGREN J; ESSEN C von; ZWETNOW NN: The pressure-volume curve of the cerebrospinal fluid space in dogs. *Acta Neurol. Scand.*, 49, 557-574, 1973.
- LÖFGREN J; ZWETNOW NN: Cranial and spinal components of the cerebrospinal fluid pressure-volume curve. *Acta Neurol. Scand.*, 49, 575-585, 1973.
- LÖFGREN J: Effects of variations in arterial pressure and arterial carbon dioxide tension on the CSF pressure-volume relationships. *Acta Neurol. Scand.*, 49, 586-598, 1973.
- LÖFGREN J; ZWETNOW NN: Influence of a supratentorial expanding mass on intracranial pressure-volume relationships. *Acta Neurol. Scand.*, 49, 599-612, 1973.
- LÖFGREN J: Mechanical basis of the pressure-volume curve. In: *Intracranial pressure II* eds. N Lundberg, U Pontén, M Brock, Springer-Verlag, Berlin-Heidelberg-New York, 79-81, 1975.
- LÖFGREN J; ZWETNOW NN: Intracranial blood volume and its variation with changes in intracranial pressure. In: *Intracranial Pressure III* eds. JWF Beks, DA Bosch, M Brock, Springer-Verlag, Berlin-Heidelberg-New York, 25-28, 1976.
- LOVE JA; LESLIE RA: Changes in resistance to cerebrospinal fluid absorption during prolonged infusion studies. In: *Intracranial Pressure IV* eds. K Shulman, A Marmarou, JD Miller, DP Becker, GM Hochwald, M Brock, Springer-Verlag, Berlin-Heidelberg-New York, 451-455, 1980.
- LOWELL HM; BLOOR BM: The effect of increased intracranial pressure on cerebrovascular hemodynamics. *J. Neurosurg.*, 34, 760-769, 1971.
- LUNDBERG N: Continuous recording and control of ventricular fluid pressure in neurosurgical practice. *Acta Psychiat. Neurol. Scand.*, 36, Suppl.149, 1960.
- LUNDBERG N; CRONQVIST S; KJÄLLQUIST A: Clinical investigations of interrelations between intracranial pressure and intracranial hemodynamics. *Progr. Brain Res.*, 30, 69-75, 1968.

- MAGENDIE F: Recherches physiologiques et cliniques sur le liquide céphalo-rachidien ou cérébro-spinal, Paris, 1842.
- MAIRA G; ROSSI GF; VIGNATTI A: Intracranial pressure and pathogenesis of "normotensive" hydrocephalus. In: Intracranial Pressure II eds. N Lundberg, U Pontén, M Brock, Springer-Verlag, Berlin-Heidelberg-New York, 128-132, 1975.
- MARMAROU A: A theoretical and experimental evaluation of the cerebrospinal fluid system, PhD Thesis, Drexel University, 1973.
- MARMAROU A; SHULMAN K; LaMORGESE J: A compartmental analysis of compliance and outflow resistance and the effects of elevated blood pressure. In: Intracranial Pressure II eds. N Lundberg, U Pontén, M Brock, Springer-Verlag, Berlin-Heidelberg-New York, 86-88, 1975.
- MARMAROU A; SHULMAN K; LaMORGESE J: Compartmental analysis of compliance and outflow resistance of the cerebrospinal fluid system. J. Neurosurg., 43, 523-534, 1975.
- MARMAROU A; SHULMAN K; ROSENDE RM: A nonlinear analysis of the cerebrospinal fluid system and intracranial pressure dynamics. J. Neurosurg., 48, 332-344, 1978.
- MARTINS AN; WILEY JK; MYERS PW: Dynamics of the cerebrospinal fluid and the spinal dura mater. J. Neurol. Neurosurg. Psychiat., 35, 468-473, 1972.
- MARTINS AN: Resistance to drainage of cerebrospinal fluid: Clinical measurement and significance. J. Neurol. Neurosurg. Psychiat., 36, 313-318, 1973.
- MARQUARDT DW: An algorithm for least-squares estimation of nonlinear parameters. J. Soc. Indust. Appl. Math., 11, 431-441, 1963.
- MASON J; PRICE DJ; TRIMNELL S: The integration of ICP with other monitoring signals on a single computer data base. In: Intracranial Pressure IV eds. K Shulman, A Marmarou, JD Miller, DP Becker, GM Hochwald, M Brock, Springer-Verlag, Berlin-Heidelberg-New York, 429-431, 1980.
- MASSERMAN JH: Cerebrospinal hydrodynamics. Arch. Neurol. Psychiat., 32, 523-553, 1934.
- MASSERMAN JH: Correlations of the pressure of the cerebrospinal fluid with age, blood pressure and the pressure index. Arch. Neurol. Psychiat., 34, 564-566, 1935.
- MASSERMAN JH: Studies of the volume elasticity of the human ventriculo-subarachnoid system. J. Comp. Neurol., 61, 543-552, 1935.
- McDOWALL DG: Interrelationships between blood oxygen tensions and cerebral blood flow. Int. Anaesth. Clin., 4, 205-219, 1966.

- McKISSOCK W; RICHARDSON A; BLOOM WH: Subdural hematoma. A review of 389 cases. *Lancet*, I, 1365-1370, 1960.
- MILLER JD; GARIBI J: Intracranial volume-pressure relationship during continuous monitoring of ventricular fluid pressure. In: *Intracranial Pressure* eds. M Brock, H Dietz, Springer-Verlag, Berlin-Heidelberg-New York, 270-274, 1972.
- MILLER JD; GARIBI J; PICKARD JD: Induced changes of cerebrospinal fluid volume. *Arch. Neurol.*, 28, 265-269, 1973.
- MILLER JD; PICKARD JD: Intracranial volume/pressure studies in patients with head injury. *Injury*, 5, 265-268, 1974.
- MILLER JD: Volume and pressure in the craniospinal axis. *Clin. Neurosurg.*, 22, 76-105, 1975.
- MILLER JD; LEECH PJ: Assessing the effects of mannitol and steroid therapy on intracranial volume-pressure relationships. *J. Neurosurg.*, 42, 274-281, 1975.
- MILLER JD; LEECH PJ; PICKARD JD: Volume pressure response in various experimental and clinical conditions. In: *Intracranial Pressure II* eds. N Lundberg, U Pontén, M Brock, Springer-Verlag, Berlin-Heidelberg-New York, 97-99, 1975.
- MILLER JD; BECKER DP; WARD JD; SULLIVAN HG; ADAMS WE; ROSNER MJ: Significance of intracranial hypertension in severe head injury. *J. Neurosurg.*, 47, 503-516, 1977.
- MILLER JD; SAKALAS R; WARD JD; YOUNG EF; ADAMS WE; VRIES JK; BECKER DP: Methylprednisolone treatment in patients with brain tumours. *Neurosurg.*, 1, 114-117, 1977.
- MILLER ME; CHRISTENSEN GC; EVANS HE: *Anatomy of the dog*. WB Saunders Co., Philadelphia, 1964.
- MONRO A: *Observations on the structure and function of the nervous system*. Creech and Johnson, Edinburgh, 1783.
- MOSKALENKO YuE; KISLYAKOV YuYa; VAINSHTEIN GB; ZELIKSON BB: Biophysical aspects of the intracranial circulation. *Am. Heart J.*, 83, 401-414, 1972.
- MOSSO A: *Über den Kreislauf des Blutes in menschlichen Gehirn*. Leipzig, Veit and Comp., 1881.
- NAGAI H; IKEYAMA A; FURESE M; MAEDA S; BANNO K; HASUNO M; KUCHIWAKI H: Effect of increased intracranial pressure on cerebral hemodynamics. Observations on CBF, CBV and pO_2 . *Eur. Neurol.*, 8, 52-56, 1972.
- NAKAGAWA Y; TSURU M; YADA K: Site and mechanism for compression of the venous

- system during experimental intracranial hypertension. *J. Neurosurg.*, 41, 427-434, 1974.
- NAKATANI S; OMMAYA AK: Volume pressure curves and pial vascular pressure gradients in the rhesus monkey. In: *Intracranial Pressure II* eds. N Lundberg, U Pontén, M Brock, Springer-Verlag, Berlin-Heidelberg-New York, 89-96, 1975.
- NELSON JR; GOODMAN SJ: An evaluation of the cerebrospinal fluid infusion test for hydrocephalus. *Neurology*, 21, 1037-1053, 1971.
- NOELL W; SCHNEIDER M: Zur Haemodynamik der Gehirndurchblutung bei Liquor-drucksteigerung. *Arch. Psychiat. Nervenkr.*, 118/180, 713-730, 1948.
- NORNES H; AASLID R; LINDEGAARD KF: Intracranial pulse pressure dynamics in patients with intracranial hypertension. *Acta Neurochir.* 38, 177-186, 1977.
- OBENCHAIN TH; STERN WE: II. The origin of undulating ventricular waves and periodic respiration. *Arch. Neurol.*, 29, 295-297, 1973.
- O'CONNELL JEA: The vascular factor in intracranial pressure and the maintenance of the cerebrospinal fluid circulation. *Brain*, 66, 204-228, 1943.
- OLESEN J; PAULSON OB; LASSEN NA: Regional cerebral blood flow in man determined by the initial slope of the clearance of intra-arterially injected Xe-133. *Stroke*, 2, 519-540, 1971.
- OLESEN J: The effect of intracarotid epinephrine, norepinephrine and angiotensin on the regional cerebral blood flow in man. *Neurology*, 22, 978-987, 1972.
- OLESEN J: Quantitative evaluations of normal and pathologic cerebral blood flow regulation to perfusion pressure. Changes in man. *Arch. Neurol.*, 28, 143-149, 1973.
- OPPELT WW; MAREN TH; OWENS ES; RALL DP: Effects of acid-base alterations on cerebrospinal fluid production. *Proc. Soc. Exp. Biol. Med.*, 114, 86-89, 1963.
- OPPELT WW; PATLAK CS; RALL DP: Effect of certain drugs on cerebrospinal fluid production in the dog. *Am. J. Physiol.*, 206, 247-250, 1964.
- PAPPENHEIMER JR; HEISEY SR; JORDAN EF: Active transport of diodrast and phenolsulfonphthalein from cerebrospinal fluid to blood. *Am. J. Physiol.*, 200, 1-10, 1961.
- PAPPENHEIMER JR; HEISEY SR; JORDAN EF; DOWNER JC: Perfusion of the cerebral ventricular system in unanesthetized goats. *Am. J. Physiol.*, 203, 763-774, 1962.

- PETTOROSSO VE; Di ROCCO C; MANCINELLI R; CALDARELLI M; VELARDI F:
Communicating hydrocephalus induced by mechanically increased amplitude
of the intraventricular cerebrospinal fluid pulse pressure: rationale
and method. *Exp. Neurol.*, 59, 30-39, 1978.
- PHELPS ME; GRUBB RL; TER-POGOSSIAN MM: Correlation between PaCO₂ and
regional cerebral blood volume by X-ray fluorescence. *J. Appl. Physiol.*,
35, 274-280, 1973.
- PLUM F; POSNER JB: *Diagnosis of stupor and coma*. Blackwell Scientific Publ.,
1966.
- POLLAY M; CURL F: Secretion of cerebrospinal fluid by the ventricular
ependyma of the rabbit. *Am. J. Physiol.*, 213, 1031-1038, 1967.
- POLLOCK LJ; BOSHES B: Cerebrospinal fluid pressure. *Arch. Neurol. Psychiat.*,
36, 931-974, 1936.
- PONSSSEN H; VAN DEN BOS GC: Influence of the circulation on the CSF pressure
wave. *J. Neurol. Neurosurg. Psychiat.*, 34, 108, 1971.
- PORTNOY HD; CROISSANT PD: A practical method for measuring hydrodynamics
of cerebrospinal fluid. *Surg. Neurol.*, 5, 273-277, 1976.
- PORTNOY HD; CROISSANT PD: Pre- and postoperative cerebrospinal fluid
absorption studies in patients with myelomeningocele shunted for
hydrocephalus. *Child's Brain*, 4, 47-64, 1978.
- QUINCKE H: *Die Lumbalpunktion des Hydrocephalus*. *Berl. Klin. Wschr.*, 28,
929-965, 1891.
- RAICHLE ME; POSNER JB; PLUM F: Cerebral blood flow during and after
hyperventilation. *Arch. Neurol.*, 23, 394-403, 1970.
- RAPELA CE; GREEN HD: Autoregulation of canine cerebral blood flow.
Circ. Res., 15, Suppl. 1, 205-212, 1964.
- REIVICH M; HOLLING HE; ROBERTS B; TOOLE JF: Reversal of blood flow through
the vertebral artery and its effect on cerebral circulation. *New Eng.
J. Med.*, 265, 18, 878-885, 1961.
- REIVICH M: Arterial Pco₂ and cerebral hemodynamics. *Am. J. Physiol.*, 206,
25-35, 1964.
- RICKHAM PP; PENN IA: The place of the ventriculostomy reservoir in the
treatment of myelomeningoceles and hydrocephalus. *Develop. Med. Child
Neurol.*, 7, 296-301, 1965.
- RISBERG J; LUNDBERG N; INGVAR DH: Regional cerebral blood volume during
acute transient rises of the intracranial pressure (plateau waves).
J. Neurosurg., 31, 303-310, 1969.

- ROSOMOFF HL; HOLADAY DA: Cerebral blood flow and cerebral oxygen consumption during hypothermia. *Am. J. Physiol.*, 179, 85-88, 1954.
- ROUGEMONT J de; BENABID AL; CHIROSSEL JP; BARGE M: The brain vasomotor tone index as prognosis leader in severe head injuries. In: *Intracranial Pressure III* eds. JWF Beks, DA Bosch, M Brock, Springer-Verlag, Berlin-Heidelberg-New York, 119-122, 1976.
- ROWAN JO; JOHNSTON IH; HARPER AM; JENNETT WB: Perfusion pressure in intracranial hypertension. In: *Intracranial Pressure* eds. M Brock, H Dietz, Springer-Verlag, Berlin-Heidelberg-New York, 165-170, 1972.
- ROWED DW; LEECH PJ; REILLY PL; MILLER JD: Hypocapnia and intracranial volume-pressure relationship. *Arch. Neurol.*, 32, 369-373, 1975.
- RUBIN RC; HENDERSON ES; OMMAYA AK; WALKER HD; RALL DP: The production of cerebrospinal fluid in man and its modification by acetazolamide. *J. Neurosurg.*, 25, 430-436, 1966.
- RYDER HW; ESPEY FF; KIMBELL FD; PENKA EJ; ROSENAUER A; PODOLSKY B; EVANS JP: Modification of effect of cerebral blood flow on the cerebrospinal fluid pressure by variations in the craniospinal blood volume. *Arch. Neurol. Psychiat.*, 68, 170-174, 1952.
- RYDER HW; ESPEY FF; KIMBELL FD; PENKA EJ; ROSENAUER A; PODOLSKY B; EVANS JP: The mechanism of the change in cerebrospinal fluid pressure following an induced change in the volume of the fluid space. *J. Lab. Clin. Med.*, 41, 428-435, 1953.
- RYDER HW; ESPEY FF; KIMBELL FD; PENKA EJ; ROSENAUER A; PODOLSKY B; EVANS JP: The elasticity of the craniospinal venous bed. *J. Lab. Clin. Med.*, 42, 944, 1953.
- SAGAWA K; GUYTON AC: Pressure-flow relationships in isolated canine cerebral circulation. *Am. J. Physiol.*, 200, 711-714, 1961.
- SAHAR A; HOCHWALD GM; RANSOHOFF J: Experimental hydrocephalus: Cerebrospinal fluid formation and ventricular size as a function of intraventricular pressure. *J. Neurol. Sci.*, 11, 81-91, 1970.
- SAHAR A; HOCHWALD GM; RANSOHOFF J: Cerebrospinal fluid and cranial sinus pressures. Relationship in normal and hydrocephalic cats. *Arch. Neurol.*, 23, 413-418, 1970.
- SAHAR A: Choroidal origin of cerebrospinal fluid. *Isr. J. Med. Sci.*, 8, 594-596, 1972.
- SATO K; FUCHINOUE T; YAHAGI Y: CSF pulse pressure wave changes with normal pressure hydrocephalus. In: *Intracranial Pressure II* eds. N Lundberg,

- U Pontén, M Brock, Springer-Verlag, Berlin-Heidelberg-New York, 133-136, 1975.
- SEVERINGHAUS JW: Blood gas calculator. *J. Appl. Physiol.*, 21, 1108-1116, 1966.
- SHAPIRO HM; LANGFITT TW; WEINSTEIN JD: Compression of cerebral vessels by intracranial hypertension. II. Morphological evidence for collapse of vessels. *Acta Neurochir.*, 15, 222-233, 1966.
- SHAPIRO HM, WYTE SR; HARRIS AB; GALINDO A: Acute intra-operative intracranial hypertension in neurosurgical patients: Mechanical and pharmacologic factors. *Anaesthesiol.*, 37, 399-405, 1972.
- SHAPIRO K; MARMAROU A; SHULMAN K: Characterization of clinical CSF dynamics and neural axis compliance using the pressure-volume index. I. The normal pressure-volume index. *Ann. Neurol.*, 7, 508-514, 1980.
- SHAPIRO K; MARMAROU A: Abnormal brain compliance as a cause of hydrocephalus in children. In: *Intracranial Pressure V*, in press 1983.
- SHAPIRO K; MARMAROU A; CONWAY E: Comparison of bolus and constant infusion technique for determining the resistance to the absorption of CSF. In: *Intracranial Pressure V*, in press 1983.
- SHULMAN K; YARNELL P; RANSOHOFF J: Dural sinus pressure. In normal and hydrocephalic dogs. *Arch. Neurol.*, 10, 575-580, 1964.
- SHULMAN K: Small artery and vein pressures in the subarachnoid space of the dog. *J. Surg. Res.*, 5, 56-61, 1965.
- SHULMAN K; VERDIER GR: Cerebral vascular resistance changes in response to cerebrospinal fluid pressure. *Am. J. Physiol.*, 213, 1084-1088, 1967.
- SHULMAN K; MARMAROU A: Pressure-volume considerations in infantile hydrocephalus. *Develop. Med. Child Neurol.*, 13, Suppl. 25, 90-95, 1971.
- SKLAR FH; ELASHVILI I: The pressure-volume function of brain elasticity. *J. Neurosurg.*, 47, 670-679, 1977.
- SKLAR FH; BEYER CW; RAMANATHAN M; ELASHVILI I; COOPER PR; CLARK WK: Servo-controlled lumbar infusions: A clinical tool for the determination of CSF dynamics as a function of pressure. *Neurosurg.*, 3, 170-175, 1978.
- SKLAR FH; BEYER CW; RAMANATHAN M; CLARK WK: Servo-controlled lumbar infusions in children. *J. Neurosurg.*, 52, 87-98, 1980.
- SKLAR FH; BEYER CW; CLARK WK: Physiological features of the pressure-volume function of brain elasticity in man. *J. Neurosurg.*, 53, 166-172, 1980.
- SKLAR FH; BEYER CW; HAGLER H; RAMANATHAN M; CLARK WK: The pressure-volume function of brain elasticity and its relationship with ventricular size. In: *Intracranial Pressure IV* eds. K Shulman, A Marmarou, JD Miller,

- DP Becker, GM Hochwald, M Brock, Springer-Verlag, Berlin-Heidelberg-New York, 81-84, 1980.
- SMALL HS; WEITZNER SW; NAHAS GG: Cerebrospinal fluid pressures during hypercapnia and hypoxia in dogs. *Am. J. Physiol.*, 198, 704-708, 1960.
- SMITH RW; ALKSNE JF: Infections complicating the use of external ventriculostomy. *J. Neurosurg.*, 44, 567, 1976.
- SNODGRASS SR; LORENZO AV: Temperature and cerebrospinal fluid production rate. *Am. J. Physiol.*, 222, 1524-1527, 1972.
- STALHAMMER D; ARKELSJÖ P; LINDSTRÖM L; ÖRTENGREN R: Intracranial pressure registration administrated by a microprocessor. In: *Intracranial Pressure* IV eds. K Shulman, A Marmarou, JD Miller, DP Becker, GM Hochwald, M Brock, Springer-Verlag, Berlin-Heidelberg-New York, 404-408, 1980.
- STERN WE: Intracranial fluid dynamics. The relationship of intracranial pressure to the Monro-Kellie doctrine and the reliability of pressure assessment. *J. Royal College Surgeons Edinburgh*, 9, 18-36, 1963.
- SULLIVAN HG; MILLER JD; BECKER DP; FLORA RE; ALLEN GA: The physiological basis of intracranial pressure change with progressive epidural brain compression. *J. Neurosurg.*, 47, 532-550, 1977.
- SULLIVAN HG; MILLER JD; GRIFFITH RL; BECKER DP: CSF pressure-volume dynamics in neurosurgical patients. A preliminary evaluation in six patients. *Surg. Neurol.*, 9, 47-54, 1978.
- SULLIVAN HG; MILLER JD; GRIFFITH RL; BECKER DP: CSF pressure transients in response to epidural and ventricular volume loading. *Am. J. Physiol.*, 234, R167-R171, 1978.
- SULLIVAN HG; MILLER JD; GRIFFITH RL; CARTER W; RUCKER S: Bolus versus steady-state infusion for determination of CSF outflow resistance. *Ann. Neurol.*, 5, 228-238, 1979.
- SULLIVAN HG; SEARLE JR; BEVERIDGE WD; ALLEN MB; FLANIGAN HF: Effect of pressure on cerebrospinal fluid absorption in cats, baboons and humans: Comparison of the linear and logarithmic models. *Neurosurg.*, 10, 210-223, 1982.
- SUNDBÄRG G; KJÄLLQUIST A; LUNDBERG N; PONTÉN U: Complications due to prolonged ventricular fluid pressure recording in clinical practice. In: *Intracranial Pressure* eds. M Brock, H Dietz, Springer-Verlag, Berlin-Heidelberg-New York, 348-352, 1972.
- SYMON L; ISHIKAWA S; LAVY S; MEYER JS: Quantitative measurement of cephalic blood flow in the monkey. A study of vascular occlusion in the neck using electromagnetic flowmeters. *J. Neurosurg.*, 20, 199-218, 1963.

- SYMON L: Transmission of arterial pulsations in the cerebral vascular bed of the baboon. *J. Physiol.*, 196, 52P-53P, 1963.
- SYMON L: Regional vascular reactivity in the middle cerebral arterial distribution. An experimental study in baboons. *J. Neurosurg.*, 33, 532-541, 1970.
- SYMON L; HELD K; DORSCH NWC: On the myogenic nature of the autoregulatory mechanism in the cerebral circulation. *Europ. Neurol.*, 6, 11-18, 1972.
- SYMON L; PASZTOR E; DORSCH NWC; BRANSTON NM: Physiological responses of local areas of the cerebral circulation in experimental primates determined by the method of hydrogen clearance. *Stroke*, 4, 632-642, 1973.
- SYMON L; PASZTOR E; BRANSTON NM; DORSCH NWC: Effect of supratentorial space-occupying lesions on regional intracranial pressure and local cerebral blood flow: An experimental study in baboons. *J. Neurol. Neurosurg. Psychiat.*, 37, 617-626, 1974.
- SYMON L; CROCKARD HA; JUHASZ J: Some aspects of cerebrovascular resistance in raised intracranial pressure: An experimental study. In: *Intracranial Pressure II* eds. N Lundberg, U Pontén, M Brock, Springer-Verlag, Berlin-Heidelberg-New York, 257-262, 1975.
- SYMON L; CROCKARD HA; JUHASZ J; BRANSTON NM: The effect of intracranial hypertension on cerebrovascular resistance - an experimental study. *Acta Neurochir.*, 35, 221-232, 1976.
- SZEWCZYKOWSKI J; SLIWKA S; KUNICKI A; DYTKO P; DIP PG; KORSAK-SLIWKA J: A fast method of estimating the elastance of the intracranial system. *J. Neurosurg.*, 47, 19-26, 1977.
- TAKAGI H; WALSTRA G; MARMAROU A; SHULMAN K: The effect of blood-pressure and PaCO₂ upon bulk compliance (PVI). In: *Intracranial Pressure IV* eds. K Shulman, A Marmarou, JD Miller, DP Becker, GM Hochwald, M Brock, Springer-Verlag, Berlin-Heidelberg-New York, 163-166, 1980.
- TAKIZAWA H; CHISHIKI T; MURAOKA K; SUGIURA K: A combination of bed side ICP recordings; histogram, trend-graph and digital print. In: *Intracranial Pressure IV* eds. K Shulman, A Marmarou, JD Miller, DP Becker, GM Hochwald, M Brock, Springer-Verlag, Berlin-Heidelberg-New York, 400-403, 1980.
- TANS JTJ: Differentiation of normal pressure hydrocephalus and cerebral atrophy by computed tomography and spinal infusion test. *J. Neurol.*, 222, 109-118, 1979.

- TANS JTJ; POORTVLIET DCJ: Intracranial volume-pressure relationship in man. *J. Neurosurg.*, 56, 524-528, 1982.
- TANS JTJ; POORTVLIET DCJ: Steady state and bolus infusion in hydrocephalus. In: *Intracranial Pressure V*, in press 1983.
- TINEL J: Études sur le pouls cérébral. *L'Encéphale*, 22, 229-244, 1927.
- TROTTER JL; LUZECKY M; SIEGEL BA; GADO M: Cerebrospinal fluid infusion test. Identification of artifacts and correlation with cisternography and pneumoencephalography. *Neurology*, 24, 181-186, 1974.
- TROUPP H; McDOWALL DG: Summary of session on patient management. In: *Intracranial Pressure III* eds. JWF Beks, DA Bosch, M Brock, Springer-Verlag, Berlin-Heidelberg-New York, 279-280, 1976.
- TURCHETTI A: Le onde di tensione del liquor cefalo-rachidiano in rapporto all' attività respiratoria e cardiovascolare. *Boll. Soc. Ital. Biol. Sper.*, 22, 924-927, 1946.
- TURNER JM; McDOWALL DG; GIBSON RM; KHALILI H: Computer analysis of intracranial pressure measurements: Clinical value and nursing response. In: *Intracranial Pressure III* eds. JWF Beks, DA Bosch, M Brock, Springer-Verlag, Berlin-Heidelberg-New York, 283-287, 1976.
- VELA AR; CAREY ME; THOMPSON BM: Further data on the acute effect of intravenous steroids on canine CSF secretion and absorption. *J. Neurosurg.*, 50, 477-482, 1979.
- VIERHOUT RR: The response of catheter manometer systems used for direct blood pressure measurements. PhD Thesis, no. 7, University of Nijmegen, Netherlands, 1966.
- WEED LH; McKIBBEN PS: Pressure changes in the cerebrospinal fluid following intravenous injection of solutions of various concentrations. *Am. J. Physiol.*, 48, 512-530, 1919.
- WEED LH; McKIBBEN PS: Experimental alteration of brain bulk. *Am. J. Physiol.*, 48, 531-558, 1919.
- WEED LH; HUGHSON W: Systemic effects of the intravenous injection of solutions of various concentration with special reference to the cerebrospinal fluid. *Am. J. Physiol.*, 58, 53-84, 1921.
- WEED LH; HUGHSON W: The cerebrospinal fluid in relation to the bony encasement of the central nervous system as a rigid container. *Am. J. Physiol.*, 58, 85-100, 1921.
- WEED LH; HUGHSON W: Intracranial venous pressure and cerebrospinal fluid pressure as affected by intravenous injection of solutions of various concentrations. *Am. J. Physiol.*, 58, 101-130, 1921.

- WEED LH: Some limitations of the Monro-Kellie hypothesis. Arch. Surg., 18, 1049-1068, 1929.
- WEED LH; FLEXNER LB; CLARK JH: The effect of dislocation of cerebrospinal fluid upon its pressure. Am. J. Physiol., 100, 246-261, 1932.
- WEED LH; FLEXNER LB: Cerebrospinal elasticity in the cat and macaque. Am. J. Physiol., 101, 668-677, 1932.
- WEED LH; FLEXNER LB: The relations of the intracranial pressures. Am. J. Physiol., 105, 266-272, 1933.
- WEISS MH; NULSEN FE: The effect of glucocorticoids on CSF flow in dogs. J. Neurosurg., 32, 452-458, 1970.
- WELCH K; FRIEDMAN V: The cerebrospinal fluid valves. Brain, 83, 454-469, 1960.
- WELCH K; SADLER K; GOLD G: Volume flow across choroidal ependyma of the rabbit. Am. J. Physiol., 210, 232-236, 1966.
- WELCH K: The principles of physiology of the cerebrospinal fluid in relation to hydrocephalus including normal pressure hydrocephalus. Adv. Neurology, 13, 247-332, 1975.
- WESSELING KH; BENEKEN JEW: Spurious transfer of pressure changes through the catheter wall: A theoretical evaluation of its effect on the accuracy of pressure measurements. Progress Report no. 2, Inst. Med. Phys. TNO, Netherlands, 25-31, 1970.
- WIENER N: Cybernetics or control and communication in the animal and the machine. The MIT press, Cambridge, Massachusetts, 1948.
- WILSON CB; BERTAN V: Interruption of the anterior choroidal artery in experimental hydrocephalus. Arch. Neurol., 17, 614-619, 1967.
- WISE BL; CHATER N: The value of hypertonic mannitol solution in decreasing brain mass and lowering cerebrospinal fluid pressure. J. Neurosurg., 19, 1038-1043, 1962.
- WOLFF HG; FORBES HS: Cerebral circulation. V. Observations of the pial circulation during changes in ICP. Arch. Neurol. Psychiat., 20, 1033-1047, 1928.
- WOLFF HG; LENNOX WG: Cerebral circulation. XII. The effect on pial vessels of variations in the oxygen and carbon dioxide content of the blood. Arch. Neurol. Psychiat., 23, 1097-1120, 1930.
- WRIGHT RD: Experimental observations on increased intracranial pressure. Aust. N. Z. J. Surg., 7, 215-235, 1938.
- WYLER GR; KELLY W: Use of antibiotics with external ventriculostomies. J. Neurosurg., 37, 185-187, 1972.

YOSHIDA K; MEYER JS; SAKAMOTO K; HANDA J: Autoregulation of cerebral blood flow. Electromagnetic flow measurements during acute hypertension in the monkey. *Circ. Res.*, 19, 726-738, 1966.

ZYLBERLAST-ZAND N: Sur la modification de la pression du liquide céphalo-rachidien sous l'influence du changement de position du corps et de la tête. *Rev. Neurol.*, 37, 1217-1221, 1921.

SYMBOLS AND ABBREVIATIONS

CBF	Cerebral Blood Flow
CBV	Cerebral Blood Volume
CMP	Cisterna Magna Pressure
CSF	Cerebrospinal fluid
CSFPP	CSF Pulse Pressure
C_1	Constant related to parameters of CSF formation and absorption
E	Elastance of craniospinal system
E_1	Elastance coefficient
ECG	Electrocardiogram
F_a	Cerebral arterial blood flow
F_{csf}	Rate of change in CSF volume
F_{cs}	Rate of change in craniospinal volume
F_f	Forcing function: volume-pressure test or infusion test
F_i, F_1	CSF formation rate
F_{in}	Rate of infusion
F_o	CSF absorption rate
F_v	Cerebral venous blood flow
HR	Heart Rate
ICP	Intracranial pressure
P	Intracranial pressure
P_a	Arterial pressure in choroid plexus
$PaCO_2$	Arterial carbon dioxide tension
P_b	Base-line ICP
P_{br}	ICP at breakpoint in VPR-ICP relationship
P_d	Dural sinus pressure
P_{db}	Dural sinus pressure corresponding with the normal base-line ICP
P_{eq}	Equilibrium pressure

P_p	Peak pressure in response to bolus injection
P_{ss}	Steady state ICP during infusion
P_o, P_1	Constant pressure terms
PVI	Pressure-Volume Index
ΔP	Pressure change in response to change in craniospinal volume (ΔV)
R_i	Inflow resistance of CSF
R_o	Outflow resistance of CSF
SAP	Systemic Arterial Pressure
ΔSAP	Systemic arterial pulse pressure
S_1	Slope of VPR-ICP relationship
S_2	Slope of CSFPP-ICP relationship
V_{br}	Craniospinal volume at breakpoint in VPR-ICP relationship
V_e	Elastic volume: change in craniospinal volume with respect to equilibrium volume
V_{eq}	Equilibrium volume of craniospinal system at which ICP = P_{eq}
VFP	Ventricular Fluid Pressure
VPR	Volume-Pressure Response
V_{total}	Total volume of craniospinal system
ΔV_b	Pulsatile change in CBV
ΔV_c	Part of injected volume which is compensated for
ΔV_e	Elastic volume change of craniospinal system
ΔV_i	Volume of bolus injection

ACKNOWLEDGEMENTS

We should like to thank all those who have assisted us in our investigations over the years and those who have contributed to the completion of this thesis.

PROF. DR. S.A. DE LANGE suggested the idea of CSF pulse pressure analysis. He, PROF. DR. G. VAN DEN BRINK and PROF. DR. M. DE VLIETGER have encouraged and supported us in the writing of the thesis. They also put just enough gentle pressure on us, towards the end of the study, to make us meet the dead-line.

The STAFF of the INSTITUTE OF NEUROLOGICAL SCIENCES and of the WELLCOME SURGICAL RESEARCH INSTITUTE (DR. A.M. HARPER) kindly gave us hospitality during our four months stay in Glasgow and provided us with the facilities for the experimental work described in Chapters 5 and 6. PROF. W.B. JENNETT, head of the Department of Neurosurgery, and DR. JACK O. ROWAN discussed the preliminary results with us and offered valuable criticism. DR. DAVID J. WYPER participated in the animal experiments and was co-author of the publications on these studies. PROF. GRAHAM TEASDALE and his wife EVELYN lent us their house and their 'limousine'.

The NETHERLANDS ORGANISATION FOR THE ADVANCEMENT OF PURE RESEARCH (ZWO) granted financial support.

MRS. HANNI VAN RIGTEREN typed, retyped and re-retyped the manuscript with devotion and great skill. She especially enjoyed the mathematical equations. She also helped with the manuscripts for most of our publications.

PROF. DR. R. BRAAKMAN enabled us to work on the thesis for several periods at a stretch and he also made it possible for us to attend international conferences on the subject of ICP.

DR. IR. WIM A. VAN DUYL offered constructive criticism during the progress of the study.

PROF. DR. K.G. GO and PROF. DR. IR. H.G. STASSEN read the manuscript thoroughly and took the time to discuss it with us.

DIRK DE JONG participated in many clinical ICP measurements in the early phase of the project.

The TECHNICAL STAFF OF THE EEG DEPARTMENT (Piet Megens, Hans van der Sluijs, Ton Mus en Ben de Vos) built the ICP recording system and were always present when technical help was needed.

WOUT MOOLENAAR, HUGO VAN STEENIS and LOURENS VAN BRIEMEN wrote parts of the computer programs.

MRS. SUE CRAIG resisted the temptation to rewrite the whole English text. She corrected only the most obvious mistakes in order not to interfere with our own 'special' style.

The AUDIOVISUAL CENTRE of the Erasmus University, Rotterdam, provided the illustrations and tables.

MISS RIA VAN SCHELVEN typed parts of the manuscript when time was running out.

The JOURNAL OF NEUROSURGERY, ACTA NEUROLOGICA SCANDINAVICA and SPRINGER-VERLAG kindly permitted reproduction of material from published papers.

CURRICULUM VITAE

Cees J.J. Avezaat werd op 2 maart 1942 te Amsterdam geboren. Hij bezocht het Onze Lieve Vrouwe Lyceum te Breda, waar hij in 1960 het eindexamen Gymnasium B aflegde. Hij studeerde geneeskunde aan de Katholieke Universiteit te Nijmegen en werd in 1968 tot arts bevorderd. Daarna volgde hij gedurende een jaar de opleiding algemene heekkunde in het St. Hippolytus Ziekenhuis te Delft (Dr. G. Olthuis en Dr. W.M. Oosterwijk). Eind 1969 volgde hij de Tropencursus voor artsen aan het Koninklijk Instituut voor de Tropen te Amsterdam. Vervolgens vertrok hij voor een periode van drie jaar naar Tanzania, alwaar hij werkzaam was in het Bukumbi Hospital te Bukumbi, Mwanza District. In 1973 begon hij zijn opleiding tot neurochirurg in het Academisch Ziekenhuis Rotterdam (Prof. Dr. S.A. de Lange en Prof. Dr. R. Braakman, voor de stage neurologie Prof. Dr. A. Staal). Sinds 1978 maakt hij deel uit van de staf van de afdeling neurochirurgie van hetzelfde ziekenhuis.

CURRICULUM VITAE

John van Eijndhoven werd op 19 januari 1948 te Haarlem geboren. Hij bezocht het Triniteits Lyceum te Haarlem, alwaar hij in 1965 het HBS-B diploma behaalde. Vervolgens studeerde hij aan de Technische Hogeschool te Delft afdeling Werktuigbouwkunde. In 1972 studeerde hij af in de Werktuigbouwkundige Meet- en Regeltechniek (Prof. Ir. R.G. Boiten) sectie Mens Machine systemen (Prof. Dr. Ir. H.G. Stassen). Van 1 juli 1972 tot 31 december 1972 was hij bij de sectie Mens Machine systemen werkzaam als ingenieur-assistent. Sedert 1973 is hij bij de afdeling Neurologie van de Medische Faculteit Rotterdam werkzaam als wetenschappelijk medewerker.

